

Some pages of this thesis may have been removed for copyright restrictions.

If you have discovered material in Aston Research Explorer which is unlawful e.g. breaches copyright, (either yours or that of a third party) or any other law, including but not limited to those relating to patent, trademark, confidentiality, data protection, obscenity, defamation, libel, then please read our [Takedown policy](#) and contact the service immediately (openaccess@aston.ac.uk)

ASTON UNIVERSITY

Thermochemical Conversion of Brewers Spent Grain combined with Catalytic Reforming of Pyrolysis Vapours

Doctor of Philosophy in Chemical Engineering in The
Department of Chemical Engineering and Applied Chemistry

Asad S N Mahmood

September 2014

© Asad S N Mahmood, 2014

© Asad S N Mahmood asserts his moral right to be identified as the author of this thesis

This copy of thesis has been supplied on condition that anyone who consults it is understood to recognise that its copyright rests with its author and that no quotation from the thesis and no information derived from it may be published without proper acknowledgement.

THE APPLICATION OF METAL CATALYSIS TO BIOMASS THERMOCHEMICAL PROCESSING

ASAD SHAZAAD NIRYAR MAHMOOD

Doctor of Philosophy

2014

Thesis Summary

The brewing process is an energy intensive process that uses large quantities of heat and electricity. To produce this energy requires a high, mainly fossil fuel consumption and the cost of this is increasing each year due to rising fuel costs. One of the main by-products from the brewing process is Brewers Spent Grain (BSG), an organic residue with very high moisture content. It is widely available each year and is often given away as cattle feed or disposed of to landfill as waste. Currently these methods of disposal are also costly to the brewing process. The focus of this work was to investigate the energy potential of BSG via pyrolysis, gasification and catalytic steam reforming, in order to produce a tar-free useable fuel gas that can be combusted in a CHP plant to develop heat and electricity. The heat and electricity can either be used on site or exported.

The first stage of this work was the drying and pre-treatment of BSG followed by characterisation to determine its basic composition and structure so it can be evaluated for its usefulness as a fuel. A thorough analysis of the characterisation results helps to better understand the thermal behaviour of BSG feedstock so it can be evaluated as a fuel when subjected to thermal conversion processes either by pyrolysis or gasification.

The second stage was thermochemical conversion of the feedstock. Gasification of BSG was explored in a fixed bed downdraft gasifier unit. The study investigated whether BSG can be successfully converted by fixed bed downdraft gasification operation and whether it can produce a product gas that can potentially run an engine for heat and power. In addition the pyrolysis of BSG was explored using a novel "Pyroformer" intermediate pyrolysis reactor to investigate the behaviour of BSG under these processing conditions. The physicochemical properties and compositions of the pyrolysis fractions obtained (bio-oil, char and permanent gases) were investigated for their applicability in a combined heat power (CHP) application.

The third stage of this work was the addition of post-pyrolysis vapour catalysis to the intermediate pyrolysis process, which aims to reform the pyrolysis vapours so increasing the quality of the bio-oil, and enhancing the content of the permanent product gases, H₂, CO and CH₄. Three different catalysts were selected; a commercial steam reforming nickel catalyst (Ni/Al₂O₃), rhodium (Rh/Al₂O₃) and platinum (Pt/Al₂O₃) all supported on alumina. A bench-scale fixed bed batch pyrolysis reactor was used to conduct intermediate pyrolysis experiments of BSG at the same temperature as the Pyroformer but at different heating rates in an attempt to simulate the Pyroformer. The aim was to validate the use of this bench-scale unit to replicate the Pyroformer, which could not be adapted for catalytic work. The bench-scale unit was then used for the study of catalytic steam reforming of pyrolysis vapours. The incorporation of the catalysts was done via a fixed tube reactor downstream of the pyrolysis reactor.

The effect of catalyst at different reforming temperatures (500, 750 & 850°C) without steam and then with the addition of steam was investigated and the performances of the catalysts were compared. The initial catalytic experiments without steam made use of the aqueous phase or the water/steam present in the hot organic pyrolysis vapours to serve the steam reforming reactions within the secondary reactor, so as to observe quantity of syngas produced (in particular H₂ content) and the catalyst performance utilising the water already present in the system.

The passing of hot pyrolysis vapours over a fixed bed of catalysts will upgrade and enrich the pyrolysis gas prior to condensation in terms of heating value, due to an increased yield of methane, and hydrogen formation. Results indicated that catalytic reforming produced a significant increase in permanent gases (mainly H₂ and CO) and reduced liquids yield as reforming temperature increased. All catalysts had a beneficial effect; however the commercial nickel reforming catalysts using a high surface area support had a noticeably higher activity than the PGM catalysts.

Dedication

All praises be to Allah, the Exalted, the most gracious, merciful and beneficent, whom has provided me with so much and gave me strength and patience to bare and succeed through the struggles of this work. May Allah's peace and blessings be on the prophet Mohammed (pbuh).

“In the name of Allah,
The Most Beneficent, the Most Merciful,
All the praises and thanks be to Allah, the Lord of all creation,
The Most Beneficent, the Most Merciful,
The only owner and the only ruling judge of the day of recompense,
You alone we worship, and You alone we ask for help,
Guide us to the straight way, the way of those on whom You have bestowed Your grace,
Not the way of those who have earned Your anger, nor of those who went astray.”
- **The Holy Quran (1:1-7)**

“Verily, we have given you a manifest victory,
That Allah may forgive you your sins of the past and the future, and complete His favour on
you, and guide you on the straight path,
And that Allah may aid you with a mighty victory.”
- **The Holy Quran (48:1-3)**

“Verily, with hardship, there is relief.”
- **The Holy Quran (94:6)**

Allah is sufficient for us, and He is the best Disposer of affairs. So they returned with
Grace and Bounty from Allah. No harm touched them; and they followed the good
Pleasure of Allah. And Allah is the owner of Great Bounty.”
- **The Holy Quran (3:173-174)**

"And put your trust in Allah if you are believers indeed..."
The Holy Quran (5:23)

O' you who believe! Seek help in patience and the Prayer."
- **The Holy Quran (2:153)**

To my beloved parents and family who have given me so much love and support. To my son Younus. To my late nana-ji Mohammed Aslam whom sadly I did not ever get to meet.

Acknowledgments

All praise is for Allah, the Exalted, the all compassionate and all merciful. May Allah's peace and blessings be on Muhammad, on his family, and on his Companions.

The author would like to express his gratitude to Professor Andreas Hornung and the European Bioenergy Research Institute (EBRI) for providing the facilities for this research project; Dr Andrew Steele, Dr Stephen Poulston of Johnson Matthey who were collaborating as well as the Engineering and Physical Science Research Council (EPSRC) for funding and financial support; and my supervisor Dr. John Brammer who showed faith in me and that I have a tremendous amount of respect and time for.

The author also wishes to thank:

The European Bioenergy Research Institute staff and researchers for their selfless support in particular Zsuzsa Mayer for her analysis work and general assistance with laboratory equipment. Miloud Ouadi and Yang Yang for support with the pyroformer and gasification apparatus. Saifullah Abu-Bakr for his assistance during biomass compositional analysis and during the construction of the bench scale pyrolysis rig; the commissioning, alteration; the running of the completed system.

Stephen Williams glassware blower of Birmingham University.

Sheffield University technicians Stuart Richards, Oz Mcfarlane, Dave Pearson and Mike Omara for their expertise in construction of the Circulating Fluidised Bed Gasification rig; commissioning; and running then completed system.

My family for their endless support, (in particular my parents Mr Arshad Mahmood and Mrs Sofia Mahmood) and backing throughout my time at Aston University as both an undergraduate and postgraduate.

My friends both inside and outside university for their wise words and entertainment value.

List of Symbols & Abbreviations

Symbols

A	Amp
Al ₂ O ₃	Aluminium Oxide
C	Carbon
CaO	Calcium Oxide
Cl	Chlorine
Ca	Calcium
cm	Centimetre
cm ²	Centimetre square
cm ³	Centimetre cubed
C _p	Specific Heat Capacity
Cst	Centi Stokes
CO	Carbon Monoxide
CO ₂	Carbon dioxide
CH ₄	Methane
C ₂ H ₄	Ethane
C ₂ H ₆	Propane
C ₃ H ₆	Propylene
C ₄ H ₈	Butenes
C ₄ H ₁₀	Butane
°C	Degrees Celcius
°C/min	Degress Celcius per minute
Fe ₂ O ₃	Iron oxide
g	gram
g/Nm ³	grams per Normal Meter Cube
h	hours
H	Hydrogen
H ₂	Hydrogen
H ₂ S	Hydrogen Sulphide
id	internal diameter
od	outer diameter
K	Kelvin
K	Potassium
kJ	Kilo joule
kJ/mol	Kilo joule per mol
kg	kilo gram
Kg/h	kilo gram per hour
Kgh/m ³	kilogram hour per meter cube
Kg/m ² s	kilogram per meter square second
kW	kilo Watt
kV	kilo Volt
L	Litre
l/h	litre / hour
m	Meter
ṁ	Mass flowrate
m ²	Meter square
m ³	Meter cube
m ² /g	Meter square per gram
m ³ /h	Meter cube per hour
m/s	meter / second

MJ/Nm ³	Mega Joule per Normal meter cubed
MJ/kg	Mega joule per Kilo-gram
ml	Millilitre
ml/min	Millilitre per minute
Mg	Magnesium
Mg/KOH/g	Milligram per potassium hydroxide per gram
MgO	Magnesium Oxide
Mt	Million tonnes
Mpa	Mega Pascal
MW	Mega Watt
μl	Micro litre
μm	micro meter
N	Nitrogen
Na	Sodium
NaCl	Sodium Chloride
N ₂	Nitrogen
Ni	Nickel
O	Oxygen
P	Phosphorous
Q	Energy (MJ)
pH	power of Hydrogen
ppm	parts per million
Pt	Platinum
Rh	Rhodium
Ru	Ruthenium
Rpm	Revolutions per minute
s	seconds
S	Sulphur
Si	Silicon
SiO ₂	Silica Oxide
ΔT	Temperature Difference
Vol%	volume percent
v/v	volume/volume
Wt%	weight percent
w/w	weight/weight
>	greater than
<	less than
±	plus-minus
~	approximately
%	Percentage

Abbreviations

ADL	Acid Detergent Lignin
ADS	Acid Detergent Solution
ASTM	American Society for Testing Materials
BET	Brunauer, Emmet and Teller
BFB	Bubbling Fluidised Bed
BSG	Brewers Spent Grain
BTXN	Benzene-Toluene-Xylene-Naphthalene
CGE	Cold Gas Efficiency
CFB	Circulating Fluidised Bed
CHP	Combined Heat & Power
DC	Direct Current
DTG	Derivative thermo-gravimetric
EBRI	European Bioenergy Research Institute
ECN	European Research Centre of Netherlands
EFB	Empty Fruit Bunch
EPA	Environmental Protection Agency
EPSRC	Engineering & Physical Science Research Council
ER	Equivalence Ratio
FTIR	Fourier-transform Infra-red
GC	Gas Chromatograph
GCMS	Gas Chromatograph Mass Spectrometer
GC-TCD	Gas Chromatograph Thermal Conductivity Detector
GCU	Gasifier Control Unit
GCV	Gross Calorific Value
GEK	Gasifier Experimenters Kit
GHSV	Gas Hourly Space Velocity
HHV	Higher Heating Value
HT	High temperature
HCG	Hydrocarbon Gases
HCL	Hydrocarbon Liquids
HPLC	High-Performance Liquid Chromatography
IC	Internal Combustion
IOG	Inorganic Gases
IR	Infra-Red
KF	Karl Fischer
KOH	Potassium Hydroxide
LHV	Lower Heating Value
LPG	Liquid Petroleum Gas
LT	Low Temperature
MSBS	Molecular beam mass Spectrometer
MSW	Municipal Solid Waste
MW	Molecular Weight
NDF	Neutral Detergent Fibre
NDS	Neutral Detergent Solution
NREL	National Renewable Energy Laboratory
NO _x	Nitrogen dioxide

O/C	Oxygen/Carbon Ratio
PAH	Poly-aromatic hydrocarbon
PGM	Precious Group Metal
PPFB	Dual Particle Powder Fluidised bed
PWM	Pulse Width Modulation
R&D	Research and Development
RDF	Refuse Derived Fuel
RMM	Relative Molecular Mass
RO	Renewable Obligation
ROC's	Renewable Obligation Certificates
S/C	Steam Carbon Ratio
SHS	Super-heated steam
SV	Space Velocity
TAN	Total Acid Number
TGA	Thermo-gravimetric Analysis
UCI	United Catalysts Incorporation
UK	United Kingdom
USA	United States of America
WSG	Wheat Spent Grains
WHSV	Weight Hourly Space Velocity

List of Contents

Thesis Summary	1
Dedication.....	3
Acknowledgments	4
List of Symbols & Abbreviations	5
List of Contents	9
List of Tables	14
List of Figures.....	16
1 Introduction.....	20
1.1 Project Description	20
1.2 Background.....	20
1.3 Brewers Spent Grain (BSG)	20
1.4 Brewing Process and Brewers Spent Grain Generation	22
1.4.1 Steeping	22
1.4.2 Germination	22
1.4.3 Drying or Kilning	22
1.5 BSG Preservation Methods.....	25
1.6 Organisation of Thesis	26
2 Thermochemical Conversion of Biomass Techniques	28
2.1 Introduction.....	28
2.2 Biomass	28
2.2.1 Water.....	29
2.2.2 Cellulose	29
2.2.3 Hemicellulose	30
2.2.4 Lignin.....	31
2.2.5 Organic extractives	32
2.2.6 Inorganic materials	32
2.3 Pyrolysis	32
2.3.1 Modes of Pyrolysis	34
2.4 Intermediate Pyrolysis Principles	35
2.4.1 ‘Pyroformer’ Intermediate pyrolysis reactor	36
2.4.2. Haloclean Intermediate pyrolysis reactor	37
2.5 Feedstock variables effecting Intermediate pyrolysis.....	38
2.6 Intermediate Pyrolysis Products	40

2.6.1	Bio-oil.....	40
2.6.2	Char.....	40
2.6.3	Permanent Gases.....	40
2.7	Gasification.....	41
2.7.1	Biomass gasification process.....	41
2.7.2	Gasification reaction mechanism.....	43
2.7.3	Comparison of Biomass gasification systems.....	43
2.7.4	Tars.....	50
2.8	Catalytic Upgrading Options.....	52
2.8.1	Pyrolysis upgrading.....	52
2.8.2	Gasification upgrading.....	54
3	Previous Work on Thermochemical Conversions of Biomass & Catalytic Upgrading.....	58
3.1	Introduction.....	58
3.1.1	Biomass Pyrolysis Studies.....	58
3.1.2	Biomass pyrolysis vapour upgrading studies.....	66
3.1.3	Biomass Gasification studies.....	77
3.1.4	Biomass Gasification, Steam reforming and catalytic conversion.....	83
3.2	Summary of previous work.....	89
3.3	Project Aims and Objectives.....	95
3.3.1	Project aim.....	95
3.3.2	Project Objectives.....	95
4	Characterisation Methods of Biomass Feedstock and Pyrolysis Products.....	97
4.1	Introduction.....	97
4.2	Materials and Methods.....	97
4.2.1	Raw Materials.....	97
4.3	Feedstock Pre-treatment.....	97
4.3.1	Freezing.....	97
4.3.2	Drying.....	97
4.3.3	Grinding.....	98
4.3.4	Pelletizing.....	98
4.4	Feedstock Characterisation.....	99
4.4.1	Proximate analysis.....	99
4.4.2	Ultimate analysis.....	99
4.4.3	Chemical compositional analysis.....	100
4.4.4	Inorganic elements.....	101
4.4.5	Ash Fusion (Oxidising).....	101

4.4.6 Heating Values.....	101
4.4.7 Thermo-gravimetric Analysis (TGA)	102
4.5 Characterisation of Intermediate Pyrolysis Products.....	103
4.5.1 Bio-oil Analysis.....	103
4.5.2 Char Analysis.....	108
4.5.3 Permanent gases Analysis.....	108
4.6 Results and Discussion	109
4.6.1 Freezing	109
4.6.2 Drying.....	110
4.6.3 Grinding.....	111
4.6.4 Pelletizing.....	112
4.6.3 Feedstock Characterisation.....	113
4.7 Summary.....	119
5 Experimental Gasification Methodology & Results.....	120
5.1 Introduction.....	120
5.2 Fixed Bed Downdraft Gasifier.....	120
5.2.1 Gasification preparation and assembly	122
5.2.2 Gasifier Control Unit (GCU).....	124
5.2.3 Tar Analysis – Guideline Method ECN.....	124
5.2.4 Rotary Evaporation Unit.....	125
5.2.5 Water condensate analysis.....	126
5.2.6 Product Syn-gas analysis	127
5.3 Gasification Results and Discussion.....	128
5.3.1 Product gas analysis.....	131
5.3.2 Tar analysis.....	133
5.3.3 Mass balance.....	134
5.3.4 Gasifier bed inspection	134
5.4 Summary.....	135
6 Experimental Intermediate Pyrolysis Methodology	138
6.1 Introduction.....	138
6.2 Pyroformer Intermediate Pyrolysis.....	138
6.3 Experimental Bench Scale Intermediate Pyrolysis Methodology.....	142
6.3.1 Non-catalytic pyrolysis experiments	143
6.3.2 Catalytic pyrolysis experiments.....	144
6.4 Mass and Energy Balance Calculation	147
7 Intermediate Pyrolysis Results and Discussion	148

7.1	Introduction.....	148
7.2	Pyroformer Intermediate Pyrolysis.....	148
7.3	Mass Balance.....	149
7.4	Characterisation of Intermediate Pyrolysis Products.....	150
	7.4.1 Bio-oil Analysis.....	150
	7.4.2 Char Analysis.....	156
	7.4.3 Permanent gases.....	158
7.5	Summary.....	158
8	Non-Catalytic Bench Scale Intermediate Pyrolysis Results and Discussion.....	160
8.1	Introduction.....	160
8.2	Bench Scale Intermediate Pyrolysis Reactor.....	160
8.3	Mass Balance.....	162
8.4	Characterisation of Non-Catalytic Bench Scale Intermediate Pyrolysis Products ...	168
	8.4.1 Bio Oil Analysis	168
	8.4.2 Char Analysis.....	178
	8.4.3 Permanent gases.....	179
9	Catalytic Intermediate Pyrolysis Results and Discussion.....	183
9.1	Introduction.....	183
9.2	Catalytic Bench Scale Intermediate Pyrolysis Reactor.....	184
9.3	Mass Balance.....	186
	9.3.1 Pyrolysis and Catalytic Reforming with Commercial Nickel (Ni/Al ₂ O ₃) Catalyst without steam.....	190
	9.3.2 Pyrolysis and Catalytic Reforming with Commercial Nickel (Ni/Al ₂ O ₃) with Steam	190
	9.3.3 Pyrolysis and Catalytic Reforming with PGM Catalysts (Pt/Al ₂ O ₃) & (Rh/Al ₂ O ₃) without Steam	191
	9.3.4 Pyrolysis and Catalytic Reforming with PGM Catalysts (Pt/Al ₂ O ₃) & (Rh/Al ₂ O ₃) with Steam	192
9.4	Bio-oil Analysis.....	193
	9.4.1 GCMS Bio-oil at 500°C with Nickel (Ni/Al ₂ O ₃) catalysts and without steam.....	196
	9.4.2 GCMS Bio-oil at 750°C with Nickel (Ni/Al ₂ O ₃) catalysts and without steam.....	198
	9.4.3 GCMS Bio-oil at 850°C with Nickel (Ni/Al ₂ O ₃) catalysts and without steam.....	200
	9.4.4 GCMS Bio-oil at 500°C with Nickel (Ni/Al ₂ O ₃) catalysts and steam.....	201
	9.4.5 GCMS Bio-oil at 750°C with Nickel (Ni/Al ₂ O ₃) catalysts and steam.....	203
	9.4.6 GCMS Bio-oil at 850°C with Nickel (Ni/Al ₂ O ₃) catalysts and steam.....	204
	9.4.7 GCMS Bio-Oil at 500°C with Platinum (Pt/Al ₂ O ₃) catalyst and without steam	207
	9.4.8 GCMS Bio-Oil at 850°C with Platinum (Pt/Al ₂ O ₃) catalyst and without steam	210

9.4.9 GCMS Bio-Oil at 500°C with Rhodium (Rh/Al ₂ O ₃) catalyst and without steam....	211
9.4.10 GCMS Bio-Oil at 850°C with Rhodium (Rh/Al ₂ O ₃) catalyst and without steam..	213
9.4.11 GCMS Bio-Oil at 500°C with Platinum (Pt/Al ₂ O ₃) catalyst and steam	214
9.4.12 GCMS Bio-Oil at 850°C with Platinum (Pt/Al ₂ O ₃) catalyst and steam	216
9.4.13 GCMS Bio-Oil at 500°C with Rhodium (Rh/Al ₂ O ₃) catalyst and steam.....	217
9.4.14 GCMS Bio-Oil at 850°C with Rhodium (Rh/Al ₂ O ₃) catalyst and steam.....	219
9.5 Permanent gases.....	221
9.5.1 Heating Value	225
10 Implications, Conclusions and Recommendations	228
10.1 Implications	228
10.2 Conclusion	238
10.3 Recommendation	246
References	248
Appendix A: Published Work.....	256
Appendix B: Mass Balance Sheets	257
Appendix C: Energy Required for Drying Spent Grains	259
Appendix D: Proformer Mass & Energy Balance	260
Appendix E: GEK Downdraft Gasifier Energy Balance	264

List of Tables

Table 1: Modes of Pyrolysis	34
Table 2 Product yields and distribution of various feedstock's [37]	63
Table 3 GCMS analysis of bio-oil produced using the Haloclean [37]	64
Table 4 Chemical composition & heating values of the biomass used in the gasification experiments[120]	77
Table 5 Average composition and LHV values of the product gases[120]	79
Table 6 Detergent fibre system according to Van Soest[141-143]	101
Table 7 Particle size distribution of BSG and barley straw	111
Table 8 Results of proximate and ultimate analysis of BSG	113
Table 9 Ultimate analysis of other biomass [2]	114
Table 10 Chemical compositional analysis and comparison	115
Table 11 Inorganic elements Metal oxides	116
Table 12 Ash Fusion by using characteristic temperatures	116
Table 13 Product Syngas composition	132
Table 14 Comparison of gasifier performance with literature	133
Table 15 Mass balance – BSG Fixed bed downdraft gasification	134
Table 16 Yield of Products (Mass %) Pyrolysis Final Temperature = 450 °C	149
Table 17 Comparison of results for Intermediate pyrolysis using Haloclean reactor (extracted from [37])	150
Table 18 Elemental Analysis of BSG bio-oil produced from Pyrformer	151
Table 19 Physical properties of Bio-oil produced from Pyroformer in comparison to bio-oil produced from Halo-clean	153
Table 20 GC/MS Tests of the (Organic Phase) Bio-oil Produced (Pyroformer)	154
Table 21 BSG Pyroformer char proximate analysis	156
Table 22 Elemental analysis of Char produced from Pyroformer	156
Table 23 Elemental Analysis of char ash produced from Pyroformer	157
Table 24 Yield of permanent gases produced from Pyroformer	158
Table 25 Summary of mass balance for non-catalytic bench-scale pyrolysis experiments	163
Table 26 Summary of mass balances for experiments with the addition of secondary catalytic reactor (without catalysts)	166
Table 27 Non catalytic bio-oil analysis produced at different heating rate	170
Table 28 Composition of BSG bio-oil without catalysts at 25°C/min heating rate	172
Table 29 Composition of BSG bio-oil without catalysts at 50°C/min heating rate	174
Table 30 Composition of BSG bio-oil without catalysts at 50°C/min heating rate with secondary reactor at 850°C (no catalyst)	176
Table 31 Bio-oil chemical groups	176
Table 32 Proximate analysis of char produced using bench scale reactor	178
Table 33 Ultimate analysis of BSG char	178
Table 34 Summary of mass balances for catalytic experiments using commercial nickel catalysts (with and without steam)	188
Table 35 Summary of mass balances for catalytic experiments using PGM catalysts (Platinum and Rhodium) with and without steam	189
Table 36 Compositional analysis of Bio-oils produced from catalytic bench scale pyrolysis/reforming experiments using Nickel catalysts (Ni/Al ₂ O ₃)	194

Table 37 Compositional analysis of Bio-oils from catalytic bench scale pyrolysis/reforming experiments using PGM catalysts Platinum (Pt/Al ₂ O ₃) and Rhodium (Rh/Al ₂ O ₃)	195
Table 38 Composition of BSG Intermediate Pyrolysis oil after catalytic reforming at 500°C Nickel catalyst and no steam	197
Table 39 Composition of BSG Intermediate Pyrolysis oil after catalytic reforming at 750°C Nickel catalyst and no steam	199
Table 40 Composition of BSG Intermediate Pyrolysis oil after catalytic reforming at 850°C Nickel catalyst and no steam	201
Table 41 Composition of BSG Intermediate Pyrolysis oil after catalytic reforming at 500°C with steam.....	203
Table 42 Composition of BSG Intermediate Pyrolysis oil after catalytic reforming at 750°C with steam.....	204
Table 43 Composition of BSG Intermediate Pyrolysis oil after catalytic reforming at 850°C with steam.....	205
Table 44 Composition of BSG Intermediate Pyrolysis oil after catalytic reforming 500°C with Platinum and no steam.....	209
Table 45 Composition of BSG Intermediate Pyrolysis oil after catalytic reforming 850°C with Platinum and no steam.....	211
Table 46 Composition of BSG Intermediate Pyrolysis oil after catalytic reforming 500°C with Rhodium and no steam	212
Table 47 Composition of BSG Intermediate Pyrolysis oil after catalytic reforming 850°C with Rhodium and no steam	214
Table 48 Composition of BSG Intermediate Pyrolysis oil after catalytic reforming 500°C with Platinum and with steam.....	215
Table 49 Composition of BSG Intermediate Pyrolysis oil after catalytic reforming 850°C with Platinum and with steam.....	216
Table 50 Composition of BSG Intermediate Pyrolysis oil after catalytic reforming 500°C with Rhodium and with steam	218
Table 51 Composition of BSG Intermediate Pyrolysis oil after catalytic reforming 850°C with Rhodium and with steam	219

List of Figures

Figure 1 Brewers Spent Grain [6].....	21
Figure 2 Representation of a Barley Grain [3]	21
Figure 3 Representation of the process to obtain BSG from Barley Grain (extracted from [3] .	24
Figure 4 Biomass Composition [15].....	29
Figure 5 Structure of Cellulose [17]	30
Figure 6 Structure of Hemi cellulose [18]	31
Figure 7 Structure of Lignin [19].....	32
Figure 8 Pyrolysis, Gasification and Combustion [23].....	33
Figure 9 Pyroformer Twin screw mechanism (Engineering Diagram)	36
Figure 10 Pyroformer schematic	37
Figure 11 Scheme of Haloclean Rotary Kiln [37]	37
Figure 12 Pyrolysis curves of hemicellulose, cellulose and lignin TGA[38]	39
Figure 13 Diagram of (downdraft) gasification; notice pyrolysis occurring above and prior to gasification before the biomass is exposed to oxygen [51]	42
Figure 14 Comparison of gasification reactors [57]	44
Figure 15 Updraft Gasifier Design [58].....	45
Figure 16 Downdraft Gasifier design [58].....	46
Figure 17 Bubbling Fluidised Bed (left) & Circulating Fluidised Bed Gasifiers (right) [58]	47
Figure 18 Entrained Flow Gasifier[58].....	48
Figure 19 Scale potential of different type of gasifiers [66].....	49
Figure 20 Formation of biomass tar and example of compounds formed[57].....	51
Figure 21 Haloclean Pyrolysis (Intermediate) and LT reforming experimental setup [34].....	67
Figure 22 Comparison yields from measurements with and without catalysis (700g catalyts, LT reforming temperature 450°C) [34]	68
Figure 23 Determined flow rates of the pyrolysis gases with and without catalysis after the condensation (700 g catalyts, LT-reforming temperature 450°C)][34]	68
Figure 24 Schematic of continuous feed screw-kiln pyrolysis-gasification/catalytic steam reforming system [114].....	69
Figure 25 Pathway tar formation as a function of temperature [117].....	73
Figure 26 The downdraft gasifier system setup used in the experiments[120]	78
Figure 27 Typical vertical gasifier temperature profiles for the different fuels and respective dry composition [120].....	79
Figure 28 Chemical Groups found in Haloclean Pyrolysis Oils.....	91
Figure 29 Chemical Groups found in Waste Derived Pyrolysis s Oil produced in the Pyroformer	91
Figure 30 Biomass Cutting Mill	98
Figure 31 Roller shaft pellet mill with BSG pellets.....	99
Figure 32 Detergent fibre system according to Van Soest[141-143]	100
Figure 33 Parr 6100 bomb calorimeter	102
Figure 34 Perkin Elmer Pyris 1 TGA	103
Figure 35 Mettler Titrator for Water Content.....	104
Figure 36 Mettler Toledo Titrator for Acid Number	106
Figure 37 Cannon-Fenske Routine glass capillary viscometer.....	107
Figure 38 (right) Wet BSG with signs of degradation, (left) dried and ground BSG material.	109
Figure 39 Degradation of wet BSG over 3 days if left untreated	109

Figure 40 Oven drying rate of BSG at 70°C.....	110
Figure 41 Ground BSG material.....	111
Figure 42 BSG pellets.....	112
Figure 43: BSG TGA and DTG Pyrolysis Profile	118
Figure 44: Barley TGA and DTG Pyrolysis Profile	118
Figure 45 GEK Fixed Bed Downdraft Gasifier[165]	120
Figure 46 Downdraft gasification operation [166]	121
Figure 47 Gasification chamber.....	123
Figure 48 Gasification reactor and pre-heated air inlet pipes	123
Figure 49 Producer gas cleaning system [61].....	125
Figure 50 Rotary evaporator system.....	126
Figure 51 Karl Fischer titration: Water condensate analysis	127
Figure 52 (left) Feed hopper with BSG pellets (right) screw feeder feeding BSG pellets	128
Figure 53 Gasification of BSG flare.....	129
Figure 54 Gasification Air flow rate.....	130
Figure 55 BSG Averaged Product Syngas Composition	132
Figure 56 Tar laden flask.....	134
Figure 57 (left) Pellets broken into fines within screw feeder, (right) collected BSG fines and pellets.....	135
Figure 58 (left) unprocessed pellets and fines (right) BSG ash and char	135
Figure 59 The Pyroformer 20kg/hr. Intermediate pyrolysis unit.....	139
Figure 60 Pyroformer (Intermediate Pyrolysis) schematic diagram.....	140
Figure 61 Pyroformer twin coaxial screw system[25, 36].....	141
Figure 62 Bench scale pyrolysis reactor cylindrical quartz tube and electrically heated furnace	143
Figure 63 Bench Scale Pyrolysis reactor	143
Figure 64 Secondary reactor dimensions and packed catalyst bed.....	145
Figure 65 Bench Scale Pyrolysis and Catalytic reactor	146
Figure 66 Copper strip immersed in BSG bio-oil after 24h/40°C	152
Figure 67 GC/MS Analysis of Bio-oil (Organic phase) produced from Pyroformer	153
Figure 68 Pyroformer 'Bio-oil' Chemical Groups.....	155
Figure 69 Biochar produced from Pyroformer	157
Figure 70 Pyroformer BSG Char TGA and DTG curve.....	158
Figure 71 Carbolite pyrolysis reactor and biomass temperature for BSG	161
Figure 72 Permanent gas release rate for BSG at 25°C/min & 50°C/min heating rate	161
Figure 73 Comparison of the yields of products from different pyrolysis heating rates	165
Figure 74 Quartz wool before (a), after (b) 500°C and then after (c) 850°C.....	166
Figure 75 Comparison of the yields of products from different pyrolysis heating rates and with 2nd reactor at 500°C and 850°C (no catalyst)	167
Figure 76 Bio-oil samples received different heating rates (left) 25°C/min (right) 50°C/min .	168
Figure 77 GC/MS analysis of BSG bench scale bio-oil at 25°C/min (chemical abundant vs. Retention time)	171
Figure 78 GC/MS analysis of BSG bench scale bio-oil at 50°C/min (chemical abundant vs. Retention time)	173
Figure 79 GC/MS analysis of BSG bench scale bio-oil at 50°C/min heating rate with secondary reactor at 850°C (no catalyst) (chemical abundant vs. Retention time)	175
Figure 80 Chemical groups and the peak areas for non-catalytic bench scale intermediate pyrolysis bio-oil.....	177

Figure 81 BSG char TGA and DTG combustion profiles	179
Figure 82 Comparison of the Permanent gas yields from different pyrolysis heating rates.....	180
Figure 83 Comparison of the Permanent gas yields from different pyrolysis heating rates and with 2nd reactor at 500°C and 850°C (no catalyst)	181
Figure 84 Permanent gas heating value of non-catalytic pyrolysis experiments.....	181
Figure 85 The bifunctional reaction mechanism, where possible side reactions are indicated as well. Figure adapted from [188]	185
Figure 86 Space velocity vs Mass of catalysts for Nickel catalysts (supplied as pellets).....	186
Figure 87 Space velocity vs Mass of catalysts for PGM catalysts (supplied as spheres).....	186
Figure 88 Condenser 1 before and after.....	187
Figure 89 Comparison of the yields of products from measurements with Ni/Al ₂ O ₃ catalysts and without steam.....	190
Figure 90 Comparison of the yields of products from measurements with Ni/Al ₂ O ₃ catalysts and with steam added	191
Figure 91 Comparison of the yields of products from measurements with Pt/Al ₂ O ₃ & Rh/Al ₂ O ₃ catalysts at low temperature and without steam	192
Figure 92 Comparison of Bio-oil samples.....	193
Figure 93 GC/MS analysis of BSG Intermediate pyrolysis oil after catalytic reforming at 500°C Nickel catalysts and no steam (Chemical abundant vs. Retention time)	196
Figure 94 GC/MS analysis of BSG Intermediate pyrolysis oil after catalytic reforming at 750°C Nickel catalysts and no steam (Chemical abundant vs. Retention time)	198
Figure 95 GC/MS analysis of BSG Intermediate pyrolysis oil after catalytic reforming at 850°C Nickel catalysts and no steam (Chemical abundant vs. Retention time)	200
Figure 96 GC/MS analysis of BSG Intermediate pyrolysis oil after catalytic reforming at 500°C Nickel catalysts with steam (Chemical abundant vs. Retention time).....	202
Figure 97 GC/MS analysis of BSG Intermediate pyrolysis oil after catalytic reforming at 750°C (Chemical abundant vs. Retention time).....	203
Figure 98 GC/MS analysis of BSG Intermediate pyrolysis oil after catalytic reforming at 850°C with steam (Chemical abundant vs. Retention time)	205
Figure 99 Effects of Nickel catalysts without steam	206
Figure 100 Effects of Nickel catalyst with the addition of steam.....	207
Figure 101 GC/MS analysis of BSG Intermediate pyrolysis oil after catalytic reforming 500°C with Platinum and no steam (Chemical abundant vs. Retention time)	208
Figure 102 GC/MS analysis of BSG Intermediate pyrolysis oil after catalytic reforming 850°C with Platinum and no steam (Chemical abundant vs. Retention time)	210
Figure 103 GC/MS analysis of BSG Intermediate pyrolysis oil after catalytic reforming 500°C with Rhodium and no steam (Chemical abundant vs. Retention time).....	211
Figure 104 GC/MS analysis of BSG Intermediate pyrolysis oil after catalytic reforming 850°C with Rhodium and no steam (Chemical abundant vs. Retention time).....	213
Figure 105 GC/MS analysis of BSG Intermediate pyrolysis oil after catalytic reforming 500°C with Platinum and with steam (Chemical abundant vs. Retention time).....	214
Figure 106 GC/MS analysis of BSG Intermediate pyrolysis oil after catalytic reforming 850°C with Platinum and with steam (Chemical abundant vs. Retention time).....	216
Figure 107 GC/MS analysis of BSG Intermediate pyrolysis oil after catalytic reforming 500°C with Rhodium and with steam (Chemical abundant vs. Retention time)	217
Figure 108 GC/MS analysis of BSG Intermediate pyrolysis oil after catalytic reforming 850°C with Rhodium and with steam (Chemical abundant vs. Retention time)	219

Figure 109 Effect of bio-oil chemical groups using Platinum and Rhodium Catalysts catalyst without steam.....	220
Figure 110 Effect of bio-oil chemical groups with Platinum and Rhodium catalysts with the addition of steam.....	221
Figure 111 Comparison of the yields of Permanent gases produced from measurements with Ni/Al ₂ O ₃ catalyst and without steam	222
Figure 112 Comparison of the yields of Permanent gases produced from measurements with Ni/Al ₂ O ₃ catalyst and with steam added.....	223
Figure 113 Comparison of the yields of permanent gases produced from measurements with Pt/Al ₂ O ₃ & Rh/Al ₂ O ₃ catalyst at low temperature and without steam.....	224
Figure 114 Comparison of the yields of Permanent gases from measurements with/Al ₂ O ₃ & Rh/Al ₂ O ₃ catalysts at low temperature and with steam.....	225
Figure 115 Comparison of permanent gas heating value of bench scale pyrolysis/reforming experiments with catalysts and without steam.....	226
Figure 116 Comparison of permanent gas heating value of bench scale pyrolysis/reforming experiments with catalysts and with steam.....	227

1 Introduction

1.1 Project Description

The present work is funded by an EPSRC Industrial CASE studentship in collaboration with Johnson Matthey plc.[1]

The main aim of this research is to study the pyrolysis/reforming/gasification of Brewers Spent Grain (BSG), and the effects of tar cracking using different catalysts to attain a tar free product-fuel gas that can be suitable to run an engine, gas turbine or a combined heat and power plant.

1.2 Background

Recently there has been growing concern over the need to reduce emissions of greenhouse gases, principally CO₂, and a drive to produce energy from alternative and renewable sources including biomass.

Biomass is a generic term that is used for any organic matter of recent origin including crops, wood and wood wastes, agricultural residues, animal wastes and both municipal and industrial wastes. Biomass has stored solar energy in chemical bonds via the photosynthesis process.

There are various types of biomass falling into four main categories: woody plants, herbaceous plants, grasses and wastes.[2] By-products from the food processing industry are an abundant source of biomass which can be made available for energy recovery.

1.3 Brewers Spent Grain (BSG)

Brewers spent grain (BSG), shown in Figure 1, is the widely available non-fermentable main by-product of the brewing process. It is the solid residue that remains from the barley after separation and filtration of the wort [3]. It has been estimated by the UK Environment Agency that UK breweries generate more than 250 million tons of wet BSG every year. BSG is either sent to landfill, or used as animal feed, primarily for cattle, but also for pigs, goats, fish and other livestock. It is used as animal feed due to its large content of fibre (60%) and protein (20%). [4]

Wet BSG contains a large amount of moisture, typically 67-81% (w/w). Due to its high moisture content as well as its fermentable sugar content, BSG is difficult to store and transport as it deteriorates rapidly due to microbial activity. [5] Therefore to be considered as a potential energy feedstock, methods must be adopted to reduce its moisture content significantly.



Figure 1 Brewers Spent Grain [6]

BSG has received little or no attention as a marketable commodity, but as it is now becoming increasingly expensive to dispose of as well as presenting an increasing environmental problem, options for its uses are starting to be considered. The chemical composition of BSG indicates that it can be of value as a raw material for energy production. [6]



Figure 2 Representation of a Barley Grain [3]

After wheat maize and rice, barley grain is one of the world's most important cereals. Its main uses are either as a cattle feed or as the primary feedstock in the production of beer and whisky via fermentation and distillation processes.

1.4 Brewing Process and Brewers Spent Grain Generation

Barley is the main raw material used in the beer brewing industry. During preparation of the barley feedstock it is initially screened, cleaned and graded according to a specific size requirement, any larger grains usually >2.5mm are malted separately. The barley grain is left dormant up to 4-6 weeks prior to a controlled malting germination process.

Malting occurs in three steps:

- Steeping
- Germination
- Drying or kilning

1.4.1 Steeping

During the steeping stage the cleaned grains are placed into tanks with water at a temperature between 5°C and 18°C for approximately 2 days. This stage of the process allows the barley grain to soak and hydrate as water begins to enter the embryo through the micropylar region as can be seen from Figure 2. The moisture content of the barley grain reaches approximately 42-48%. Through this method of hydration the grain is able to initiate a germination process.

1.4.2 Germination

After the steeping process the barley grain is sent via screw conveyors to a germination vessel, where it is continuously turned and contacted with humid air which maintains the bed temperature between 15°C and 21°C. The germination process activates enzymes that are present in the aleurone layer and starchy endosperm of the barley grain, such as amylases, proteases, β -glucanases and others.

1.4.3 Drying or Kilning

The enzymes that are activated initiate modification of the structure of the barley grain, mainly of the starchy endosperm; this process usually requires up to 6 or 7 days until the endosperm is fully modified.

The malted barley is then able to be dried reducing the moisture content down to 4-5% at a temperature between 40°C and 60°C. This is important as it avoids any microbial contamination, and allows generation of flavour components. Once the malted barley grain is dried it is usually stored for up to 3-4 weeks to reach homogeneity.

The malted barley is then ready for the brewery where the malted barley is milled and mixed with water. The temperature is slowly increased from 37°C to 78°C to promote enzymatic

hydrolysis. During this process any of the starch that is present is converted to fermentable and non-fermentable sugars and any proteins are converted or partially degraded to polypeptides and amino acids.

The enzymatic conversion stage produces a sweet liquid known as wort. The insoluble undegraded part of the malted grain is allowed to settle to form a bed in the mash and the sweet wort is able to filter through it. The filtered wort is used as the fermentation medium to produce beer. The residual fraction is known as BSG. [3, 7] Figure 3 illustrates the process of obtaining BSG from barley grain.

The main difference between Barley and BSG during these steps is the level of substitution of the phenolic hydroxyl groups along the chain of starch, changing the physicochemical and functional properties of the starches[8, 9]. BSG when wet as it has undergone chemical modification is part of the hydroxyl group.

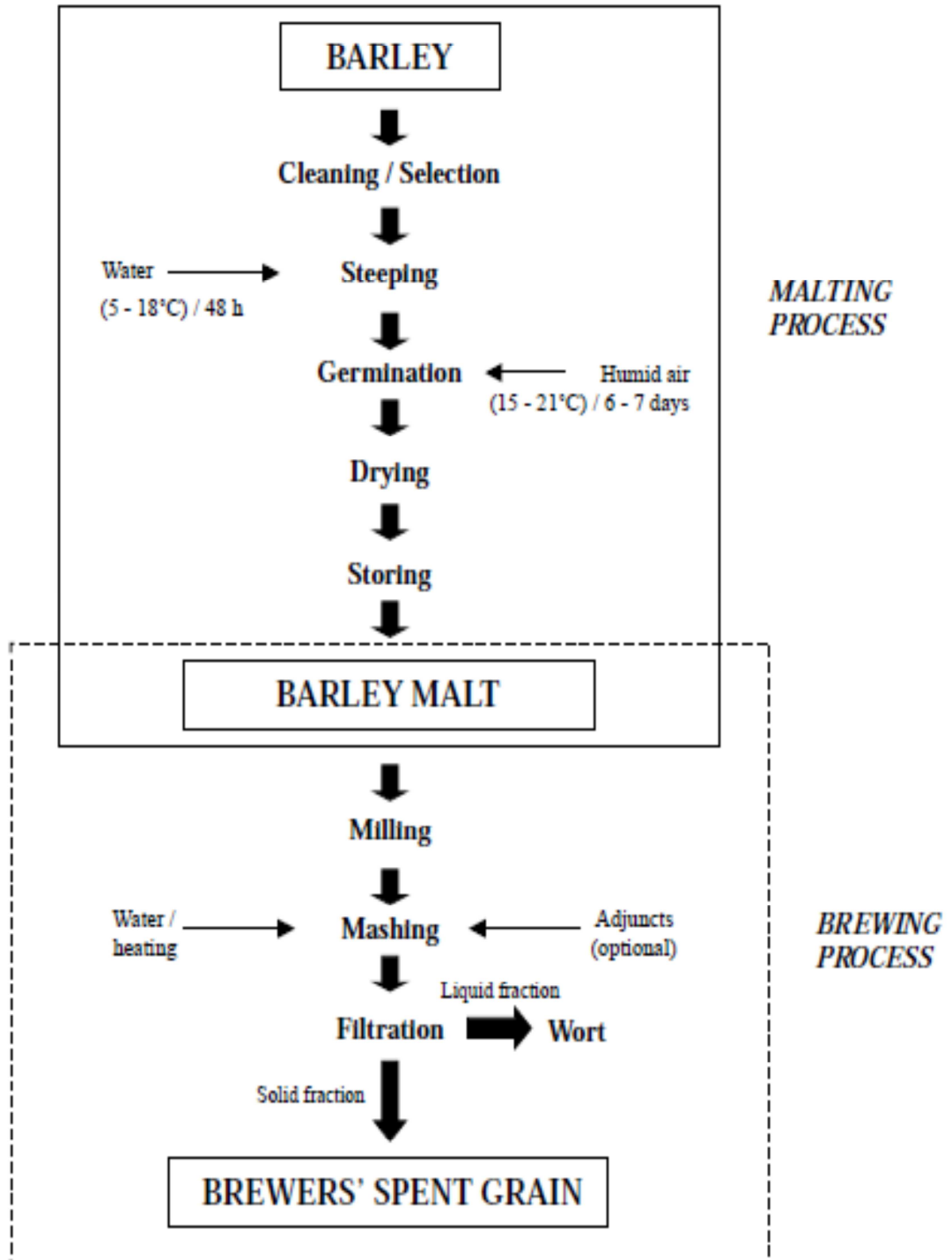


Figure 3 Representation of the process to obtain BSG from Barley Grain (extracted from [3])

1.5 BSG Preservation Methods

BSG when wet is a very unstable material due to microbial activity which causes problems if the moisture is not removed or reduced to below 10%. As described earlier, wet BSG contains approximately 70% water and in some cases it has been reported to be as high as 81%.[5] Therefore to prevent the degradation of BSG enabling it to be stored and transported easily as well as increasing its market value, preservation methods must be adopted.

There are three different methods that can be and evaluated for preserving BSG, namely freeze drying, oven drying and freezing.[10, 11] Freezing can be regarded as the most inappropriate method due to the large volumes of wet BSG that must be stored, and can alter the composition of BSG in particular the arabinose content which can deteriorate due to the microbial alteration during defrosting.

Preservation by oven drying and freeze drying reduces the volume of the product and do not alter the composition of the spent grain, however oven drying was deemed to be the preferred method to freeze-drying as freeze drying is not economically viable. Oven drying temperatures for very high moisture content of BSG are typically at 60°C [12].

BSG is most commonly dried using rotary super-heated steam (SHS) dryer (Figure 4). This approach was investigated as an attractive alternative to conventional air drying in that it provides a wide range of potential advantages, such as increased efficiency, reduction in the risk of fire and explosion, no odorous or particulate emission, the combination of drying with material sterilization and pasteurization, and faster drying rates.

Also, stickiness is a common problem in food handling and processing, as BSG is a sticky material due to its large moisture content, it has a tendency to foul drying equipment. Grain sticking to the surface of dryer equipment can also cause product degradation from the inclusion of blackened deposits and can increase the risk of fire and explosions, especially in air drying. [13]

1.6 Organisation of Thesis

This thesis comprises 10 chapters. In this first chapter an overview is provided of BSG with a description of how it is generated within the brewing process, and its current and potential uses are given along with important issues relating to preservation.

Chapter 2 gives an overview of biomass and its basic constituents with a brief discussion of pyrolysis principles with a particular focus on the intermediate pyrolysis process and associated reactors. A discussion of gasification is also provided, in particular outlining the process and the reactions that take place, leading to a comparison of biomass gasification systems and problems associated with tar. Catalytic upgrading options for the two techniques described presents a brief outline of different catalysts that have been used for bioenergy, in particular reforming catalysts used for tar reforming during gasification and bio oil upgrading during pyrolysis.

Chapter 3 reviews previous relevant studies focusing on pyrolysis, pyrolysis vapour upgrading, gasification and gasification with steam reforming mainly of residue or waste feedstock's. This then leads to the detailed specification of project aims and objectives. The primary focus is to investigate BSG using advanced thermochemical conversion such as gasification and intermediate pyrolysis, followed by subsequent upgrading of the vapours using steam reforming catalysts to improve product quality.

As BSG is a material that has not been widely investigated in open literature for thermo chemical conversion and is relatively new to the bioenergy field, **Chapter 4** presents a range of biomass analysis methods for a full characterisation study of BSG. This is followed by a discussion of results comparing BSG to other biomass feedstocks.

Chapter 5 provides a description of the experimental methodology for downdraft gasification of BSG using the GEK fixed bed downdraft gasification unit, describing its preparation and assembly and associated instrumentation. This is followed by a discussion of results for the gasification of BSG comparing to gasification of other biomass feedstocks.

Chapter 6 provides a description of the experimental methodology for intermediate pyrolysis of BSG, using both a new 'Pyroformer' reactor and a bench scale fixed bed pyrolysis reactor which attempts to simulate the Pyroformer but allows greater versatility for experimentation, and which also allows the investigation of catalytic upgrading of the vapours (not possible on the Pyroformer itself). The methodologies for full characterisation of the gas, liquid and solid product streams are described.

Results for the intermediate pyrolysis of BSG using the Pyroformer are presented and discussed in **Chapter 7**. Included in this chapter is the calculation of mass balance, and the characterisation results for all pyrolysis products formed (bio-oil, char and permanent gases).

In **chapters 8** and **9** the results obtained for the bench-scale intermediate pyrolysis experiments (non-catalytic and catalytic) are presented and discussed in terms of mass balances, properties of bio-oil, char and permanent gases.

Chapter 10 provides the overall discussion for the implications of this work followed by conclusions of the work conducted and provides recommendations for further work in the future.

2 Thermochemical Conversion of Biomass Techniques

2.1 Introduction

Thermochemical conversion technologies such as pyrolysis, gasification and combustion can convert biomass to energy. Pyrolysis is described as the thermal decomposition/degradation of biomass or a solid fuel in the absence of oxygen to produce solid char, liquid and gases. Biomass gasification is the partial oxidation of a combustible material, usually a solid fuel (biomass), which converts biomass into a gaseous component where the process is starved of oxygen. Pyrolysis and gasification are the most studied conversion processes for advanced thermal conversion. Combustion is the oldest and most common biomass conversion technique and has been practised for centuries. It consists of direct burning of biomass to convert the chemical energy into heat, mechanical power or electricity using stoves furnaces, boilers or steam turbines. Combustion processes are used mostly today for heat generation. The heat energy generated must be used immediately, as the heat cannot be stored or transported like the liquid and gaseous products from pyrolysis or gasification. This chapter will begin with a description and overall definition of biomass and its constituents, then move on to discuss both advanced thermochemical conversion techniques as well as give an overview of catalytic upgrading options to use with these advanced techniques.

2.2 Biomass

Biomass is a generic term that is used for any organic matter of recent origin including crops, wood and wood wastes, agricultural residues, animal wastes and both municipal and industrial wastes. Biomass has stored solar energy in chemical bonds via the photosynthesis process.

Biomass contains the elements carbon (45-55 wt.%), hydrogen (5-7 wt.%), oxygen (40-50 wt.%) and small amounts of sulphur (0-0.05%) and nitrogen (0-10 wt.%). Carbon and hydrogen are the main combustible components of the biomass. [14]

The main building blocks of biomass are water, lignin, cellulose, hemicelluloses, organic extractives and inorganic matter, as is illustrated in Figure 4 below. The following sub- sections describe each of the major biomass components in more detail.

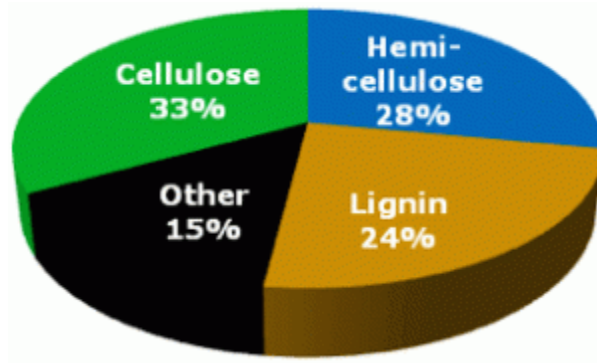


Figure 4 Biomass Composition [15]

2.2.1 Water

The amount of water present in biomass can vary depending on the type of biomass. Crops and woody biomass can contain high levels of water approximately 50%; this is dependent on weather effects and conditions when planted. Agricultural or industrial waste can contain much higher quantities of water up to 80%; this is dependent on storage as-well as how wet the residue material is when it exits the industrial process. For most thermo-chemical processes, biomass must be pre-treated to reduce the moisture content to 10-15%. For pyrolysis much of the water will end up in the bio-oil product, ultimately for both pyrolysis and gasification processing higher moisture contents will reduce the thermal efficiency of the process as energy will be used to evaporate the unwanted water. The moisture content can be determined using proximate analysis which will be discussed in chapter 4.

2.2.2 Cellulose

The cellulose component is the same in all types of biomass, except for the degree of polymerisation which can vary slightly in the most uniform sample. Cellulose is a glucan polymer consisting of linear chains of β (1, 4)-D-glucanpyranose units. The aggregation of these linear chains within the micro fibrils provides a crystalline structure, highly inert and inaccessible to chemical reagents. The cellulose content for most deciduous and coniferous trees varies between 40% and 45%, but can reach 55% for some. [16] An illustration of the structure is provided in Figure 5.



Figure 5 Structure of Cellulose [17]

2.2.3 Hemicellulose

Hemicellulose is a mixture of polysaccharides composed almost entirely from glucose, mannose, galactose, xylose, arabinose, 4-O-Methylglucuronic acid and galacturonic acid residues. It is generally much lower in molecular weight than cellulose. In contrast to cellulose, the hemicelluloses are amorphous. For deciduous trees the hemicelluloses (xylans or pentosans) represent 20-35% of the total mass. For coniferous trees, there are 20-40% hemicelluloses (mannans and xylans). [9] An illustration of the structure of hemicellulose is given in Figure 6.



Figure 6 Structure of Hemi cellulose [18]

2.2.4 Lignin

Lignin is a randomly linked, amorphous, high molecular weight phenol compound. It is more abundant and has a higher degree of polymerisation in softwoods than in hardwoods. Its composition in these two types of wood also present some differences. The lignin content is 24% to 30% for coniferous trees and 17 % to 24% for deciduous trees. [14] The structure of lignin is illustrated in Figure 7.



Figure 7 Structure of Lignin [19]

2.2.5 Organic extractives

Biomass contains a small fraction of organic extractives that are low in molecular weight. The fraction can vary quite significantly. Examples of biomass extractives are fats, waxes, alkaloids, proteins, phenolics, simple sugars, pectins, mucilages, gums, resins, terpenes, starches, glycosides, saponins[20]. These can be extracted from biomass by using various solvents. The extractive contents can be determined by chemical compositional analysis using neutral and acidic detergents and will be discussed in Chapter 4.

2.2.6 Inorganic materials

The inorganic elements present in biomass, namely chlorine (Cl), calcium (Ca), Iron (Fe), potassium (K), magnesium (Mg), sodium (Na), silicon (Si), sulphur (S) and phosphorous (P) are collectively known as ash. These ash materials vary in concentration depending on the biomass.[21] The ash content can be determined by proximate analysis which will be discussed in Chapter 4.

2.3 Pyrolysis

Pyrolysis is the thermal decomposition/degradation in the absence of oxygen. As well as a conversion method in its own right, it is also the first step in combustion and gasification, where it is then followed by total or partial oxidation of the primary products. [22] An example of all three is taken place in a flaming match, illustrated in Figure 8.



Figure 8 Pyrolysis, Gasification and Combustion [23]

Pyrolysis is considered to be an attractive technology as reactions take place under controlled conditions with a wide range of products suitable for different applications.[24, 25] The products of the pyrolysis process are char (a solid), bio-oil (a liquid formed from condensable pyrolysis vapours) and permanent gases. There are several processes in which the pyrolysis of biomass has been applied for heat and power applications, or combined with gasification as a pre-conditioning step for hydrogen production or sequential catalysis to produce methanol or synthetic fuels. [26]

Table 1 below provides the distribution of products from different modes of pyrolysis process. Low process temperatures and long solids residence time favor the production of charcoal. High temperature and long solids residence time increase the biomass conversion to gas. Moderate temperature, short solid and vapour residence times and high heating rates favor production of liquids. [26] The distribution of the products can be controlled to some extent by controlling these main reaction parameters.

Table 1: Modes of Pyrolysis

Mode	Conditions	Liquid	Char	Gas
Fast	Moderate temperature, around 500°C, short vapour and solids residence times ~ 1 sec	75%	12%	13%
Intermediate	Moderate temperature, around 450°C, moderate solids residence time ~ 1-30 mins	50%	20%	30%
Slow	Low temperature, around 400°C, very long solids residence time ~ hours/days	30%	35%	35%

2.3.1 Modes of Pyrolysis

2.3.1.1 Slow Pyrolysis

The classical ‘slow’ approach leads to charcoal (with a woody feedstock). Conventional slow pyrolysis is the irreversible thermal degradation of organic components in biomass, (usually lignocellulosic) in the absence of oxygen. Slow pyrolysis is also known as carbonisation and is used to maximise solid charcoal production. This method of pyrolysis has been practiced for centuries and requires relatively slow reaction at low temperatures to maximise solid char yield [27-29].

2.3.1.2 Fast Pyrolysis

Fast pyrolysis occurs with solids and vapour residence times of few seconds or less and very high heating rates. It is used primarily to maximise liquid products (up to 75 wt.%). After cooling and condensation of the pyrolysis vapours, a dark brown mobile liquid is formed (“bio-oil”) which has a heating value about half that of conventional fuel oil. While it is related to the traditional pyrolysis processes for making charcoal, fast pyrolysis is an advanced process, with carefully controlled parameters to give high yields of liquid.

The essential features of fast pyrolysis process for producing liquids are:

- very high heating and heat transfer rates at the reaction interface, which usually requires a finely ground biomass feed,
- a carefully controlled pyrolysis reaction temperature of around 500 °C and,
- short vapour residence times of typically less than 2 seconds and,
- rapid cooling of the pyrolysis vapours to give the bio-oil product.[22]

Most successful work with fast pyrolysis has been carried out with woody, low-ash, highly homogeneous feedstock’s, and the process is often not successful with more “difficult” feedstock’s which can produce highly reactive liquids rich in high-MW tars leading to storage and processing issues. [26, 30-32].

2.3.1.3 Intermediate Pyrolysis

Intermediate pyrolysis takes place at moderate temperatures of 350-450°C with moderate solids residence times of 1-30 minutes. It can process a diverse range of feedstocks such as waste wood, food wastes, sewage sludge, grass and algae, and is relatively insensitive to feedstock ash and to some extent moisture content. The distribution of the product phases and the composition of the liquid phase depend strongly on the feedstock and to a lesser extent on process conditions.

The ability of intermediate pyrolysis to deal with “difficult” high-ash feedstocks with relatively high moisture contents is a significant advantage over fast pyrolysis for feedstocks such as BSG. In particular, the liquids produced from non-woody biomass are very low in high molecular weight tars and can be suitable for direct application in engines.

For the reasons given in the previous section the present work will focus on the intermediate pyrolysis route for the experimental pyrolysis of BSG.

2.4 Intermediate Pyrolysis Principles

The temperature range of intermediate pyrolysis is 350-450°C, to which biomass is heated smoothly in the absence of any oxidising agent. Under these conditions, biomass decomposes producing a product distribution of typically 50% liquids, 25% char and 25% gas (although this is strongly dependent on the feedstock).

The essential features of intermediate pyrolysis process are: (1) smooth slow to intermediate heating and heat transfer rates, (2) long solids residence times of approximately 5-30 minutes at a temperature around 350-450°C, (3) short vapour residence times of a few seconds, (4) hot vapour filtration and rapid cooling of pyrolysis vapours to give bio-oil product.

In addition to the advantage of producing liquids with lower high-MW tar content, the process delivers a brittle dry char suitable for co-combustion in thermal plants or for use as a soil conditioner and carbon sequestration medium. Another advantage is that the product streams are easily separated without contamination.

Even though intermediate pyrolysis can produce a liquid with lower-MW components than other pyrolysis processes, it would still be attractive to further reduce the average-MW and hence viscosity, and to increase the proportion of permanent calorific gases (notably H₂), to improve suitability for prime movers such as IC engines, and also for further upgrading to high-value products.

Previous work in this area has mainly aimed to upgrade the bio-oil from fast pyrolysis processes by reducing the oxygen content so as to improve properties such as viscosity, thermal stability and

corrosiveness. Other studies have investigated steam reforming of bio-oil to produce hydrogen by the use of catalytic hydro-treatment and catalytic cracking [33-35].

Intermediate pyrolysis can be carried out in a range of reactor types, most commonly rotary kiln and screw auger reactors. Examples of these will be described in the next section.

2.4.1 'Pyroformer' Intermediate pyrolysis reactor

The Combined Pyrolysis Reformer or 'Pyroformer' is the new state of the intermediate pyrolysis reactor, developed at the European Bioenergy Research Institute (EBRI) at Aston University in the UK. The pyroformer relies on a screw auger system for moving the solids through the reactor. The design is illustrated in Figure 9.



Figure 9 Pyroformer Twin screw mechanism (Engineering Diagram)

- (A) Biomass feed inlet; (B) Inner feed screw, (C) Gas/Vapour product outlet, (D) Outer recycle screw, (E) Char product outlet

There are two screw augers, mounted co-axially to form a forward inner and an outer passage. See Figure 10. Apertures at either end of the arrangement allow material to pass between the inner and outer augers. Biomass is fed into the inner auger (green arrow) via a screw-fed feed hopper. The inner auger pushes the biomass forward through the reactor. A portion of the char formed (black arrow) during the passage of the biomass through the inner auger falls into the outer auger and is moved backwards to join the fresh feed at the inlet. Hence there is a recycle of char within the unit. The char has two important effects: it promotes catalytic cracking of the vapours so that the condensable fraction has reduced MW and there are a greater proportion of permanent gases; and it also acts as a heat transfer medium. [36]



Figure 10 Pyroformer schematic

2.4.2. Haloclean Intermediate pyrolysis reactor

The 'Haloclean' reactor was developed and patented by Sea Marconi Technologies. It is a single screw auger design see Figure 11. The biomass is transported along the screw in a nitrogen-purged oxygen free zone maintained at 450-500°C. Heat to the reactor is provided via an external jacket and by means of steel spheres that are continuously recirculated and reheated.[37]



Figure 11 Scheme of Haloclean Rotary Kiln [37]

The Haloclean reactor can process biomass in different forms including chips, blocks, pellets or dusts and materials processed to date include rapeseed residues, olive and sunflower seed residues, residues of coconuts and other nuts, beech wood, residues from beer production, wheat straw, rice husks and pomace. The balance of plant consists of a high temperature dust filtration unit, a water cooled condensation unit, and an electrostatic precipitator for aerosol removal.[37]

2.5 Feedstock variables effecting Intermediate pyrolysis

Numerous studies have been conducted on the pyrolysis of biomass. Many of the recent studies show that biomass pyrolysis can be divided into four individual stages: moisture evolution, hemicellulose decomposition, cellulose decomposition and lignin decomposition[38].

However different feedstocks have varying compositions of hemicellulose, cellulose, lignin, ash and water content that can have a direct impact on the intermediate pyrolysis products and yields.

Moisture bound in the biomass would lead to a high content of water in the final product bio-oil. The moisture is bound originally in the feedstock and formed during dehydration reactions during pyrolysis. High moisture content in the bio-oil lowers the heating value and flame temperature, but on the other hand, water reduces the viscosity and enhances the fluidity which is good for the atomization and combustion of bio-oil in an engine.[39] Oasmaa et al reported that bio-oils may phase separate if the water content is greater than 30 wt. %. [40]

Feedstock with very low moisture content is likely to increase the organic fraction in the pyrolysis liquid yield in turn increasing the viscosity which is undesirable if the bio-oil is to be considered as a fuel for engines. It is recommended that biomass should be dried to moisture content of 10wt.% in order to control the amount of water collected in the final product and to reduce the risk of phase separation [31].

The ash content is one of the most influential parameter in the pyrolysis process which affects the yield and chemical composition of the pyrolysis products. It has been reported that agricultural residues and grassy biomass have higher ash contents than lignocellulosic woody biomass. High ash containing feedstocks are not desirable for biomass pyrolysis because ash catalyses reactions which compete with biomass pyrolysis, leading to increased formation of water and gas at the expense of liquid organics [31, 41-46]. The minerals present in ash mainly alkali components are responsible for secondary catalytic cracking [46].

It is also reported that biomass with ash content greater than 2.5% causes phase separation of the bio-oil and biomass with an ash content less than 2.5% gives a more homogeneous bio-oil liquid.[31] However a feedstock may contain a high ash composition but then may contain a large amount of inactive constituents that do not lead to catalytic cracking or bio-oil phase separation. Therefore the ash compositional analysis must be carried out to support this.

The pyrolysis temperature, heating rate and residence time has a profound effect on the pyrolysis product yields and compositions. In a study conducted by Horne and Williams [47] they reported that high heating rates at temperatures less than 650°C with rapid quenching favours the formation of liquid products and minimizes char and gas formation. High heating rates with temperatures greater

than 650°C tend to favour the formation of gaseous products at the expense of liquids and slow heating rates coupled with low maximum temperature maximises the yield of char.[48]

The essential features of intermediate pyrolysis process are: (1) smooth slow to intermediate heating and heat transfer rates, (2) long solids residence times of approximately 5-30 minutes at a temperature around 350-450°C, (3) short vapour residence times of a few seconds, (4) hot vapour filtration and rapid cooling of pyrolysis vapours to give bio-oil product.

Temperature has a big effect on the pyrolysis process and product yields. Yang et al [38] investigated the thermal analysis of the three main components of biomass (hemicellulose, cellulose and lignin). Figure 12 shows the mass loss (wt.%) as a function as temperature, the pyrolysis of hemicellulose and cellulose occurred quickly with the weight loss of hemicellulose at 220-315°C and that of cellulose 315-400°C. Lignin was more difficult to decompose. Its decomposition happened slowly under the whole temperature range from ambient to 900°C.



Figure 12 Pyrolysis curves of hemicellulose, cellulose and lignin TGA[38]

The pyrolysis of biomass usually occurs at low to moderate temperatures between 300 to 500°C as reported by Bridgwater, 2004 [22]. A further increase in the temperature will lead to secondary cracking of the pyrolysis vapours leading to a decrease of liquid organics and char yields and increase the gas yields. Moreover, the increase in temperature from 400°C to 550°C results in higher polycyclic aromatic hydrocarbon (PAH) formation.

2.6 Intermediate Pyrolysis Products

2.6.1 Bio-oil

The bio-oil yield from intermediate pyrolysis is typically between 40-60 wt.%. The bio-oil liquids are usually lower in molecular weight than fast pyrolysis oils and contain a mixture of complex oxygenated compounds. The composition of bio-oils depends on the nature of the feedstock and process conditions. Roggero et al, 2011 [37] described intermediate pyrolysis oils as being generally dark liquids, giving off a particularly strong smell of carbonised organic material. It was also stated that the physical and chemical properties of intermediate pyrolysis oil fall into the typical ranges for typical pyrolysis oils. The oils are usually phase separated with an aqueous at the bottom and oily organic phase at the top, this is due to pyrolysis vapours being cracked by char. The pyrolysis vapours can be further processed to electricity, heat and transportation fuels.

2.6.2 Char

The bio-char yield from intermediate pyrolysis is approximately 15-25 wt.%. The bio-char has a dry brittle texture and is suitable for further applications either as solid fuel, or as a soil amendment or a fertiliser. Hornung et al 2011 [25] described pyrolysis char as having a high water holding capacity, therefore if mixed with sand or soil (known as Black Earth) can preserve water longer than natural soil [25].

2.6.3 Permanent Gases

The permanent gas yield from intermediate pyrolysis is approximately 20-30 wt.%. It comprises mainly a mixture of hydrogen (H_2), nitrogen (N_2), methane (CH_4), carbon monoxide (CO) and carbon dioxide (CO_2). Other hydrocarbons may be present in the gases such as ethene (C_2H_4), ethane (C_2H_6), propane (C_3H_8), propylene (C_3H_6), butane (C_4H_{10}) and butenes (C_4H_8).

2.7 Gasification

Biomass gasification is a thermo chemical process which converts biomass into a gaseous component. It is defined as the partial oxidation of a combustible material usually a solid fuel (biomass), by either pure oxygen or air. Partial oxidation takes place when there is not enough oxygen present for full oxidation to occur, i.e. when less than the stoichiometric amount of oxygen needed for complete combustion is present

This produces a combustible gas known as product syngas. This gas can be used as a low to medium calorific value fuel in gas turbines, engines and fuel cells or as a synthesis gas for the production of methanol, hydrocarbons and hydrogen.[49] Various contaminants such as small char particles, ash and tars (condensable oxygenated hydrocarbons) are present with the gases.

The product gas is composed of:

- hydrogen (H_2)
- carbon monoxide (CO)
- small amounts of methane (CH_4) and higher hydrocarbons
- carbon dioxide (CO_2)
- water (H_2O)
- nitrogen (N_2) (if air is used as the oxidising agent)

If air is used as the gasification medium, the combustible components in the fuel gas are diluted with nitrogen which significantly lowers the gas HHV ($4-7 \text{ MJ/Nm}^3$). Oxygen blown or steam gasification produces a synthesis gas with a medium heating value ($10-18 \text{ MJ/Nm}^3$).

As a result of this, partially oxidised products are formed. Gasification of biomass into product syngas is of growing interest as it offers many more substantial advantages to the environment, as gases can be produced and converted to clean alternative fuels that contribute significantly to the reduction of CO_2 emissions [50].

2.7.1 Biomass gasification process

Biomass gasification can be illustrated as a series of steps: drying, pyrolysis (de-volatilisation), combustion (oxidation) and reduction. These can occur separately or simultaneously depending on the type of gasifier. They will be described here as occurring separately. As would be the case in a downdraft gasifier see section 2.7.3.2.

The first step involves drying the biomass feedstock and this occurs at temperatures usually between $70-105^\circ\text{C}$. The moisture that is released through evaporation passes through the gasifier and contributes towards reduction reactions (Equations 7&9). The biomass feedstock then moves through

the gasifier and is heated to 300-500°C (pyrolysis temperatures) at this point, in the absence of an oxidising agent, it pyrolyses.

The volatile gases released move through the gasifier into the combustion zone where they react with an oxidizing agent. Figure 13 illustrates gasification steps.



Figure 13 Diagram of (downdraft) gasification; notice pyrolysis occurring above and prior to gasification before the biomass is exposed to oxygen [51]

The products of the combustion zone pass to the reduction zone, where they are reduced to combustible gases primarily by heterogeneous reactions with the char from the pyrolysis step. In fact we see the combination of several gas-solid and gas-gas reactions in which solid carbon is oxidised to carbon monoxide and carbon dioxide, and hydrogen is generated through the steam reforming reaction. The gas-solid reactions are the slowest and limit the overall rate of the gasification process.

Not all the products from the pyrolysis step are completely converted due to the physical or limitations of the reactions involved, and these give rise to contaminant tars (condensable organic vapours in the final product gas).

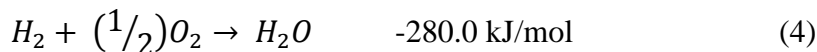
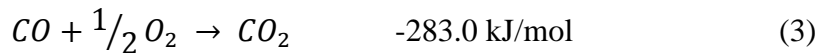
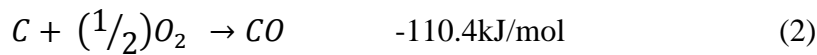
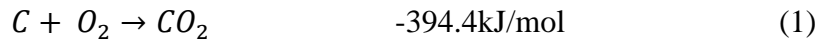
The final gas composition is influenced by many factors such as:

- Feed composition
- Water content
- Reaction temperature [52-55]

2.7.2 Gasification reaction mechanism

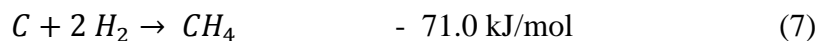
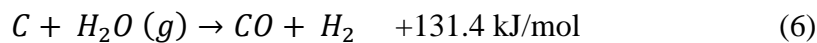
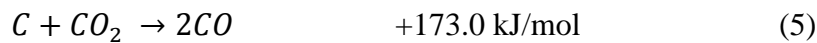
It is important to note that gasification is a series of reactions, in fluidised bed applications they can occur simultaneously. The reactions that take place are below:

2.7.2.1 Oxidation reactions

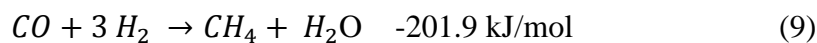
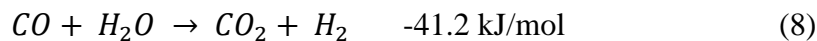


These reactions are highly exothermic and occur very fast. They also provide the energy that is required to sustain the endothermic heterogeneous reactions.

2.7.2.2 Heterogeneous reactions



2.7.2.3 Homogeneous reactions



The extent of these reactions will depend on operating conditions, and on the design of the gasifier. Other important secondary reactions occur under different operating temperature and pressures forming tars. [56]

2.7.3 Comparison of Biomass gasification systems

There are many different types of gasification reactor. The most common and basic form of gasifier is the moving bed gasifier, alternatively known as the fixed bed reactor. Fixed bed gasifiers have been traditionally used for gasification at operating temperatures around 1000°C. There are two types depending on the direction of air flow:

- Updraft (counter-current gasifier)
- Downdraft (co-current gasifier)

More recently fluidised bed gasifiers have been developed. Two main types are:

- Dense (bubbling) fluidised bed gasifier (BFB)
- Circulating fluidised bed gasifier (CFB)



Figure 14 Comparison of gasification reactors [57]

2.7.3.1 Fixed Bed Updraft gasifier (counter- current)

Fuel is fed at the top of the updraft gasifier, flows down the reactor vessel through the drying, pyrolysis, gasification and combustion zones. The gasifying medium usually air is introduced from the bottom of the reactor and passes upwards through the moving bed. Ash is also removed from the bottom part of the gasifier. As the solid fuel is pyrolysed moving downwards, the pyrolysis vapours generated are carried upwards by the hot up-flowing product gas. The tars present in the vapour either condense on cool descending fuel or are carried out of the reactor with the product gas contributing to its high tar content. The tars and solid char end up at the bottom of the gasifier reaction zone, where they are partially oxidised by incoming air and further cracked. The product gas contains a significant proportion of tars and hydrocarbons. The product gas does not pass through a hot char bed where much of the tars are cracked; therefore the product gas exit temperature is usually 200-400°C.

Therefore, the main disadvantage of updraft moving bed gasifiers is that the product gas has a high tar yield of up to 10 to 20 wt.%. This Figure 15 illustrates the design of a updraft fixed bed gasifier [58, 59]

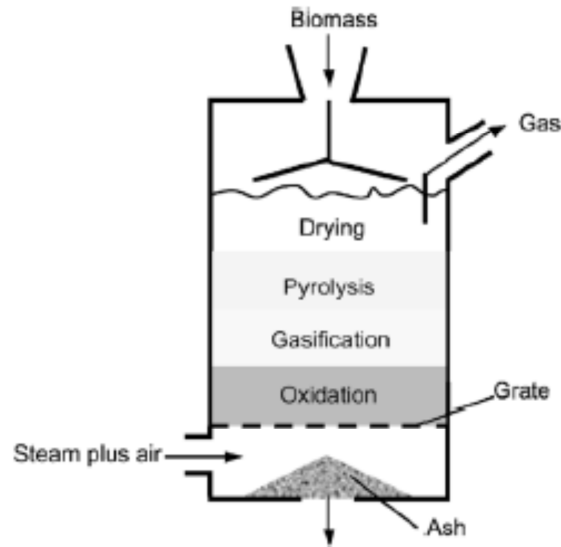


Figure 15 Updraft Gasifier Design [58]

2.7.3.2 Fixed Bed Downdraft gasifier (co current)

In this design the fuel and the gasifying medium (usually air) flows co-currently. Fuel is fed from top and the introduction of air can be introduced near the middle of the gasifier forming the combustion zone where most volatiles are oxidised. See section 2.6.1 for a general description of a downdraft gasifier. Downdraft gasifiers suffer from less tar in the product gas in comparison to product gas from updraft gasifiers. The hot product gas passes through a hot char bed which cracks the tars (reported up to 99.9%) and acts as a filter. The low tar levels obtained in the downdraft gasifier can enable the gas produced to be used in a combustion engine after filtration and cooling; however the actual level of tar is still dependent on the quality of biomass. The main advantage of downdraft gasifiers is that they are simple, reliable and proven for certain fuels, require minimal or no tar clean up however, there major drawback is they suffer from flow problems if the fuel is fluffy or has a low density. Fuels containing high ash are problematic resulting in slagging. Pellets or briquetted fuels are recommended before use. [59] Figure 16 illustrates the design of a downdraft gasifier.

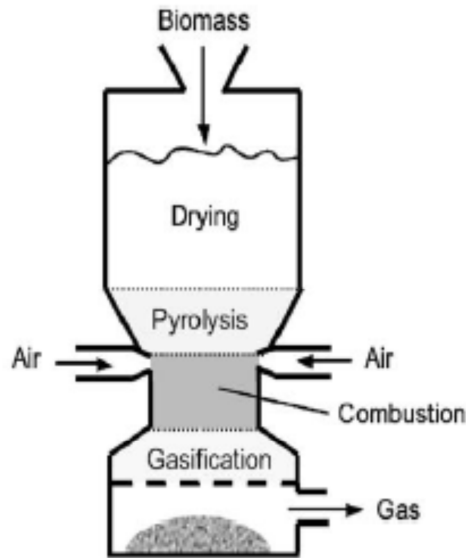


Figure 16 Downdraft Gasifier design [58]

2.7.3.3 Fluidised bed gasifier (*Bubbling and Circulating*)

Fluidised bed technologies are very promising in biomass gasification. They have previously been used extensively for coal gasification. The advantage fluidised bed gasifiers have over fixed bed gasifiers is the uniform temperature distribution achieved in the gasification zone. This is achieved as fluidised beds comprise of an inert fine bed material (usually heated particles) that are not consumed in the oxidation reaction. Biomass is fed into or on top of the bed material and due to high heat transfer between the fuel and heated bed material the fuel is heated very quickly. Air, oxygen, steam or a combination of steam and oxygen can be used as the gasification medium in fluidised bed gasifiers.

The gasification medium is injected usually into the bottom of the gasifier through a distribution plate into the bed material.

Secondary injection points can also be introduced and these are usually located at the freeboard area to assist in cracking reactions. The four conventional steps of gasification as described earlier for fixed bed gasification (drying, pyrolysis, oxidation and reduction), are not as clearly distinguishable in a fluidised bed. Figure 17 illustrates the design of both bubbling and circulating fluidised bed gasifiers.



Figure 17 Bubbling Fluidised Bed (left) & Circulating Fluidised Bed Gasifiers (right) [58]

As mentioned earlier, there are two main types of fluidised bed gasifier they are: low-velocity bubbling fluidised bed and a high-velocity circulating fluidised beds.[60]

Bubbling fluidised bed (BFB) gasifiers consist of a vessel, a distribution plate and usually a freeboard. In a BFB when particles are fluidised with a gas flow rate which is below the terminal velocity of the particles it is considered as Bubbling or Dense. The terminal velocity is defined as the velocity that is large enough to lift single particles and carry it out of the fluidised bed. The freeboard at the top of the reactor is usually wider in diameter than the bottom of the reactor. The role of the freeboard is to ultimately prevent any entrainment of solids. This process allows the biomass and sand to mix allowing a small carryover of char. [61]

In circulating fluidised beds (CFB) the inert bed material is transported and circulated between the gasifier vessel and a cyclone separator. The cyclone removes the ash and recycles the char and bed material back to the gasifier vessel.

In a CFB the gas velocity is increased above the terminal velocity of the particles. The terminal velocity is defined as the velocity that is large enough to lift single particles and carry it out of the fluidised bed.[62] The CFB is a natural extension of the BFB concept, as it includes extra equipment such as cyclone and separators in order to capture and recycle solids back to the gasifier to extend the solids residence times.

The attractiveness of the fluidised bed offers scalability and good fuel flexibility in comparison to fixed bed gasifiers. They have very good temperature distributions, high specific capacity and fast

heat up rates. They have the ability to tolerate a variation of fuel quality and particle sizes and most importantly are suitable for large commercial or industrial scale. [49, 50, 58, 63, 64]

2.7.3.4 Entrained flow gasifier

An entrained flow gasification reactor is mainly used to gasify coal which is usually operated at high temperatures and pressures. Entrained flow reactors usually require the feedstock to be prepared as a fine granular powder and it is then entrained with a steam/oxygen mix when entering the gasifier in a co-current flow that allows rapid gasification to take place. Entrained flow gasification reactors have short residence times; involve extremely high temperatures, and high pressures as well as large capacities. Figure 18 illustrates the design of an entrained flow gasifier.



Figure 18 Entrained Flow Gasifier[58]

Commercial or large demonstration scale gasification plants, fluidised bed gasifiers are usually implemented rather than fixed bed gasifiers. Fluidised beds are preferred due to the scalability and flexibility in feed properties requirement.[65] Figure 19 illustrates the scale potential of different type of gasification systems available to date.

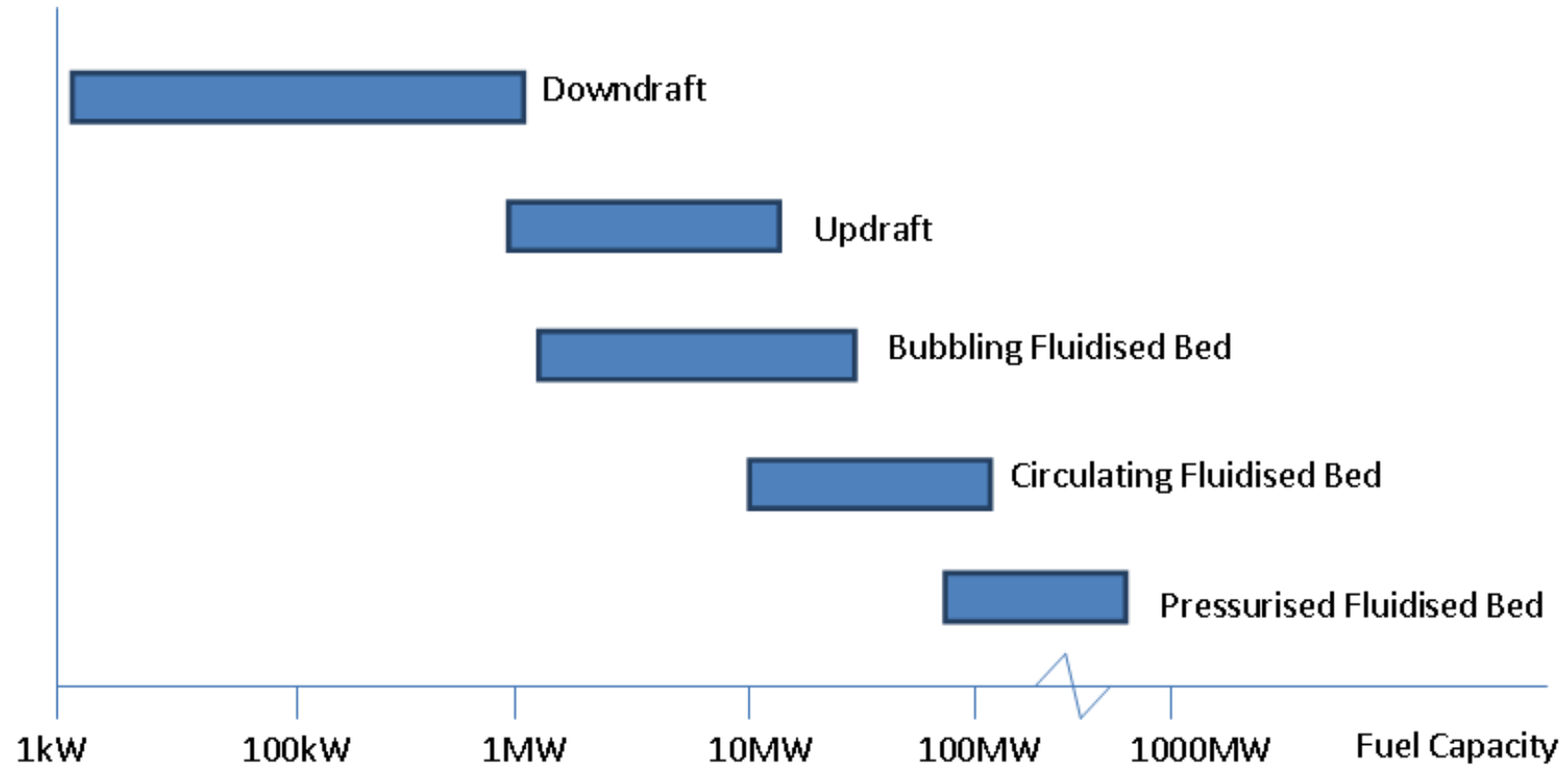


Figure 19 Scale potential of different type of gasifiers [66]

2.7.4. Tars

Different types of tars are present in the product gas generated from biomass gasification. Evans and Milne described the tar level from the three main categories of gasifier (updraft, downdraft and fluidised bed), with updraft regarded as producing the most tar $100\text{g}/\text{Nm}^3$, and fluidised beds at $10\text{g}/\text{Nm}^3$ and downdraft at $1\text{g}/\text{Nm}^3$. One of the most common problems caused by tar is condensation. If the temperature of the product gas is decreased below the tar dew point (below 300°C) the tars present will cool on cooler surfaces. The condensation of tar can lead to several problems in downstream equipment's. Polymerisation of tar is also problematic, as tar compounds polymerise at high temperature usually between $900\text{--}1250^\circ\text{C}$ in the gas phase. At lower temperatures between $100\text{--}200^\circ\text{C}$ tars can also polymerise in the liquid phase.

Therefore cleaning of the product gas is required and is often the major area of concern in biomass gasification. Trying to reduce the tar and particulates content is a major challenge, as possible blocking of process equipment downstream of the gasification process can occur as well as other issues such as:

- Fouling and plugging due to tar condensation and soot formation
- Difficulty in handling tar-water mixtures
- Contamination of waste streams [61]

In order to reduce tar content in the produced gases from the gasification process there are two approaches. One is to apply a downstream cleaning process, either a catalytic reforming system or alternatively the use of scrubbers and separators (known as secondary measures). The other is to optimise the biomass fuel properties or the gasification design and operating conditions so as to reduce tar formation (known as primary measures).

As has been indicated earlier, tar is the term given to volatile oxygenated hydrocarbon compounds that remain liquid at room temperatures (i.e. are condensable). Tar is a complex mixture of condensable hydrocarbons, including single and multiple ring aromatic compounds as well as other hydrocarbons containing oxygen[67]. The formation of biomass tar and examples of compounds formed are illustrated in Figure 20.

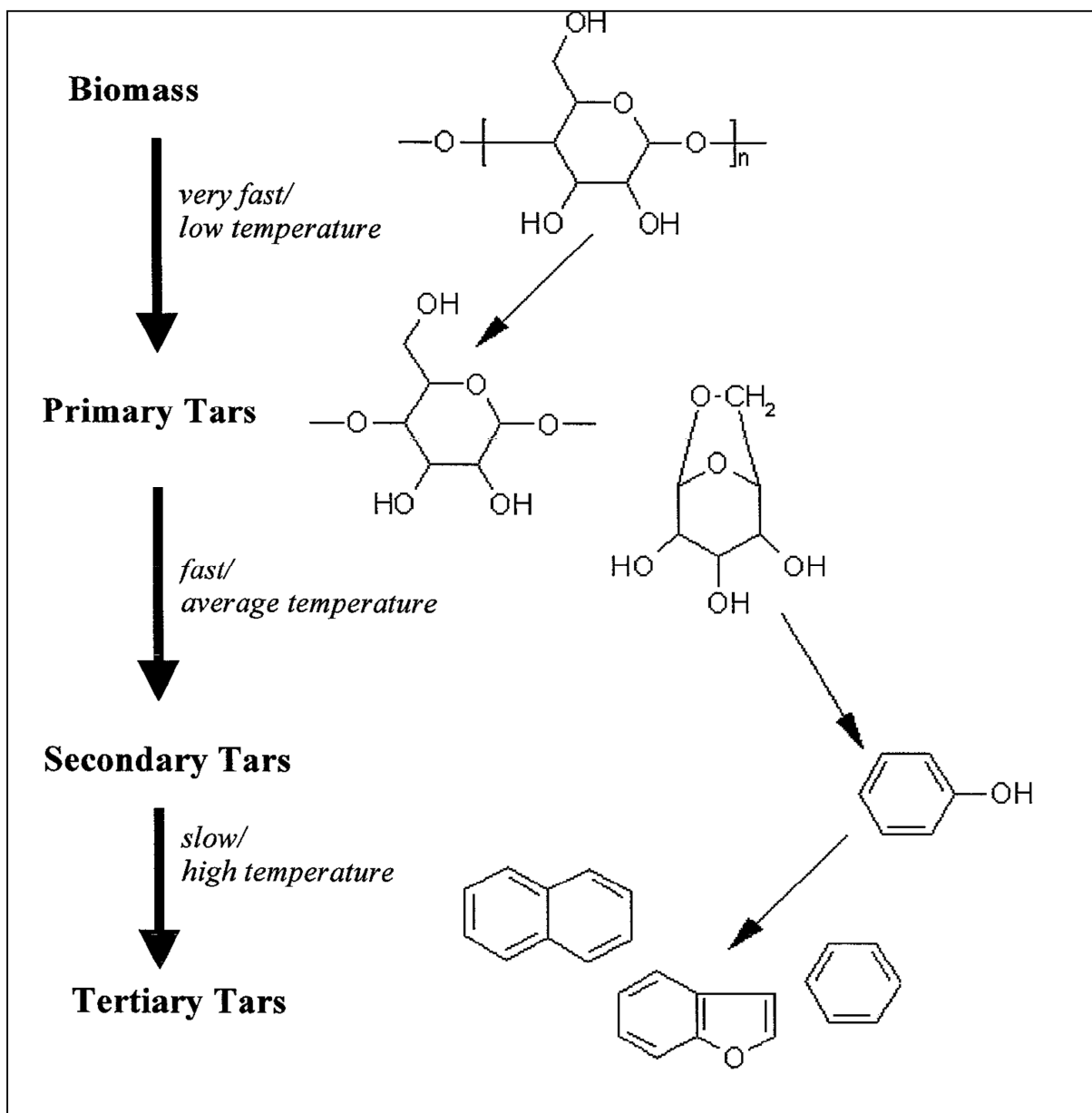


Figure 20 Formation of biomass tar and example of compounds formed[57]

The formation of biomass tars can be categorised according to the temperature within the gasifier and the series of complex reactions that are taking place. The amount of tar formed is dependent on the gasification process itself as well as the reaction conditions and the gasification temperature.

As the gasification temperature increases (usually above 800°C) it can result in the conversion of the oxygenated compounds into hydrocarbons, aromatics, oxygenates and olefins. Evan and Milne[68] proposed a new method to classify tars formed from different biomass gasification systems are as follows:

1. Primary Tars; these are characterised by cellulose, hemicelluloses and lignin derived products; these are the main components of biomass (temperatures around 400-600°C)

2. Secondary Tars: During the conversion of primary tars, phenolic's and olefins are formed (temperatures around 700-850°C)
3. Alkyl tertiary tar, these are characterised by methyl derivatives of aromatics (styrene and/or xylene) (temperature around 900-1200°C)
4. Condensed Tertiary tar: these are polyaromatic hydrocarbons (PAH) without substituents.[68]

The next section discusses the role of catalysis in both pyrolysis and gasification systems. It will describe some of the different catalytic upgrading options that have been practised widely in research and give an overview of the type of catalysts used to either upgrade the product gas or to remove contaminants and unwanted tars.

2.8 Catalytic Upgrading Options

The catalytic upgrading of pyrolysis products (pyrolysis vapours or bio-oil) and gasification product gas is attractive and is often considered. This section aims to discuss some of the catalytic upgrading options for both pyrolysis and gasification processes.

2.8.1 Pyrolysis upgrading

Direct catalytic upgrading options for pyrolysis systems have mainly been carried out to increase the quantity or the quality of the liquid product yield. One of the objectives in utilising catalysts is to attempt to reduce or remove the oxygen content from the liquid bio-oil to produce a hydrocarbon rich liquid fuel.

Hydrotreating is an upgrading option that improves bio-oil properties by rejecting the oxygen in the form of water. The products that are formed are nearly pure hydrocarbons equivalent to naphtha. The process conditions involve high hydrogen pressure with (up to 200 bar) and temperatures (about 400°C). The catalysts used in typical hydro-treating studies are usually sulphided CoMo and NiMo based catalysts. The bio-oil at high hydrogen pressure reacts with the catalysts to form water and carbon-carbon bonds. Up to 95% of the oxygen in the bio-oil can be removed, but the drawback of this process is the requirement of a high pressure and high hydrogen consumption which makes it economically unattractive[31]. Hydrotreating as a bio-oil upgrading option has been extensively researched from literature [69-73].

Zeolite catalysts have been tested in catalytic pyrolysis to upgrade the bio-oil at temperatures (400-600°C) by reducing the oxygenated compounds in the oils mainly consisting of phenols, cresols, benzenediols, guaiacol and their alkyl derivatives. William and Nugranad, 1999 [74], identified that the presence of zeolite catalysts reduce the yield of bio-oil, and reduces the oxygen content of the oil. At low catalyst temperatures the oxygen in the bio-oil is converted to water and at high catalyst temperatures to CO and CO₂. Zeolite catalysts are usually placed in a fixed bed reactor coupled to a

pyrolysis reactor where direct catalytic conversion of the pyrolysis vapours can occur. Unlike hydro treating the process conditions do not require high pressures or consumption of hydrogen operating at atmospheric pressure and at around 450°C.

Biomass-derived oils are generally best upgraded by HZSM-5 or ZSM-5, as these zeolite catalysts promote high yields of liquid products and propylene. Unfortunately, these feeds tend to coke easily, and high TANs and undesirable by-products such as water and CO₂ are additional challenges. The catalytic vapour cracking of bio-oil over acidic zeolite catalysts provides deoxygenation by simultaneous dehydration-decarboxylation producing mostly aromatics at 450°C and atmospheric pressure. The aromatic product produced would still be required to be sent for refining in a conventional refinery[53]. Significant research can be found in literature where authors have investigated different types of zeolite catalysts for bio-oil upgrading [52, 75-85]

2.8.2 Gasification upgrading

The presence of tars and effective gas cleaning of gasification product gases is still the main barrier to gas utilisation generated from biomass to produce electricity. Catalysts are preferred as the cost associated with secondary or auxiliary equipment downstream to produce clean gas is the major challenge. Build-up of tars or non-condensable hydrocarbons can cause blockages and corrosion to equipment as well as reduce the efficiency of a process.

The use of catalysts in biomass gasification systems has been attempted by many researchers and reported in literature since the mid-1980s[86]. The advances in this area have been driven by the need to produce a tar free product gas from the gasification of biomass. This is because it has been reported that the removal of tars and the reduction of the methane content increases the economic viability of the gasification process. [87]

Sutton et al, 2001 [87] conducted a review where it was reported catalysts criteria as follows:

1. Catalysts must be effective in the removal of tars
2. Catalysts must be capable of reforming Methane (CH_4) if the desired product is syngas
3. The catalysts should provide a suitable syngas ratio for the intended process
4. The catalysts should be resistant to deactivation as a result of carbon fouling and sintering
5. The catalysts should be easily regenerated
6. The catalysts should be strong
7. The catalysts should be inexpensive.

The catalytic decomposition of unwanted hydrocarbons, referred to as by Sutton et al [87] as hot gas cleaning, is achieved by passing raw gasifier product gas over a solid catalyst in a fluidised bed or fixed bed reactor under atmospheric temperature and pressure. As the raw gases pass over a solid catalyst, hydrocarbons may be reformed on a catalyst. The use of a catalyst to reform condensable organic compounds and methane can increase the overall efficiency of biomass conversion process by 10%.

There are a large number of different catalysts that have been used to eliminate tars in the product gas from the gasification process[88]. However, there are three main types of catalysts that have predominantly been reported in many literature studies for biomass gasification and they are Nickel, Dolomite and Olivine.

Dolomite catalysts contain alkaline earth metal oxides. It usually consists of a magnesium ore with chemical formula $\text{MgCO}_3 \cdot \text{CaCO}_3$ and usually contains approximately 30 wt.% CaO, 21 wt.% MgO and 45 wt.% CO_2 it also includes some trace minerals such as SiO_2 , Fe_2O_3 and Al_2O_3 . Dolomite has attracted a lot of interest in biomass gasification as it is a relatively cheap disposable catalyst that can

significantly reduce tar content from the raw product gases in a gasifier, achieving as close to 95-100% conversion of tar at 700-875°C under steam reforming conditions. Dolomite shows catalytic activity for tar elimination when the material is calcined. Calcination occurs because of the loss of bound carbon dioxide when the material is heated.

Pangmei et al, 2004 [89] reported dolomite being used mainly as a guard bed or a primary catalyst that is usually dry mixed with biomass, to protect the expensive and sensitive metal catalysts from deactivation caused by coke formation, tars, or other impurities such as H₂S. The advantage of this material is that it is inexpensive and abundant, and considered as the most popular cheap catalyst for tar elimination. The main problem with this material is its fragility. Dolomite catalysts are very soft and can quickly erode in fluidised bed systems with high turbulences.

Almost all authors have reported increased gas yields ranging from 10-20 vol. %, and an increase of 15% of (LHV) lower heating value of the gas. Naphthalene is often reported to be the most abundant condensable product after reforming tars over dolomite, highlighting the limitation in the use of dolomites as catalysis for the complete elimination of tars from product gases [90-94].

Olivine catalysts are represented by the formula (MgFe)SiO₄ and consist of silicate mineral in which magnesium and iron cations are set in the silicate tetrahedral. Olivine catalysts are useful for tar elimination and this is related to the magnesite (MgO) and iron oxide (Fe₂O₃) contents where the latter is much higher than in dolomite.

In terms of catalytic activity and on the basis of tar elimination olivine performs well and similarly to calcined rocks but less well than dolomite. It is cheap similar to dolomite catalysts but has a much higher attrition resistance. It often performs better than dolomite in fluidised bed environments due to its mechanical strength and is at times preferred to sand. Olivine is mainly deactivated by the formation of coke which covers and cloaks the active sites and reduces the surface area of the catalysts [95-97].

Much of work carried out today by researchers for steam and dry reforming of methane and hydrocarbons is performed using transition metal based catalysts. Nickel catalysts supported on alumina is most widely used in industry. Much has been published in research for biomass gasification using commercial reforming catalysts with nickel as the active element[98]. Other noble metals such as platinum (Pt), ruthenium (Ru) and rhodium (Rh) are other materials which can be potentially considered and applied in biomass gasification processes [99].

Supported noble metal based catalysts are the main catalysts used in the automotive industry for controlling emissions from exhaust gases from internal combustion engines. When used in biomass gasification they can demonstrate high tar conversion and no tendency to form coke deposits.

Nickel based catalysts have been widely used commercially in the petrochemical industry for naphtha reforming and methane reforming to produce syngas, and have been extensively demonstrated in reforming biomass gasification tars.

Nickel is represented as the active site of the catalysts and has been designed for steam reforming of hydrocarbons and also of methane. The support material gives the catalysts mechanical strength and protection against severe conditions such as attrition and heat. Alumina is the primary support that is used for most reforming catalysts. This steam reforming catalysts exhibits high activities for tar elimination and gas upgrading in biomass gasification. The catalytic activity of these catalysts depends on the nickel content, support type and the promoter type and content.

Nickel based catalysts have proven successful and useful in biomass gasification for gas cleaning and upgrading. They have high activity for tar destruction, for methane reforming, and water gas shift to adjust CO/H₂.

Literature [100, 101] has reported that using nickel catalysts designed for steam reforming at temperatures higher than 740°C there is a general increase in the hydrogen and carbon monoxide content by either reducing or eliminating the hydrocarbon and methane content. Only at lower temperatures the methanation reaction is favoured thermodynamically when methane is the desired component in the gases. Commercial Nickel catalysts can be divided into two groups

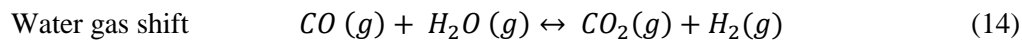
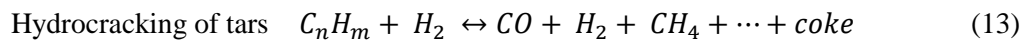
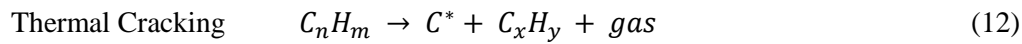
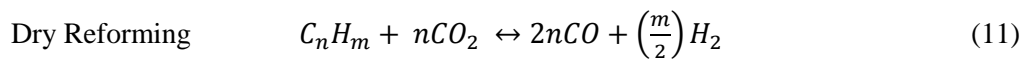
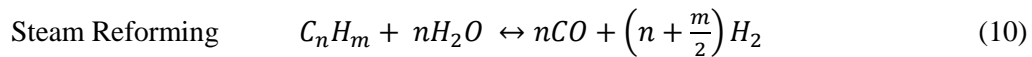
- Pre-reforming catalysts operating at lower temperatures (450-500°C)
- Reforming catalysts operating in the range (750-900°C)

Nickel catalysts are often employed downstream of a gasifier in a secondary reactor at temperatures between 730 – 900°C with space times of 0.1s for hot gas cleaning. Nickel catalysts are reported to deactivate in several ways and they can be as follows, (i) due to carbon fouling, tars and other impurities such as hydrogen sulfide (H₂S) reduces the life span of the catalyst, (ii) mechanical deactivation due to loss of catalytic material through attrition and loss of surface area, (iii) sintering causing loss of surface area and occurs as a result of severe conditions and high temperatures. Sulphur, chlorine and alkali metals can act as Ni poisons.

Reduction of tar content by conditioning the feed gas prior to nickel catalysts is a possible way to prevent poisoning and increasing the longevity of the catalyst lifetime. Thus many authors have reported using a guard bed of dolomite catalysts to pre-condition the feed gas prior to nickel catalyst which is placed in a secondary reactor that is usually a fixed bed.

The main advantage of Ni-based catalysts is their ability to attain complete tar elimination at temperature of around 900°C and to increase yields of H₂ and CO. It has been reported that Nickel based catalysts are 8-10 times more active than calcined dolomites under the same operating conditions. The main disadvantage of nickel-based catalysts are their rapid deactivation from sulphur and high tar contents in the feed and the need for preconditioning the feed gas before it enters the catalysts bed. In addition, these catalysts are relatively expensive [102-106].

Some of the important reactions that take place in a secondary catalytic reactor downstream of a gasifier have been reported by Abu El-Rub. Z et al, 2004 [107] they are as follows:



The reactions involved in tar elimination are very difficult to determine and often are not well known, however some reactions involved in tar removal have been illustrated above.

3 Previous Work on Thermochemical Conversions of Biomass & Catalytic Upgrading

3.1 Introduction

This chapter will analyse the current state of the art for advanced thermo chemical conversion studies of biomass, biomass residues and catalytic upgrading. As mentioned in chapter 1 there has not been much focus of thermo chemical processing of BSG, therefore similar feedstock's and different forms of waste feedstock in particular from industry have been considered for review. The scope of the review is to assess peer reviewed journals of previous research carried out on the pyrolysis, gasification and catalytic upgrading of waste feedstock's including BSG and similar compositional wastes.

The overall objective is to carry out an assessment of the research that has already been achieved within this area and to identify gaps or areas of further work and improvement. Other thermal conversion technologies or feedstock types are beyond the scope of this review. A summary and critical analysis of the findings from the review is presented in section 3.2.

3.1.1 Biomass Pyrolysis Studies

Yang et. al, 2013 [108] investigated the characteristics of intermediate pyrolysis derived oil from sewage sludge (water industry) and de-inking sludge (paper industry). The objective of this study was to obtain intermediate pyrolysis oils with a view to use in diesel engines. The feedstock's used was processed using the Pyroformer intermediate pyrolysis reactor at Aston University. Sewage sludge was received by Severn Trent Water from an anaerobic digestion process. De-inking sludge, the solid residue generated during the de-inking stage of recovered paper production containing mainly fibers and inert fillers, was provided by Kimberly-Clark.

Both feedstock's are industrial residual wastes with very high moisture contents, and so were dried to less than 15 wt.% moisture and then pelletized. From the ultimate analysis study it was noted that sewage sludge contained carbon 24 wt.%, hydrogen 3.5 wt.%, oxygen 35.7 wt.%, nitrogen 2.9 wt.% and sulphur 1.3 wt.% and ash 32.6 wt.%. De-inking sludge had carbon 21.7 wt.%, oxygen 29.8 wt.%, hydrogen 2.8 wt.%, nitrogen 2.1 wt.%, sulphur <0.1wt.% and 43.6 wt.%, so both have low carbon contents. From the proximate analysis it was noted that both feedstock's have high volatiles and ash contents with sewage sludge 63.7 wt.% and 32.6 wt.%, and de-inking sludge 55.1wt.% and 43.6 wt.% respectively. The ash contents for both feedstock's are reported to be very high, however the authors did not analyse the mineral content present in the ash.

The Pyroformer was fed at a rate of 15 kg/h with the inner and outer screws set to 4 rpm and 1.25 rpm, with solid residence time estimated to be between 7-10 minutes and vapour residence time of a few seconds, at a temperature of 450°C.

The reported product yields from sewage sludge were liquids 40 wt.%, permanent gas 12 wt.% and solids 48 wt.%. The liquid readily separated into two phases with an organic layer at the top (25 wt.%) and an aqueous phase at the bottom (75 wt.%). For de-inking sludge the corresponding yields for liquids, permanent gas and solids were 10 wt.%, 11 wt.% and 79 wt.% respectively. Again the liquid readily separated into organic and aqueous phases, however in this case the organic phase was 90 wt.%. Both organic phase oils (referred to henceforth just as “oils”) were analysed and compared to each other, to biodiesel and to regular diesel using various analytic techniques. GC/MS analysis reported that both oils were complex organic mixtures and consisted of carbon chains ranging from C₇ to C₁₇ for sewage sludge and C₅-C₁₅ for de-inking sludge. Aromatic hydrocarbons were the most abundant components in the pyrolysis oils accounting for 31% of oil derived from sewage sludge and 48% for de-inking sludge. Phenols were the other major compound found in the oils accounting for 22% and 15% for sewage sludge and de-inking sludge. It is reported that the aromatics have poorer combustibility compared with paraffin’s and naphthenes.

An interesting finding was that the intermediate pyrolysis process had significantly reduced the oxygen content of the oil from that of the original feed stocks, making them favorable as fuel oils. The oxygen contents reported for sewage sludge oil were 8.73 wt.% and for deinking sludge oil 11.27 wt.%, comparable to bio-diesel at 8.36 wt.%. Both oils were found to have high carbon and hydrogen contents and their higher heating values were comparable to that of biodiesel (sewage sludge oil 39.38 MJ/kg and de-inking sludge oil 36.54 MJ/kg, compared to biodiesel 39.85 MJ/kg. The authors concluded that both oils had satisfactory characteristics for use as diesel engine fuels; however some characteristics of the oils may cause issues overtime leading to poor engine performance such as poor combustion due to carbon deposition. The authors suggested that preliminary tests indicate that both oils are largely immiscible with water, but miscible with biodiesel, and blending the oils with biodiesel could address these issues and should be further investigated and tested in a diesel engine.

In a follow up study conducted by Hossain et al, 2012 [109] de-inking sludge intermediate pyrolysis oil was blended with biodiesel derived from waste cooking oil and was tested in an unmodified multi-cylinder indirect injection type CI diesel engine. Blends of 20 and 30% (v/v) of de-inking sludge were prepared with both biodiesel and fossil diesel and then characterized. All blends were prepared by mixing and agitated without the use of surfactants and were allowed to settle for a period of 24 hours. The blended oils were then filtered using a 1µm sock filter to remove any fine particulates prior to any engine tests. The blended oils (de-inking sludge: biodiesel) showed that density, acid number and carbon residues had reduced significantly in comparison to the pure oil, and a slight increase in

heating value was also observed. The flash point temperatures of biodiesel and de-inking sludge oil were almost the same.

Engine tests were carried out by initially starting and warming the engine up for 10 minutes with fossil diesel or biodiesel before switching over to the blend. After the tests the engine was reverted back to a fossil diesel supply to remove any blend remaining within the injectors. Various engine performance parameters were measured when operating on the blends, and compared with biodiesel and fossil diesel.

The author reported that running on 20 % (v/v) blended oil, smooth running and stable operation of the engine was observed, however when on the higher blend of 30% (v/v) some minor knocking was experienced. The engine knocking is attributed to cylinder pressure and the crank angle position at the time of combustion. The low cetane number of the 30% blend caused this behavior. All engine tests lasted approximately 3 hours with stable operation at 20% blend.

Samanya et al, 2011 [110] investigated the co pyrolysis of sewage sludge with wood, straw and rapeseed on the upper phase of the bio-oil. The pyrolysis process was carried out using a laboratory scale batch fixed bed reactor with 100g of fuel loaded inside the reactor for the production of bio-oils using a moderate heating rate. The reactor was a cylindrical shaped quartz tube measuring 40 cm in length and with an internal diameter of 6cm that was housed inside a furnace. The outlet of the reactor was connected to two cooling traps for the condensation of pyrolysis vapours into bio-oils.

The fuels were in different forms, both sewage sludge and wheat straw were as pellets, wood mixed with bark were chippings and the rapeseed was as seeds. Three biomass fractions were made up containing 60% sewage sludge with the remaining 40% made up with mixed wood, rapeseed and straw.

The reactor was purged with N₂ gas at a rate of 100 ml/min for the first 10 minutes to ensure the removal of oxygen. The reactor was then heated at a rate of 25°C/min to a pyrolysis temperature of 450°C and held for 15 minutes. The vapours were cooled using liquid nitrogen traps and permanent gases were expelled through the electrostatic precipitator and extractor.

It was reported that the co pyrolysis of sewage sludge with other biomass produced a variation in product yield. The bio-oils that were produced had phase separated into two layers, the upper and bottom phase. The upper layer contains the organic fraction. The co-pyrolysis with rapeseed produced the highest char yield of 53.3% and the wood fraction has the lowest char yield at 46.8%. The rapeseed and sewage sludge fraction produced the highest bio-oil yield of 33.2 %, with an equal amount of upper and bottom layers, with straw and sewage sludge yielding the least amount of bio-oil at 27.8 %.

The oils were characterised for their composition, it was reported that the 40% straw bio-oil fraction contained hydrocarbons, alkyl phenols and nitrogen compounds originating from sewage sludge. The compounds that were originating from the straw bio-oil are phenols and amino compounds. The 40% mixed wood bio-oil fraction contained a high percentage of components detected as a result of the decomposition of wood. They were found to be aromatic hydrocarbons, furans from cellulose, phenols and derivatives from methoxyphenols (from lignin). The compounds detected in rapeseed bio-oil are aromatic hydrocarbons, phenol, alkane hydrocarbons, long chain alkenes, alkane nitriles, fatty acid, and alcohol.

Sewage sludge mixed with rapeseed was reported to have the highest heating value at 34.8 MJ/kg compared to other fractions and also decreased the viscosity of sewage sludge upper phase. It was reported the 40% rapeseed increased the bio-oil yield compared to the pyrolysis of sewage sludge alone. The sulphur content was also found to be lower and the hydrogen content higher.

The co-pyrolysis of mixed wood and sewage sludge improved some of the properties found in the upper phase of wood bio-oil. The co-pyrolysis with 40% mixed wood, increased the higher heating value from an average of 17 to 31.3MJ/kg. It was also found to reduce the acidity of the bio-oil; however the viscosity was found to be the highest amongst the upper phases. The changes in bio-oil characteristics found with co-pyrolysis of 40% straw were not very significant.

Beciden et al, 2007[111] performed a study on the pyrolysis on large samples (thermally thick samples) of biomass residue's. The author proposed to investigate thermally thick particles for industrial fixed bed thermal conversion of biomass as industrial applications rarely use solid fuels in the form of particles. The biomass residues investigated for this study were brewers spent grains, fibre board and coffee beans. These biomass residues were selected due to their relevance in agricultural areas and where the intensive production of a plant may generate large amounts of wastes or by-products.

The biomass residues were investigated under pyrolysis conditions using an in-house fabricated macro-TGA. The study focuses on the temperature and heating rate dependence of the product yields and gas compositions during pyrolysis. Two procedures were investigated fast/high heating rate pyrolysis (sudden introduction in a hot reactor) and slow/low heating rate pyrolysis (application of a 10 K/min heating rate at the walls).

The reactor used is a stainless steel vertical tube with an inner diameter of 0.1m and height of 1m. It is heated with five independent heating elements, and a preheater is used to heat up the purge gas before it enters the reactor. A suspension system holds the cylindrical wire mesh basket which is then connected to a Sartorius CP 153 precision balance. The product gases were analysed by online micro-GC and FTIR analyser.

It was reported that an increase in pyrolysis temperature increases the yield of gases, resulting in a decrease of char and liquid yields which is in agreement to what is reported in literature. The gas yields for biomass residues BSG and fibreboard, increased from 30-35% for all to 52-57 wt.%, and 65 wt.% for coffee waste.

The main gaseous products were CO and CO₂, with CO yield increasing 2-3 folds between 600°C and 900 °C. The study reported that the CO₂ is a product of the pyrolysis of cellulose and hemicellulose by a path less favoured by increasing temperature. It was also reported that CH₄, C₂ hydrocarbons and H₂ are minor components of pyrolysis gases, with CH₄ yield for coffee waste and fibreboard ranging from 2.4wt.% at 600°C to around 6% at 900°C, and C₂ yields increasing with temperature from 1.6 wt.% at 600°C to 5.2 wt.% at 900°C for coffee waste. The researchers reported that at temperatures between 825°C to 900°C the C₂ yields are stable at 5.2 wt.% for coffee waste, decreasing moderately from 3.9 to 3.6 wt.% for fibreboard and from 6.1 to 5.9 wt.% for BSG. The hydrogen yield was reported to be a product of cracking and increases sharply with temperature from less than 0.5 wt.% at 600°C to approximately 1.1- 1.2 wt.% for BSG and fibreboard and 1.7 wt.% for coffee waste at 900°C. As temperature increased there was definite trend of decreasing char yield, with char yield being fairly similar for all the residues tested. Yield fell from approximately 23 wt.% at 600°C to approximately 17-19 wt.% at 900°C.

The researchers also evaluated the liquid yield that was obtainable for the biomass residues at 600°C and 900°C. It was reported that liquid yields were not the focus of their study, however the liquid yield generated for fibreboard decreases from 47 wt.% at 600°C to around 25 wt.% at 900 °C. It was reported that trends concerning all the different product yields are similar and the range of the results is in agreement with literature.

The authors reported the gross calorific values (GCV) of the pyrolysis gases of the biomass residues. The GCV of the pyrolysis gas increased with temperature between 600°C and 750°C to attain approximately 19 MJ/kg for BSG, 15.7 MJ/kg for coffee waste and 16.3 MJ/kg for fibreboard. For all fuels investigated the higher the temperature favoured gas yield at the expense of char and liquid. The high heating rate also promoted gas yield.

Roggero et al, 2011 [37] investigated a new type of “intermediate” pyrolysis technology patented under the name Haloclean at Sea Marconi Technologies in 2002. The Haloclean reactor is an auger screw design which has already been described in Section 2.4.2. It was claimed to be a new form of pyrolysis process that is rapid and very flexible in terms of processing any kind of biomass such as chips, pellets, and dusts up to 50mm wide, or even mixtures of the materials.

The aim of this investigation was to pyrolyse several different biomass residues to obtain product yields with the main interest focusing on bio-oils, and to carry out physio-chemical characterisation of

the oils. The biomass residue samples tested included rapeseed, olive and sunflower residues, residues of coconut and nuts, beech wood, residues from beer production, wheat straw, rice husks and pomace.

The yield and composition of the bio-oils, char and gas produced depended on the nature of the feedstock and process conditions such as the temperature and residence time. The researchers reported that most of the oils produced were suitable for either direct co-generation or for fuels after refining.

The researchers reported that any form of biomass can be used as a feedstock for pyrolysis; this can be seen in the Table 2 below illustrating the product yields obtained along with operating temperature and feed rate.

Table 2 Product yields and distribution of various feedstock's [37]

Biomass type	Feed, kg	Temperature, °C	Yield, %		
			Coke	Liquid	Gas
Wheat straw	PS \approx 15 t	450	50	30	20
Rape residues	PS 1292	450	38	45	17
		550	25	50	25
Olive stones	PS 169	450	30	47	23
Rapeseeds	PS 611	450	33	47	10
		500	15	52	33
Beech wood	PS 149	450	23	56	21
		500	21	57	22
Rice husk	PS 86	450	41	41	18
Coconut	LS 13	450	34	52	14
Rice bran	LS 3	500	20	38	42
Brewers grain	LS 2	450	23	51	26

Table 3 illustrates the compounds found in pyrolysis oils produced at 450°C by GCMS, as peak area percentages.

Table 3 GCMS analysis of bio-oil produced using the Haloclean [37]



It was reported that the oils obtained were fairly similar and share common features, having a dark appearance with a particularly strong smell of carbonized organic material. The oils were found to be acidic and in most cases highly viscous. GCMS analysis reported that each oil composition differed widely which can be seen in the Table 3 above. The variability in results for the bio-oils obtained is dependent on the nature of the feedstock to be treated.

Mullen et al [112] investigated the production of bio-oil and bio-char from corn cobs and corn stover by fast pyrolysis within a bubbling fluidised bed of quartz sand at 500°C and at a feed rate varied between 1 and 1.6kg/h. The reactor section was reported as 3 inches in diameter, with 2 cyclones for bio-char collection and separation followed by a series of condensing canisters maintained at 4°C. Bio-oil and bio-char produced from the fluidised bed reactor were characterised for energy and soil amendment properties.

The author reported corn stover to be the largest quantity of agricultural crop biomass produced in the United States at 23 Mt per year, and claimed its suitability as a biomass feedstock for bio-fuel production. One of the concerns for the harvesting of corn stover from fields is that it could have an impact and effect on the soil quality, nutrients and available water, which can increase water run-off and soil erosion. It was suggested that bio-char application to these soils can be a potential solution to these problems, and could enhance the soil quality as well as sequester large portions of carbon. The

use of the bio-char can release some of the nutrients originally found in the biomass and can be released back in the soil. The high absorbent nature of the bio-char can increase the soil's ability to retain water, nutrients and agricultural chemicals.

The bio-oil yield from corn crop residue feedstock was approximately 60%, with a heating value around 20 MJ/kg confirming that oil had a greater energy density of biomass feedstock reported 20-32 times making storage and transportation of bio-oil easier.

The bio-char was reported to be a potentially valuable soil amender because of the mineral nutrients it contains from the original feedstock. These important mineral nutrients such as K, P, Ca and Mg concentrated in the ash act as good absorbents and agricultural chemicals. It was also reported that bio-char had a heating value between 21-30 MJ/kg and would serve well a renewable solid fuel as it compares well to some natural coals.

Asadullah et al, 2007 [113] investigated the characterisation of Bangladesh based bagasse for pyrolysis to produce bio-oil. The objective of their work was to produce renewable liquid fuel (bio-oil) from locally produced bagasses by pyrolysis in a batch feeding fixed bed reactor. The author reported approximately 7.3tons of can-sugar is produced per year in Bangladesh, with about 21 million metric tonnes of bagasse being produced as a by-product per year. Part of the bagasse is used for steam power generation for the sugar industry with the rest used for energy in unorganised sectors.

Raw bagasse was obtained from the sugar industry and dried in sunlight to obtain moisture content less than 10 wt.% and then analysed for proximate and ultimate analyses. The result indicate that bagasse has carbon of 49 wt.%, hydrogen 6 wt.%, oxygen 39 wt.%, nitrogen 0.2 wt.%, chlorine 0.05 wt.% and sulphur 0.05 wt.%. Proximate analysis shows the fuel has high volatile matter ranging between 68-70 wt.%, fixed carbon 28.7-31wt.% with typical higher heating value (HHV) of 19.2 MJ/kg and a low ash content of 1.26 wt.%. The fuel was prepared to undergo pyrolysis as it was crushed using a crushing machine to particles of about 0.5-1.0mm in particle size. The author reported that the thickness of the of the particle has an important role in the surface area per unit weight, indicating that the lower particle size the higher the surface area which leads to the high heat transfer rate from the outer surface to the centre of the particles. Overall the fuel composition was found to be comparable to that of some woody biomass in terms of density and energy content giving clear indication that bagasse can be used for the production of bio-energy.

A laboratory fixed bed batch scale reactor was used for pyrolysis constructed of stainless steel with dimension of 50cm in height and 10cm inner diameter. Approximately 200g of bagasse was fed in batch inside the reactor with N₂ as the purge set at 200ml/min which was passed from the bottom of the reactor to the top. The experiments were performed at different temperatures ranging from 300 to 600°C. The temperature was increased at the rate of 50°C/min. The purge vapour and pyrolysis

vapours formed during the pyrolysis process are passed through the reactor and escape at the top of the reactor and through two condensers. The first condenser is cooled with tap water reducing the vapour temperature to 60°C and the second condenser is cooled with the circulation of ice water mixed with NaCl using a small pump reducing the temperature to -5°C. The liquid products were collected in conical flasks beneath each condenser, with permanent gases collected in gas bags.

The effect of temperature on the product distribution was investigated and was found that at low temperatures of 300°C where the decomposition of bagasse just starts, the quantity of liquids produced and collected in both collectors was very low as was the gas yield. Most of the carbon in the bagasse was found to have been converted to char at this temperature. It was reported that the yield of bio-oil increased as the temperature increased to 500°C, however the total bio-oil yield decreased above 500°C with further increase of the temperature. This was due to secondary cracking of the pyrolysis vapours to lower molecular weight organic products such as CO, CO₂, CH₄ and other gaseous hydrocarbons. Char yield is reported to be a function of temperature, as the temperature increased from 300-450°C the char yield decreased slowly. The author reports that at low temperature (300°C) the secondary cracking and cracking of biomass derived high weight molecules is difficult and usually proceeds at temperatures usually above 400°C. Thus the yield of char in this process was very high at 300°C where cracking of high molecular weight compounds did not take place.

The bio-oils were analysed and found comparable to various grades of pyrolysis oils, containing organic acids, the pH was found to be around 3.5 and 4.5. The other impurities found in the bio-oil was found to be comparable with other reported work and was found it can be used as a liquid fuel.

3.1.2 Biomass pyrolysis vapour upgrading studies

Hornung et al, 2009 [34] conducted a study to implement a low temperature (420-490°C) reforming unit containing a commercial pre-reforming catalyst (C11-PR) on a nickel (Ni) basis downstream of a Haloclean intermediate pyrolysis unit. The aim of this work was to achieve an enhanced heating value of the pyrolysis gases. Much of the focus of this work was to produce a gas quality that was suitable for use in power generation.

The biomass feedstock used in this study was wheat straw in pellet form. It was reported that the pyrolysis of wheat straw at 450°C by means of Haloclean intermediate pyrolysis leads to 28% char, 50% condensate (bio-oil) and 22% of permanent gas. The bio-oil was found to have separated into a water phase and an organic phase. The organic phase was a liquid but not homogeneous and contained viscous compound. These compounds overtime could polymerize with age due to the phenolic components and can lead to solid tars which can cause post processing problems. The authors reported that this is also typical of other lignocellulosic biomasses and could lead to solid tars at room temperature.

The authors stated that these difficult components could be converted into lower alkanes like methane as well as hydrogen and carbon oxides in a sequential low temperature reforming unit after the pyrolysis step.

The authors claimed that such a process with temperatures below 500°C is attractive compared to simple gasification which needs temperatures of about 800-1000°C.



Figure 21 Haloclean Pyrolysis (Intermediate) and LT reforming experimental setup [34]

Downstream of the Haloclean reactor two flow paths are possible, one with a catalytic reforming unit followed by a condensation unit, the other with an identical condensation unit but no reformer as is illustrated in Figure 23.

Wheat straw pellets was pyrolysed at 450°C at a flow rate of 40g/min, with solid phase residence times from 1 to 10 minutes and a gas phase residence time of approximately 2 seconds.

Two identical studies were performed, one without catalyst and one with catalyst. A total feed of 1.6kg of biomass was used in each 40 min run. The space velocities of the reforming reactors were altered by varying the amount of catalyst used from 310g to 700g as well as by varying the nitrogen flow through the Haloclean reactor from 0.75 to 1.79 m³/h. The catalyst was activated with a 15 vol% hydrogen/nitrogen mixture in advance as NiO is inactive and required to be activated to Ni.

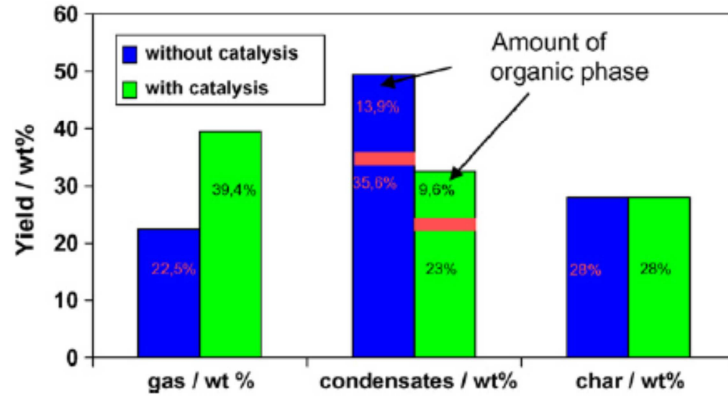


Figure 22 Comparison yields from measurements with and without catalysis (700g catalysts, LT reforming temperature 450°C) [34]

Figure 22 shows a comparison of the product yields with and without catalyst. The condensate yield collected with catalyst was about 33 wt.%, compared with 50 wt.% without catalysts. The pyrolysis gas yield rose to more than 32 wt.%. As the catalyst activity began to decline, the condensate yield rose to over 40 wt.%.

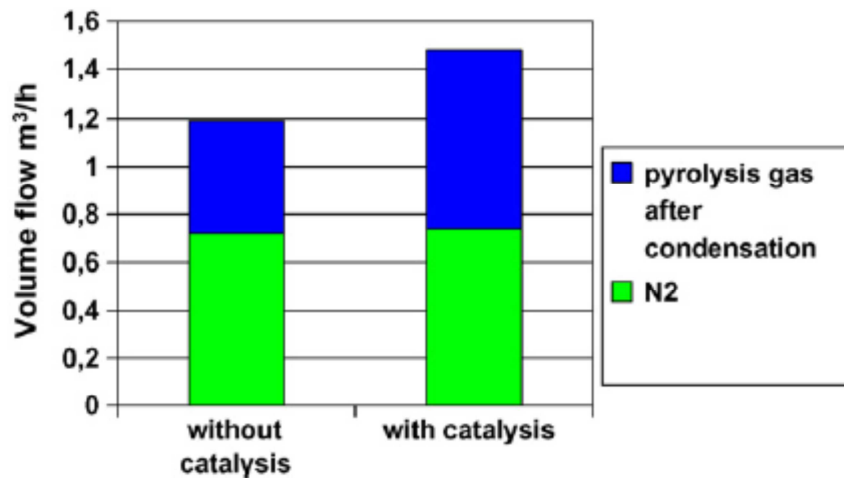


Figure 23 Determined flow rates of the pyrolysis gases with and without catalysis after the condensation (700 g catalysts, LT-reforming temperature 450°C)[34]

Illustrated in Figure 23 are flow rates of the pyrolysis gases after the condensation together with the flow of nitrogen. It was reported that the pyrolysis gas flow increased with the catalysts compared to without catalysts from 0.47 m³/h to 0.74m³/h, an increase of 58%, together with a sharp increase in heating value of the gas. The best measurement of the heating value obtained with catalysts was about 5.1 MJ/m³, which is a factor of 1.64 higher than without catalyst and is equivalent to 22-24% of the heating value of biogas (21.5-23.5 MJ/m³) as well as 15% of the heating value of the methane (35 MJ/m³).

It was reported that with catalyst hydrogen contents increased to 14 vol%., CO₂ concentration between 15-20 vol%, with CO concentrations about 5-7 vol% and methane about 12 vol%. An increase in CO₂ was detected and this was attributed to decarboxylation reactions. The gained heating value is attributed to the formation of H₂, CO and CH₄, through the use of catalysis.

The authors reported that the wheat straw contained some level of chlorine and was present in the pyrolysis gases post reforming, and this was responsible for the loss of activity and poisoning of the catalyst with time rather than coking. This was a new finding in the study as much of the chlorine in wheat straw was expected to be bound in inorganically and be transferred to the char.

Chidi et al, 2012 [114] investigated the production of synthesis gas using a two-stage continuous screw-kiln reactor. Waste wood and sawdust was used as the biomass with the objective to catalytic steam reform the pyrolysis vapours and oils within a second stage fixed bed reactor containing Ni catalysts. The first stage of the system utilises a horizontal screw kiln pyrolysis reactor (54cm long x 6.2cm diameter) where biomass was pyrolysed. The reactor is constructed of stainless steel and is heated by an electric furnace to achieve a maximum temperature of 500°C with a heating rate of 40°C/s. The second stage comprises a fixed bed catalytic gasification/steam reforming reactor (26cm high x 2.5cm diameter) constructed of stainless steel and with a maximum fixed operating temperature of 760°C. See Figure 24 below.



Figure 24 Schematic of continuous feed screw-kiln pyrolysis-gasification/catalytic steam reforming system [114]

Pyrolysis took place in the screw-kiln reactor with the biomass (waste-wood) being transported with the motion of the screw reactor at (0.24 kg/h) with a solids residence time of 40s. The evolved pyrolysis gases were then transported via nitrogen purge to react with steam and either of the four nickel based catalysts within the second stage fixed bed vertical reactor, a process similar to catalytic or steam reforming. Solid char was collected in a solids collection pot.

The four nickel based catalysts investigated were NiO/CeO₂/Al₂O₃ (20 wt.% CeO₂), NiO/Al₂O₃ and NiO/SiO₂ (denoted as NiO/SiO₂ (a)) prepared by a sol-gel method. The catalysts were synthesised using the wet impregnation method using an aqueous solution of (Ni(NO₃)₂.6H₂O), an aqueous solution of Ce(NO₃)₂.6H₂O (for the NiO/CeO₂/Al₂O₃ catalyst) and two supports (γ -Al₂O₃ and SiO₂). These were dried overnight at 105°C before calcination at 450°C for 3hours in an atmosphere of air. A further catalysts NiO/SiO₂ catalysts (20 wt.% Ni) (denoted as NiO/SiO₂ (b)) was prepared using a different preparation method (modified sol-gel-method).

The catalysts were ground and sieved to sizes between 50 and 180 μ m. The catalysts surface area was measured using the Brunauer, Emmet and Teller (BET) method via nitrogen adsorption. The adsorption and desorption isotherms were obtained by measuring the quantity of gas absorbed or desorbed on the surface of the catalysts sample at a constant temperature over a wide range of relative pressures. The BET surface areas were measured and are as follows; NiO/Al₂O₃ is 147m²/g, NiO/CeO₂/Al₂O₃ is 111 m²/g, NiO/SiO₂ (a) 136 m²/g and NiO/SiO₂ (b) 765m²/g.

Approximately, 5g of catalysts were used in each experiment. The results indicated that the presence of catalysts increased the yield of syngas, in particular hydrogen. The liquid content in the condenser system was a mixture of mostly water and pale yellow coloured oil. The quantity of the liquid yield had decreased indicating an effect of the catalysts on cracking the pyrolysis products to produce more gases.

The studies also suggested the catalyst with the highest surface area NiO/SiO₂ (b) (765 m²/g) and prepared by the sol-gel method was found to generate the highest gas yield of 54 wt.% and the NiO/SiO₂ (a) prepared by the incipient method yielded a lower gas yield of 49.8 wt.%. This is an indication the different preparation of catalysts has an effect on surface area and the catalytic activity. The authors also reported that filamentous carbon was detected on the NiO/Al₂O₃ catalyst.

Gas compositions for the four different catalysts indicated a significant increase in the product gas yield and compositions. H₂ and CO₂ compositions increased while CO and CH₄ as well as C₂-C₄ compositions decreased. The introduction of catalyst and steam indicates the promotion of the water gas shift, methane and steam reforming and tar (C₂-C₄) reforming reactions.

The gas composition for each of the four catalysts tested were in the range of H₂ 18.2-44.1 vol %, CO 29.9-47.5 vol%, CO₂ 11.6-17.5 vol%, CH₄ 5.5-14.5 vol% and C₂-C₄ 2.8-8.2 vol%. The results show that catalysts NiO/Al₂O₃ and NiO/CeO₂/Al₂O₃ appeared to display the most activity towards H₂ production as well as CH₄ and C₂-C₄ hydrocarbon gas decomposition. This indicates that the Ni catalysts have been effective in promoting formation of hydrogen and tar decomposition post pyrolysis at 500°C.

Sanna et al 2011 [115] investigated the pyrolysis of wheat and barley spent grains between 460°C and 540°C using an activated alumina bed. The study focuses on low temperature pyro-catalytic conversion of spent grains into low oxygen containing bio-oil and high nitrogen containing bio-char using alumina catalysts. Spent grains were obtained as by-products from a pilot scale brewer at the University of Nottingham.

Wheat and barley spent grains (referred to as WSG and BSG henceforth) were analysed for both proximate and ultimate analysis and was found to have carbon content of 43.2 and 49.8 wt.%. The calorific values reported for both fuels were 18.35 MJ/kg and 18.55 MJ/kg for both WSG and BSG. The author reported that BSG exhibits lower level of volatile matter 61.4 wt.% and an oxygen content of 39.4 wt.% compared with WSG 75.2 wt.% and 45.8 wt.%. Both feedstock contained high nitrogen content 4.5 and 4.1 for WSG and BSG, suggesting this is attributed to the presence of proteins within the sample. The presence of proteins 4.9 wt.% in WSG and 6.6 wt.% in BSG may represent a limitation towards fuel use due to the possible emission of nitrogen oxides, however the spent grains were found to be rich in fatty acids showing 13 and 17 wt.% for WSG and BSG respectively.

Approximately 114g of alumina sand with an Al_2O_3 content of 91% and a particle size between 250 μm and 355 μm was used in the fluidised bed reactor. Alumina is reported to be a synthetic white oxide of aluminium Al_2O_3 and has shown to be very active towards reducing tar and coke formation during gasification. The pyro-catalytic setup comprised of a pressurized injection system, a sample chamber, a fluidised bed reactor, an electrical heater and a tar trap. The tar trap comprised 3 Dreshel bottles 500, 250 and 150 ml in series with ice and water to condense the condensable gases to bio-oil. The reactor was 65cm in height with an internal diameter of 4.1 cm, and a volume of 858.5 cm^3 . A total of 5g sample was applied and inserted into the reaction chamber for pyrolysis experiments and were conducted at the following temperature: 460-490-520°C and 540°C. After each run the bio-oil was collected in a vial, and bio-gas was collected in gas-bags, were weighed and then both stored in a refrigerator.

The effect of temperature on the bio-oil yield for WSG and BSG presented a similar trend due to their similar composition of original materials. The maximum yield was obtained at 520°C with 53 and 49 wt.% for WSG and BSG. At 460°C the bio-char yield was 20 wt.% while at 540°C the yield decreases to about 15 wt.%, indicating that char yield decreases with increasing temperature.

Pyrolysis reactions with the presence of alumina is said to be shifted at low and moderate temperature in that it maximises the yield of the bio-oil compared to that of non-catalytic reactions. The char yield was also reported to decrease with increasing temperature due to secondary decomposition reaction of char residue enhanced by the presence of acid sites in the alumina sand at high temperature, maximising the gaseous yield due to acid cracking principally C-C bonds due to their low bond energy and also due to secondary reactions including thermal cracking, re-polymerisation and condensation of

the char residues. The oils produced were characterised for proximate and elemental analysis. The moisture content of the oils was found to be high ranging from 11 to 16 wt.% for oil from WSG and 17-21wt.% for BSG oil. The volatile matter showed a slight decrease with increasing temperature whereas the fixed carbon tended to increase. The sulphur content was very low for all the bio-oils as the ash content was virtually absent. The carbon and oxygen content ranged from 50% to 53% and from 31% to 37% respectively. Also 5-6% of hydrogen and 6-9% of nitrogen was present in the bio-oils. The energy content of the bio-oil varied between 22 and 26 MJ/kg for bio-oils was higher at 460°C compared to 520°C, the oxygen content was lower at 460°C than 520°C however higher yields were reported at the higher temperature. The increase in energy content in the oils as compared to the original feedstock is approximately 35%.

The oxygen content in the oils was found to be significantly lower than the feedstock's, indicating the pyrolysis process has partially deoxygenated the biomass. The author reports that the O/C ratios at 460°C was found to be the lowest for both samples investigated suggesting that at lower temperatures may favour and enhance deoxygenation. The H/C molar ratios of the bio-oils indicate that the hydrogen level decreases with increasing temperature thus high temperature favour's dehydrogenation perhaps due to increased cracking reactions.

The bio-chars were found to have a high nitrogen content 13-19 wt.% and tend to increase with decreasing temperature. Also the amount of nitrogen in the bio-oil is lower at 460°C compared to 490 and 520°C. Therefore pyrolysis at low temperatures can be considered for its effectiveness on bio-oil quality improvements in terms of nitrogen reduction. Moreover bio-chars rich in nitrogen might be used as soil amendment, and possibly for carbon sequestration. As a result pyrolysis at low temperature could be used to reduce the nitrogen level of spent grains producing bio-chars and bio-oils with enhanced quality.

Blanco et al,2012 [116]investigated the pyrolysis-gasification of refuse derived fuel (RDF) using a two stage reaction system. RDF is derived from municipal solid waste (MSW) with removal of recyclable glass and metals. The properties of RDF were analysed for both proximate and ultimate analysis. A low moisture content of 7.3 wt.% was reported but a relatively high ash content of 15 wt.%. The volatile matter and fixed carbon were reported to be 67.5 wt.% and 10.2 wt.% respectively. The ultimate analysis (dry ash free basis) reports a carbon content of 42.7 wt.%, hydrogen 6.1wt.%, oxygen 32 wt.% and nitrogen 0.5 wt.%.

Two nickel catalysts with different weight percentages (5 wt.% and 10 wt.%) were prepared by an impregnation method and investigated for their influence on tar and aromatic compounds as well as the product gas yield using sand at gasification temperatures. The authors were interested in one of the major issues of the process which is the formation of tar as it can significantly reduce the quality of

the gas produced. The formation pathway for the different types of tar as function of temperature is depicted in Figure 25.

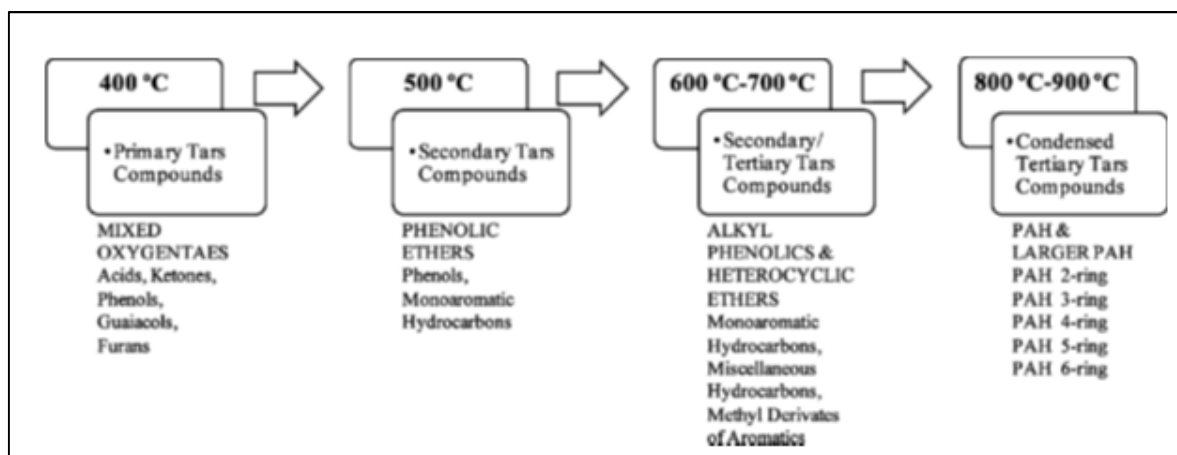


Figure 25 Pathway tar formation as a function of temperature [117]

A two stage fixed bed pyrolysis-gasification reactor was used. The pyrolysis reactor was constructed of stainless steel having a length of 25cm and a diameter of 5cm. The gasification reactor, also constructed of stainless steel, was 35cm in length and 2.5cm in diameter. The pyrolysis reactor was the upper part of the reactor and the catalytic gasification the lower section. Both were housed in separated electrically heated furnaces. Approximately 1.0g of RDF was used within the pyrolysis reactor (first stage) purged with nitrogen, and the evolved pyrolysis vapours were directly passed to the second stage reactor over the nickel catalyst (about 0.5g at 800°C) with steam being introduced. This allowed the vapours formed from the first stage to be gasified in the second stage.

The results were compared with experiments conducted using a bed of sand with and without the presence of steam. The char yield was approximately 30 wt.% and the conversion of RDF to gas and liquid was approximately 69 wt.%, with gas production increasing from 25.40 to 34.71 wt.% as the gasification temperature increased from 600 to 800°C. Higher gas yield was achieved when the Ni (Ni/Al₂O₃) content of the catalysts increased from 5 wt.% to 10 wt.%, rising from 30.85 wt.% to 45.89 wt.%. The hydrogen content in the product gas was about 32 vol% for 5 wt.% and reached approximately 45 vol% for 10 wt.%. When sand was used in place of a catalyst bed, the H₂ molar fraction increased from 18.70 vol% to 31.61 vol% and CO concentration decreased from 27.09 vol% to 18.15 vol% when steam was added at 800°C. Overall the addition of a bed of nickel catalyst increased the hydrogen content, CO₂ content increased slightly whereas the methane and C₂-C₄ concentrations were decreased and the CO concentration remained constant.

The major tar compounds identified were indene, naphthalene, methylnaphthalene, biphenyl, acenaphthylene, fluorine and phenanthrene. These have been identified as tar compounds in different thermal processes such as pyrolysis and gasification of both biomass and wastes. It was found that

lower gasification temperatures of 600°C promote the formation of oxygenated compounds and at higher temperatures aromatic compounds are formed.

Evans et al, 2002 [118] were investigating the production of renewable hydrogen from agricultural residues at a comparable cost to existing methane reforming technologies. The authors of this study at NREL had originally began development of this work (biomass to hydrogen) in 1993 with the concept of producing pyrolysis oil and fractionating it into two fractions based on water solubility. The authors identified two pathway strategies whereby biomass can be converted to hydrogen thermochemically with the first using gasification followed by shift conversion and the second, fast pyrolysis of biomass followed by catalytic steam reforming and shift conversion of specific fractions. The authors of this study investigated the latter route.

The process begins by converting biomass into a liquid product (bio-oil) using fast pyrolysis which can be stored or further converted to hydrogen via catalytic steam reforming followed by a shift conversion step. The authors claim that this method can be cost effective for hydrogen production using biomass of either agricultural or forest origin. Bio oil has two fractions, and each of the fractions, organic or monomer rich aqueous, can be converted using catalytic steam reforming, with the authors concentrating on reforming the aqueous fraction containing the monomers.

The tests in this study were conducted in two systems; a micro-reactor coupled to a molecular beam mass spectrometer (MSBS) and a bench scale fixed bed unit. The bench scale unit comprised a reactor (stainless steel tube) with 1.65cm i.d x 24.6cm length which was housed in a tubular furnace with three controlled heating zones. The reactor was packed with 100g of a commercial, nickel based catalyst (particle size 2.4-4.0 mm). Steam was generated in a super heater and was introduced by nozzles; to be mixed with organic feed from a diaphragm metering pump sprayed using nitrogen. The products formed were passed through a condenser, and the permanent gases output was recorded. The bio-oil and its aqueous fraction were prepared by NREL using fast pyrolysis of Poplar. A poplar oil generated by fast pyrolysis in the NREL vortex reactor system was separated into aqueous (carbohydrate derived) and organic (lignin derived) fractions by simply adding water to the oil with a weight ratio of water: oil =2:1. The aqueous fraction (55% of the whole oil) contained ca. 20% organics and 80% water. Most catalysts used were supplied by industry such as United Catalysts, Inc. (UCI) G-90 catalysts (and its K₂O promoted version G-91) and a dual catalysts bed of 46-1 and 46-4 from ICI Katalco. Two research catalysts were provided by the University of Sherbrooke (UDeS, Canada) and by the University of Zaragoza (UZ), Spain. The UDeS catalyst was a steam reforming catalysts containing NiO, Cr₂O₃, MgO, La₂O₃ and Al₂O₃. UZ catalyst is a stoichiometric nickel aluminate of a spinel lattice structure, with 20% NiO replaced by MgO.

Catalytic steam reforming experiments were conducted at 700°C initially with the objective of finding the best performing catalysts and operating conditions for steam reforming of oxygenates. All of the catalysts tested were reported to be capable of successfully reforming the model compounds (cellulose, xylan and lignin) at high conversion levels (>99%). The H₂ yields for all catalysts and model compounds were high, averaging approximately 90 % (±5%) of the stoichiometric value. No catalyst was reported as being superior in this investigation. Other parameters were investigated such as catalyst bed temperature, molar steam: carbon ratio, methane-equivalent gas hourly space velocity and residence time.

Temperature was reported to have the most significant effect on steam reforming reactions. Varying the residence time from 0.04s to 0.15s and increasing the S/C ratio from 4.5 to 7.5 showed no significant effects on the yield of hydrogen under the condition 600°C and gas hourly space velocity GHSV – 1680 h⁻¹ however these affected the concentration of CH₄ in the product gas.

For tests conducted using the bench scale unit much emphasis was placed on how to feed bio-oil or its fractions into the reactor. Model compounds (methanol, acetic acid 67%, syringe 16%, and m-cresol 16%, both separately and in mixtures) and bio-oil (whole oil and its aqueous fraction) were used as feedstock. The UCI G-90 catalyst was found to have some carbonaceous deposits on the catalysts bed after tests after taking the reactor apart. The carbon conversion to gas was 96%, other catalysts such as ICI Katalco showed excellent and steady performance without any carbonaceous deposits. The ICI Katalco catalyst is used in commercial naphtha reforming plants to reduce coke formation and extend catalyst lifetime.

Steam reforming of bio-oil and its fractions was reported to be a more difficult task than that of model compounds, mainly due to feeding the bio-oil into the reactor. Vaporizing bio-oil is a challenging task as it cannot be totally vaporised as significant amounts residual solids can cause blockage of the feeding line. The poplar bio-oil prepared was fed successfully at an inlet temperature of >500°C together with superheated steam 850°C, and with a high nitrogen content. A very stable gas composition and production rate was observed after 4hours, as well as satisfactory performance of the ICI 46 series catalyst.

Aqueous fraction could be successfully fed using a triple nozzle spraying system. Excellent hydrogen yields were reported as high as 86% with the potential to achieve 98% with a water-gas shift reactor. Hence both catalysts can efficiently convert oxygenates to hydrogen, with catalysts easily regenerated by steam or CO₂ gasification of carbonaceous deposits.

Qinglan et al, 2010 [119] investigated the catalytic pyrolysis of plant biomass using a dual-particle powder fluidised bed (PPFB) aiming to produce a gas rich in hydrogen. The authors aimed to achieve this at low temperature and pressure.

The raw biomass material samples used were chips of pine, Alaskan spruce, tropical laun and rice husks that were ground and sieved to less than 104 μm (150 mesh) in size, and dried at 375K in vacuum for 2 hours to a moisture content between (4.7-9.2 wt.%). The authors had chosen commercial NiMo/Al₂O₃ and inert SiO₂ for the solid bed, and these were also ground and sieved to 250-560 μm particle size.

The reactor apparatus consisted of a PPFB, temperature controller, and micro-feeder providing a continuous supply of fine chip powder, product collection system including a cyclone, two colds traps and a gas bag.

Experiment duration was approximately 40 minutes in which the biomass powder was loaded into the micro feeder, with the fluidising medium loaded into the pyrolysis reactor. The reactor was fluidised using helium and heated up to the desired temperature of 723K at atmospheric pressure. Once the desired temperature was reached the micro feeder would feed the fluidised bed reactor at a rate of 5g/hour. Initial pyrolysis experiments were conducted in the absence of catalysts to see the effect of pyrolysis temperature on product gas yields. The results showed that as pyrolysis temperature increased the yields of low molecular weight products increased, yields such as IOG (Inorganic gases), HCG (Hydrocarbon gases) and HCL (Hydrocarbon Liquids) increase from 2.72%, 0.34% and 0.07% at 773K to 43.37%, 12.17% and 3.17% at 1173K. It was noted that bio-oil and char were the main pyrolysis products formed with very little gas produced. At increasing temperature the tar and other components underwent secondary reactions to enhance the production of low molecular weight components.

The yield of inorganic gases and hydrocarbon gases is 55.4% which accounts for 94.60% of total gas and liquid products. Hydrogen is 1.38% at 1173K and accounts for 2.35% of total gas and liquid product. High temperature pyrolysis favours the formation of gas products but without catalysts the production of hydrogen is low. BTXN (benzene- toluene- xylene-naphthalene) usually derived from fossil fuels are also value-added intermediate products formed during secondary reactions at high temperature conditions. The study also observed the increase of BTXN produced from tar with increase of pyrolysis temperature.

Under catalytic conditions using NiMo/Al₂O₃ and inert SiO₂ as the solid bed the yields and distributions of the pyrolysis products differ dramatically. It was demonstrated that NiMo/Al₂O₃ and inert SiO₂ accelerates the decomposition of tar but also the decomposition of BTXN. It was observed that xylene had decomposed completely during the secondary reaction, toluene was minimised and yield of inorganic gases increased significantly. Hydrogen yield (3.75 wt.%) is 8.3 times higher than in the absence of a catalyst at a given temperature.

Therefore the presence of catalysts improved and promoted the production of hydrogen-rich gas through secondary reactions. It was also observed that woody biomass produced a higher hydrogen yield than that of rice husks under the same operating conditions. The authors also commented on one of the major drawbacks of the investigation of biomass catalytic pyrolysis, the rapid deactivation of catalysts due to tar formation and carbon deposits on the catalyst surface.

3.1.3 Biomass Gasification studies

A study performed by Erlich & Fransson, 2011 [120] investigated the downdraft gasification of pellets made of wood, palm oil residues and bagasse. The authors reported that little gasification data is available of ‘before disregarded’ fuels such as sugar cane bagasse from sugar/alcohol production and empty fruit bunch (EFB) from palm oil production. Much of their research was focused on improving the performance and optimization of the gasifier as well as testing different biomass fuels. They also investigated the possibility of finding possible uses for the product gases other than in an internal combustion engine, such as liquid fuel production.

Pellets of wood, sugar cane bagasse and EFB were used in the gasification experiments, with their chemical compositions and heating values illustrated in Table 4 below.

Table 4 Chemical composition & heating values of the biomass used in the gasification experiments[120]

Composition	Analysis method	Biomass sort		
		Bagasse	EFB	Wood
C (wt.% dry)	LECO-1	48.2 ± 2.9	47.2 ± 2.8	50.4 ± 3.0
H ₂ (wt.% dry)	LECO-1	6.1 ± 0.5	6 ± 0.5	5.9 ± 0.5
N ₂ (wt.% dry)	LECO-1	0.3 ± 0.1	0.6 ± 0.2	<0.1 ± 0.03
O ₂ (wt.% dry)	Calculated	44.3	38.2	43.3
Ash (wt.% dry)	SS 18 71 71:1	1.1 ± 0.1	7.9 ± 0.4	0.3 ± 0.1
S (wt.% dry)	SS 18 71 77:1	0.03 ± 0.007	0.12 ± 0.01	<0.01 ± 0.002
Cl (wt.% dry)	SS 18 71 54:1	0.05 ± 0.01	0.46 ± 0.1	<0.01 ± 0.002
HHV (MJ/kg dry substance)	SS-ISO 1928:1	19.26 ± 0.39	19.35 ± 0.39	20.27 ± 0.41
LHV (MJ/kg dry substance)	SS-ISO 1928:1	17.93 ± 0.36	18.05 ± 0.36	18.99 ± 0.38

The wood has the highest LHV and HHV as well as the lowest ash content, with EFB having the highest ash content. EFB was also reported to have the higher concentration of sulphur and chlorine which could potentially corrode equipment on a long term basis.

The gasifier a downdraft type reactor operated with suction generated from a frequency regulated centrifugal blower that allows air to enter the reactor through three adjustable air nozzles from an air flow meter. The researchers in this study highlighted the importance of air nozzles being equally

positioned with the combustion zone, placed directly by the air intake, where the gases are forced through a constriction zone (90mm) to the char zone where gasification reactions take place. The illustration of the gasification equipment is shown in Figure 26.



Figure 26 The downdraft gasifier system setup used in the experiments[120]

The constricted area concentrates the high temperature zone and favours tar cracking. The gasifier unit did not have a conventional grate to support the bed, to prevent any ash sintering blockage that could lead to the obstruction of gases passing if high ash fuels were to be utilised. It is reported that many gasifiers similar of this type have grid/bed shaking devices to avoid problems such as bridging and fouling. In this design however the gases were allowed to pass through with much of the dust entrained in the gas stream and then trapped in the filters. Pellets were also reported to perform better as they have a higher density than commonly used wood chips and provide better bed dynamics.

The gas was collected and cleaned in three steps by passing through a cyclone followed by two packed bed filters trapping dust and ash, before it was then allowed to pass into a blower to be flared off. This sequence also allows cooling of the product gases to prevent any temperature related problems. A small gas stream supplies a GC after the blower for gas composition analysis. Each biomass fuel was fed from inlets at the top of the reactor, and the char bed was pre-filled up to the constriction zone. Both pellets and char were weighed before the experiment.

The researchers reported that stable combustible gas was obtained after 3-4 min for wood pellets, 5-7 min for bagasse with EFB pellets being difficult and producing very little gas.

Table 5 Average composition and LHV values of the product gases[120]

Pellet sort and diameter	Volumetric gas composition (%) on dry gas					Energy content
	N ₂	CO	H ₂	CH ₄	CO ₂	LHV (MJ/m ₃ dry gas)
Bagasse, 6 mm	52.6±0.9	23.3±1.2	9.9±0.6	2.8±0.3	11.4±0.9	5.0±0.1
Wood, 6 mm	50.4±1.7	25.7±1.7	11.9±1.1	2.6±0.2	9.9±1.0	5.4±0.3
EFB, 6 mm	53.3±2.2	17.0±0.9	13.5±0.8	1.9±0.4	14.5±1.2	4.3±0.2
EFB, 8 mm	55.0±1.0	17.4±1.5	12.9±0.3	1.5±0.2	13.7±0.6	4.1±0.2

Table 5 presents the average gas composition and lower heating value (LHV) of the dry product gases for each biomass type and pellet size. Wood produced the highest LHV gas and EFB the lowest. The larger EFB pellets gave a slightly lower LHV than the smaller ones.

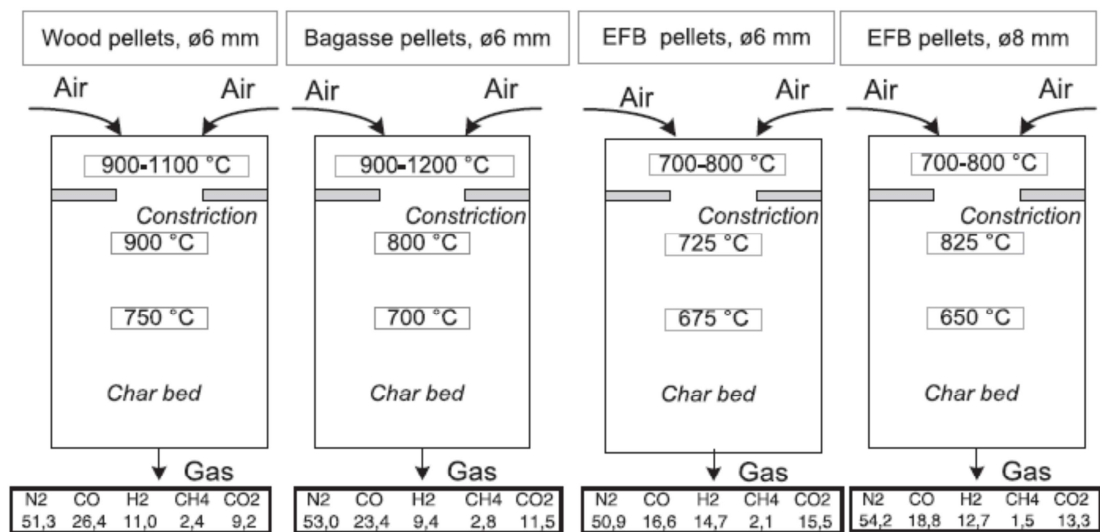


Figure 27 Typical vertical gasifier temperature profiles for the different fuels and respective dry composition [120]

The authors also reported that the gas composition was directly related to the reactivity of the biomass types, which affects the temperature level in the gasification reactor. A more reactive fuel gives higher temperature levels and a richer gas whereas a less reactive fuel gives lower temperature levels and more N₂ in the product gas. This is illustrated in Figure 27.

From the same figure it can also be observed that the temperature profiles seem to have a large impact on the gas composition. The bagasse and wood temperature profiles are similar and their gas composition is also relatively close.

Olgun et al, 2010 [121] investigated a small scale downdraft gasifier system that used agricultural and forestry residues, specifically hazelnut shells and woodchips. The gasifier was designed and constructed with a throat to achieve gasification with lower tar content. The setup consisted of a

throated downdraft fixed bed gasifier capable of 10kg feeding capacity, an ignition unit, cyclone, and a gas cleaning system, a flare and a data recording unit. Air was used as the gasification agent, which was supplied by an air blower with an electrical motor that can generate up to 120 m³/h maximum air flow-rate.

Much of the work focused on the design and construction of the reactor and equipment, which was constructed of 3mm thick stainless steel. It measured a diameter of 300mm and the throat diameter at 100mm, with the gasifier height 1095mm and throat height 200mm. A lid at the top of the reactor connected with 8 hinges around the gasifier was used to prevent any gas leakages. The reactor design also comprises of an air jacket located near to the gasifier combustion zone, primarily to allow the air to be heated at ambient conditions before entering the gasification combustion zone through 3 air nozzles. The producer gas leaves the throat area at temperatures above 900°C; this promotes a low tar content product gas.

A cyclone constructed of stainless steel was used to remove the particulates that may be present in the gas stream. The ignition system located at the air inlet has a LPG cylinder and an ionization burner with a capacity of 2.5 kW. The gas cleaning system consists of a cooler, a scrubber and a filter bed. The product gas is initially cooled with water in counter current flow using a cooler column before it is brought into contact with biodiesel in the scrubber to remove any tar components in the gas. A perlite-bed column was used to adsorb the remaining tar and moisture from the product gas as well as filtering fine particulates.

The woodchips were in the size range 10-30mm and hazelnut shells 5-10mm. The hazelnut shells and woodchip were subjected to proximate and ultimate analysis. Hazelnut shells were found to have about 55% more fixed carbon than wood chips on a dry basis while the wood chips have higher volatile matter content, and have a higher heating value than hazelnut shells. The gasification experiments were reported to have run smoothly without any major problems with either the hazelnut shells or woodchips. No problems such as gas leakage or agglomeration problems occurred in the gasifier. All tars present in the product gas had condensed within the gas cleaning system.

The gasification results were obtained after about hour duration for a batch of 10kg of woodchips. The gasifier reached a temperature of 1000°C in the combustion zone within 10 minutes of operation and stayed below 1200° C. The product gas heating value within the first 30 minutes had reached about 5 MJ/Nm³ and had gradually decreased to less than 1MJ/Nm³. The results for the gasification of hazelnut shells were comparable to those obtained for woodchips, with the highest heating value of 5.5 MJ/Nm³ achieved at an equivalence ratio of 0.35. The equivalence ratio is defined as the actual oxygen to fuel weight ratio divided by the oxygen to fuel ratio stoichiometrically needed. The product gas composition obtained at the highest heating value had carbon monoxide as the major combustible

component at 20-24%, hydrogen at 12-13%, methane at 3-4%, carbon dioxide at 11-14% and oxygen less than 1%. Product gas composition was found to be acceptable between ER 0.25-0.4.

The tar levels were quantitatively determined but it was observed that hazelnut shell gasification produced more tar than woodchips gasification. However the researchers had identified that fixed bed batch operated throated downdraft gasifiers are suitable for biomass gasification, which can also be upgraded for continuous operation.

Sheth & Babu, 2008 [122] carried out gasification experiments in a downdraft biomass gasifier with waste generated while making furniture in the carpentry section of the institute's workshop. 'Dalbergiasoo' also known as sesame wood or rose wood is the material usually used in making furniture. The waste generated from this same material is used as the biomass material in the gasification studies. In general the waste is usually used for either direct combustion or sold to pottery makers at a cheap rate to fuel their kilns as pottery making is an energy intensive process due to high temperature requirements in the kiln. The drawback of this is the poor control of temperature in the firing kiln and the high amount of ash and emissions. The researchers proposed that using biomass gasification technology can avoid these issues and evaluated the performance of the gasifier in terms of equivalence ratio, producer gas composition, calorific value, gas production rate and cold gas efficiencies.

The total height of the Imbert type downdraft gasifier used in the study was 1.1m; the diameter of the pyrolysis zone was 310mm, diameter of the reduction zone 150mm. The height of the reduction zone is 100mm and the oxidation zone is approximately 53mm. The pyrolysis zone height was dependent on biomass loading. The reduction zone, loaded with charcoal of approximately 500g, is supported by a rotating grate located at the bottom of the gasifier. Ash produced during the gasification process is collected and removed by using a rotating grate lever to unclog the grate. The grate if moved regularly during gasification can avoid grate clogging and encourage bridging of biomass thus allowing the biomass to undergo gasification. Air is introduced into the biomass gasifier through a gate valve at a constant flow rate (measured using a rotameter) and enters the gasifier through air nozzles.

The biomass consumption rate was found to be from 1.0 to 3.6 kg/h when air flow rate was varied from 1.85 to 3.4m³/h. The effects of moisture content present in the biomass was varied from 4% to 12% and was reported that as the moisture content increased the biomass consumption rate decreased with the energy requirement for drying increases reducing biomass pyrolysis. Moisture content was reported to have an effect on the operation of the gasifier and the producer gas with the authors reporting that the upper limit acceptable for a downdraft reactor considered being around 40% on dry basis. It was reported that as the air flowrate increased the biomass consumption also increased, allowing more oxygen to oxidise the higher amount of biomass would get combusted.

Carbon monoxide and hydrogen were reported as the main gas components of the producer gas resulting in a higher calorific value. It was found that at an equivalence ratio of 0.17 the calorific value was approximately 4.5 MJ/Nm^3 , with a slight increase 0.205 the calorific value reaches a maximum of 6.34 MJ/Nm^3 . A higher equivalence ratio than 0.205 the calorific value decreases steadily, which signifies a higher air flow rate for a specific biomass consumption rate.

The process of air biomass gasification was investigated by Plis & Wilk, 2010 [123] in this study using an auto-thermal fixed bed updraft biomass gasifier in order to produce a fuel gas suitable for small scale co-combustion systems. The gasifier was connected by a pipe with a water boiler fired with coal. The syngas obtained in the gasifier was supplied into the coal firing zone of the boiler and co-combusted with coal. The authors stated that the major drawback of the updraft gasification process is the high amount of tars resulting from the process, but this problem is of less importance if the syngas is immediately combusted in a boiler. The tars in this case may be an advantage in the case of immediate combustion of the obtained syngas in a stoker boiler because of its high heating value.

The authors in this study also conducted theoretical equilibrium calculations to predict the composition of the syngas and its calorific value taking into consideration the biomass composition, fuel moisture content, air ratio, gasification temperature, and external heat losses from the reactor. The model was based on four different biomass wood pellets, rape straw, corn straw and sunflower stems; however any biomass fuel can be carried out if the proximate and ultimate analyses are known. The model mainly used for theoretical investigations was also able to estimate whether the residence time of the reactants inside the reactor was able to achieve equilibrium. The author has made a more detailed analysis of this theoretical approach, however for the purpose of this review it will not be considered.

The experimental investigation was carried out using two kinds of biomass wood pellets, and oats husk. Both biomasses were cylindrical in shape with a diameter of 6mm and length 10-30mm. The gasifier system was designed and built from four cylindrical segments lined with refractory rings having an internal diameter of 0.25m with a total height of 0.60m and having a maximum loading capacity of 20kg wood pellets.

Biomass was fed from the top of the reactor and air was supplied and fed from the bottom which was supplied from a blower and measured by a flow meter. The experiment began by firing and heating the boiler until it reached steady state, the gasifier is then fired up and takes approximately 2 hours to reach experimental temperature. A syngas generator was placed on a scale to measure the mass decrement of gasified fuel. The syngas sampling point was located at the outlet of the gasifier where the syngas is collected and cleaned by a system of filters and then supplied to CO and H₂ analysers. Both feedstocks' had fairly comparable lower heating value 17.7 MJ/kg for wood and 16.3 MJ/kg for oats husk with very low ash contents between 1-2.6%.

The influence of excess air ratio on syngas composition was investigated at an excess air ratio of 0.29. It was found that the molar fraction of CO and H₂ were within the range of 23-29% and 5-9%. The author reported that the higher amounts of air provided into the gasifier caused a high molar fraction of CO in the syngas and was confirmed by theoretical calculations using their model. The moisture content in the fuel was said to have greatly affected the operation parameters of the gasifier and the composition of the syngas. A temperature drop was noted inside the gasifier which is heat needed to evaporate the moisture, which influences the quality of the syngas.

Three moisture contents were investigated for a few cases at 7%, 13% and 16% and was reported that the moisture content in the biomass was not favorable influencing change in the composition of the syngas between molar fractions CO and CO₂. For dry biomass the cold gas efficiencies (CGE) exceeded 50% while with wet biomass gasification the CGE dropped to 40%.

3.1.4 Biomass Gasification, Steam reforming and catalytic conversion

The researchers in this study Okamoto et al, 1999 [124] investigated direct conversion of brewers' spent grains to gas in the presence of a catalyst using a batch-type laboratory scale reactor. The grains were produced by Asahi breweries, and had a high moisture content of approximately 77%. The reactor operated at 350°C and 18Mpa, and a nickel catalyst was used (NI-3288).

The composition of the gas produced was 49-50% carbon dioxide, 33% methane, and 14% hydrogen. The researchers reported that the conversion of spent grains is a good means of producing energy, and forecasted that catalytic gasification of spent grain for energy production is a promising method of treating spent grain in the future.

In this study performed by Steele et al, 2011 [125] the authors were primarily concentrating on the use of catalysts for the efficient clean-up of biomass gasification gas, as this is a major barrier preventing commercialisation of this technology. The formation of tar during the gasification process is a limitation and the use of catalysis technology is well suited to the efficient clean-up of tars that are formed in the product gas. However one of the prime challenges with catalytic tar reforming of raw bio-syngas is the potential to deactivate catalysts via carbon deposition and poisoning with sulphur and other inorganic impurities.

There has been much work [126-130] that has concentrated on the use of relatively cheap catalysts materials such as dolomite/olivine and supported nickel based catalysts. Other work [96, 99, 102, 103, 106, 116, 131] has looked at attempts to improve nickel based catalysts on different supports such as Ni on alumina or silicate/spinal with alkali promoter. These attempts are only partially effective in reducing tar to acceptable levels due to poisoning by H₂S, alkali and chlorine containing compounds. Therefore in this study rhodium (precious metal catalyst) recognised for its S (sulphur) tolerance as

well as resistance to carbon was investigated. The aim of this work was to assess and compare the relative effectiveness of catalytic conversion of model tar compounds (toluene and naphthalene) using nickel and precious metal catalysts.

The authors tested catalysts in a quartz plug-flow reactor consisting of a quartz tube (4mm id) containing 0.15g of catalysts (particle size range 250-355um) at temperatures of 700-900°C under atmospheric pressure using a synthetic sulphur containing gas mix. The gas flow rate was 720 ml/min of (dry) composition 35% H₂, 18% CO, 14% CO₂, 32% N₂, 0.9% CH₄, 100ppm H₂S to which 10% steam and 0.5 vol% toluene/naphthalene were added as tar surrogates. These conditions generated a very high space velocity of ~300 lg-1h-1. The catalyst reactor was contained in a tube furnace which was in turn housed in an oven maintained at 180°C to prevent water and tar condensation. The catalysts prepared were pre-reduced at 900°C for 2 hours using 40%H₂/N₂ at 200 ml/min.

The results demonstrated that both Ni and Rh based catalysts were able to significantly contribute to the conversion of tar in the presence of H₂S between 700-900°C, however little methane conversion was observed. Without the presence of H₂S, methane conversion increased significantly for the best catalysts at 800°C, as did tar conversion. It was evident that H₂S was a significant poison to the catalysts when present in the gas, possibly blocking some of the active sites. A high surface area support with the Ni catalyst gave a much higher activity than commercial Ni catalysts. Rh based catalysts with low metal loading were found to give superior activity than the high surface area Ni catalysts over 10h timescales.

In a study conducted by Sang Jun Yoon et al, 2009 [67] the catalytic steam reforming of model biomass tar was investigated, with toluene being a major tar component. The study was performed at various conditions of temperature, steam injection rate, catalyst size and space time. In the study two nickel based catalysts, namely, Katalco 46-3Q and Katalco 46-6Q, were used in a lab scale steam reforming fixed reactor/gasifier. Both catalysts were supplied by Johnson Matthey. The system had a volumetric capacity of 12 l/h, the diameter of the reactor area was 30mm and the total length was 520mm. The reactor was heated to 800°C. To imitate the properties of tar 1000g/Nm³ of toluene (over ten times as much as tar emitted from a biomass gasification plant) was injected into the reactor at a rate of 50mg/min with argon used as a carrier gas.

The catalyst was crushed into sizes of 0.045-1mm; 5g of catalyst was used to fill the reactor. The space time in this study was controlled by adjusting the carrier gas flow rate at a constant catalyst weight of 5g. The effect of space time on hydrogen production yield with Katalco 46-6Q catalyst at four different temperature ranges was tested (600, 700, 800 and 900°C) at a constant steam ratio of 3. At 600°C and a space time of 1 kg h/m³ the dependency of hydrogen production yield on space time was not significant, however at a higher temperature of 900°C and a space time of 3 kg/h/m³ hydrogen

productions increased linearly with increasing space time. Therefore as space time increases, residence time increases and tars that are difficult to reform are cracked.

The results demonstrated that for all catalysts tested the composition of hydrogen increased with temperature while CO content decreased. Notably zirconia nickel based catalysts produced a 100% toluene conversion even at low temperatures of 600°C, and the applied Katalco 46-3Q and Katalco 46-6Q catalysts achieved a 100% conversion at 900°C under the presence of high tar concentration. The production of hydrogen also increased when increasing the amount of steam and with decreasing catalyst size

In the study performed by Safitri, 2005 [57] the aim of this work was to investigate the process of biomass gasification using a bubbling fluidised bed gasifier. The study involved varying some of the important parameters which influence the performance of the gasifier, and the most important was the investigation of tar formation and decomposition by several types of bed materials. The gasifier was 10cm in diameter and 120cm in length and was operated at a temperature between 800-950°C at atmospheric conditions. The author did not state the biomass used in the investigation.

The author identified that there are many parameters which influence the performance of a fluidised bed gasifier such as temperature, gasifying agent, type of bed materials and catalysts, residence time, biomass feed rate. For this work the effect of different type of catalysts, gasifying agent and residence time are studied

The fluidised bed contained sand and additives such as catalysts were added as its solid material, the diameter of the particles being 0.3mm and the density 2600kg/m³ with 600g being used in the experiment. When a catalyst is used within the bed the sand material is 540g and the catalyst 60g (10%). The temperature was set at 800°C and the biomass feedrate was set at 1kg/hr.

Air was used initially as the gasifying medium with a flow rate of 1000l/h and 2000l/h. Nitrogen was added to aid bubbling in the fluidised bed. The minimum fluidisation velocity for the reactor was calculated to be 0.0226 m/s, superficial gas velocity 0.1133 m/s, and the cross sectional area of the reactor 0.00785 m². The equivalence ratio [ER] is the ratio of gasifying gas to biomass. It is defined as the actual oxygen to fuel weight ratio divided by the oxygen to fuel ratio stoichiometrically needed. The ER ratio in the study was defined as being between 0.2 – 0.4, and was dependant on the temperature of the freeboard. This may be likely that ER was too high, therefore combustion taking place instead of gasification. The ER ratio for the use of catalysts was set at 0.3. A variety of catalysts were tested.

The experimental result shows that gasification using sand as the bed material with air as the gasifying medium gives a better temperature distribution than gasification using steam, therefore the biomass

conversion is higher. The biomass conversion using air as the gasifying medium reaches 99.5% while the gasification using steam results in only 87% of the conversion. A considerable less amount of soot or char can be found in the reactor and almost no carbon is deposited on the sands surface for gasification with air, whereas the gasification with steam gives a big amount of char or soot and carbon is deposited on the surface of the sand.

The addition of different type of catalysts in the bed material gives positive effect in reducing tars, For 4 hours of experiment, and the use of olivine catalysts added to the bed material can reduce up to 77% of the total tar produced from the gasification process using only sand as the bed material. The addition of calcined olivine catalysts results in higher tar destruction up to 94%. Other types of catalysts are made by impregnating (20 wt.%) NiO on olivine and calcined olivine in order to enhance the activity of the catalysts. The result showed that both were capable of tar removal of up to 98%.

The catalysts used in this case are mentioned below with their corresponding findings:

1. Olivine (tars reduced by 77% after 4h)
2. Calcined olivine (approximately 94% tars removed)
3. NiO-olivine (up to 97% tars decomposed and 5 times higher H₂ than biomass gasification using sand)
4. NiO-calcined olivine (same as above catalyst 3)
5. Calcinations of NiO-olivine, (2h experiment, already 98% tars converted and 6 times higher H₂)
6. Recalcination of NiO-calcined olivine

In a study performed by Li et al, 2003 [64] biomass gasification was investigated on a test pilot scale 6.5m tall and 0.1m diameter, air blown circulating fluidised bed reactor. A high temperature cyclone was employed for the solids recycle and a ceramic fibre filter was used for gas cleaning. The temperature profile of the reactor was in the range of 700-850°C. The biomass feedstock was sawdust with the feed rate being applied in the range between 16 to 45kg/h, with throughput estimated to be 0.7-2.0kg/m²s.

Air was the fluidizing agent which was supplied to the reactor from the bottom, with an air flow of 40-65 Nm²/h. Steam was injected at a pressure of 5 bar, with a varying steam flow rate tested in the range of 0-10.5 kg/h.

The system also consisted of a gas cleaning train, with the ability to capture and gases and tar for further analysis. The tar gas sampling device, also known as 'The Guideline method'. The tar sampling consists of 4 impinge bottles (250ml) with acetone acting as the main solvent which works alternately at -3°C and room temperature approximately 35°C.

Six different sawdust species were analysed and used as feedstock. Any of the bed ash collected from a previous run was used as the starting bed material for each new run, with silica sand making up for the loss of solids.

The last two runs in the study involved the use of two nickel based catalysts (C11-9 LDP, Sud-Chemie) for tar removal and methane reforming. The particle density was 2829 kg/m³. Approximately 11-14kg of catalysts were crushed and screened to 0.25-1.7mm in diameter.

The main aim of this study was to investigate whether temperature, air ratio, suspension density, fly ash rejection and steam injection were found to influence the composition and heating value of the product gas.

The findings however revealed:

1. The product gas heating value depends heavily on the air or O/C ratio and suspension temperature.
2. Gas heating value can be increased by increasing the suspension density.
3. Ash re-injection improved carbon conversion, while steam injection improved the quality (heating value) of the product gas.
4. Tar yield decreased with increasing operating temperature.
5. Addition of a reforming catalyst significantly reduced tar yield, while secondary air had only a very limited effect on tar removal for a constant total air ratio.

In a study performed by Pangmei et al, 2003 [89] a fluidised bed gasifier system was developed to investigate the hydrogen-rich gas produced from biomass gasification with the direct use of calcined dolomite in the gasifier and a fixed bed catalytic reactor containing nickel catalysts post gasification. The purpose of the study was to characterise the influence of operating parameters in the gasifier and catalytic reactor on the production of hydrogen as well as to test the performance of the system to obtain useful data for the design of industrial units.

Pine sawdust was the feedstock, with particle sizes between 0.3 and 0.45mm. Calcined dolomite and nickel based catalysts were used in the experiments; the dolomite was first crushed and sieved to obtain a particle size of 0.3-0.45mm then calcined in air at 900°C for 4h. The dolomite catalyst acted as the guard bed and was placed in the gasification reactor. The function of the guard bed is to decrease the tar content at the inlet to the catalytic bed, so preventing the nickel catalyst from being deactivated. Nickel-based catalyst Z409R was used in the second catalytic reactor. This had a size of ϕ 16 x ϕ 6 x 6.0-6.8mm and a composition of NiO \geq 22 wt.%, K₂O 6.5 \pm 0.3 wt.%.

The apparatus included an atmospheric pressure, indirectly heated, fluidised bed gasification system. The major components in this system included:

- Fluidised bed gasifier
- A steam generator
- Air compressor
- A cyclone
- Catalytic fixed bed reactor
- Electric heated furnaces

The fluidised bed was constructed of 1Cr18Ni9Ti stainless steel pipe and was externally heated by two electric furnaces. The total height of the reactor is 1400mm, with the bed diameter of 40mm and a freeboard diameter of 60mm.

Air was used as the fluidising agent and came from an air compressor. Before entering the reactor the air was heated to 65°C to improve performance. The steam entered the reactor at 154°C and is produced using a steam generator. The produced gas flow passed through a cyclone at 200°C to prevent tar in the gas from condensing, and then into the fixed bed catalytic reactor. The fixed bed catalytic reactor was constructed of the same material used to construct the fluidised bed gasifier and was externally heated by an electric furnace. The length of the reactor was 400mm with an inner diameter of 38.5mm.

120g/kg h⁻¹ of biomass and calcined dolomite mixed with 30 g silica sand (0.2-0.3 mm) was put in the gasifier. Since calcined dolomite is soft it erodes during the test and is eluted out of the bed with flue gas exit.

3.2 Summary of previous work

The review of the literature highlights the opportunity to explore the advanced thermochemical conversion of BSG further. There have been some studies that have explored both the pyrolysis and gasification of BSG however the quantity of searchable work was very limited, therefore work conducted with biomass and biomass residue as feedstock's for thermochemical conversion was reviewed. Furthermore there has been limited literature that explores intermediate pyrolysis systems.

Becciden et al [111] uses small equipment but temperatures are higher almost that of gasification rather pyrolysis. It was reported hydrogen yield increases sharply with temperature. Liquid yields were not focus of the study but liquid yield decreased also. The author reported higher temperature favoured gas yield at the expense of char and liquid. This is consistent as reported by Asadullah et al [132] that at lower temperatures of 300°C the quantity of liquids was very low as was the gas yield. Increasing the temperature to 500°C increased the bio-oil, however the yield started to decrease above 500°C with further increase of the temperature.

Most of the work found in the literature on intermediate pyrolysis mainly focused on the production and characterisation of the pyrolysis oils from waste residue feedstocks. Reviewed work of Yang et al [133], Ouadi et al [134], focused using the state of the art Pyroformer reactor and Roggero et al [37] focused on using the Haloclean reactor using different waste feedstock.

The work of Roggero et al[37] explored intermediate pyrolysis of a variety of biomass and residue feedstocks using a single screw auger (Haloclean) that is externally heated but also uses steel spheres that are continuously re-circulated to transport heat within the system. The author investigated different biomass residues and reported on the product yields with the main focus on bio-oils and its characteristics.

The author did not report on the characteristics of the biomass residue feedstock before they were processed, therefore it is unknown the effect the feedstock properties such as moisture and ash has on the product distribution was not reported. Roggero et al[37] reported the yield distribution of coke, gas and liquid depended mainly on processing conditions mainly temperature and residence time. However the author did not report on the solids and vapour residence times as well as the heating rate.

Yang et al [108], explored intermediate pyrolysis of sewage sludge and paper industry waste using the pyroformer a externally heated twin screw auger reactor that recycles a fraction of the char within the reactor. The recycling of char within the pyroformer is reported to increase the char to feedstock ratio in the reaction zone which promotes catalytic cracking of the primary higher molecule weight vapours to lower molecular weight vapours and permanent gases. It also serves to recycle heat within the reactor and increase the heating rate experienced by the feed rate. Yang et al [108]carried out

characterisation of the feedstock and reported high ash content for the fuel (sewage sludge and paper waste) but did not analyse the mineral content of the ash. Therefore it is unclear the role ash plays in the product distribution in this work or whether the pyroformer twin screw arrangement plays a role in producing a phases separated oil suitable for blending in biodiesel or is it entirely dependent on the feedstock

The ash content is one of the most influential parameter in the pyrolysis process which affects the yield and chemical composition of the pyrolysis products. It has been reported that agricultural residues and grassy biomass have higher ash contents than lignocellulosic woody biomass. High ash containing feedstock's are not desirable for biomass pyrolysis because ash catalyses reactions which compete with biomass pyrolysis, leading to increased formation of water and gas at the expense of liquid organics [31, 41-46]. The minerals present in ash mainly alkali components are responsible for secondary catalytic cracking [46].

Bridgwater, 2012 [31] reported that biomass with ash content greater than 2.5% causes phase separation of the bio-oil and biomass with ash content less than 2.5% gives a more homogeneous bio-oil liquid. [31] However a feedstock may contain a high ash composition but then may contain a large amount of inactive constituents that do not lead to catalytic cracking or bio-oil phase separation. Therefore the ash compositional analysis must be carried out.

Yang et al [133] reported a solids residence time between 7-10 minutes but did not report the heating rate but defined intermediate pyrolysis as slow heating rates and intermediate solid residence times. Samanya et al [110] reported used blends of fuel in different forms in a bench scale fixed bed reactor at a heating rate of 25°C/min to 450°C and held at this temperature for 15 minutes and reported bio-oils phase separating into two layers. Roggero et al [37] did not report on the heating rate but reported processing at temperatures from 450-500°C.

Both authors mainly reported on the characteristics of the bio-oils produced reporting on the major chemical compounds detected using a GC/MS mass spectrum. Roggero et al [37] reported that the oils chemical groups from the feedstocks processed were mainly alkenes and phenols and with small proportions of organic acids, alkanes and cyclopentanones, see Figure 28.

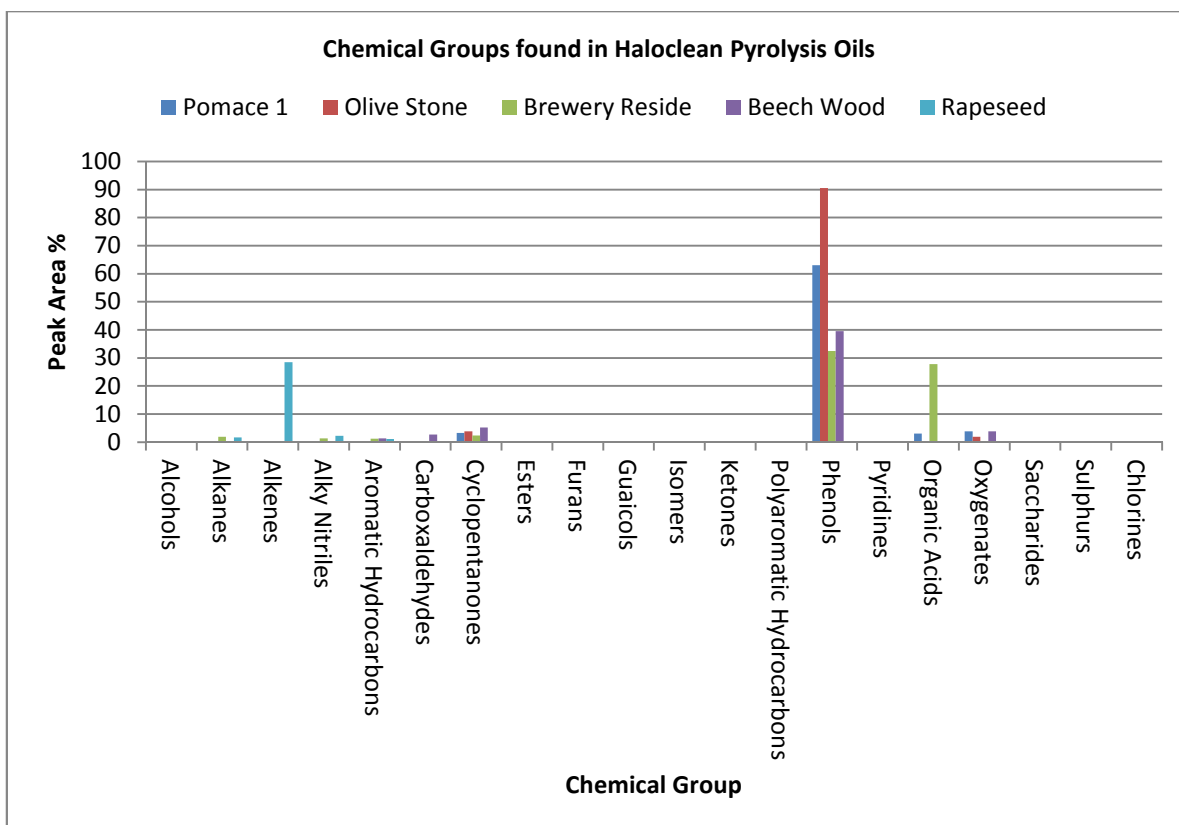


Figure 28 Chemical Groups found in Haloclean Pyrolysis Oils

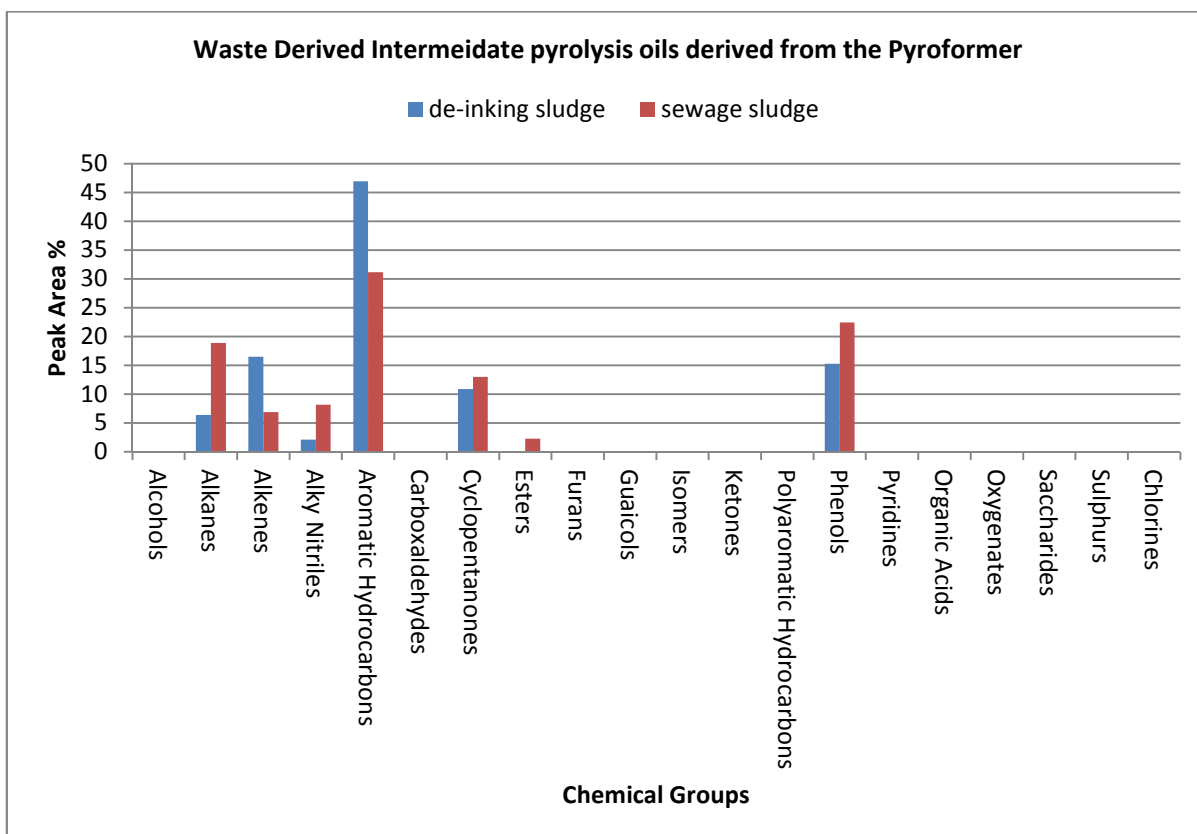


Figure 29 Chemical Groups found in Waste Derived Pyrolysis s Oil produced in the Pyroformer

The major chemical compounds reported in the work of Yang et al [133] shifted towards alkenes, alkane aromatics, alkyl nitriles, cyclopentanones and phenols, see Figure 29.

Yang et al [133] reported that the bio-oils produced in the pyroformer had readily separated into two phases with an organic phase at the top and an aqueous phase at the bottom. It was also reported that the organic phase had reduced oxygen content from that of the original feedstock, making them favourable as fuels and making them able to be miscible with biodiesel and diesel. Roggero et al [37] did not discuss phase separation for any of the oils but reported results giving oil/water distribution ratio only. Hornung et al [34] reports bio-oil from straw had phase separated into a water phase and organic phase using the haloclean and a solids residence time of 1-10mins and vapour residence time of 2 seconds. It is not reported in the work of Yang et al [133], Hornung et al [34], Roggero et al [37] and Semanya et al [110] of what the real causes of the oil to phase separate with respect to their investigations.

The concentration and composition of the chars or permanent gases was not reported in either of the studies although the heating value of the chars and permanent gases was reported. It is unclear in either of studies whether the quality and characteristics of pyrolysis products change dramatically with the feedstock characteristics, feedstock residence times, heating rates, or the role ash plays in the formation of pyrolysis products mainly the phase separated bio-oils or if it's a combination. It is also unclear whether the processing technology employed plays a role in producing phase separated oil.

Sanna et al [135] reported using alumina as a bed for the pyrolysis of barley and wheat straw and reported that the presence of alumina at low and moderate temperatures maximised the liquid yield compared to non-catalytic, char yield decreased due to increasing temperature. Phase separation of the oils did not occur however the oxygen content of the oil was reported to have been lower than the original feedstock.

Further work using the Haloclean was conducted by Hornung et al [34] focusing on upgrading pyrolysis vapours intermediate pyrolysis via steam reforming. To date there is no existing work using the pyroformer and upgrading pyrolysis vapours.

Hornung et al [34] investigated combined intermediate pyrolysis (450°C) steam reforming (450°C-500°C) with the aim of converting pyrolysis vapours into pyrolysis gases with an increased heating value using a LT reforming catalyst. Pyrolysis of biomass is connected to the formation of water during thermal degradation of biomass and is abundant so could serve in reforming reactions as a source for hydrogen. The topic of this investigation was to see the influence of temperature and space velocities by varying the amount of catalysts and inert gas flow on gas quality. The author reported that such a process below 500°C is attractive compared to simple gasification which needs 800-1000°C. The heating rate and the nickel loading content of the catalysts was not reported although the

catalysts had to be activated using a 15vol% H₂/N₂ mixture. Chidi et al [114] did not report on reducing the catalyst stating this would have been expected to have occurred in situ by the process gases. The study reports an increase in H₂ content and decrease in bio-oil of 17%. The colour of the pyrolysis oils was not reported but was found to still phase separate into both aqueous and organic phases. Chidi et al [114] also reported the quantity of the liquids yield had decreased indicating the affect pf the catalysts on cracking pyrolysis products to more gases and also observed that liquid content was mostly water and pale yellow coloured.

As the catalytic activity began to decline, the condensate yield rose over to 40wt%. The major chemical components of the bio-oils was not analysed or reported in this study and therefore it is unclear the affects the catalysts had on the composition of the bio-oil. However the permanent gases were reported to have hydrogen contents increased to 14% and an increased heating value of 5.1MJ/m³ from 3MJ/m³. Catalytic declining activity with time was reported to be due to poisoning with the amount of chlorine detected and actually very little carbon precipitated on the surface of the catalysts was observed. Chidi study filamentous carbon was detected on the catalysts surface.

Chidi et al [114]carry out combined pyro steam reforming but with first stage at 500°C at a heating rate of 40°C/s and a second stage at 760°C but using 5g of catalyst. This study reported on the effect of different catalysts being prepared using different methods and different catalysts loading. The author reported that Nickel catalysts are effective in promoting formation of hydrogen tar decomposition post 500°C. The author also reported that catalysts with a higher surface area performed best producing the most hydrogen. It is unclear from the study of Hornung et al [34] what the actual Nickel loading content and the surface area of the catalysts was as this could also influence the performance. Blanco et al [117] reported that the higher gas yields are achieved when the second stage temperature is increased from 600°C to 800°C, and overall when the content of the catalysts increases in particular the Nickel content the hydrogen content increases also.

Therefore one can argue catalysts perform better at higher temperatures, with higher surface area and higher Nickel content. In the work of Chidi et al [114]the introduction of catalyst and steam indicates the promotion of the water gas shift, methane and steam reforming and tar (C₂-C₄) reforming reactions. Horning reported using the aqueous phase present in the pyrolysis vapours as the reaction partner for steam reforming and hydrogen. None of the two studies mention the effect of steam or report the quantity of additional steam consumed.

Literature [100, 101] has reported that using nickel catalysts designed for steam reforming at temperatures higher than 740°C there is a general increase in the hydrogen and carbon monoxide content by either reducing or eliminating the hydrocarbon and methane content. Only at lower temperatures the methanation reaction is favoured thermodynamically when methane is the desired component in the gases. Commercial Nickel catalysts can be divided into two groups

Evans et al [118] reported that it would be cost effective to produce a liquid product using fast pyrolysis so this can be stored or further converted to hydrogen using steam reforming. Hornung et al [34] reported that bio-oil organic phase is liquid but not homogeneous and contains viscous compounds which could accumulate and polymerise with age due to the phenolic structure of the components. Bridgwater reports most successful work with fast pyrolysis has occurred mainly with woody, low ash highly homogenous feedstock, and the process would not be successful with more difficult feedstock's which can produce highly reactive liquids in high MW tars leading to storage and processing issues.

Steam reforming of bio-oil and its fractions was reported by Evans et al[118] to be a more difficult task than that of model compounds, mainly due to feeding the bio-oil into the reactor. Vaporizing bio-oil is a challenging task as it cannot be totally vaporised as significant amounts residual solids can cause blockage of the feeding line.

To vaporise and reheat bio-oil would be difficult and expensive. The process would be best served if carried out in situ. In particular, the liquids produced from non-woody biomass are very low in high molecular weight tars and can be suitable for direct application in engines.

As described earlier the work of Beciden et al [111] the pyrolysis of BSG was conducted in a small laboratory scale macro TGA reactor investigating the pyrolysis products formed. Roggero et al [37] reported on and compared the product distribution of various waste biomass feedstock including residues from beer production under intermediate pyrolysis condition using the Haloclean, however no further work has been conducted to upscale or further investigate BSG in both the authors findings.

Okamoto et al [124], investigated the direct conversion high moisture spent grains in the presence of a catalysts using batch type laboratory reactor. The author reported that the conversion of spent grains is a good means of producing energy, and forecasted that catalytic gasification of spent grain for energy production is a promising method of treating spent grains in the future. Very little research work has been carried out to further explore the gasification of BSG using the various gasification technology configurations available.

Again much of the work reviewed has been investigated on small laboratory scale and has not been up-scaled. Much of this can be explained by the problems BSG can present as a potential fuel mainly its high moisture and protein content if not treated can microbiologically degrade fairly quickly making it a very difficult material to handle, store and transport.

From the literature review it is important to carry out the full pre-treatment and full investigation and characterisation of brewers spent grain to understand its suitability as a fuel. Hornung et al[34] and Roggero et al [37] did not report on the characterisation of the fuel prior to processing. It is also

important to carry out a full compositional analysis of the ash. Yang et al did not report on the composition of ash even though the fuel processed had high ash loading and therefore it was unclear the role ash played in catalysing the pyrolysis vapours from high MW to low MW components and the effects it has on the product distribution. It would also be best to identify the active and inactive components in the ash.

There has been limited or no published work which investigates the use of BSG in intermediate pyrolysis systems and there also exists limited or no literature on the use of BSG for Gasification systems.

There has been no published literature that investigates the intermediate pyrolysis of BSG using the 'Pyroformer' which is the state of the art intermediate pyrolysis reactor at Aston University, and there also does not exist any literature reporting the upgrading of intermediate pyrolysis products from BSG or as a fuel source for engines.

The review identifies the potential of investigating the use of BSG for pyrolysis followed by steam reforming with the use of different steam reforming catalysts at different reforming temperatures. The review identified that the mass of catalyst, the catalyst loading, the surface area of the catalyst and the catalytic temperature are important parameters when considering the production of hydrogen. Much of the catalysts reported in the literature review were nickel based on an alumina support. It will be worthwhile to explore nickel catalysts and the use of different metal catalysts for steam reforming post pyrolysis to produce hydrogen rich syngas and to understand the effects it has on the pyrolysis products. It is also important whilst investigating catalyst is to determine the composition of the gases in particular hydrogen and determine catalytic activity.

The review identifies there has been much work conducted on pyrolysis and gasification of various biomasses, and waste feedstock's but very limited work can be found of the thermochemical conversion of BSG. Therefore there remains much scope for further research in these areas.

3.3 Project Aims and Objectives

3.3.1 Project aim

The main aim of this research is to study the pyrolysis/reforming/gasification of BSG, the effects of tar cracking using different catalysts to attain a tar free product-fuel gas that can be suitable to run an engine, gas turbine or a combined heat and power plant.

3.3.2 Project Objectives

There are three key objectives to this project.

The first objective involves the pre-treatment followed by the full investigation and characterisation of BSG and its suitability for advanced thermo-chemical conversion. The method requires, drying and preparing the fuel to enable thermal conversion, followed by various analysis techniques to obtain detailed characterisation such as moisture, ash and elemental composition.

The second objective is the application of intermediate pyrolysis technology to brewer's spent grain in order to produce three product streams, liquid, solid and gas. The three product streams will then be further analysed for fuel properties and capabilities.

The third objective is to explore the introduction of steam reforming catalysts into the intermediate pyrolysis process. This will involve the coupling of a catalytic tar cracking reactor to reform the vapors, increasing the quality of the bio oil and enhance heating value of the product gases.

A further objective if time allows will be an investigation of the gasification of BSG using both fixed bed downdraft and fluidized bed configurations.

4 Characterisation Methods of Biomass Feedstock and Pyrolysis Products

4.1 Introduction

In this project, BSG is used as the industrial waste biomass feedstock for advanced thermochemical processing. Before commencing any thermochemical conversion study, the feedstock is pre-treated and then characterised to determine its basic composition and structure so it can be evaluated for its usefulness as a fuel. The objective of this chapter is to describe the pre-treatment and detailed characterisation of the biomass feedstock using a combination of analytical methods, which include proximate, ultimate, chemical compositional, inorganic elemental, heating value, thermo-gravimetric (TGA) and derivative thermo-gravimetric (DTG) analyses. A thorough analysis of the characterisation results helps to better understand the thermal behaviour of BSG feedstock so it can be evaluated as a fuel when subjected to thermal conversion processes either by pyrolysis or gasification.

4.2 Materials and Methods

4.2.1 Raw Materials

Approximately 50kg of wet brewers spent grain was obtained from Molson Coors brewery R&D pilot plant in Burton on Trent approximately 35 miles away from Aston University, Birmingham.

4.3 Feedstock Pre-treatment

As described earlier in Chapter 1, preservation methods must be adopted in order to prevent the degradation of BSG enabling it to be stored or transported easily. BSG when wet is a very unstable material caused by microbial activity. Therefore as reported by Di Blasi et al[12], preservation by oven drying reduces the volume of the product but does not alter the composition of the spent grain. Therefore, freezing of the wet grain followed by oven drying was adopted in this study.

4.3.1 Freezing

The grain was initially stored in double black bin liner bags in a cold store room at the breweries at 0°C to preserve the grain and prevent microbial degradation. When collected they were immediately placed and stored in a freezer box (-18°C) available at Aston University labs.

4.3.2 Drying

A fan assisted oven was used to dry the frozen or wet BSG to a moisture content of about 10-15%, suitable for thermochemical conversion.

4.3.3 Grinding

A Heavy-Duty Cutting Mill, Type SM 2000 supplied by Retsch Ltd. of was used to reduce the size of the dried BSG (see Figure 30).



Figure 30 Biomass Cutting Mill

A fold back feed hopper, smooth surfaces and push fit rotor are provided for quick and easy cleaning after the feed material has been reduced. Selections of bottom sieves are available for this cutting mill, dependant on the fineness required. Stainless steel bottom sieves with a perforation size up to 10mm, 4mm and 1mm are available at Aston University. For this study a 1mm sieve was selected.

Ground biomass samples were graded using a series of sieves. The sieve sizes were 250, 300, 400, 425, 500, 600, 850 and 1000 μ . The different sieves sizes were placed on top of one another with approximately 200g of biomass added. With the lid securely placed on the sieves, the sieves were then placed in an Endecott's EFL2000 sieve shaker for 10minutes. This was done to understand the particle distribution of milled BSG as well as to prepare for further analysis.

4.3.4 Pelletizing

A roller shaft pellet mill 9PK-250 [136] was used to pelletize dry ground BSG. Pelletising is required to prepare the BSG feedstock so that it is suitable for both thermochemical reactors available at Aston University.



Figure 31 Roller shaft pellet mill with BSG pellets

4.4 Feedstock Characterisation

BSG was characterised for proximate and ultimate analysis and heating value. Barley straw and wheat straw pellets were obtained and analysed in the same way, for comparison purposes. Barley in this work is of some interest as it is the main raw material used in the brewing industry and could perhaps be used as a substitute feedstock for BSG during thermochemical conversion experiments.

4.4.1 Proximate analysis

The proximate analysis is used for the determination of moisture, volatile matter, ash and fixed carbon contents of biomass samples. The moisture content was determined using British Standard 14774-3:2009[137]. The prepared sample is dried at a temperature of $105 \pm 2^\circ\text{C}$ in an air atmosphere until constant mass is achieved and the percentage moisture is calculated from the loss in mass of the sample. The ash content is determined using British Standard (BS EN 14775-2:2009) [138], in which the ash content was determined by calculation from the mass of the residue remaining after the sample is heated in air under rigidly controlled conditions of time, sample weight and equipment specifications to a controlled temperature of $550 \pm 10^\circ\text{C}$. Volatiles and Fixed Carbon was determined using the British Standard (BS EN 15148:2009) [139].

4.4.2 Ultimate analysis

Ultimate analysis was performed in order to determine the basic elemental composition of the biomass samples; carbon, hydrogen, nitrogen, and sulphur was measured, while oxygen is calculated by difference. Prepared samples of dried, ground and sieved biomass was sent to an external company (MEDAC Ltd., Surrey, UK)[140]for CHN analysis using a Carlo-Erba EA1108 CHNS-O analyser.

4.4.3 Chemical compositional analysis

Chemical compositional analysis of BSG was conducted using the FiberCap 2021/2023 Fibre analysis system to determine the cellulose, hemicelluloses, and lignin and extractive contents. The FiberCap equipment used for this analysis is based on the Van Soest method. Biomass samples are subjected to extractions using Neutral Detergent Solution (NDS) to obtain the Neutral Detergent Fibre (NDF) value; Acid Detergent Solution (ADS) to obtain the Acid Detergent Fibre (ADF) value and 72% Sulphuric Acid to obtain the Acid Detergent Lignin (ADL) value. Values of cellulose, hemicellulose and lignin can be obtained from subtractions of the weight loss from the extractions [141-143]. See Figure 32 for the detergent fibre system diagram and Table 6 describing the principles.

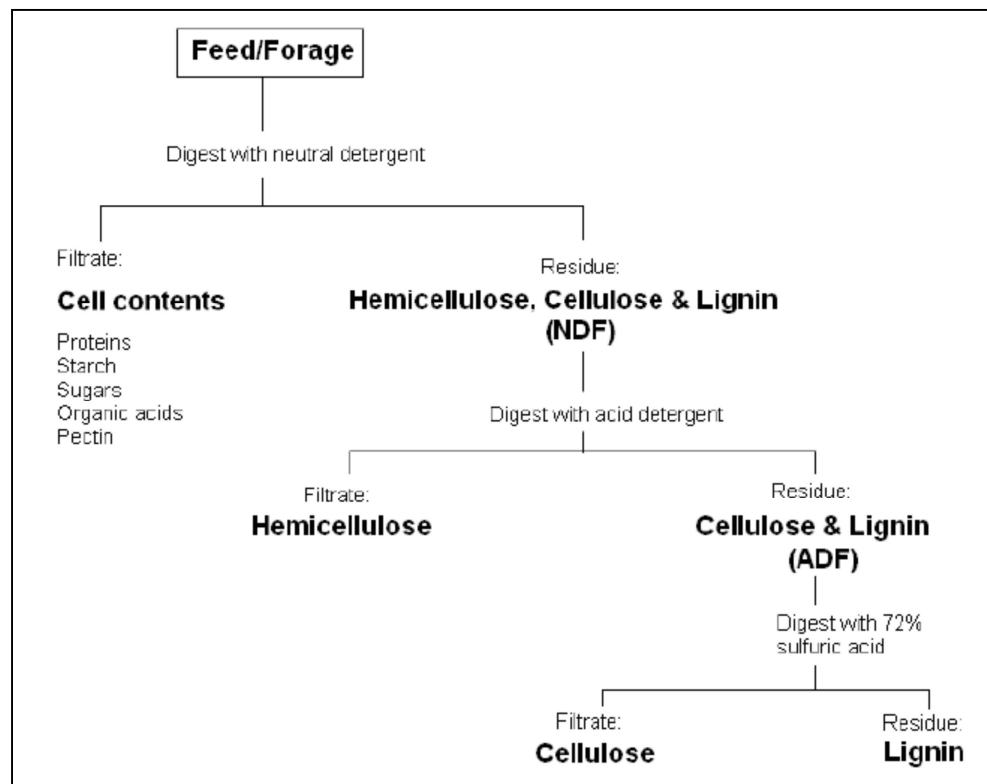


Figure 32 Detergent fibre system according to Van Soest[141-143]

Table 6 Detergent fibre system according to Van Soest[141-143]

Methods	Principle	Residue Content
NDF (Van Soest)	Neutral Detergent Fibre is defined to be the residue after treatment with a neutral detergent solution (Sodium lauryl sulphate and EDTA)	Cellulose, 100% Hemi cellulose, 100% Lignin, 100%
ADF (Van Soest)	Acid Detergent Fibre is defined to be the residue after treatment with an acid detergent solution (Cetyltrimethylammonium bromide in Sulphuric acid solution)	Cellulose, 100% Lignin, 100%
ADL (Van Soest)	Acid Detergent Lignin is defined to be the residue after initial treatment by the ADF method followed by removal of the cellulose fraction through extraction using 72% H ₂ SO ₄	Lignin, 100%

4.4.4 Inorganic elements

The contents of inorganic elements present in biomass, namely chlorine (Cl), calcium (Ca), Iron (Fe), potassium (K), magnesium (Mg), sodium (Na), were determined by calculation based on ash content and composition. The ash content was obtained from the proximate analysis and the ash composition analysis was performed by an external company (MARCHWOOD SCIENTIFIC SERVICES, Marchwood, Southampton, UK) [144] using ICP-OES (inductively coupled plasma-optical emission spectrometer) technique.

4.4.5 Ash Fusion (Oxidising)

Ash Fusion Temperatures (ash melting behavior) of the inorganic constituents of ash was measured after ashing as above. Ash fusion, ash initial deformation, ash softening, and ash hemispherical temperatures were determined using the CEN/TS 15404 [145] method.

4.4.6 Heating Values

The gross heating value was determined using an oxygen bomb calorimeter model Parr 6100 according to ASTM D5865[146]. The bomb calorimeter is a device that is used for determining heats of combustion by igniting a sample in oxygen at a high pressure in a sealed vessel, which is called a bomb. The sample was then burnt completely in an excess oxygen environment and the reaction takes place at constant volume. The energy released by combustion is absorbed within the calorimeter allowing the temperature change (ΔT) to be recorded.



Figure 33 Parr 6100 bomb calorimeter

The results were then compared using the unified correlation for fuels developed by Channiwala et al. [147, 148], which the authors claim can be used to calculate the (HHV) higher heating value of gases, solids, liquids, biomass and residue derived fuels. The mass fractions (expressed as percentages) obtained from the ultimate analysis for C, H, S, O, N and ash were used in the chemical equation 16 below.

$$\text{HHV}_{\text{dry}} (\text{MJ/kg}) = 0.34912 * \text{C} + 1.1783 * \text{H} + 0.1005 * \text{S} - 0.1034 * \text{O} - 0.0151 * (\text{N}) - 0.0211 * (\text{A}). \quad (16)$$

4.4.7 Thermo-gravimetric Analysis (TGA)

BSG and barley straw were also analysed using TGA and DTG techniques. Thermo-gravimetric analysis pyrolysis profiles were produced using a computerised Perkin Elmer Pyris 1 TGA apparatus auto sampler with either air or nitrogen gas flow of 40mL/min at 10°C/min heating rate see Figure 34 for illustration. TGA is a valuable technique as it can be used to determine a material's thermal stability and its fractions of volatile components by monitoring the weight change that occurs as the sample is heated.



Figure 34 Perkin Elmer Pyris 1 TGA

Approximately, 4-5 mg of duplicate sample was loaded into a tarred crucible. Pyrolysis of the sample was carried out in an inert atmosphere, and combustion was carried out in a purged atmosphere of air. Both were carried out with the following temperature programme:

1. Heating from ambient to 50°C at a heating rate of 5°C/min
2. Hold for 5 minute at 50°C
3. Heat from 50°C to 105°C at 5°C/minute
4. Hold for 5 minute at 105°C
5. Heating from 105°C to 900°C at 25°C/minute
6. Hold for 15 minutes at 900°C

4.5 Characterisation of Intermediate Pyrolysis Products

The intermediate pyrolysis of BSG gives a liquid bio-oil as the main product with solid char and permanent gases as by-products. All products were analysed in order to complete the mass balance and to gain insight into the main product properties. This section describes the analytic methods used for the characterisation bio-oil, char and permanent gases.

4.5.1 Bio-oil Analysis

Bio-oil is the main product obtained by the intermediate pyrolysis of BSG. For both Pyroformer and bench-scale (catalytic and non-catalytic) intermediate pyrolysis experiments, characterization of bio-oils included gas chromatography, ultimate analysis, water content, pH value, acid number, heating value, kinematic viscosity, flash point, ash, carbon residue and corrosivity. These analysis techniques are described in the following sub-sections.

4.5.1.1 Gas Chromatography/ Mass Spectrometer (GC/MS) analysis

GC-MS was performed to identify the most abundant compounds present within the pyrolysis oil. Samples of the bio-oils obtained from the Pyroformer, catalytic and non-catalytic experiments was diluted in ethanol in a 1:10 ratio. GC-MS analysis was conducted using a Hewlett Packard HP 5890 Series II Gas Chromatograph with an automatic injector and auto sampler with a DB 1706 non-polar capillary column of 60m x 0.25 mm x 0.25 μm . Helium was used as the carrier gas at a constant flow rate of 1.5ml/min The initial oven temperature was 40°C and ramped up to 290°C. Identification of the GC-MS peaks was based on the comparison between the Mass finder library and Wiley library.

4.5.1.2 Ultimate analysis

All bio-oil liquids collected were sent to an external company MEDAC Ltd for CHN analysis to obtain carbon, hydrogen and nitrogen with oxygen determined by difference using a Carlo-Erba EA1108 CHNS-O analyser. Poisonous elemental analysis to determine sulphur and chlorine was also conducted.

4.5.1.3 Water content

The water content of the bio-oils was determined using a Mettler Toledo V30 Compact Volumetric Karl Fischer (KF) titrator in accordance with ASTM E203[149]. This method is widely used for the determination of water content of bio-oils. Before each measurement the instrument was calibrated using HPLC-grade water. Three samples of each bio-oil from pyrolysis experiments were subjected to water content analysis.

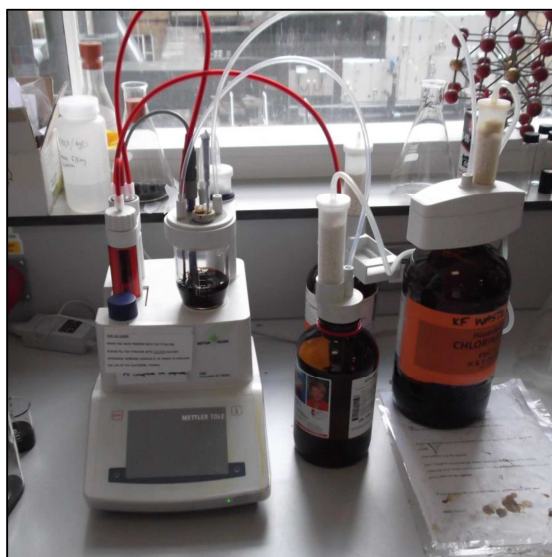


Figure 35 Mettler Titrator for Water Content

4.5.1.4 pH value

The pH was obtained using the Sartorius basic meter PB-11. Bio-oil is usually acidic due to the presence of acetic acid and formic acid. All bio-oil samples obtained from Pyroformer, bench-scale (catalytic and non-catalytic) intermediate pyrolysis experiments were subjected to pH determination. Prior to each pH measurement the instrument was calibrated with liquid calibration standards.

4.5.1.5 Acid number

Total acid number (TAN) of the oils was measured with a Mettler Toledo V20 Compact titrator using the potentiometric titration method in accordance with ASTM D664. The oil sample was dissolved in 50/50 toluene and isopropanol solution and titrated potentiometrically with 0.1N alcoholic potassium hydroxide using a combination electrode. Readings are automatically plotted against the volume of titrating KOH solution used until the titration end-point was achieved.



Figure 36 Mettler Toledo Titrator for Acid Number

4.5.1.6 Heating value

The gross heating value was determined using an oxygen bomb calorimeter model Parr 6100 according to ASTM D5865 [146]. The results were then verified using the unified correlation developed by Channiwala et al. [147, 148]

$$\text{HHV (MJ/kg)} = 0.34912 C + 1.1783 H + 0.1005 S - 0.1034 O - 0.0151 (N) - 0.0211 (A) \quad (16)$$

4.5.1.7 Kinematic viscosity

Kinematic viscosity, which is the resistance to flow of a fluid under gravity, was measured in accordance with ASTM D445[150] with a Cannon-Fenske Routine glass capillary viscometer. Bio-oil produced from the Pyroformer was analysed only. During the test, fixed volume of oil samples are passed through the capillary of the viscometer under gravity at 40°C. The sample travelling time is recorded. The kinematic viscosity was then the product of the viscometer calibration constant and the measured flow time.

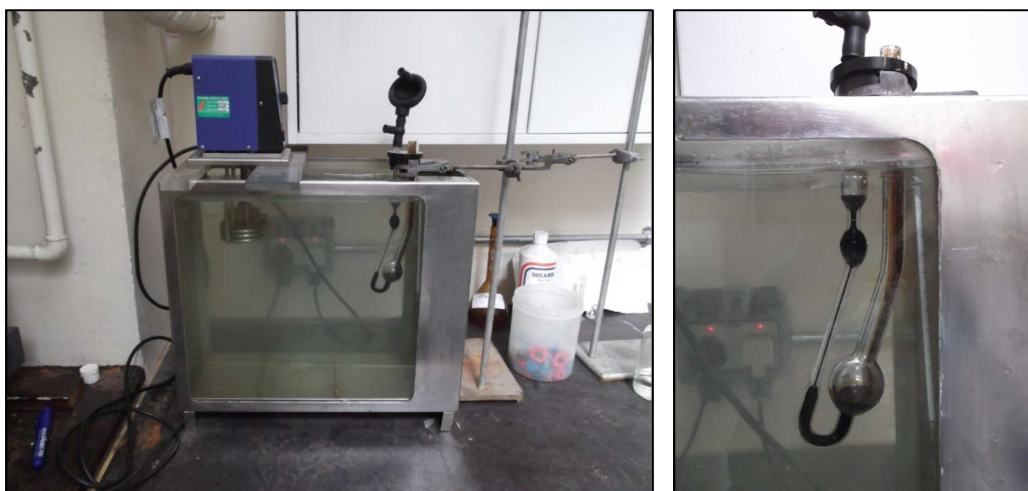


Figure 37 Cannon-Fenske Routine glass capillary viscometer

4.5.1.8 Flash point

Flash point of bio-oil only produced from the Pyroformer was determined in accordance with ASTM D7236 [151] by a Seta Flash Series 3 plus Closed Cup (Auto Ramp) Tester. A test flame is directed to the pre-set location where the vaporised oil may be released at specified temperature intervals until the flash is detected.

4.5.1.9 Ash

Ash content of bio-oil only produced from the Pyroformer was determined in accordance with ASTM D482[152]. The carbonaceous solid samples produced from the Carbon Residue test were combusted in a muffle furnace at 775°C. The remaining ash was cooled at room temperature and weighed, and then expressed as a mass percentage of the original oil sample.

4.5.1.10 Carbon residue

The Conradson Carbon Residue test was performed on bio-oil produced only from the Pyroformer in accordance with ASTM D189 [153] by a manual method. A weighed sample is placed in a crucible and undergoes strong heating by a Meeker burner. The carbonaceous residue remaining after the cracking and coking reactions is cooled to room temperature and weighed. The Conradson Carbon Residue is then the carbonaceous residue expressed as a mass percentage of the original oil sample

4.5.1.11 Corrosivity

The bio-oil produced from the Pyroformer was analysed for corrosiveness test was carried using a Stanhope-SETA cooper corrosion test station in accordance with ASTM D130[154]. A polished copper strip was immersed into the tested oil samples which were placed in a 40°C heated bath. The copper strips were compared to the ASTM corrosion standard board after periods between 6 and 24

hours.

4.5.2 Char Analysis

4.5.2.1 Ultimate analysis

The elemental analysis of char samples was performed in order to determine the carbon, hydrogen, nitrogen and sulphur contents. Only one char sample which was produced from the Pyroformer was analysed. Char samples from bench-scale intermediate pyrolysis experiments at different heating rates were collected and analysed. The technique applied is the same as described in Chapter 4.

4.5.2.2 Proximate Analysis

All char proximate analysis were performed by Medac Ltd, Surrey UK. The technique applied is the same as described earlier in section 4.4.1.

4.5.2.3 Ash analysis and composition

The ash obtained from the char was subjected to metal elemental analysis for the determination of calcium (Ca), iron (Fe), potassium (K), magnesium (Mg), and sodium (Na) content. In addition chlorine (Cl) was also obtained. The total ash content was obtained from the proximate analysis and the ash composition analysis was performed by Medac Ltd, Surrey UK.

4.5.2.4 Heating Value

The gross heating value for char samples was determined using an oxygen bomb calorimeter model Parr 6100 according to ASTM D5865. It was also obtained from the elemental analysis and the ash content of the char sample using Equation 16 as described in section 4.4.6.

4.5.2.5 Thermo-gravimetric analysis (TGA)

Char samples was analysed using TGA and DTG techniques. Thermo gravimetric analysis combustion profiles was conducted using a computerised Perkin Elmer Pyris 1 TGA apparatus auto sampler with an air gas flow of 40mL/min at 10°C/min heating rate. The same technique for thermo gravimetric analysis was conducted as described earlier in section 4.4.7.

4.5.3 Permanent gases Analysis

Analysis of permanent gases produced from experiments was analysed using a Hewlett Packard HP-5890 series 2 device Gas Chromatograph Thermal Conductivity Detector (GC-TCD) with a 60/80 Carboxen-1000, 15' x 1/8" SS (2.1mm ID) column. Helium is used as the carrier gas with a flow rate of 30ml/min. The oven temperature is programmed with an initial temperature of 35°C and was heated at a ramping rate of 20°C/min to 225°C. The column had been calibrated to detect H₂, CO, CO₂, N₂

and CH₄. Approximately 150 micro litres of clean sample gas is extracted from the gas sampling system using a gas tight micro syringe and injected into the GC for analysis.

4.6 Results and Discussion

4.6.1 Freezing

Figure 38 shows a comparison of wet BSG (70% moisture content) preserved by freezing (left) with the same material which was not (right), after three days. The unpreserved material presents black spots indicating microbial degradation; and releases strong odours and heat.



Figure 38 (right) Wet BSG with signs of degradation, (left) dried and ground BSG material



Figure 39 Degradation of wet BSG over 3 days if left untreated

4.6.2 Drying

BSG was dried using a fan assisted oven. A bag of BSG with ~70% moisture content weighing approximately 15-20kg was removed from the freezer and allowed to thaw for 24hours at room temperature. The oven comprised three shelves with trays. A full bag of wet BSG was evenly dispersed within the three trays ensuring large clump of bonded grain was broken down to smaller clumps.

The initial moisture of the wet BSG was measured using the Sartorius moisture analyser MA35. The oven drying rate was determined by drying the grain at 70°C and measuring the moisture of the grain every hour. Figure 40 illustrates the oven drying rate over 21 hours of drying. The chart shows a linear decline in moisture with the grain losing 3% moisture per hour. After 21 hours of drying a full bag of grain was dried with consistent moisture content of 5-10% and a total grain quantity of 10-12kg.

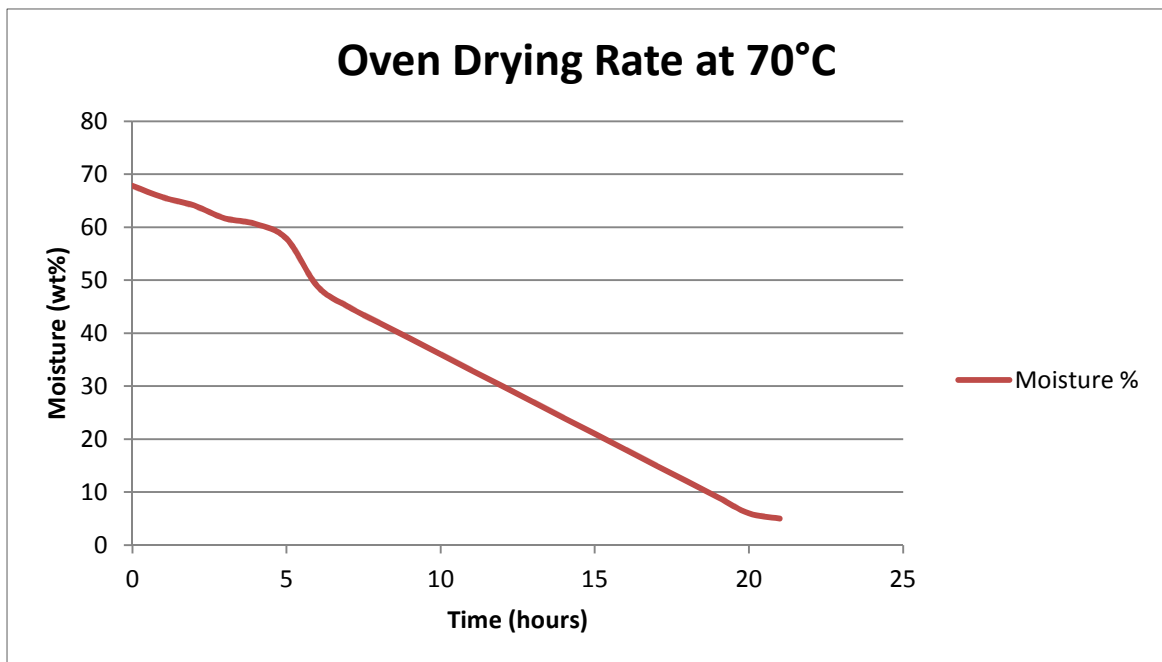


Figure 40 Oven drying rate of BSG at 70°C

Reducing the moisture content was not only important to preserve BSG but equally when undergoing thermal conversion. In pyrolysis, the amount of water present in the feed material will ultimately end up in the final liquid product. As reported by Bridgwater 2004, the water in the bio-oil has negative and positive effects, in that it lowers heating value yet it improves bio-oil flow characteristics [22]. In a gasification process a high moisture feedstock above about 30% can make ignition difficult, reduce the product gas heating value and ultimately reduce the thermal efficiency of the process. This is

because the moisture reduces the temperature achieved in the oxidation zone, resulting in the incomplete cracking of the hydrocarbons released from the pyrolysis zone.[155]

4.6.3 Grinding

In order to utilise this equipment it was important to ensure the moisture content of the feed was no higher than 15%; higher moistures would lead to blockages. It was necessary to mill the BSG as the dried material would agglomerate forming lumps of various sizes which would be difficult to handle or feed in a screw feeder.



Figure 41 Ground BSG material

Illustrated in Figure 41 is dried and ground BSG. This was now suitable for storage; ease of handling and for screw feeding systems in thermal conversion applications. Particle size distributions of the ground BSG are compared to ground barley straw in Table 7 below.

Table 7 Particle size distribution of BSG and barley straw

Particle size (μm)	Content (wt.%, as received)	
	BSG	Barley
250	7.3	10.41
300	18.98	5.41
425	12.01	17.78
500	14.6	21.05
600	27.93	28.51
850	7.49	8.99
1000	11.69	7.86
TOTAL	100	100

4.6.4 Pelletizing



Figure 42 BSG pellets

The ground BSG was added to the pellet machine hopper which feeds the material gradually into the mould and roller shaft. As the roller shaft would rotate on the mould the screws to the roller shaft was adjusted and tightened to ensure pellets would form. Initially the material emerged as fines. This was due to the grain having too low moisture content (5-7%) for binding to take place.

In order to resolve this a little water was added to the feed both prior to and during feeding to aid the binding process. More pressure was exerted by tightening the screws to ensure the space between roller shaft and mould was 0.1-0.3mm. Under these conditions pellets were formed, with a length of 4-12mm.

4.6.3 Feedstock Characterisation

4.6.3.1 Proximate and Ultimate analysis

Table 8 Results of proximate and ultimate analysis of BSG

Analysis	BSG	Barley Straw Pellets	Wheat Straw Pellets	BSG	BSG	BSG (Barley)	WSG (Wheat)	BSG (Barley-Sorghum)	BSG (Barley-Maize)
	This Study	This Study	This Study	Becidan et al 2006[111]	Okamoto et al 1999[124]	Sanna et al 2011[135]		<i>Emwermadu et al 2008[67]</i>	
<i>Proximate Analysis wt.% (dry basis)</i>									
Moisture	8	11.9	13.3	-	-	4.6	6.6	-	-
Volatiles	78	74.9	76.3	78.75	-	61.4	75.2	-	-
Fixed Carbon	9.5	7.2	6.9	16.22	-	17	16	-	-
Ash	4.5	6	6.5	5.03	4.37	6.5	2.2	4.46	6
Heating Value (MJ/kg)	18	17	18	20.83	12.1	18.55	18.35	19.52	18.09
<i>Ultimate Analysis wt.% (dry basis)</i>									
Carbon	46.6	44.2	45.7	51.59	49.85	49.8	43.2	48.36	49.1
Hydrogen	6.85	6.1	6.4	7.07	7.11	6.38	6.5	6.02	6.24
Oxygen	42.26	30.4	26.6	36.96	34.13	39.36	45.8	36.73	39.61
Nitrogen	3.54	0.4	0.5	4.15	4.54	4.14	4.5	4.11	4.69
Sulphur	0.74	0.6	0.6	0.23	-	0.1	0.1	0.32	0.36
Chlorine	0.1	0.4	0.4	-	-	-	-	-	-

The proximate analysis results in Table 8 show that BSG has relatively high volatility content in the range 61-78%. The high volatility content for BSG suggests that under intermediate pyrolysis conditions it would produce a high liquid yield and a low char yield.

The high volatility content determined for BSG is particularly good if used as a feed for gasifiers also. Therefore a suitable gasifier would be needed to convert the volatile components and heavy hydrocarbons released during the pyrolysis stage of a gasification process. The heating value as determined using the oxygen bomb calorimeter gave a higher heating value (HHV) of 18MJ/kg. This was checked with the HHV obtained using Channiwala's equation [147, 148] see section 4.4.6. The HHV result was found to be 19.2 which are in reasonable agreement with the values obtained in Table 8.

The ash contents measured for BSG ranged between 4 and 6%. Both barley and wheat straw pellets ranged between 6-6.5%. BSG has a relatively high ash content in comparison to those of wood 0.4%, beech 1% and cypress 0.4% which are far lower see Table 8 for comparison [2]. The results in Table 8 above show that BSG is comparable to barley and wheat straw. Since the ash content in BSG is relatively high in comparison to other biomass samples, it implies a higher level of inorganic compounds is expected.

Table 9 Ultimate analysis of other biomass [2]

	Ash	Cypress	Beech	Wood	Miscanthus	Rice	Barley Straw	Wheat Straw	Lignite
<i>Ultimate Analysis wt.% (dry basis)</i>									
Carbon	49.7	55	51.6	51.6	48.1	41. 4	45.7	48.5	56.4
Hydrogen	6.9	6.5	6.3	6.3	5.4	5 39.	6.1	5.5	4.2
Oxygen	43	38.1	41.4	41.5	42.2	9	38.3	41.6	18.4
Nitrogen				0	0.5	0.7	0.4	0.3	1.6
Sulphur				0.1	0.1	0.1	0.1	0.1	
Ash	0.4	0.4		1	2.8		6	4	5

The ultimate analysis from Table 8 shows that BSG contains 46.6 wt. % carbon, 6.85 wt.% hydrogen, 42.26 wt.% oxygen, 3.54 wt.% nitrogen and small amounts of sulphur and chlorine. Nitrogen is quite high in comparison to other biomass such as wood, barley and wheat straw pellets. This could be due to the higher protein content present, and could lead to higher NO_x emissions when combusted. Sulphur and chlorine are only present in small quantities but could still cause poisoning of catalysts. Table 9 provides ultimate analysis of other biomass feedstock's as a comparison and reveals that barley and wheat straw are very similar to BSG. As mentioned earlier, barley is the main raw material used in the brewing industry.

4.6.3.2 Chemical compositional analysis

The chemical compositional analysis of BSG gave values of 18.98 wt. % cellulose, 33.59 wt. % hemicelluloses, 12.61 wt.% lignin, and 34.82 wt.% extractives. In the literature cellulose varies between 14 and 26 wt. %, hemicelluloses between 21 and 34 wt.% and lignin between 6 and 28 wt.%. Therefore BSG as reported by this study has a relatively low lignin content, however literature has reported [156]that lignin contents can vary depending on the analysis method adopted. Biomass with low lignin content has been suggested by Ghetti et al to produce a lighter pyrolysis product (bio-oil), which in turn is better if used as a fuel [156, 157].

Table 10 Chemical compositional analysis and comparison

Component (dry wt.%)	BSG (This Study)	BSG (ECN) PHYLLIS[158]	BSG ^a	BSG ^b
Cellulose	18.98	14.7	25.4	16.8
Arabinoxylan	nd	nd	21.8	28.4
Hemicellulose	33.59	30.5	nd	nd
Lignin	12.61	6.1	11.9	27.8
Extractives	34.82	nd	nd	nd
Lipids	nd	5.3	10.6	nd
Protiens	nd	31.1	24	15.2
Starch	nd	nd	nd	nd
Ash	4.5	5.1	2.4	4.6

4.6.3.3 Inorganic elements – Metal oxide analysis

The analysis of inorganic elements for BSG shows mainly magnesium (Mg), alumina (Al), silica (Si), phosphorous (P), potassium (K), and calcium (Ca). The results were quite similar to barley and wheat straw. Lower ash content fuels such as wood chips (0.1%) are suitable for fast pyrolysis which has the objective of maximising organic liquid yields.

Ash has a natural catalytic effect due to the presence of these inorganic elements (mainly alkali metals) which tends to crack the vapours and reduce liquid yield [159]. The relatively high ash content of BSG (4-6%) is one reason why the present work uses intermediate pyrolysis.

In gasification processes, high ash content and high inorganic elements can cause problems of sintering, agglomeration, deposition, erosion and corrosion. Both fixed bed gasification and fluidised bed systems can exhibit lagging or agglomeration of ash within the gasifier bed[160].

Table 11 Inorganic elements Metal oxides

Component (dry wt.%)	BSG (This Study)	Barley Straw Pellets	Wheat Straw Pellets
MgO	1.3	1.6	1.8
Al ₂ O ₃	3.8	3.2	2.6
SiO ₂	44.1	42.3	41.9
P ₂ O ₅	1.2	1.1	1
K ₂ O	15.6	17.2	15
CaO	5	5.2	4.7
TiO ₂	<0.1	<0.1	<0.1
MnO	<0.1	<0.1	<0.1
Fe ₂ O ₃	<0.1	<0.1	<0.1
CuO	<0.1	<0.1	<0.1
ZnO	<0.1	<0.1	<0.1
PbO ₂	<0.1	<0.1	<0.1
SO ₃ (as above)	8.7	9.2	8.5
Chloride (as above)	1.1	4.2	3.7

4.6.3.4 Ash Fusion (Oxidizing)

The analysis of BSG ash fusion shows an initial deformation temperature of 1090°C, a softening temperature of 1140°C, a hemispherical temperature of 1180°C and a flow temperature of 1230°C. Ash fusion isn't so much of a problem for pyrolysis systems as these do not normally exceed temperatures of 500°C, considerably below the melting point of BSG ash.

Table 12 Ash Fusion by using characteristic temperatures

	Initial Deformation (°C)	Softening Temperature (°C)	Hemispherical Temperature (°C)	Flow Temperature (°C)
BSG	1090	1140	1180	1230
Barley	1080	1150	1180	1270
Wheat	1400	>1450	>1450	>1450

The melting point of biomass ash is important in gasification. The high mineral matter, in particular alkali oxides, can melt if the temperature in the oxidation zone is high enough. Alkali metals such as potassium (K) and sodium (Na) have lower melting and evaporation points than any other inorganic material present in the fuel, and can react readily with silicates during combustion. Potassium (K) can react with other elements such as chlorine to produce potassium chloride (KCl) which has two major disadvantages; in that it has a very low melting point (below 800°C) and is highly corrosive. Elements such as Al and Si are able to trap alkali metals limiting the formation of alkali chlorides [161-163]. BSG in this study has a SiO₂ of 44.1%, K₂O of 16%, CaO of 5% and Al₂O₃ of 3.8% see Table 11.

4.6.3.5 Thermo-gravimetric analysis (TGA)

The TGA differential thermo gravimetric (DTG) weight loss profiles for BSG and barley are shown below in Figure 43 and 44. Barley has been analysed as for comparison purposes only. The DTG curves for the two samples show similar thermal behaviour. Much of the weight loss for BSG occurs between temperatures of 200 and 450°C. Literature has reported that the basic biomass components, hemicellulose, cellulose and lignin, decompose thermo-chemically in the following temperature ranges: 150-350°C, 275-350°C and 250-500°C.[164] The DTG profile for BSG shows the first step shoulder peak between 170-320°C which represents the decomposition of hemicellulose and the initial decomposition of cellulose. The second step, the shoulder peak between 320-450°C signifies the final decomposition of cellulose and lignin. Due to the high volatility content, most of the volatiles are released below 450°C.

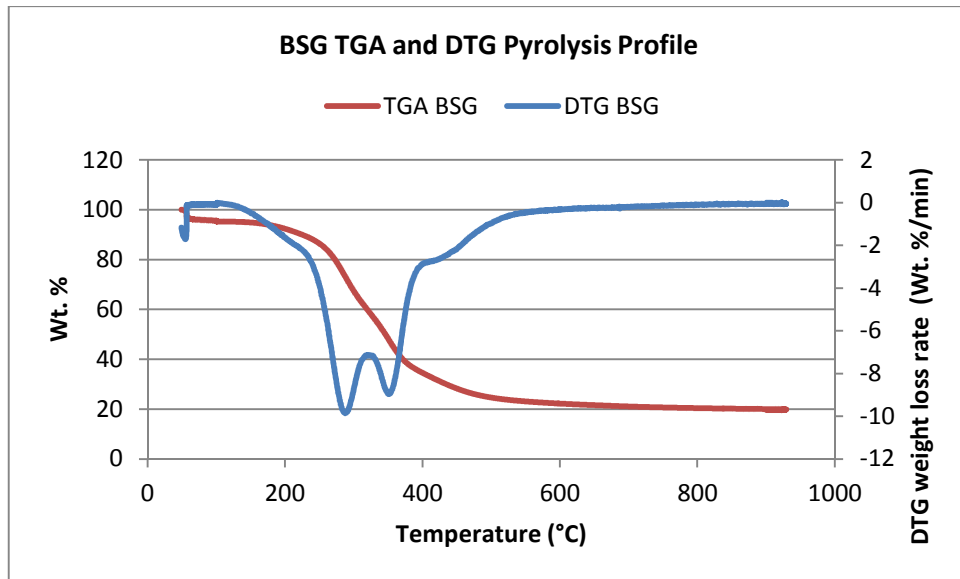


Figure 43: BSG TGA and DTG Pyrolysis Profile

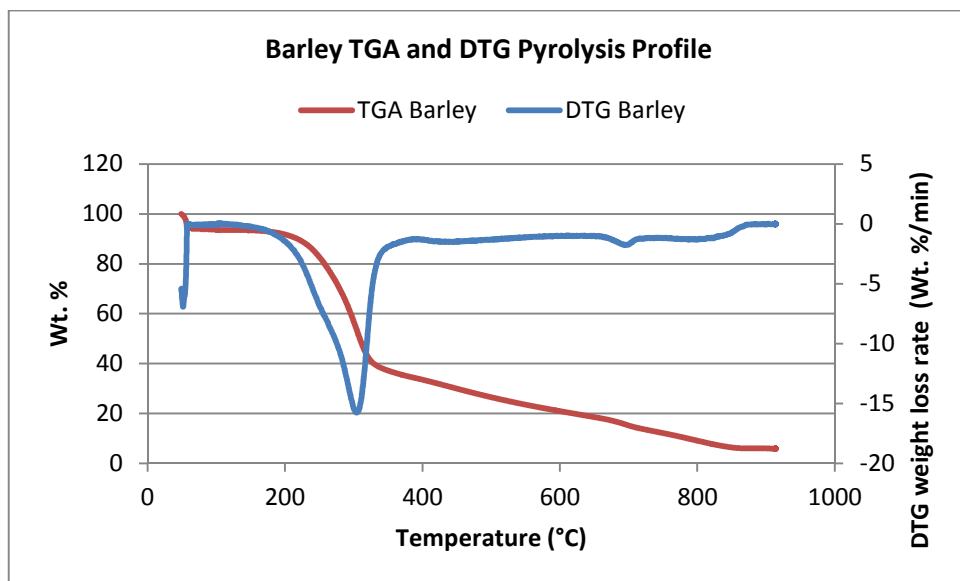


Figure 44: Barley TGA and DTG Pyrolysis Profile

4.7 Summary

The pre-treatment and characterisation of BSG has been reported in this chapter. The results improve understanding of the behaviour of the feedstock in advanced thermo chemical systems (pyrolysis and gasification). BSG was pre-treated by initial storage in a freezer followed by drying to reduce the moisture to acceptable levels for thermo chemical conversion. This was imperative as BSG is a very wet material (67-81% moisture) making it a very unstable and difficult material to store and transport due to microbial degradation. The results show that BSG can be dried to a moisture content of 8% suitable for both pyrolysis and gasification.

Proximate, ultimate, chemical composition, inorganic element, ash fusion and heating value analysis were conducted. BSG has a high volatile content (78% dry basis) and contains 46.6% carbon, 6.85% hydrogen, 42.26% oxygen, 3.54% nitrogen, 0.74% sulphur and 0.1% chlorine. Chemical compositional analysis has revealed that BSG is composed of 18.98% cellulose, 33.59% hemicelluloses, 12.61% lignin and 34.82% of extractives. The analysis of inorganic elements for BSG shows mainly magnesium (Mg), alumina (Al), silica (Si), phosphorous (P), potassium (K), and calcium (Ca). BSG has an ash initial deformation temperature of 1090°C, an ash softening temperature 1140°C, an ash hemispherical temperature 1180°C and an ash flow temperature of 1230°C. The heating value of BSG is approximately 18 MJ/kg on a dry basis. The TGA and DTG profile for BSG shows the first step shoulder peak between 170-320°C which represents the decomposition of hemicellulose and initial decomposition of cellulose. The second step the shoulder peak between 320-450°C signifies the final decomposition of cellulose and lignin. Due to the high volatility content, most of the volatiles are released below 450°C.

To date there has been very limited work on the thermochemical conversion of BSG. The results of this study show that BSG can be preserved prepared and also have thermal characteristics making it suitable as a potential fuel for either pyrolysis or gasification.

5 Experimental Gasification Methodology & Results

5.1 Introduction

This chapter describes the experimental methodology for the gasification of BSG. In this study a fixed bed downdraft gasification unit was selected to perform the gasification test. The study investigates whether BSG can be thermally converted as a feedstock for fixed bed downdraft gasification operation and whether it can produce a product gas that can potentially run an engine for heat and power. As indicated in Chapter 3, BSG thermochemical processing of BSG by gasification has not been explored previously. The studies will also consider areas for further exploration such as fluidized bed gasification, and the coupling gasification reactors with reforming reactors containing catalysts in order to reform the tars and enhance the product gases.

5.2 Fixed Bed Downdraft Gasifier

The GEK fixed bed downdraft gasifier was available at Aston University and is an Imbert type fixed bed downdraft gasification unit. It has the potential of producing a product gas with low tar suitable to power an internal combustion engine. It was designed and manufactured in the USA by All Power Labs and is shown in Figure 45.[165]



Figure 45 GEK Fixed Bed Downdraft Gasifier[165]

The gasifier has a maximum mass feed rate of 20kg/h based on wood chip and operates at negative pressure using a downstream venturi air ejector to draw the gasification air into the gasification zone. The gasification air is preheated via a heat exchanger jacket using the hot product gases leaving the reactor.

The airflow rate is in the range 10-20m³/hr. The chips/biomass must be no bigger than 2cm in length, 1 cm width and 0.5cm thickness. Moisture level of the biomass must be between 5-20% (wet basis). Temperature of gasification can range between 850°C to a maximum of 1200°C depending on the feedstock. Figure 46 provides an illustration of the gasifier operation.

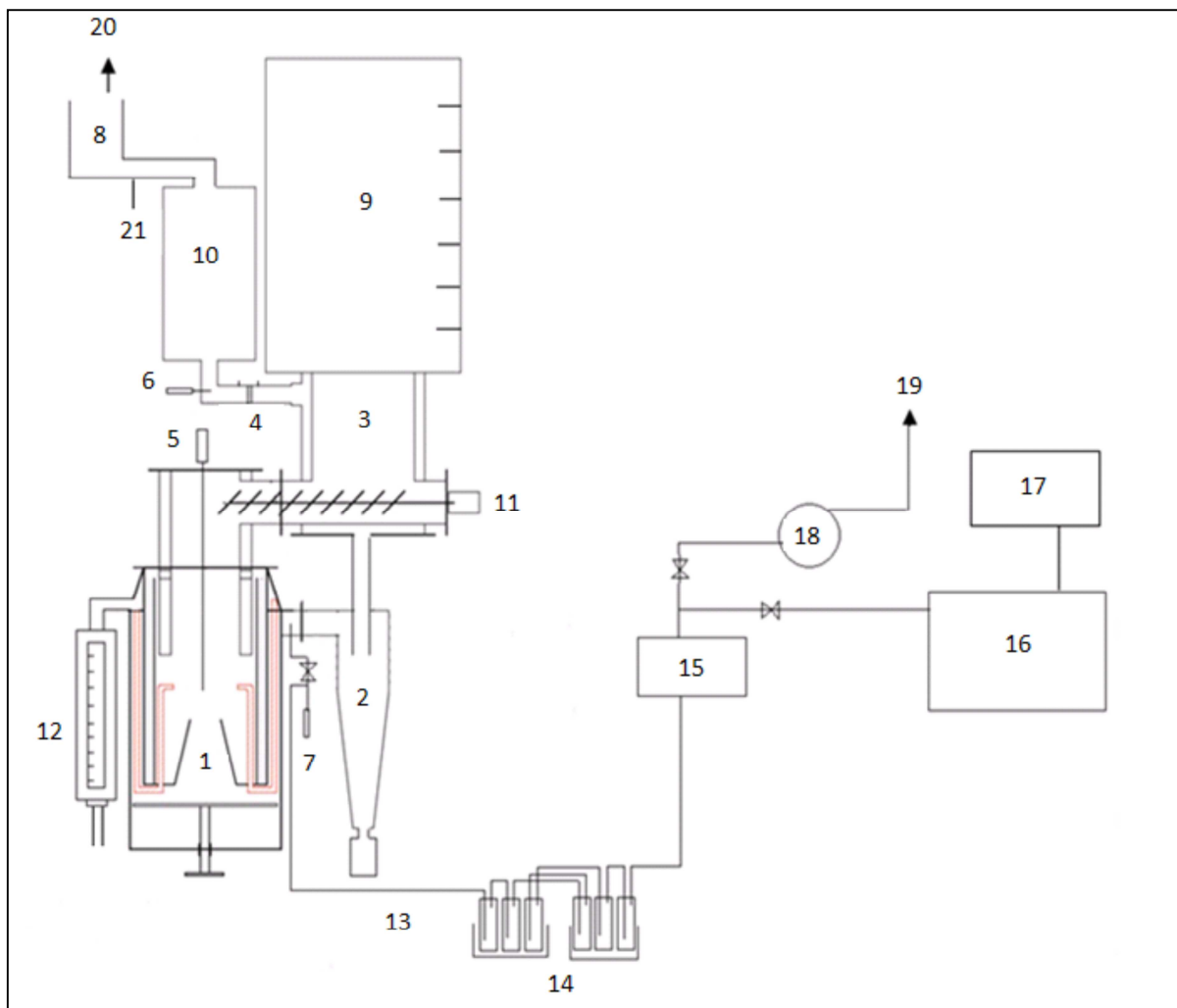


Figure 46 Downdraft gasification operation [166]

- 1 Gasifier, 2 Cyclone, 3 Heat Exchanging Drying Bucket, 4 Orifice Plate, 5 Thermocouple, 6 Thermocouple, 7 Thermocouple, 8 Swirl Burner, 9 Calibrated Glass Hopper, 10 Carbon Absorption Filter, 11 Auger, 12 Air Rotameter, 13 Gas Sampling Line, 14 Gas Wash Bottles, 15 Digital Mass Flow Meter, 16 Gas Chromatograph, 17 Computer, 18 Gas Suction Pump, 19 Vent, 20 Main Vent, Venturi Ejector

5.2.1 Gasification preparation and assembly

Before experimentation, the gasifier is disassembled and cleaned to remove any fouling from tar; char and ash build up before it can be reassembled with new gasket seals all round. The gasification chamber is then filled with approximately 3kg of charcoal before the top lid is resealed to ensure a gas tight seal. The glass hopper is filled with the biomass of known weight, and a cold run is conducted to ensure there are no gas leaks.

To begin experimentation the venturi ejector valve is opened to allow air to enter, an ignition source is then introduced into the ignition chamber using a propane burner to ignite the gasifier. With successful ignition, the feeder is then switched on to replenish any consumed biomass and the reactor is then allowed to reach steady state gasification temperatures of approximately 800-1000°C. Once these temperatures had been achieved the flare is also ignited using the propane burner. The GEK temperature can be controlled by altering the airflow rate.

After startup the nominal air flow rate is 10m³/hr. for gasification to occur, but the flow can be either increased or decreased using the ejector flow monitored by a rotameter to achieve the desired gasification temperature. The biomass feedrate is determined by multiplying the average bulk density of the feedstock by the reduction of hopper volume.

The air inlet is determined by using a calibrated air rotameter at the air inlet port to determine flow rates, k-type thermocouples for temperature measurements, pressure transducers installed to measure pressure and pressure drop, a calibrated orifice plate for outlet product gas flow rate and a gas sampling line for tar, water and product gas composition.

Figure 47 illustrates the gasifier chamber consisting of throat, ignition port and five air inlet nozzles. Figure 48 illustrates the air inlet pipes that are pre-heated within the heat exchanger jacket containing the hot product gases leaving the gasifier.

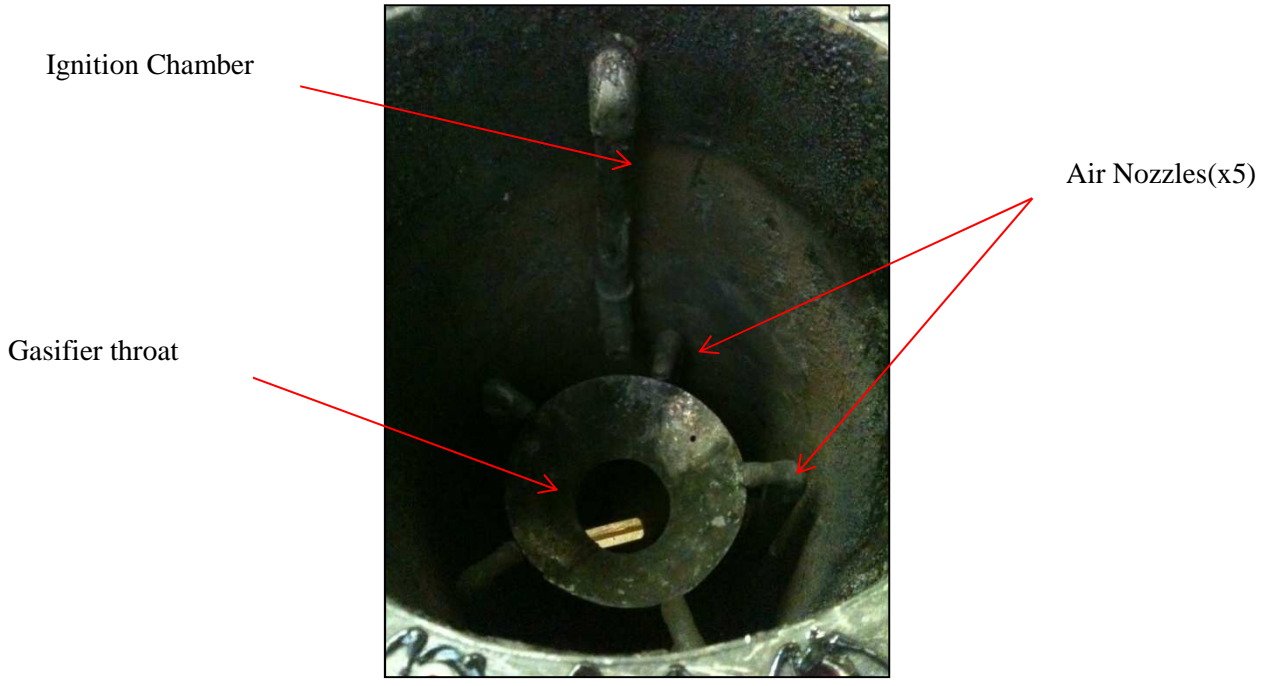


Figure 47 Gasification chamber



Figure 48 Gasification reactor and pre-heated air inlet pipes

5.2.2 Gasifier Control Unit (GCU)

The GEK Gasifier Control Unit (GCU) is an open source sensing control board designed and developed for testing and control of gasification equipment.

The GCU control unit board below offers a number of thermocouple, pressure, analogue signal and rpm timer inputs with a generous array of Pulse Width Modulation (PWM) speed control, servo driver and higher current DC switched outputs.

Thermocouple and pressure transducers from the gasifier are connected to the GCU to measure flow rates, pressure difference, gas outlet temperature and bed temperature. All recordable data is electronically measured by the GCU and sent to a computer every second.

5.2.3 Tar Analysis – Guideline Method ECN

The guideline method is a technique developed by the European research Centre of the Netherlands (ECN Biomass) [167] that allows sampling and analysing of tars and particles that may be present in biomass gasification product gases. A sample of product gas containing tar and particulates is removed through a gas outlet pipe (or sampling location) and passed through a ‘tar train’, a series of gas impinge bottles. The series of impinge bottles are placed in a temperature controlled bath to condense the tars at low temperatures. The bottles contain an extraction solvent, usually iso-propanol (propan-2-ol), and glass beads to improve scrubbing efficiency.

The tar train comprises six interconnected impinge bottles that are placed in a hot bath of 50°C (bottles 1, 2 & 4), and a cold bath containing dry ice (bottles 3, 5&6). The collection of tars takes place through both condensation and absorption in the extraction solvent contained in the impinge bottles.

Immediately after sampling the contents of the impinge bottles are further analysed. To begin with they are decanted into a dark storage bottle. The concentrations of the inorganic compounds are determined by GC analysis of the bulk solution collected [61, 131]. An illustration of the system is illustrated in Figure 49.



Figure 49 Producer gas cleaning system [61]

5.2.4 Rotary Evaporation Unit

A rotary evaporator was used to separate the tar from the tar/iso-propanol mixture with a round bottom flask using a STUART model RE-300 rotary evaporator.

The sample containing a mixture of tar/water and iso-propanol is weighed and poured into a round bottom flask. This sample flask was then attached to the rotary evaporator with the sample flask partially immersed in a heated water bath at approximately 50°C, which is then rotated at constant speed of 40rpm.

A collection flask was used to collect the condensed water and iso-propanol, which is connected to a shell and tube cooled condenser that is operated under vacuum. The evaporated water and iso-propanol is condensed and collected in the collection flask leaving the remaining tar in the sample flask. Figure 50 illustrates the rotary evaporator apparatus.



Figure 50 Rotary evaporator system

Separation of the water / iso-propanol mixture collected in the condensate flask was monitored by visual observation. The rate at which water/isopropanol solution was being collected reduced and eventually stopped. The round bottom flask that contained the initial sample mixture contained only tar at this point.

When separation had completed, the rotary evaporator was pressurised. The tar laden flask was taken and its weight was measured. The difference in weight between the empty flask and the tar laden flask was the total amount of tar collected in the product gas which passed through the tar train.

5.2.5 Water condensate analysis

The amount of water condensate was determined using a V20-compact volumetric Karl-Fischer titration unit using a Hydranol composite 5k titrant, after the extraction of tar. Karl Fischer titration was carried out on the tar free water/iso-propanol solution to determine the water content of the product gas that had passed through the tar train. The tar free water/iso-propanol mixture is weighed before titration takes place. The result that was determined from the titration unit is used to scale up the water produced per cubic metre of product gas in the gasifier. Figure 51 illustrates the Karl Fischer titration system is used to conduct water condensate analysis.



Figure 51 Karl Fischer titration: Water condensate analysis

To carry out this analysis, the glass beaker was initially cleaned by rinsing with fresh solvent Hydranol, followed by draining the contents into a dispensing buret. The empty beaker containing a magnetic stirrer was then filled with fresh solvent until the dual platinum electrode is submerged.

A clean syringe is then used to inject 1g of the water/isopropanol sample into the solvent containing beaker; the weight injected was then manually input into the system using the system control unit before the titration of the sample can start. Once titration had completed by visual observation, the water content was displayed on the control unit screen.

5.2.6 Product Syn-gas analysis

Product syn-gas analysis was conducted using a Hewlett Packard HP-5890 series 2 device Gas Chromatograph Thermal Conductivity Detector (GC-TCD) with a 60/80 Carboxen-1000, 15' x 1/8" SS (2.1mm ID) column. Helium was used as the carrier gas with a flow rate of 30ml/min. The oven temperature was programmed with an initial temperature of 35°C and was heated at a ramping rate of 20°C/min to 225°C. The column had been calibrated to detect H₂, CO, CO₂, N₂ and CH₄. Approximately 150 micro litres of clean sample gas was extracted from the gas sampling system using a gas tight micro syringe and injected into the GC for analysis.

5.3 Gasification Results and Discussion

BSG was oven dried ground and then pelletised using the methodology described earlier in Chapter 4. A pellet form was deemed necessary for satisfactory downdraft gasification. The pellets, with a moisture content of 8%, had a length of 10-21mm and a diameter of 5mm and an overall bulk density of 480kg/m³.

Before the experiment was started the gasifier was assembled with all pipelines cleaned, flange seals removed, cleaned and resealed again in order to ensure the gasifier is gas tight and has no air leaks. High temperature sealant was used on the flange seals before being bolted together.

The reduction zone and throat of the gasifier was initially loaded with approximately 3kg of charcoal as part of the gasifier preparation and assembly. The biomass hopper was loaded with approximately 12kg of BSG pellets. The BSG pellets were then tested within the GEK screw feeder system, which was switched on to ensure the pellets would feed and supply the gasifier accordingly, see Figure 52. This was done to ensure a successful start-up and to achieve steady state within the gasifier.



Figure 52 (left) Feed hopper with BSG pellets (right) screw feeder feeding BSG pellets

Once the area above the gasification zone was loaded with charcoal and BSG pellets, the gasifier lid was closed using a high temperature sealant and bolts tightened to ensure no gas leaks would occur. .

The gasifier was tested for air leaks (cold run) by connecting an airline to the ejector pipe, which creates a vacuum suction within the gasifier; any leaks can be detected by the GCU control unit connected to a computer. The gas outlet during the leak test should measure 12.5 m³/hr. as standard; however the air leak test resulted a gas outlet of 9.9m³/hr. a difference of 2.5m³/hr. Due to this air leak all bolts was checked over and tightened across flanges and the process was repeated.

To begin experimentation, the operation of the gasification unit was started by ensuring there is air flow and a vacuum suction/pressure created within the gasifier by connecting an airline to the ejector pipe. The venturi ejector valve was opened to allow the gasifying air to enter the bed, and a propane burner was used to ignite the char bed.

The ignition of the char bed allowed the char to be consumed and ultimately heated up the gasification bed as well as providing the necessary temperature to commence gasification. The gasifier started well and steady state was achieved after 10 minutes of operation. The gasifier reached a steady gasification temperature of 1000°C. The steady state air flow rate was observed to be 7.1m³/hr. As the gasifier had reached steady state the flare was ignited.

The flare was observed to be strong and stable throughout the duration of the experiment, the experiment lasted approximately 2 hours. The presence of a very strong consistent flare throughout the investigation is a good indicator to the quality of the product syngas produced. Figure 53 illustrates the flare during the gasification of BSG test.



Figure 53 Gasification of BSG flare

The oxidation zone temperature at steady state was 1000°C, and the gas outlet temperature was 65°C. The feed rate was attained by multiplying the feedstock average bulk density by the reduction in hopper volume and was determined to be approximately 9 kg/hr. The gasification air flow rate was recorded and averaged at 6m³/hr. over the duration of the experiment. Figure 54 shows the air flow rate during the experiment.

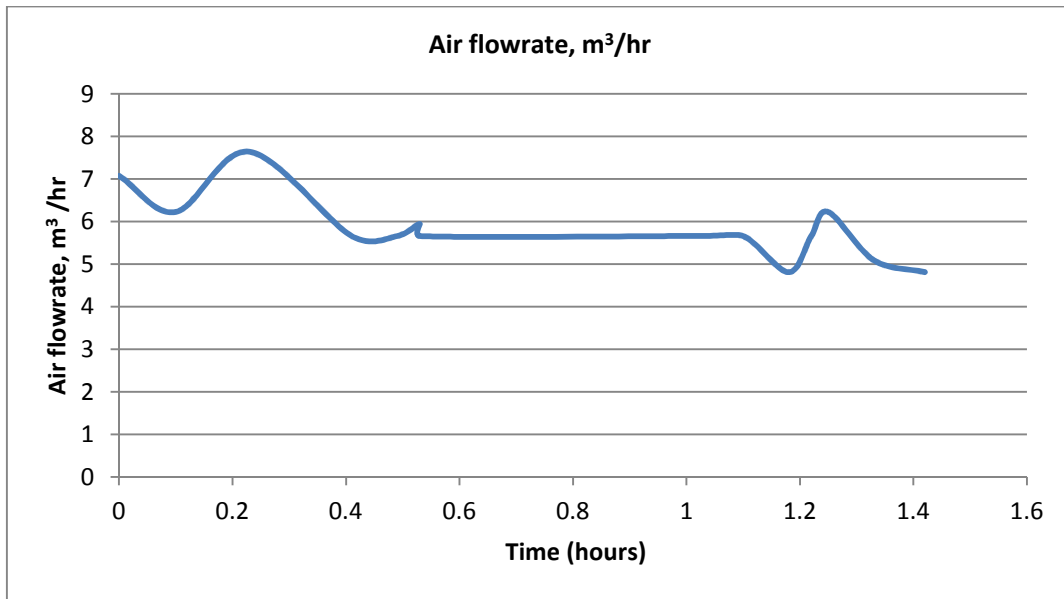


Figure 54 Gasification Air flow rate

A slight increase of air intake into the gasifier was a result of the outlet gas sampling valve leading to the tar train assembly being opened, so that a gas sample could be taken for GC/TCD detection. It was observed after an hour of operation that the air flow rate had declined gradually.

The slight decrease in air flow rate was an indication of some restriction within the bed; to alleviate this problem the ash grate was agitated in order to distribute the ash and allow better distribution of air flow. After 1 hour and 10 minutes of operation no BSG was visible in the biomass hopper and assumed to be consumed in the gasifier.

The equivalence ratio is defined as the actual oxygen to fuel weight ratio divided by the oxygen to fuel ratio stoichiometrically needed which is illustrated as Equation 17:

$$ER = \frac{\text{Actual Oxygen to Fuel Ratio to Fuel Ratio}}{\text{Stoichiometric Oxygen to Fuel Ratio}} \quad (17)$$

The ER determined for the test using air was approximately 0.3, for complete combustion the ER is usually equal to 1. The ER is a key parameter that strongly influences the type of gasification products, a high ER value results in lower concentration of H₂ and CO as well as higher CO₂ in the product gas which lowers the heating value of the product syngas.[168]

The pressure difference across the bed averaged 525Pa, and between the carbon filter outlet, gasification bed and filter 845Pa. Therefore the total pressure drop between the gasification bed and filter was 320Pa.

5.3.1 Product gas analysis

During steady state gasification approximately 380 litres of gas was withdrawn from the gasifier and routed through the tar sampling system. Gas samples for GC/TCD gas detection was taken using a micro litre syringe of approximately 150 μ l. Three samples were taken and measured for analysis over the duration of the experiment at regular 30 minute intervals.

Table 13 and Figure 55 below shows the composition of the product syngas formed from the gasification of BSG. Due to a very small air leak through the tar sampling system, oxygen was detected by the GC. The results were corrected and normalised by eliminating the proportion of air in the sample to determine the true product gas values. The higher N₂ content in sample 2 and 3 was assumed to be that of slightly higher intake of air into the gasifier to maintain and control the gasification temperature.

Table 13 Product Syngas composition

Product Syngas	Sample 1 <i>vol%</i>	Sample 2 <i>vol%</i>	Sample 3 <i>vol%</i>	Average <i>vol%</i>
N ₂	49.08	55.12	55.39	53.2
H ₂	14.05	11.07	9.55	11.6
CO	20.39	20.42	19.39	20.1
CO ₂	14.2	12.08	13.29	13.2
CH ₄	2.2	1.29	2.35	2

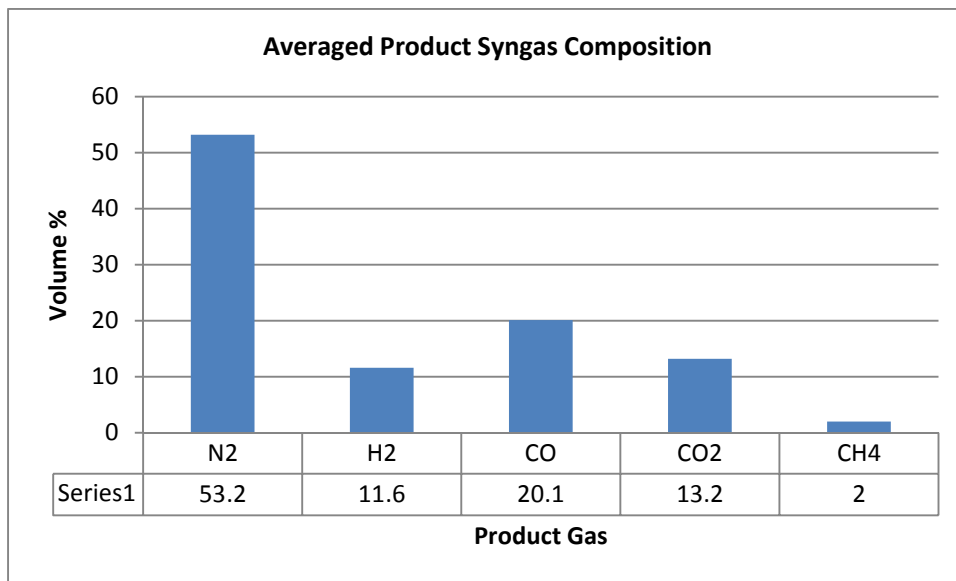


Figure 55 BSG Averaged Product Syngas Composition

The main reactions influencing the production of product syngas was the water gas shift, methane steam reforming and Boudouard reactions. With a char bed present within the reduction zone the heterogeneous gasification reactions as described in section 2.7.2.2 takes place as hot gases from the pyrolysis and oxidation zones above react with the carbon in the char. At high temperatures carbon dioxide produced from combustion in the oxidation zone reacts with carbon in the char and promotes the forward Boudouard reaction forming carbon monoxide. Similarly carbon monoxide and hydrogen produced when the carbon in the char reacts with steam in the gas; carbon in the char also reacts with some of the hydrogen produced to form methane.[56]

The comparison of these results with those reported in the literature is shown in Table 14. The CO, H₂ and in particular heating value obtained in this work was comparable with those of wood, woodchips, wood pellets and hazelnut shells.

Table 14 Comparison of gasifier performance with literature

Reference	Feedstock	CO (vol %)	H ₂ (vol %)	LHV (MJ/m ³)
BSG (This Work)	Brewers Spent Grain	20.1	11.6	4.96
Erlich&Fransson[120]	Bagasse	23.3	9.9	5
Erlich&Fransson[120]	Wood	25.7	11.9	5.4
Olgun et al [121]	Woodchips	21	13	5.1
Olgun et al [121]	hazelnut shells	22	13	5.2
Gai & Dong [169]	Corn straw	11-20	7-14	3-5.4
Sheth & Babu[122]	Furniture waste of Dalbergiosisoo	-	-	6.34
Plis & Wilk [123]	Wood Pellets	15-28	7-12	3.84-5.47
Plis & Wilk [123]	Oat husk pellets	11-16	4- 8	
Tippayawong et al[170]	Cashew nut shells	17	5	3.5
Bhoi et al[171]	Ground nut shells	-	-	4.4
Bhoi et al[171]	Cashew nut shells	-	-	4.5
Pathak et al[172]	Babul wood	-	-	5.0-5.5

5.3.2 Tar analysis

The tar content in the product gas was determined to be 1.87 g/Nm³, a figure which is similar to that with wood chips (2 g/Nm³)[173]. Evan and Milne [68] proposed that a crude generalization would have downdraft gasifiers producing 1g/Nm³. This in comparison to other types of gasification processes is fairly low, but still much too high for an engine and will seriously limit the life of the engine components. Therefore the tar content would need to be reduced to acceptable levels (approximately 100g/Nm³). The water content of the product gas was 15.52 g/Nm³. High amounts of water vapour in the product gas reduce its calorific value; therefore it is important to reduce the level if possible. This can be achieved by further evaporative drying of the feedstock before gasification, although it is important that the water content is not too low as some water vapour is required for the important water gas shift reactions occurring to produce hydrogen. Also low water containing feedstock's can result in excessive gasification temperatures. Tar appeared to form a dark highly viscous layer on the flask surface. The tar laden flask is illustrated in Figures 56.



Figure 56 Tar laden flask

5.3.3 Mass balance

The mass balance from the run is illustrated in Table 15. This shows that for every kilogram of biomass fed approximately 2.4kg of product gas was formed. Literature reports that downdraft gasifiers running with wood produce approximately between 2.6 kg of product gas. [174]. The average syngas composition had a heating value of 4.96 MJ/m³. The mass balance closed at 95%. The source of the error may have been due to a number of factors including the amount of BSG fines and the inability to measure the residual char in the gasifier. A more accurate method ensuring the mass balance closure was obtained would have been by placing the gasifier on a weighing scale to measure the total mass before and after each experiment however due to the size of the unit it was impractical to implement this strategy. As equipment is scaled up it becomes increasingly difficult to obtain accurate results as there is increased tendency for errors to occur.

Table 15 Mass balance – BSG Fixed bed downdraft gasification

Components:	Input (kg/hr.)	Output (kg/hr.)	Closure %
Air	14.70		
Biomass	9.50		
Ash		0.38	
Syngas :		22.82	
<i>H₂</i>		0.21	
<i>N₂</i>		12.42	
<i>CO</i>		4.72	
<i>CH₄</i>		5.27	
<i>CO₂</i>		0.20	
Water		0.33	
Tar		0.04	
TOTAL	24.2	23.19	95%

5.3.4 Gasifier bed inspection

With the experiment completed the reactor was allowed to cool down. Upon the removal of the gasifier top plate it was observed that the area above the oxidation zone contained some unprocessed BSG and residual char. As can be seen in Figures 57 and 58 the area was filled with unprocessed BSG pellets of varying sizes as well as a considerable quantity of BSG fines.

The BSG fines were largely present within the screw feeder housing, which feeds biomass pellets into the gasifier. The presence of fines was the result of the BSG pellets breaking down within the screw feeder due to abrasion and friction. The BSG pellets are not as durable and solidly formed as other feedstock's such as woodchips. The unprocessed material was collected and weighed approximately 2.19kg. The residual char remaining in the gasifier was unable to be measured accurately.



Figure 57 (left) Pellets broken into fines within screw feeder, (right) collected BSG fines and pellets



Figure 58 (left) unprocessed pellets and fines (right) BSG ash and char

It has been reported in literature[120] that too many fines building up within the gasifier bed may restrict the flow of air and product gases, which can ultimately prevent gasification occurring. However, in this study all of the BSG is consumed. Fine char and ash dust were accumulated and collected in the ash grate located beneath the gasifier bed. To prevent pellets breaking down into fines accumulated in the screw feeder a stronger pellet form would be more suitable.

5.4 Summary

This chapter has investigated the fixed bed downdraft gasification of BSG pellets to produce a product gas that can potentially run a combustion engine for heat and power. Currently there is no literature available on gasification of BSG.

BSG pellets were successfully prepared by oven drying, followed by grinding and then pelletising using the roller shaft pellet mill described earlier. Pellets with a moisture content of 8% and a size range of 10-21mm in length and 5mm in diameter and an overall bulk density of 480kg/m³. Pellets were prepared so that they were suitable for gasification in the GEK fixed bed downdraft gasifier. The gasifier was cleaned and assembled with no gas leaks after a cold run was performed.

Gasifier start-up was achieved; the gasifier operated successfully at steady state with no performance issues for approximately 2hrs at an approximate feed rate of ~ 4.2 kg/hr until all feedstock in the feed hopper was consumed. A strong flare was observed throughout steady state operation. For every kilogram of biomass fed, 2.0kg of product gas was formed. The mass balance closure was 100% and the average product gas composition had a heating value of 4.96 MJ/m³. The average product gas composition produced was H₂ 11.6%, CO 20.1%, CH₄ 2.0%, CO₂ 13.2% and N₂ 53.2% which is similar to what was reported in literature [120-123, 169-172] and comparable to with those of wood, and hazelnut shells.

In this work tar removal was achieved using a carbon absorption filter, but tar levels downstream of the filter were not measured. The tar content in the product syngas was determined to be 1.87 g/Nm³, a figure which is similar to that of wood chips (2 g/Nm³) [173] The water content of the product gas was 15.52 g/Nm³. High amounts of water vapour in the product gas reduce its calorific value; therefore it is important to reduce the level if possible. This can be achieved by further evaporative drying of the feedstock before gasification, although it is important that the water content is not too low as some water vapour is required for the important water gas shift reactions occurring to produce hydrogen. Tar appeared to form a dark highly viscous layer on the flask surface.

The mass balance closed at 95%. The source of the error may have been due to a number of factors including the amount of BSG fines and the inability to measure the residual char in the gasifier. A more accurate method ensuring the mass balance closure was obtained would have been by placing the gasifier on a weighing scale to measure the total mass before and after each experiment however due to the size of the unit it was impractical to implement this strategy.

Upon inspection of the gasifier chamber by the removal of the gasifier top plate there was some unprocessed BSG in the middle of the gasifier bed mainly fines. Fines may have resulted in the abrasion of the surface of the pellets and overtime the fines will build up and may block the throat that can lead to obstruction of gases. Erlich & Fransson [120] reported that many gasifiers similar of this type have grid/bed shaking devices to avoid problems such as bridging and fouling. However a shaking device may form more fines due to abrasion and breakdown of BSG pellets that may block the constricted throat. Literature does not report how to overcome breakdown of pellets in this type of

gasifier and dealing with fines. Therefore due to the fines BSG would perhaps be more suited to operate within a fluidised bed type gasifier.

It is recommended to repeat tests but to increase the duration of the experiment to assess stability and the effects of ash. Ash in this work did not seem to effect the investigation greatly but may over time. Stronger BSG pellets are required that could perhaps be binded together with a binding agent such as starch, so that the pellets hold their form better during the feeding process and not crumble.

It is recommended to further expand this work by conducting gasification of BSG using fluidised bed systems, both bubbling or circulating configurations and further coupling of these reactors to steam reforming reactors to produce a H₂ rich gas that could be combusted in an engine for heat and power.

6 Experimental Intermediate Pyrolysis Methodology

6.1 Introduction

This chapter describes the available equipment and procedures used for the intermediate pyrolysis of BSG with and without catalysts at Aston University. The primary objective of this part of the work was to conduct an experiment utilising the Pyroformer reactor to investigate the behaviour of BSG under intermediate pyrolysis conditions; to characterise the chemical compositions of the pyrolysis fractions obtained (bio-oil, char and permanent gases); then to investigate their feasibility for use in a combined heat power (CHP) application or in a post-reformer or gasifier stage. The second objective was to setup and conduct bench scale intermediate pyrolysis experiments at the same temperature as the Pyroformer but at differing heating rates. The heating rate, the time it takes the bench scale unit to reach the optimum set-point temperature, was varied to see the effects it has on the product yield. The aim of this was to determine the heating rate that will give products yields similar to that obtained from the Pyroformer with the same feedstock. The third objective was to then add a small catalytic reformer (secondary plug flow reactor) housed within an oven furnace to the bench scale pyrolysis reactor, so that pyrolysis vapours can pass through to be further cracked and reformed at varying reforming temperatures using three different catalysts.

6.2 Pyroformer Intermediate Pyrolysis

The intermediate pyrolysis of BSG was carried out using a 'Pyroformer', a 20kg/h intermediate pyrolysis unit. The Pyroformer was recently patented by A. Hornung & A. Apfelbacher at Aston University[175], was originally manufactured in Germany before being installed and commissioned at the European Bioenergy Research Institute (EBRI) at Aston university (Figures 59 and 60).



Figure 59 The Pyroformer 20kg/hr. Intermediate pyrolysis unit

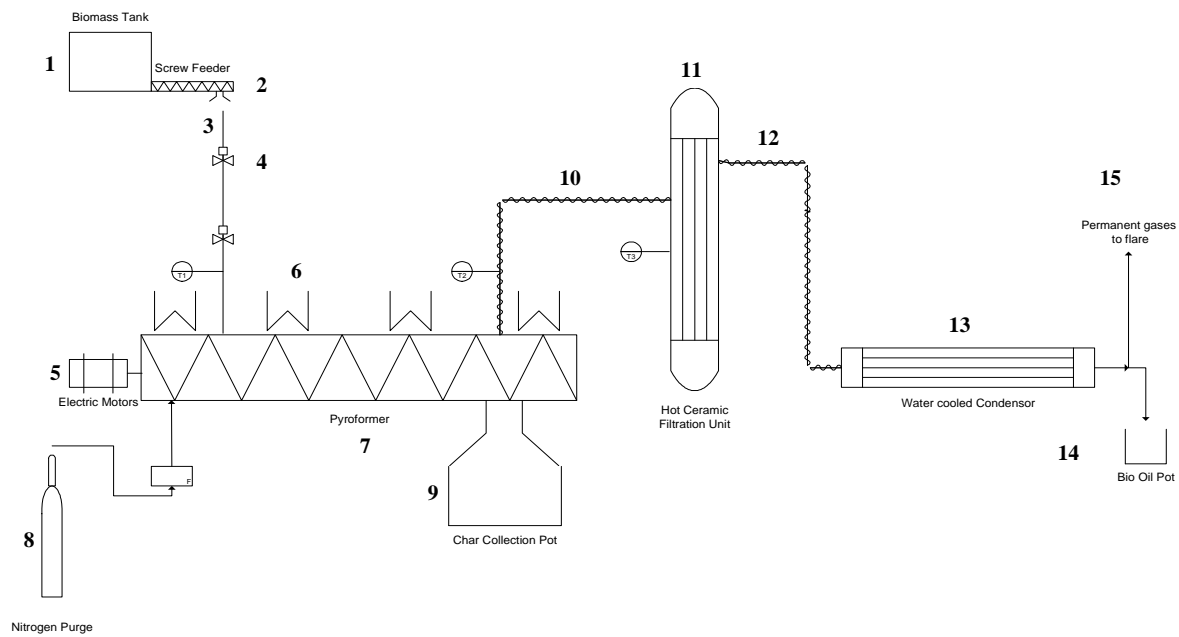


Figure 60 Pyroformer (Intermediate Pyrolysis) schematic diagram

Pyroformer Intermediate pyrolysis reactor used in the conversion of BSG; (1) Biomass Tank, (2) Biomass screw feeder, (3) Feed entry pipe, (4) Actuator Valves, (5) Electric Motors, (6) Heaters, (7) Twin coaxial screw reactor (Pyroformer), (8) N₂ bottle, (9) Char collection pot, (10) Heated vapour exit line 1, (11) Hot ceramic filtration, (12) Heated vapour exit line 2, (13) Water-cooled condenser, (14) Bio-oil collection pot, (15) Permanent gases vent line

The Pyroformer is constructed of carbon-steel and measures approximately 1.8m in length and has a diameter of 0.2m, and consists of twin horizontal rotary coaxial screws. The twin coaxial screw system offers the advantage of defined residence times which can be varied between about 1 and several minutes by adjusting the speed of the internal screw. The outer screw transports a fraction of the char produced during pyrolysis back, so that there is an internal recycling. The remainder drops out at the downstream end of the reactor. This not only ensures better heat transfer but also promotes catalytic reforming within the process[25](see Figure 61).The operating temperature range of the Pyroformer is 300- 450°C depending on the feedstock material to be pyrolysed.

Before any hot experiments commenced a cold run was conducted in order to determine the solids residence time based on the selected internal screw speeds. The solids residence time was defined as the time the fuel (solids) spends inside the reactor chamber to be fully converted under pyrolysis conditions. This was determined by measuring the time taken for the solids fed into the reactor to drop out downstream at the end of the reactor. This was established after approximately 45 minutes.



Figure 61 Pyroformer twin coaxial screw system[25, 36]

The Pyroformer was first heated to a set point temperature of 450°C, which takes approximately 3 hours. The hot ceramic filters (also known as candle filters) are also switched on and allowed to heat up to a set point temperature of 450°C. The twin screws within the reactor are then started. The reactor was then purged with N₂, and the biomass screw feeder was then started, feeding the unit at a chosen rate of 5kg/hr. from a biomass hopper.

The unit was allowed to reach steady state before any measurements took place, this took approximately 60 minutes. Hot organic vapour and permanent gases generated from the pyrolysis process first pass through the hot ceramic filters in order to pre-clean the vapours of any entrained solids. The hot vapours were then directed to a water cooled shell and tube heat exchanger (condenser) where the vapours were able to condense and be collected.

The remaining permanent gases were then routed to an electrostatic precipitator for aerosol knockout, after which the gases are suitable for GC-TCD detection. The solid products exit the reactor and are collected within a char pot. At steady state the char leaving the reactor is at a constant rate.

6.3 Experimental Bench Scale Intermediate Pyrolysis Methodology

Further pyrolysis work was carried out using a bench scale intermediate pyrolysis unit. The bench-scale fixed bed batch pyrolysis reactor was a cylindrical quartz tube measuring 400mm length x 60 mm diameter which is mounted in an externally heated electrical furnace as illustrated in Figure 62. The pyrolysis reactor lid has two entry points, one for the purge gas nitrogen inlet and one for a k-type thermocouple to measure the temperature of the bed.

The batch pyrolysis reactor is loaded with 100g of BSG feedstock. Nitrogen was the carrier gas serving as the purge, and was set to a flow rate of 50cm³/min using a flow meter. The reactor heater operates on a temperature controlled program via a heater controller, on which the heating rate and final temperature set point can be programmed.

The outlet of the pyrolysis reactor is connected to a transition tube leading to the glass liquid collection system. The reactor head together with the transition tube is lagged to ensure minimal condensation of pyrolysis vapours. The glass liquid collection system comprises two dry ice-acetone condensers (with temperatures of -70°C). The hot pyrolysis vapours flow into these, and the condensed liquid was collected in an oil pot. Downstream of condenser 2 was a cylindrical tube containing a scrubbing agent (10ml of isopropanol) with glass beads to capture any solids or tars that may still be present, and an electrostatic precipitator (voltage at 15kV and current at 0.5A) to collect aerosols.

The clean product gas may be sampled with a gas tight syringe and injected into a GC for gas analysis. The final product gas passes through an Aalborg DFM digital mass flow meter that records flow rate, temperature and pressure simultaneously and this data is sent to a computer. The clean gas was then routed to meter and then directly to a Hewlett Packard for GC-TCD detection and quantification. The char remains in the pyrolysis reactor after the experiment was conducted. Each experiment takes approximately 40-50 minutes.

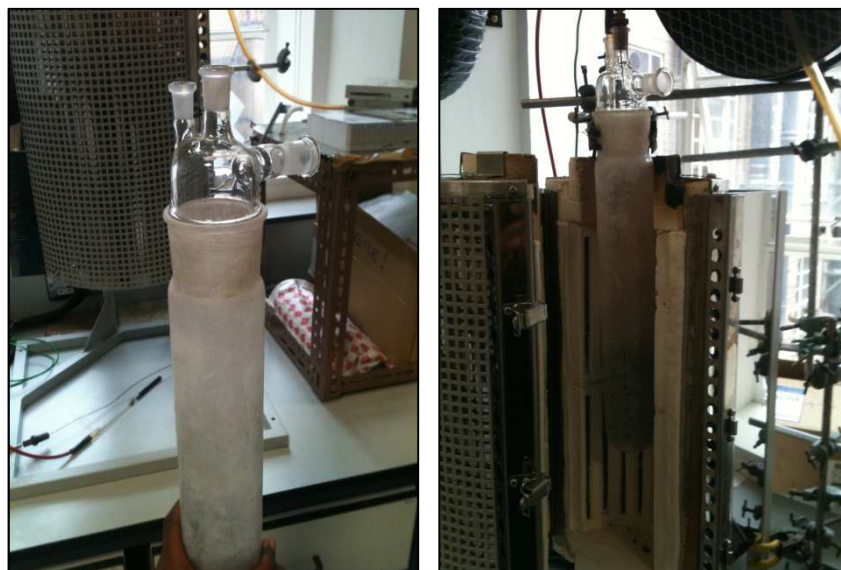


Figure 62 Bench scale pyrolysis reactor cylindrical quartz tube and electrically heated furnace

6.3.1 Non-catalytic pyrolysis experiments

Non-catalytic pyrolysis experiments was first conducted under a range of conditions of heating rate chosen to simulate continuous intermediate pyrolysis conditions of the Pyroformer unit.

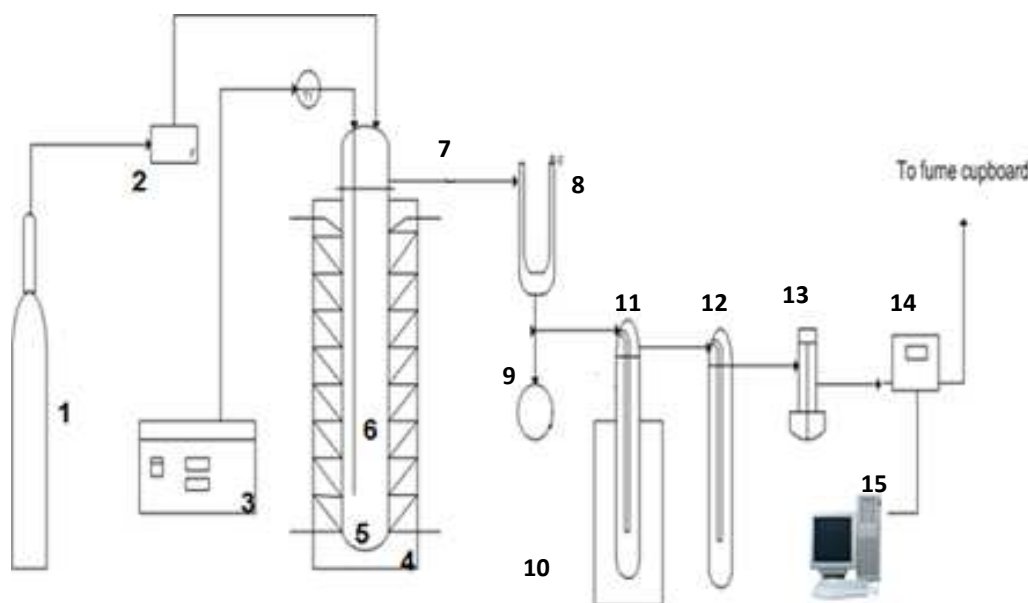


Figure 63 Bench Scale Pyrolysis reactor

Batch fixed bed pyrolysis reactor used in the conversion of BSG. (1) Nitrogen gas bottle, (2) N₂ flow meter, (3) Pyrolysis heater controller, (4) Pyrolysis heater, (5) Pyrolysis reactor, (6) Thermocouple, (7) Transition tube, (8) Condenser 1, (9) Bio-oil pot, (10) Ice bath, (11) Condenser 2, (12) Scrubber, (13) Gas sampling port, (14) Flow/Temp/Press meter (15) Gas Chromatography

6.3.1.1 Different heating rates

For these tests the unit was operated at a temperature of 450°C, the same temperature as the Pyroformer. The heating rate was varied to see the effects on the product yield. Two heating rates were selected to begin with, 25°C/min and 50°C/min. The objective of this test was to determine the heating rate that gives a product yield similar to that obtained from the Pyroformer with the same feedstock.

Before each run the glassware was thoroughly cleaned using an oven furnace to remove any solid residue, after which it was left to cool and later cleaned with acetone. The initial step was to load the pyrolysis reactor with 100g of ground BSG and secure the reactor lid using silicone grease before the reactor can be placed within the pyrolysis carbolite heater.

The N₂ purge pipe and thermocouple are then introduced within the pyrolysis reactor via the top of the pyrolysis reactor lid. The reactor lid was then lagged together with the transition tube. The solid residence time was 45 minutes, which accounts for the time taken for the biomass to be fully converted under pyrolysis conditions, and relates to the duration of the pyrolysis runs. The vapour residence time was not determined but can be assumed in the order of seconds.

6.3.2 Catalytic pyrolysis experiments

For the catalytic pyrolysis experiments a secondary catalytic reactor was added. This was housed in an electrical furnace placed directly after the batch pyrolysis reactor and before the glass liquid collection system. The glass liquid collection system and downstream of the unit is unchanged and is as described earlier.

The secondary reactor was constructed out of high temperature resistant material (quartz), with dimensions 400mm length and 25mm diameter with two female open ends (see Figure 64). The reactor was easily inserted or removed from the electrically heated furnace with manual temperature control. A handheld thermocouple inserted on the inner wall was used to measure the furnace temperature. The catalyst was inserted and supported by approximately 1g of quartz wool. The quartz wool serves two functions; firstly it supports the packed bed therefore preventing catalysts falling (Figure 64). Secondly, it functions as a hot vapour filter by capturing any char fines that can otherwise cover the catalyst surface leading to catalyst deactivation. The use of the quartz wool can also reduce the solids contents of the bio-oil.

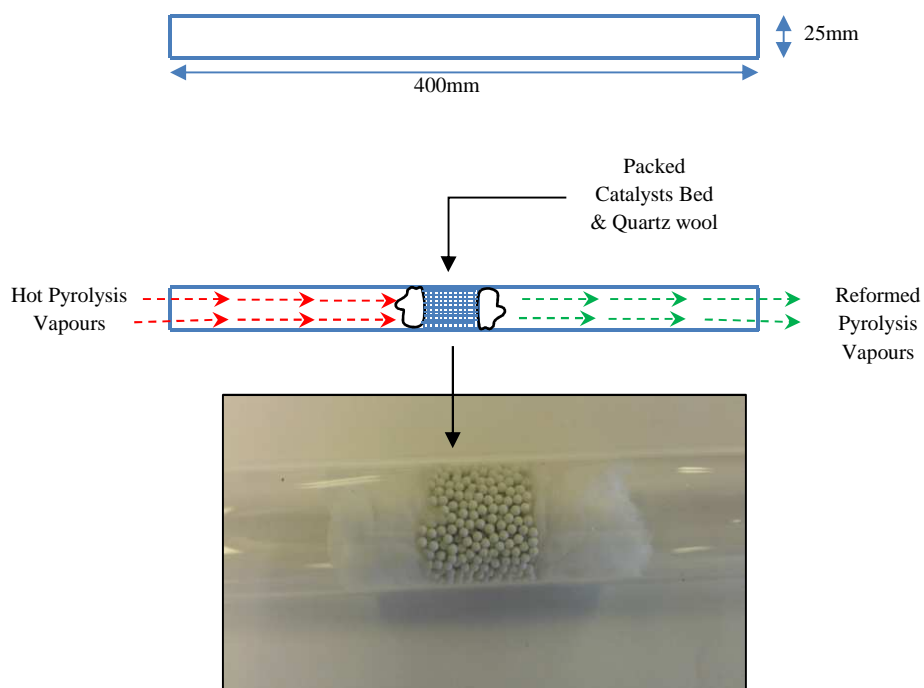
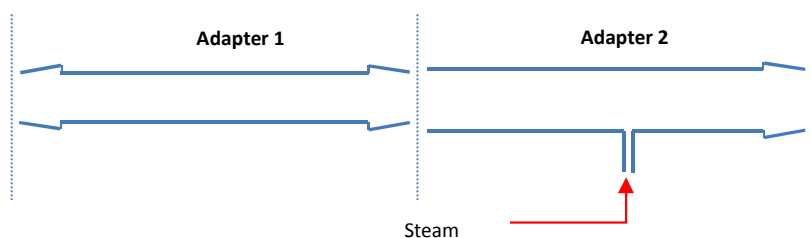


Figure 64 Secondary reactor dimensions and packed catalyst bed

The connecting (transition) tubes before and after the catalytic reactor were made of high temperature resistant material (1000°C) to cope with high vapour temperatures during reforming experiments, whilst the rest were made of mid temperature material (525°C). The arrangement is shown below, Adapter 1 is 150mm in length with male to male (b19 ends). Adapter 2 is 100mm in length having a female connection (b19/26) and a male end (b24) that fits into the secondary reactor. Adapter 2 has an inlet for the introduction of steam for steam reforming.



A copper distillation kettle mounted on top of a heated plate was used to generate steam for steam reforming experiments. The distillation kettle was filled with 200ml of water and then heated to approximately 350-400°C. The time taken for steam to be generated was established to be approximately 7 minutes. The steam flow rate determined was approximately 5ml/min.

The arrangement was tested to ensure the steam and pyrolysis vapours flowed towards the secondary catalytic reactor. Two reference tests were conducted without catalyst and steam at reactor

temperatures of 500°C and 850°C, with quartz wool placed in the secondary reactor in place of catalysts.

Three different catalysts were selected and used in this study. These were a nickel (Ni/Al₂O₃) catalyst, a platinum (Pt/Al₂O₃) catalyst and a rhodium (Rh/ Al₂O₃) catalyst, all supported on an alumina base. 10 g of nickel catalyst was used (supplied as pellets), and 5 g of rhodium and platinum catalyst (supplied as spheres) due to their low density and increased surface area. All catalysts were prepared and supplied by Johnson Matthey Ltd [1]. Catalysts were fully reduced at 900°C using a H₂/N₂ gas mixture and then passivated.

Three catalytic steam reforming temperatures were selected and investigated, 500°C, 750°C and 850°C, initially without steam and then with the addition of steam. Initial catalytic reforming experiments were conducted using the aqueous phase or the water/steam present in the hot organic pyrolysis vapours produced during the thermal degradation of biomass. This would supply the steam reforming reactions within the secondary reactor, allowing observation of the quantity of syngas produced, in particular H₂ content, and catalyst performance utilising the water already present in the system[34]. Secondary catalytic steam reforming experiments will be conducted with the addition of steam.

A schematic of the primary batch pyrolysis reactor and secondary catalytic reactor is shown in Figure 65 below.

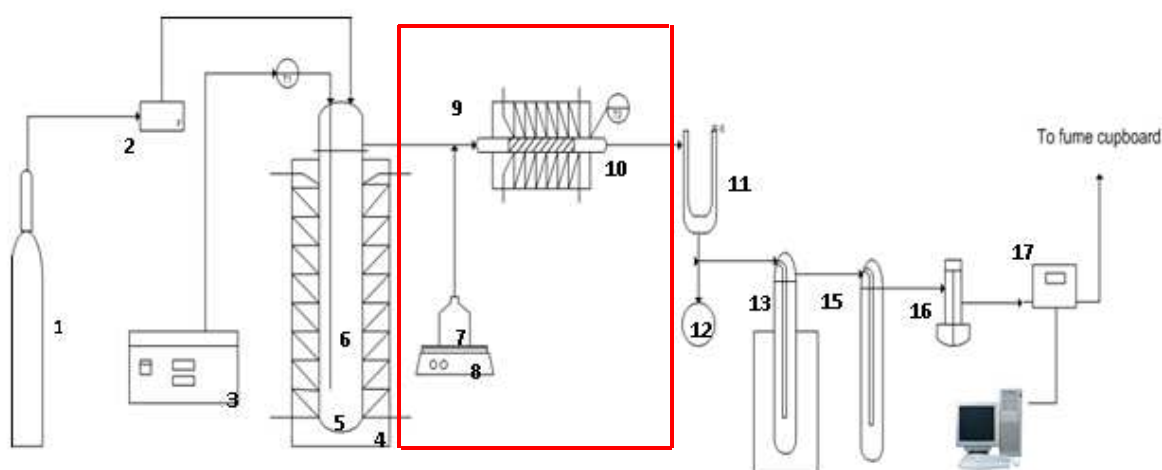


Figure 65 Bench Scale Pyrolysis and Catalytic reactor

Batch fixed bed pyrolysis and catalytic reforming reactor used in the conversion of BSG. (1) Nitrogen gas bottle, (2) N₂ flow meter, (3) Pyrolysis heater controller, (4) Pyrolysis heater, (5) Pyrolysis reactor, (6) Thermocouple, (7) Kettle, (8) Kettle heater, (9) Reformer heater, (10) Catalytic reformer, (11) Condenser 1, (12) Bio-oil pot, (13) Condenser 2, (14) Ice bath (15) Scrubber, (16) Gas sampling port, (17) Flow/Temp/Press meter

6.4 Mass and Energy Balance Calculation

For tests conducted with the Pyroformer BSG was initially weighed and loaded into the feed hopper so the amount of feedstock was known. The screw feeder feeding the Pyroformer was calibrated so that the feeding rate was known. After the twin rotary screws were switched on the BSG was fed into the reactor and the resulting solids were collected downstream to determine the solids residence time. Bio-oil and char were collected and weighed after the experiment; with the known quantity of feed the permanent gases could be calculated by difference. Pyroformer temperature was recorded every 10 minutes during start up and throughout the experiment.

All glassware items for the bench scale pyrolysis unit were weighed before and after each run in order to be able calculate the pyrolysis product yields. The amount of BSG was weighed before being loaded into the fixed bed batch pyrolysis reactor. The liquids yield is a combination of the pyrolysis vapours that may have condensed and fouled on the pyrolysis reactor lid, transfer lines (transition tubes), dry ice condensers and bio-oil collection pots. The solid yield is determined by the weight of the char that is collected in the pyrolysis reactor after each run. Having known the feed weight and the final product yields of the liquid and solids, the permanent gases were calculated by difference. This was also confirmed by the Aalborg digital flow meter. The permanent gas yields composition was calculated based on the data attained by the GC analysis. The pyrolysis temperature was recorded every 5 minutes from the temperature data recorded from the thermocouple inside the bed material within the pyrolysis reactor.

During catalytic experiments the secondary reactor was weighed before and after each run and the steps described above are repeated. The quartz wool used to hold the bed is weighed before and after. The catalyst is also weighed before and after each run. The catalysis temperature was recorded every 5 minutes from start-up and throughout experiment using a k-type thermocouple placed within the secondary furnace at the location of the catalyst bed. For tests conducted with steam the amount of water added was weighed before and after each test.

7 Intermediate Pyrolysis Results and Discussion

7.1 Introduction

The intermediate pyrolysis of BSG was conducted using the Pyroformer reactor. The overall objective was to investigate the yields and properties of the pyrolysis products, mainly bio-oil and char, in order to determine the feasibility of their use in a CHP plant or for further processing in a post reformer or gasifier stage. This included investigating the decomposition behaviour of BSG and characterising the chemical compositions of the pyrolysis fractions and the residue in terms of contaminants and inert materials and comparing them to the products produced with the Haloclean Intermediate pyrolysis reactor.

7.2 Pyroformer Intermediate Pyrolysis

The Pyroformer experiment was carried out at atmospheric pressure with nitrogen gas used as purge. The reactor controls was programmed so that a pyrolysis set-point temperature of 450°C can be achieved. The unit was heated using a set of four electrical heated bands.

The heating bands were then switched on; the hot ceramic candle filters were also switched on to a set point temperature of 450°C. The water supply to the water cooled shell and tube condenser was opened, and the electrostatic precipitator was switched on also.

The auger screws were then switched on. The inner screw was set to 16 revolutions per minute (rpm) to transport the feed forwards, and the outer screw was set to 8 rpm to recycle char in the reverse direction.

After approximately four hours all equipment had reached its operating temperature of 450°C, and the feed hopper was loaded with ground BSG (in total 15 kg). The actuator valves situated on the feed inlet pipe were switched on, followed by switching on the screw feeder. The ground BSG was fed at a mass flow rate of 5kg/hr.

Steady state conditions was achieved approximately after 45 minutes of feeding, as indicated by solids dropping out at the end of the reactor and collected in the char pot as well as operating conditions remaining unchanged. The run then proceeded at steady state for a further two hours. This experiment was then repeated for consistency.

7.3 Mass Balance

Table 16 shows the mass product yields from the trials. See APPENDIX D for Pyroformer energy balance. The Pyroformer operated at steady state for duration of two hours at a feed rate of 5kg/hr. producing 29 wt.% char, 52 wt.% liquid (bio-oil) and 19 wt.% permanent gases obtained by difference. The liquids were found to separate into two phases, an aqueous phase 79% (bottom layer) and an organic phase 21% (top layer). This is believed to be due to the internal catalytic effect of char cracking the pyrolysis vapour within the Pyroformer.

Phase separation of bio-oils using the Pyroformer is in agreement with work previously conducted by Yang et al, 2013[108] and Ouadi et al 2013[134]. Roggero et al, 2011 [37] described intermediate pyrolysis oils usually phase separated with an aqueous phase at the bottom and oily organic phase at the top due to pyrolysis vapours being cracked by char. Other studies [31, 41-46] reported that feedstock's with an ash content usually greater than 2.5% causes phase separation, as minerals within the ash such as alkali components are responsible for secondary catalytic cracking.

The organic phase of the bio-oil, the permanent gases and the char were analysed.

Table 16 Yield of Products (Mass %) Pyrolysis Final Temperature = 450 °C

Products	Pyroformer Yield (Mass %)
Char	29
Total liquid	52
Water	79.15
Organics	20.85
Gases (by difference)	19

Table 17 below shows a comparison of the performances of different feedstock's with the Haloclean intermediate pyrolysis reactor. Roggero et al, 2011 [37] found the Halo-clean product range varies significantly with different feedstock's, temperature and solids residence time. The char ranged between 15-50%, liquids 30-52% and permanent gases 10-33%.

Brewer's grain was analysed in the Halo-clean at 450°C and yielded char 23%, liquids 51% and permanent gases 21%. However the solids residence time, or the oil to water ratio for this feedstock was not reported in literature. Compared with results from the Haloclean reactor, BSG processed using the Pyroformer shows similar liquid yields; however the Pyroformer produced more char and less permanent gases.

Table 17 Comparison of results for Intermediate pyrolysis using Haloclean reactor (extracted from [37])

Biomass type	Temperature, °C	Yield %		
		Coke	Liquid	Gas
Wheat straw	450	50	30	20
Rape residues	450	38	45	17
	550	25	50	25
Olive stones	450	30	47	23
Rapeseeds	450	33	47	10
	500	15	52	33
Beech wood	450	23	56	21
	500	21	57	22
Rice husk	450	41	41	18
Coconut	450	34	52	14
Rice bran	500	20	38	42
Brewers grain	450	23	51	26
<i>BSG (This study)</i>	450	29	52	19

7.4 Characterisation of Intermediate Pyrolysis Products

7.4.1 Bio-oil Analysis

The condensed bio-oil produced was found to have an organic and an aqueous phase. The two phases was separated easily using a gravimetric settler and then analysed. The organic phase was of more interest and was analysed to assess its suitability as a fuel. The organic phase was very dark in appearance and viscous with a strong smell of carbonised organic material. The aqueous phase was red in appearance and contained some evidence of solid particles.

Table 18 indicates the elemental analysis of the organic phase(referred to as bio-oil) which shows an increase in C, H and S content by 1%, 3% and 0.56% respectively and notably a reduction in O content by 12% in comparison to the original BSG feedstock. Ouadi et al, 2013 [176] reported an oxygen content of 10-11% for de-inking sludge bio-oils produced using the pyroformer. The low oxygen content reported for these bio-oils improved the calorific value as well as making the bio-oil extremely favourable for fuel oils as they were found to be fully miscible with biodiesel without any need for surfactants or additives.

Although the oxygen content for the bio-oil reported in this study was reduced from the original feedstock, indicating that the pyrolysis process has partially deoxygenated the biomass it is still however high to be considered as a fuel. Bridgwater et al, 2004 [22] reported that bio-oil requires full deoxygenation for it to be miscible with conventional fossil diesel. Bio-oil from fast pyrolysis processes generally has a higher oxygen content of about 40-50%. [26] Therefore this bio-oil would be more suited for catalytic upgrading to further deoxygenate the bio-oil to improve its stability and miscibility if considered as a fuel for engines.

Table 18 Elemental Analysis of BSG bio-oil produced from Pyrformer

Elemental analysis	wt% (wet basis)				
	C	H	N	S	O ^a
BSG bio-oil	47.6	9.9	3.4	1.3	30.7

^a By difference

The water contents for the organic (bio-oil) phase and aqueous phase were 6.5 % and 62% respectively. The water content for the bio-oil was lower than what was reported in the literature that water content for bio-oils can vary between 10-60% [177-179]. As mentioned previously, water formation in the pyrolysis oils is largely due to moisture bound in the original feedstock, dehydration and catalytic reactions during pyrolysis between alkali components in the char and hot pyrolysis vapours.

Some water can be dissolved in bio-oil in water-soluble compounds and this can offer both advantages and disadvantages to the properties of the bio-oils. The water content improves the bio-oil's flow characteristics; however it also lowers the heating value and flame temperature of the fuel, which increases the ignition delay and decreases the combustion rate compared to petroleum fuels. It also means that the bio-oil is immiscible with petroleum fuels.

Table 19 gives physical properties of the bio-oil of relevance for use as an engine fuel. The calorific value of the bio-oil was 20 MJ/kg, which is about half the energy content of fossil diesel. The low energy content is associated with the high oxygen content of the oil.

Bio-oils are normally quite acidic with pH values ranging between 2-3[22], this is due to the presence of organic acids such as acetic and formic acid, however BSG bio-oil has a pH of 6 which is much higher than expected for a bio-oil. However the acidity number of the oil was found to be 49mgKOH/g which was relatively high in comparison to bio-diesel (0.8), indicating potential corrosion problems if considered as fuel for engine applications. The high acid number may be partly due to the presence of phenolics and some unidentified components present in the bio-oil.

The corrosive effect is related to the acidity and reactivity of the bio-oils. After 6h/40°C the copper corrosive class was 1a. After 24h/40°C the copper corrosive class was 3a, indicating that BSG bio-oil has a low ability to corrode copper. Figure 66 illustrates an image of a copper strip immersed in BSG bio-oil after 24 hours.



Figure 66 Copper strip immersed in BSG bio-oil after 24h/40°C

The carbon residue and ash were 1.93% and 0.44% respectively which in contrast to diesel and biodiesel are relatively high and could indicate potential blockage problems in engine applications such as clogging injectors and coke formation in the combustion chamber. Viscosity was very high 222 cSt; this may be due to the amount of solids present in the bio-oil and would make atomisation difficult.

The bio-oil upon visual inspection is liquid but not homogeneous as it contained many bituminous solids and viscous compounds which overtime could polymerize with age if stored at room temperature. The solids content however must remain low if the bio-oil is to be considered suitable for engine applications. Similar characteristics of intermediate pyrolysis bio-oil from wheat straw were reported by Hornung et al, 2009 [34]. The author also reported that the quality and characteristics of the pyrolysis products from biomass change dramatically with feedstock and residence times.

Table 19 Physical properties of Bio-oil produced from Pyroformer in comparison to bio-oil produced from Halo-clean

	Carbon Residue (%)	Copper Corrosion	Density (g/cm ³)	Gross Calorific Value (MJ/kg)	Viscosity @ 40°C cSt	pH	Total Acid Number (mgKOH/g)
BSG (This study)	1.93	1A	1.02	20.39	222	6.43	49.16
*Pomace 1	-	-	1.108	-	211.89	4.02	-
*Brewery Residue	-	-	1.102	-	141.38	4.7	124.45
*Olive stones	-	-	1.112	-	71.65	3.87	116.4
*Beech wood	-	-	1.065	-	78.76	3.89	174.5
*Rapeseed	-	-	0.938	-	35.97	7.46	-

*Extracted from [37]

Figure 67 shows the GC/MS mass spectrum. The major chemical components present are illustrated in Table 20. The bio-oil consists of a number of complex organic oxygenated compounds. Much of the abundant components are aromatic hydrocarbons and alkanes, followed by phenols.

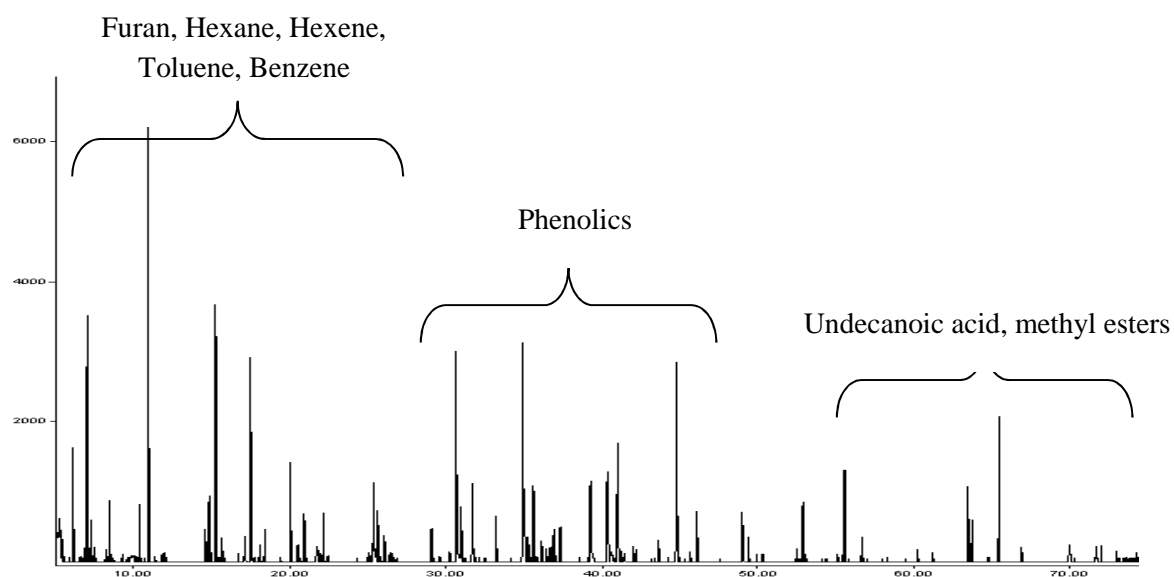


Figure 67 GC/MS Analysis of Bio-oil (Organic phase) produced from Pyroformer

The 'Area%' in Table 20 represents the peak areas of each identified component as a fraction of the whole integrated mass spectrum, thus giving an approximate mass fraction of that component.

It was found that the bio-oil contains a complex mixture of low to intermediate molecular hydrocarbon chains ranging from C₅-C₁₉. Alkenes such as, benzene, cyclooctatetraene, hexene, toluene and xylene were present with the latter two representing significant quantities of 11.29% and 7.39% respectively and cyclooctatetraene of 5%. Phenolic derived aromatic compounds were the other major components present comprising approximately 24% of the bio-oil fraction. Undecanoic acid and methyl esters, were the only acidic and fatty acid component identified. The acidity however

could be due to the large quantity of phenolic components detected and some unidentified components. Higher aromatic components were detected such as tridecane which represents approximately 6% of the mass fraction, higher aromatics have poorer combustibility compared with paraffin's and naphthenes[108].

Phenylacetonitrile and undecanenitrile are the alkyl nitrile identified peaks with a maximum of 6.85% see Table 20. Alkyl nitrile compounds are highly toxic, and the oil should be handled with care to avoid direct skin contact. Decane-1-Chloro represents approximately 2-3% of the bio-oil and is a surprise finding as it contains chlorine and would have been expected to be present in the char.

Table 20 GC/MS Tests of the (Organic Phase) Bio-oil Produced (Pyroformer)

Retention Time	Chemical Name	Chemical Group	Molecular Formula	Area %
5.271	4,6-Heptadiyn-3-one	Ketones	C ₇ H ₆ O	2.29
6.133	Furan, 2-methyl-	Furan	C ₅ H ₆ O	1.69
8.466	2,5-Dimethylfuran	Furan	C ₆ H ₈ O	1.21
10.375	2,4-Dimethyl-1-heptene	Alkene	C ₉ H ₁₈	1.07
10.938	Toluene	Aromatic	C ₇ H ₈	11.29
14.582	Cyclopentanone	Cyclopentanone	C ₅ H ₈ O	0.89
14.835	Pentane,2,2,3,4-tetramethyl-	Alkane	C ₉ H ₂₀	1.26
15.249	p-Xylene	Aromatic	C ₈ H ₁₀	6.24
17.49	Cyclooctatetraene	Alkene	C ₈ H ₈	5.4
20.031	Decane, 1-chloro-	Alkane/Chloro	C ₁₀ H ₂₁ Cl	2.63
20.916	2-Cyclopenten-1-one, 2-methyl-	Cyclopentanone	C ₆ H ₈ O	1.39
22.146	Azetidene, 3-methyl-3-phenyl-	Alcohol	C ₁₀ H ₁₃ N	1.12
25.376	Heptane, 2,4-dimethyl-	Alkanes	C ₉ H ₂₀	1.61
25.618	Benzene, (2-methylpropyl)-	Aromatic	C ₁₀ H ₁₄	1.15
29.066	5-Octen-1-ol, (z)-	Alcohol	C ₈ H ₁₆ O	1.01
30.63	Phenol	Phenol	C ₆ H ₆ O	6.95
30.951	Benzene, pentyl-	Aromatic	C ₁₁ H ₁₆	1.43
31.676	Guaiacol	Guaiacols	C ₇ H ₈ O ₂	2.47
33.17	2-Methylphenol	Phenol	C ₇ H ₈ O	1.37
34.894	Phenol, 4-methyl-	Phenol	C ₇ H ₈ O	8.2
35.584	Phenol, 4-methyl-	Phenol	C ₇ H ₈ O	2.44
36.895	2-Methoxy-4-methylphenol	Phenol	C ₈ H ₁₀ O ₂	0.96
37.308	2,4-Dimethylphenol	Phenol	C ₈ H ₁₀ O	1
39.24	4-Ethylphenol	Phenol	C ₈ H ₁₀ O	2.55
40.964	4-Ethylguaiacol	Guaicol	C ₉ H ₁₂ O ₂	3.61
44.746	Tridecane	Alkane	C ₁₃ H ₂₈	5.96
46.033	Phenylacetonitrile	Alkyl Nitriles	C ₈ H ₇ N	1.57
55.586	Benzene,1,1'-(1,3-propanediyl)bis-	Aromatic	C ₁₅ H ₁₆	2.57
63.483	Undecanoic acid, methyl ester	Ester	C ₁₂ H ₂₄ O ₂	1.77
63.736	1-Propene, 3-propoxy-	Oxygenates	C ₁₉ H ₁₈ N ₂ O ₂	0.99
65.472	Undecanenitrile	Alkyl Nitriles	C ₁₁ H ₂₁ N	3.71

Figure 68 illustrates the chemicals detected within in bio-oil produced using the pyroformer. The major components detected were aromatic hydrocarbons at 23% in the form of benzene, toluene and xylenes. The other major groups found was phenols 15.3%, alkenes 8%, alkanes 5.5%, and Guaicol 6.1%.

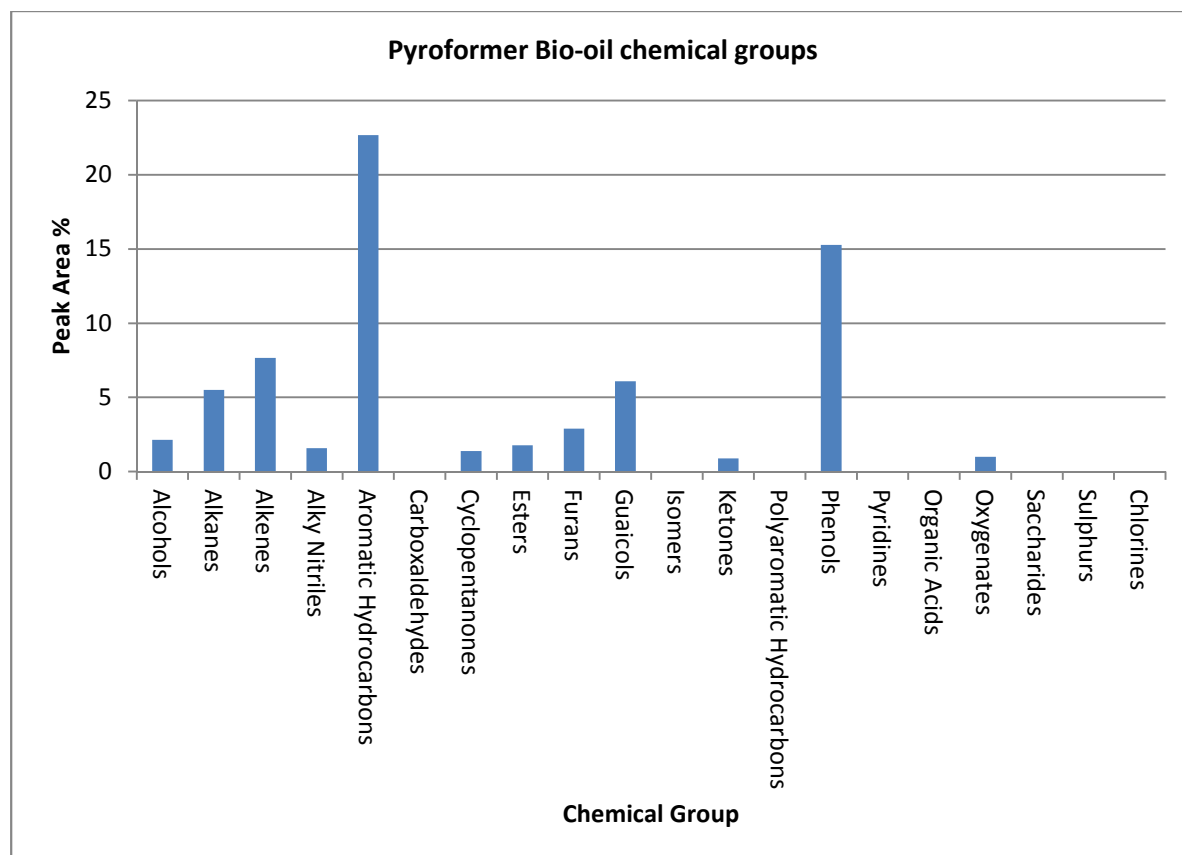


Figure 68 Pyroformer 'Bio-oil' Chemical Groups

Other notable chemicals present were furans 2.9%, alcohol 2.1%, cyclopentanones 1.4%, esters 1.8%, and alkyl nitriles 1.6%, ketones 0.9% and oxygenates 1%. In summary the bio-oil was found to have poor characteristics for use as a diesel engine fuels. As mentioned earlier, this bio-oil would be more suited for catalytic upgrading to further deoxygenate the bio-oil to improve its stability and miscibility if considered as a fuel for engines. Other studies have investigated steam reforming of bio-oil to produce hydrogen by the use of catalytic hydro-treatment and catalytic cracking.[33, 34, 180]

By placing a reforming unit after the pyrolysis process, the pyrolysis vapours prior to condensation could be upgraded by converting unfavourable compounds into lower alkanes like methane as well as hydrogen and carbon oxides, as well as leading to a lower viscosity of the final liquid.

This in turn can increase the heating value and combustible gas content of the formed pyrolysis gases and make it more suitable for application in gas engines. The large formation of aqueous phase in the bio-oil could serve as a reaction partner in reforming reactions to produce hydrogen.[34]

7.4.2 Char Analysis

The char (shown in Figure 68) was the second largest product yield in the intermediate pyrolysis of BSG. The material produced was found to be very dark, brittle, coarse and very dry. It was analysed for its heating value, proximate analysis and elemental composition. Table 21 & 22 gives the proximate and elemental analysis of the char.

Table 21 BSG Pyroformer char proximate analysis

Proximate analysis	mass %			
	Moisture	Ash	Volatiles	Fixed Carbon
BSG Char	3	18	21	57

Table 22 Elemental analysis of Char produced from Pyroformer

Elemental analysis	mass % dry ash free basis				
	C	H	N	S	O ^a
BSG Char	61.8	4	5.2	1.9	27.1

^a By difference

The fixed carbon content increased 47% and the volatile matter had decreased 57% from the original feedstock as expected from the pyrolysis process. The biochar was found to be very dry with a moisture content of 3% and containing a high ash content of 18%. The heating value obtained by bomb calorimeter was 26-28 MJ/kg which has higher energy content than the original feedstock.

The carbon contents show that the char is rich in carbon (approximately 15% higher than in the original feedstock) with oxygen determined by difference. A high level of hydrogen 4% nitrogen 5.2% and sulphur 1.9% was detected. The O/C ratio of the char was 0.43 and the H/C ratio was 0.06 indicating the char produced at 450°C is richer in oxygen content and may have retained the oxygen from the bio-oils. Crombie et al, 2012[181] reported that a char material with an O:C ratio in the range between 0.2-0.6 would be expected to have mean residence time (stability) of 100-1000 years in soils. Therefore the char would be a long-term stable biochar for soils.



Figure 69 Biochar produced from Pyroformer

The char has a useful energy content that can be of use for combustion in boilers and furnaces or to provide heat for the pyrolysis process. However the high ash content may lead to ash slagging, fouling and corrosion in boilers due to the low melting points of alkali and alkaline earth metals. The presence of a high nitrogen and sulphur content in the char may also lead to the release of NO_x and SO_x along with their precursors such as NH_3 and SO_2 when combusted.

Sanna et al, 2011[135] obtained biochar from spent grains WSG and BSG. The author reported high carbon (63-67%) and nitrogen (4-5%) contents that can provide nutrients to soil and crop productivity making it very attractive as a soil amendment leading to an overall process with carbon negative emissions.

The use of char/biochar as a soil improver or fertiliser is attracting widespread attention, as reported by Hornung et al, 2011 [25]Industrial agriculture has a high demand for fertilizer. Nutrients such as nitrogen, phosphorous, potassium and carbon are important for plant growth, and were found to be present with mass fractions of 5.2%, 1.68%, 0.1% and 61.8%. Therefore applying char to agricultural land could improve soil fertility promoting plant growth as well as storing carbon.

Table 23 Elemental Analysis of char ash produced from Pyroformer

	mass %,					
	Al	Ca	Fe	K	Mg	P
BSG char	0.2	0.9	0.3	0.1	0.4	1.68

The TGA and DTG combustion profile of the char is shown in Figure 70 below. Combustion profiles were carried out in an air atmosphere. The weight loss can be seen to occur between 300°C and 770°C with peaks between 500-600°C. Much of the cellulose and hemicellulose fibres would have degraded therefore the peaks that are likely to be and still be present within the char solids are lignin fibres.

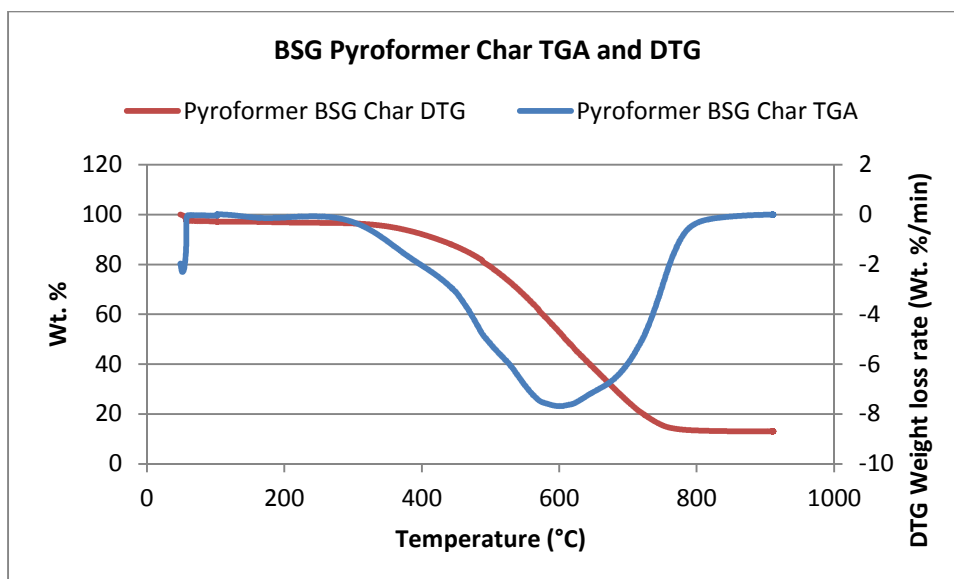


Figure 70 Pyroformer BSG Char TGA and DTG curve

7.4.3 Permanent gases

The permanent gases were analysed post quench using an offline GC-TCD analyser and the results are given in Table 24. The permanent gases detected were hydrogen, nitrogen, carbon monoxide, methane and carbon dioxide. Hydrogen of about 1-2vol% was produced; this may be due to cracking reforming reactions taking place between hot char and pyrolysis vapours. Other species that were formed included methane and carbon monoxide. The heating value of the gas was 6.7MJ/m^3 , largely due to the high methane content. The gas can be combusted along with some char to meet heat demands of the Pyroformer or a feedstock dryer. Carbon dioxide was relatively high at 64vol% and is likely to be due to decarboxylation reactions taking place.

Table 24 Yield of permanent gases produced from Pyroformer

Gases	vol% permanent gases					
	H ₂	O ₂	N ₂	CO	CH ₄	CO ₂
	1.6	0.45	4.6	19.74	9.43	64.18

7.5 Summary

Intermediate pyrolysis products bio-oil 52%, char 29% and permanent gas 21% of BSG have been produced using the Pyroformer reactor. The condensed bio-oil produced was found to have an organic and an aqueous phase. The two phases were separated easily using a gravimetric settler.

The organic phase was very dark in appearance and viscous with a strong smell of carbonised organic material. The aqueous phase was red in appearance and contained some evidence of solid particles.

The calorific value of the bio-oil (organic phase) was 20 MJ/kg, which is about half the energy content of fossil diesel. The low energy content is associated with the high oxygen content of the oil. Due to the high moisture, solids content and poor physical properties of the bio-oil, it is unsuitable as a fuel source in an engine without upgrading. The bio-oil upon visual inspection is liquid but not homogeneous as it contained many bituminous solids and viscous compounds which overtime could polymerize with age if stored at room temperature. The solids content however must remain low if the bio-oil is to be considered to be suitable for engine applications.

The carbon residue and ash for the bio-oil was 1.93% and 0.44% respectively which in contrast to diesel and biodiesel are relatively high and could indicate potential blockage problems in engine applications such as clogging injectors and coke formation in the combustion chamber. Viscosity was very high at 222 cSt; this may be due to the amount of solids present in the bio-oil and would make atomisation difficult. The major components detected in the bio-oils were aromatic hydrocarbons at 23% in the form of benzene, toluene and xylenes. The other major group found was phenols 15.3%, alkenes 8%, alkanes 5.5%, and Guaiacol 6.1%.

The biochar was found to be very dry with a moisture content of 3% and containing a high ash content of 18%. The heating value for the char was found to be 26-28 MJ/kg which has higher energy content than the original feedstock. The char has a useful energy content that can be of use for combustion in boilers and furnaces or to provide heat for the pyrolysis process. However the high ash content may lead to ash slagging, fouling and corrosion in boilers due to the low melting points of alkali and alkaline earth metals. The presence of a high nitrogen and sulphur content in the char may also lead to the release of NO_x and SO_x along with their precursors such as NH_3 and SO_2 when combusted.

The carbon contents show that the char is rich in carbon (approximately 15% higher than in the original feedstock) with oxygen determined by difference. A high level of hydrogen 4% nitrogen 5.2% and sulphur 1.9% was detected. The O/C ratio of the char was 0.43 and at 450°C is richer in oxygen content and may have retained the oxygen from the bio-oils, and would be expected to have mean residence time (stability) of 100-1000 years in soils.

Hydrogen of about 1-2vol% was produced; this may be due to cracking reforming reactions taking place between hot char and pyrolysis vapours. Other species that were formed included methane and carbon monoxide. The heating value of the gas was 6.7MJ/m³, largely due to the high methane content. The gas can be combusted along with some char to meet heat demands of the Pyroformer or a feedstock dryer. Carbon dioxide was relatively high at 64vol% and is likely to be due to decarboxylation reactions taking place.

8 Non-Catalytic Bench Scale Intermediate Pyrolysis Results and Discussion

8.1 Introduction

Intermediate pyrolysis of BSG using a non-catalytic bench-scale fixed bed pyrolysis reactor was conducted in an attempt to simulate the Pyroformer. The objectives of these experiments were to investigate the yields and properties of the pyrolysis products formed at a temperature of 450°C at two different pyrolysis heating rates, in order to identify the optimum pyrolysis heating rate to obtain liquid, solid and gas product yields similar to those produced from the Pyroformer. The optimum heating rate will be adopted for the study of catalytic steam reforming pyrolysis presented in Chapter 9. A secondary catalytic reactor was added to the bench scale reactor as described in Section 6.3. Two further pyrolysis experiments were conducted as an essential reference point without catalysts prior to catalytic experiments. The analysis of the product yields properties based on methods discussed from chapter 6, and the mass balance from the experiments are discussed below.

8.2 Bench Scale Intermediate Pyrolysis Reactor

Approximately 100g of dried and ground BSG feedstock was placed into the batch fixed bed reactor. The nitrogen purge was set at 50cm³/min then introduced into the reactor, afterwards the reactor heater was switched on to heat the pyrolysis reactor to the desired temperature of 450°C at two different heating rates, 25°C/min and then 50°C/min.

The BSG particles are heated by radiation in the heated furnace and finally reach the desired temperature. At the desired temperature the biomass is kept for approximately 20 minutes until no further pyrolysis volatiles form. In these initial experiments no catalysts were used, however a catalytic reforming reactor housed in a furnace was later added downstream and set at 500°C and then at 850°C.

The pyrolysis temperature of 450°C was selected based on results obtained from the TGA and pyroformer experiments as discussed in Chapters 4 and 6. Figure 71 below shows the temperature profiles for BSG inside the carbolite bench scale pyrolysis reactor at the two different heating rates. Figure 72 below illustrates the permanent gas release rate of BSG at both different heating rates.

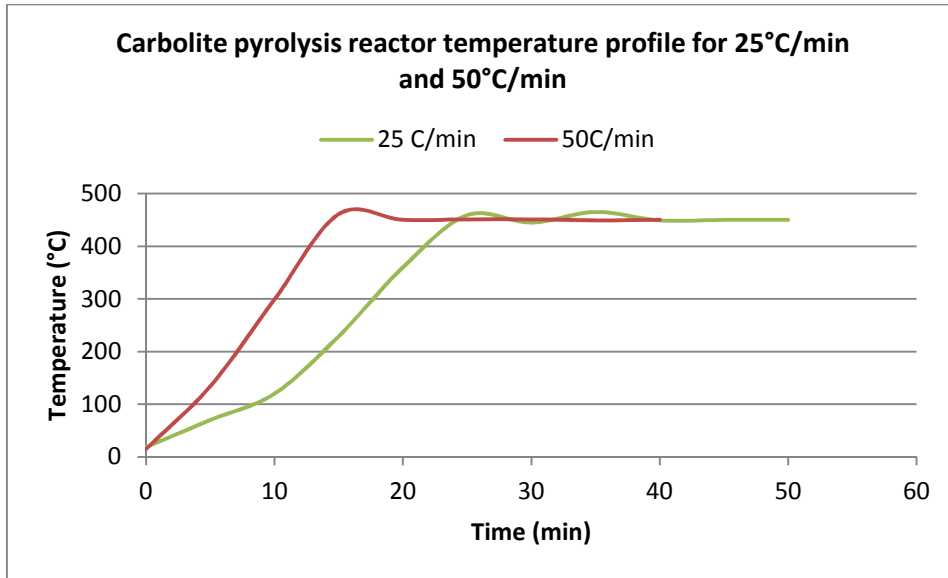


Figure 71 Carbolite pyrolysis reactor and biomass temperature for BSG

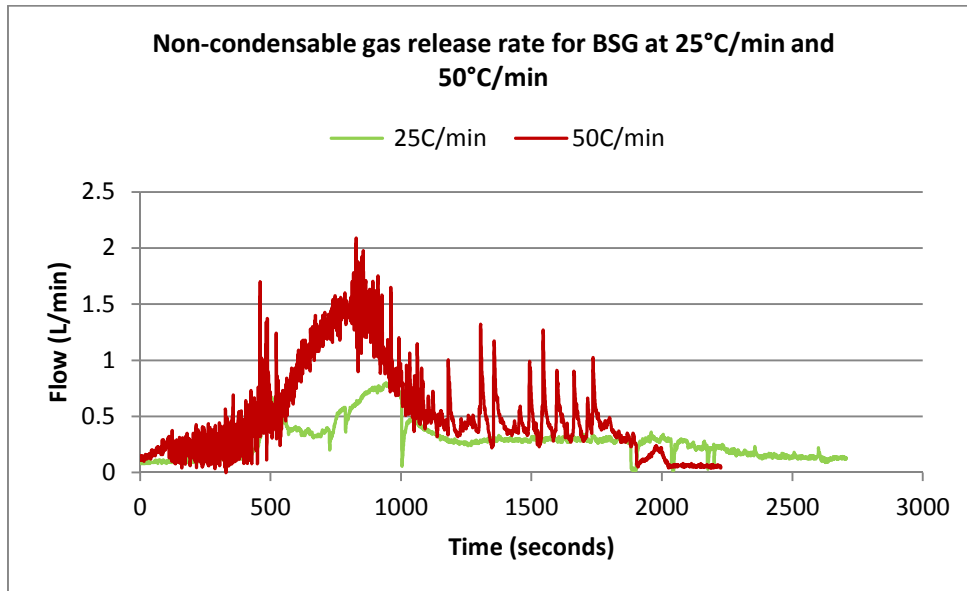


Figure 72 Permanent gas release rate for BSG at 25°C/min & 50°C/min heating rate

The reactor temperature was recorded every two minutes, with each experiments lasting approximately 40 minutes. The duration of each experiment represents the solids residence time as the time taken for the feed to be fully converted inside the reactor. The reactor takes approximately 13-15 minutes to reach set-point temperature at the higher heating rate and 20-23 minutes at the lower heating rate. The vapour residence time was not determined but can be assumed to be in the order of a few seconds.

The vapour residence time seemed to be affected by the amount of feed inside the reactor and the purge gas flow rate. Phan et al, 2008 [182] reported that the bed depth inside the reactor had a strong influence on the properties of pyrolysis products but a small effect on the yield of pyrolysis products.

The purge gas flow rate affected the velocity of the pyrolysis vapours leaving the pyrolysis zone; therefore both these factors are kept constant throughout the pyrolysis experiments.

Much of the BSG pyrolysis vapours release BSG occurs between temperatures 150°C and 450°C. Literature has reported that the basic biomass components, hemicellulose, cellulose and lignin, decompose thermochemically in the following temperature ranges: 150-350°C, 275-350°C and 250-500°C [164]. Between temperatures 170-320°C represents the decomposition of hemicellulose and the initial decomposition of cellulose, and between temperatures 320-450°C signifies the final decomposition of cellulose and lignin. Due to the high volatility content of BSG, most of the volatiles are released below 450°C.

8.3 Mass Balance

The mass balance sheet used for recording data can be found in APPENDIX B. For each experiment the reactor transition tubes and condensers are weighed before and after each experiment, this allows determination of the product yields, and the overall mass balance. Much of the char was retained in the primary quartz reactor, and the transition tubes and oil-pots contained the bio-oils. Prior to weighing, all the glassware apparatus was thoroughly cleaned and dried. Permanent gases composition was normalised and obtained by difference. The mass balance for these tests are summarised in Table 25 and then discussed.

Table 25 Summary of mass balance for non-catalytic bench-scale pyrolysis experiments

	Unit	BSG	BSG	Barley	Brunei Rice Husk [183]
Moisture content	wt.%	8%	8%	12%	8.43%
Ash content	wt.%, dry basis	4.5	4.5	6	14.83
Pyrolysis temperature	°C	450	450	450	450
Pyrolysis heating rate	°C/min	25	50	50	25
Catalysts		-	-	-	-
Catalytic reforming temperature	°C	-	-	-	-
Steam flow rate	ml/s	-	-	-	-
Steam : Carbon Ratio		-	-	-	-
Biomass feed	g, dry basis	100.33	100.11	100.64	-
<i>Pyrolysis Yields (as received):</i>					
Liquids	wt.%	34.39	47.83	39.32	39.61
Char	wt.%	32.44	30.87	30.13	41.92
Permanent Gas:	wt.%	33.5	21.41	30.55	18.47
H ₂	vol%	0%	0%	-	-
O ₂	vol%	1%	0%	-	-
N ₂	vol%	32%	28%	-	-
CO	vol%	13%	17%	-	-
CH ₄	vol%	4%	9%	-	-
CO ₂	vol%	50%	45%	-	-
HHV	MJ/kg	1.12	1.3	-	-

All bio-oils produced at 450°C but at different heating rates were found to have phase separated into two phases. As was found for bio-oils produced using the pyroformer in chapter 7, the top layer contained the oily organic fraction referred to as bio-oil, and the bottom layer contained the water fraction referred to as the aqueous phase. This is due to pyrolysis vapours being cracked by char.[31, 41-46]

At the lower heating rate (25°C/min) the product yield was 35% bio-oil, 31% char and 34% gas, and at the higher heating rate 48% bio-oil, 31% char and 21% permanent gases. Table 25 and Figure 73 show these data comparatively.

The yield of char remains the same and therefore appears unaffected by heating rate; however the yield of condensable liquids increased by 13% and the amount of permanent gases reduced correspondingly at the higher heating rate.

Dried and ground barley was tested at the same temperature but heating rate at 100°C/min for comparison purposes and the yields were 39% for bio-oil, 30% for char and 31% permanent gases. The bio-oil produced from barley was found to have phase separated into two phases and was expected. Abu-Bakr [183] investigated Brunei rice husk using the same reactor at 450°C at a heating rate of 25°C/min and found the product yields to be 40% for bio-oil, 42% for char and 19% for permanent gases. The bio-oils produced were also reported to have phase separated. The author reported that the pyrolysis condition can be classified as intermediate pyrolysis due to the moderate temperature used and the yields produced were comparable to the patented Halo-clean process for rice husks.

Therefore the products yielded for BSG at 50°C/min are comparable to the yields produced by the Pyroformer and the Haloclean at the same temperature. Therefore in order to carry out reforming experiments simulating the Pyroformer the higher heating rate of 50°C/min was selected for all subsequent experiments.

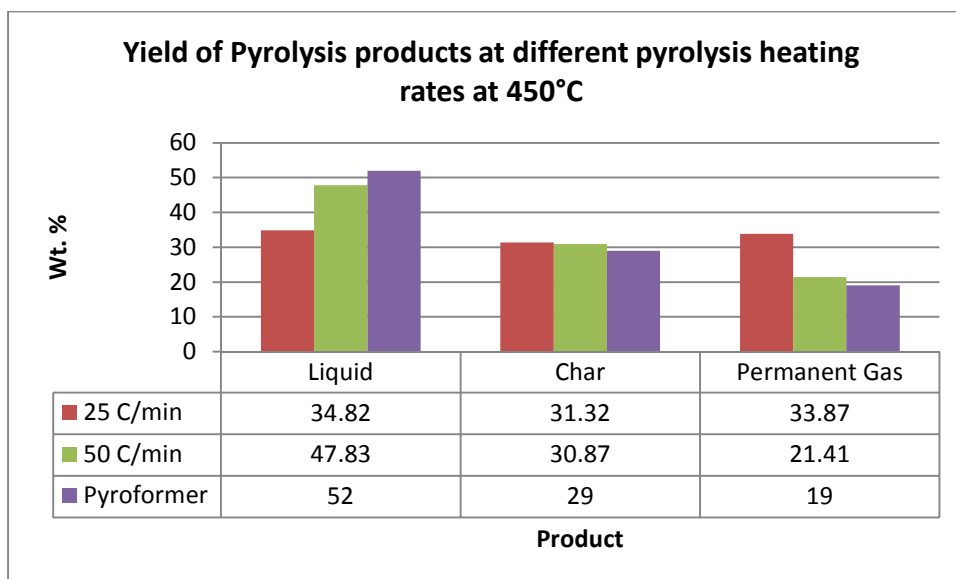


Figure 73 Comparison of the yields of products from different pyrolysis heating rates

A secondary catalytic reactor was added to the bench scale reactor as described in Section 6.3. The secondary reactor is housed in an electrical furnace placed directly after the batch pyrolysis reactor and before the glass liquid collection system. The glass liquid collection system downstream of the unit is unchanged. Two pyrolysis experiments were conducted as an essential reference point without catalysts prior to catalytic experiments. Quartz wool was placed inside the secondary reactor and was tested initially at 500°C and then at 850°C during the pyrolysis runs.

The quartz wool serves two functions; firstly it will support the catalysts as a packed bed therefore preventing the catalysts from falling and secondly functions as a hot vapour filtration by capturing any char fines that can otherwise cover catalysts surface leading to catalyst deactivation. The use of quartz wool can also reduce the solids content of the bio-oil.

The photographs below (Figure 74) show the quartz wool before and after use at 500°C and then at 850°C. The quartz wool was effective in capturing some char fines which otherwise may cover the catalysts surfaces leading to catalysts deactivation. The wool however contained condensed pyrolysis vapours photo (b) 500°C quartz wool contained far more char fines and condensed pyrolysis vapours than that wool photo (c) on right which was at 850°C.

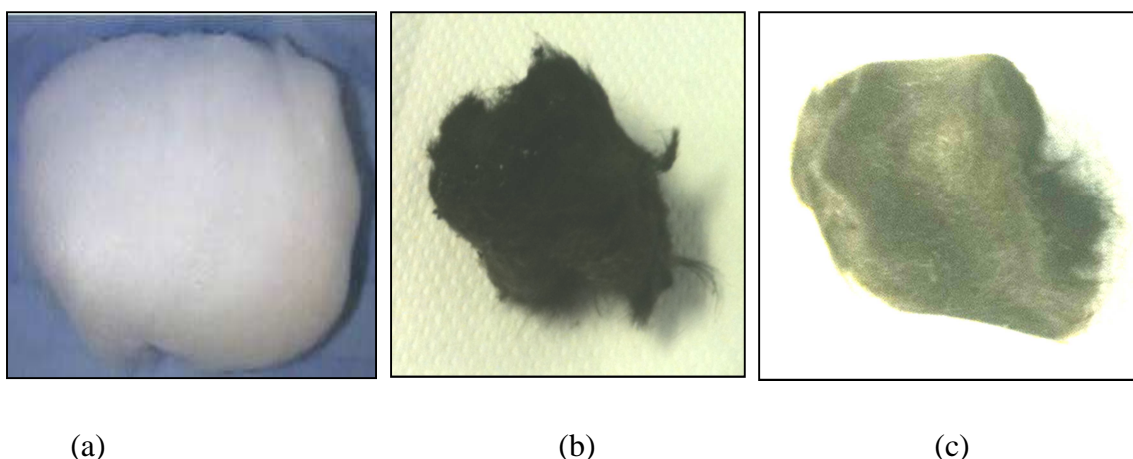


Figure 74 Quartz wool before (a), after (b) 500°C and then after (c) 850°C

The mass balance analysis for the pyrolysis runs with the addition of the secondary catalytic reactor using quartz wool is summarised in Table 26.

Table 26 Summary of mass balances for experiments with the addition of secondary catalytic reactor (without catalysts)

	Unit	BSG 100deg/min + 500°C	BSG 100 deg/min +850°C	BSG 100 deg/min +850°C (repeated)
Moisture content	wt.%	8%	8%	8%
Ash content	wt.%, dry basis	4.5	4.5	4.5
Pyrolysis temperature	°C	450	450	450
Pyrolysis heating rate	°C/min	50	50	50
Catalysts		-	-	-
Catalytic reforming temperature	°C	500	850	850
Steam flow rate	ml/s	-	-	-
Steam : Carbon Ratio		-	-	-
Biomass feed	g, dry basis	100.8	100.22	100.01
<i>Pyrolysis Yields (as received):</i>				
Liquids	wt.%	47.67	34.98	34.82
Char	wt.%	35.6	36.95	31.32
Permanent Gas:	wt.%	17.53	28.29	33.87
H ₂	vol%	0%	9%	8%
O ₂	vol%	0%	0%	0%
N ₂	vol%	16%	4%	5%
CO	vol%	24%	9%	11%
CH ₄	vol%	5%	9%	11%
CO ₂	vol%	55%	69%	65%
HHV	MJ/kg	1	1.7	1.9

Two experiments were conducted at different catalytic temperatures one at 500°C and then at 850°C. The mass balance for these runs are compared to the non-catalytic experiments conducted and discussed earlier in the section.

It appears that the presence of the secondary reactor with quartz wool at 850°C led to a reduction of liquid yields, with an increase in char and gas yields. This was due to thermal secondary reaction of pyrolysis vapours when exposed to high secondary heat.

The experiment conducted with a secondary reactor at 500°C using quartz wool in comparison to bench scale pyrolysis without the addition of the secondary reactor, no real difference was noted however char yield increased 4.73 wt.% which is likely to be due to experimental error. The general error of each experiment was approximately $\pm 3\%$.

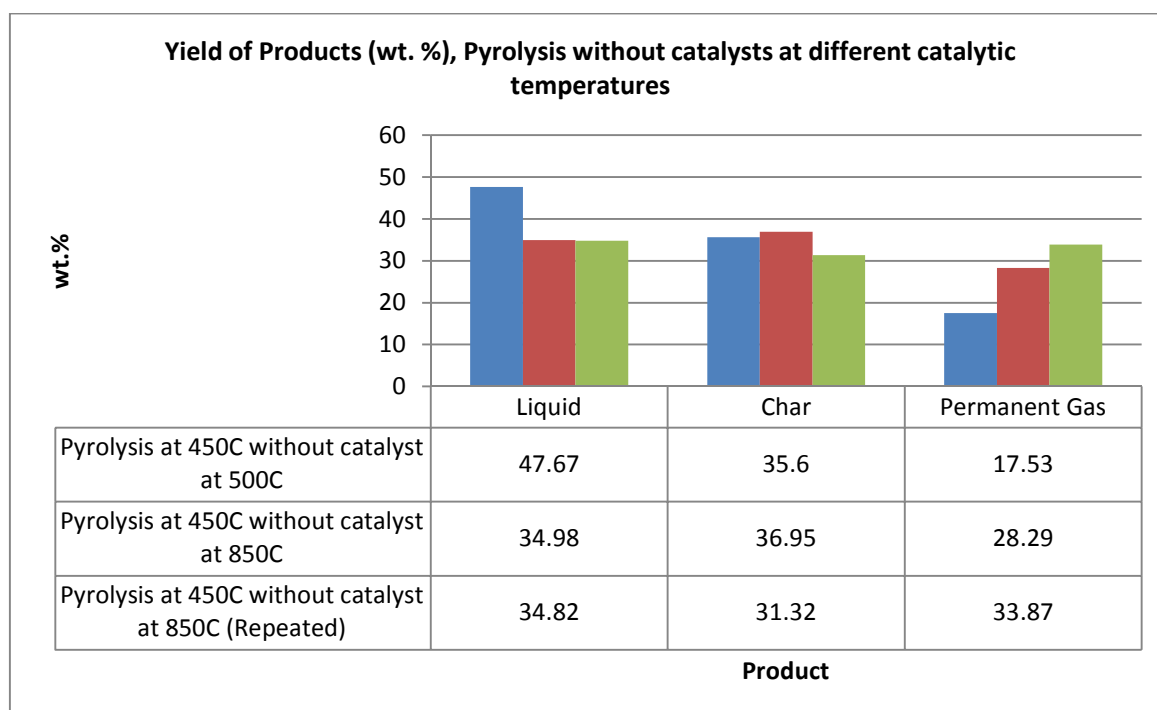


Figure 75 Comparison of the yields of products from different pyrolysis heating rates and with 2nd reactor at 500°C and 850°C (no catalyst)

At the higher temperature of 850°C, the mass balance yields were compared to the bench scale pyrolysis experiments without the addition of a secondary reactor. The mass balance yields show liquids had reduced to 34.98 wt.% from 47.83 wt.%, char increased to 36.95 wt.% from 30.87 wt.% and permanent gases increased to 28.29 wt.% from 21.41 wt.%. Again the increase in char content is likely to be due to experimental error.

The batch pyrolysis reactor was inspected; it was observed that a small fraction of char and condensed pyrolysis vapours had fouled the k thermocouple housed inside the pyrolysis reactor to measure the

temperature of the bed. As a result of fouling the inaccurate temperature readings were recorded which ultimately affected the heating rate and overall the product distribution. The thermocouple was cleaned and a test at a catalytic temperature of 850°C was repeated. The product yield obtained for the repeated tests was 34.82 wt. % for liquids, 31.32 wt. % for char and 33.87 wt. % for permanent gases.

8.4 Characterisation of Non-Catalytic Bench Scale Intermediate Pyrolysis Products

8.4.1 Bio Oil Analysis

The properties of the bio-oils produced from non-catalytic experiments using the bench scale intermediate pyrolysis reactor were characterized using various analytical techniques in order to determine ultimate (C, H, N, O,S & Cl), water content, pH, acid number and heating values as described in Chapter 6. Chemical composition analysis was conducted by GC/MS.

Figure 76 illustrates the bio-oil liquids produced at different heating rates, left at 25°C/min and right at 50°C/min. Both oils show significant phase separation with a dark oily organic layer (top) and an aqueous phase (lower). As was mentioned earlier this is believed to be due to pyrolysis vapours making contact with the generated char causing a catalytic effect within the fixed bed pyrolysis reactor [4-10]. The lower heating rate has produced a lower quantity bio-oil in comparison the higher heating rate, this may be due to restrictions of heat and mass transfer between the BSG particles.[184] It is known that generally increasing the pyrolysis temperature has a significant effect on product distribution in particular increasing oil and gas yields[185].



Figure 76 Bio-oil samples received different heating rates (left) 25°C/min (right) 50°C/min

Table 27 shows the ultimate analysis of the bio-oil liquids (organic – top layer) produced at the different heating rates without the addition of the secondary reactor. The bio-oil produced with the secondary catalytic reactor at 850°C using quartz wool as a reference was also analysed and is included for comparison. As the heating rate increased there was a reduction in the carbon content (from 70.27 wt.% to 36.22 wt.%) and an increase in the oxygen content (from 14.48 wt.% to 25.79 wt.%). Hydrogen content remained unchanged at 8 wt.% for all three oils.

Compared with the oil produced in the Pyroformer, the bench scale oil without catalysis showed an increase in C by approximately 15%, and a reduction in H, N, and O (1.78%, 1.99%, and 4.91% respectively). Increases in S and Cl were seen of 0.7% and 0.1% respectively. The increase in carbon content is likely due to the presence of fine chars.

The presence of the secondary reactor at 850°C caused a further reduction in the carbon content to 47.9 wt.% and an increase in oxygen content to 37.32 wt.% (determined by difference). Other components (hydrogen, nitrogen and poisons like sulphur and chlorine) did not vary too much.

This indicates that a secondary reactor at higher temperature there is noticeable extent of thermal decomposition reactions taking place mainly the cracking of the oxygenated compounds in the pyrolysis vapours. As the temperature increases there was evidence of some trace hydrogen starting to appear as product of non-catalytic reactions over the inert surfaces. Also the carbon conversion to gas seems to become more important as temperature increases. This suggests that at high temperatures such as 850°C the compounds could easily react without a catalyst, however if a catalyst was introduced part of the reaction could well be controlled by the thermal effects plus the contribution of catalytic reactions due to either reforming of oxygenates or the catalytic conversion of the intermediate generated.

Table 27 Non catalytic bio-oil analysis produced at different heating rate

Bio-oil	BSG 25°C/min	BSG 50°C/min	BSG 50°C/min +850°C (2 nd reactor)
C	70.27	62.57	47.9
H	8.64	8.12	8.28
N	4.16	1.41	4.04
S	2.23	2.01	2.27
O	14.48	25.79	37.32
Cl	0.22	0.1	0.19
Water Content:			
Organic (wt.%)	3.8	3.8	-
Aqueous (wt.%)	65	65	-
pH:			
organic	5.26	5.3	-
aqueous	5.1	5.1	-
Acid Number			-
mgKOH/g	60.19	60.2	
HHV	33.4	28.9	

The water content of the bio-oils produced from BSG at different heating rates was determined using a Mettler Toledo V30 Compact Volumetric Karl Fischer (KF) titrator in accordance with ASTM E203. The pH was obtained using the Sartorius basic meter PB-11.

Due to the bio-oil's phase separation the organic and aqueous phase were analysed. The organic and aqueous phases were 3.8 wt.% and 65% for both the bio-oil respectively. Much of the moisture from the BSG feedstock was reduced through drying; however the high water content is due to reaction water which is produced during pyrolysis following complex thermal degradation reactions. Water present in bio-oils produced from fast pyrolysis considered for CHP reduces the heating value, and increases the ignition delay but improves the viscosity. Due to phase separation of bio-oils the organic phase forms a layer which can be easily separated from the aqueous phase through gravimetric settling as was described in chapter 7; so much of the organic phase can be collected and stored.

The pH for bio-oil (top phase) and aqueous (lower phase) was observed to be about 5 and the acidity number to be 60mg KOH/g. It has been reported that the typical pH of bio-oils (wood-derived) is usually between 1-2.5 making them quite acidic and corrosive to materials and equipment if stored for a period of time [53]. The pH not being as low as typical bio-oils may be due to the absence of acids such as carboxylic, acetic and formic acids.

Water, pH and acid number analysis was not able to be conducted for bio-oil produced with a secondary reactor at high temperature. The quantity of organic phase was very low due to the further

breakdown of organic components at higher temperatures. The appearance of this bio-oil was very dark and the lower aqueous appeared to have a yellow aqueous phase.

8.4.1.1 GCMS Bio-oil without catalyst at 25°C/min heating rate

The bio-oil produced at a heating rate of 25°C/min was dissolved in ethanol and was characterised for its chemical composition using liquid gas chromatography. The chromatograph for this oil is presented in Figure 77 and Table 28.

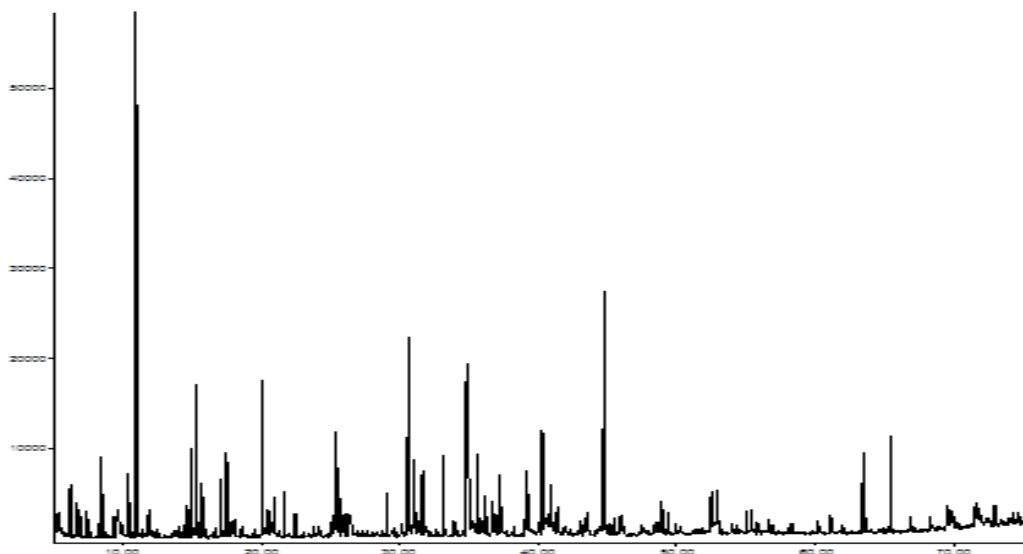


Figure 77 GC/MS analysis of BSG bench scale bio-oil at 25°C/min (chemical abundant vs. Retention time)

More than 100 peaks were detected corresponding to different organic compounds. Each peak identified has an 'Area%' given in Table 28 representing each identified component as a fraction integrated over the whole mass spectrum. The major peaks detected and identified with the highest abundance were toluene 11.48%, phenol, 4-methyl- 7.13%, tetradecane 6.76%, carbamic acid, and methyl- phenyl ester 6.69%. These were the largest components present. The average molecular weight of the bio-oil components at the lower heating rate was determined to be 145.

Table 28 Composition of BSG bio-oil without catalysts at 25°C/min heating rate

Retention Time	Chemical Name	Chemical Group	Molecular Formula	RMM	Area %
6.171	Furan, 2-methyl-	Furan	C ₅ H ₆ O	82.1	0.77
7.286	1,5-Pentanediol, 3-methyl-	Alcohol	C ₆ H ₁₄ O ₂	118.17	0.84
8.493	2,5-Dimethylfuran (96, 96, RI 0)	Furan	C ₆ H ₈ O	96.13	1.51
9.654	trans,trans-1,3,5-Heptatriene	Isomers	C ₇ H ₁₀	94.15	1.88
10.413	1-Octene, 3,7-dimethyl-	Alkene	C ₁₀ H ₂₀	140.27	1.2
10.965	Toluene	Aromatic	C ₇ H ₈	92.14	11.48
11.678	Pyridine (79, 79, RI 0)	Pyridines	C ₅ H ₅ N	79.1	0.62
14.564	Cyclopentanone	Cyclopentanone	C ₅ H ₈ O	84.12	1
15.265	Ethylbenzene	Aromatic	C ₈ H ₁₀	106.17	3.6
15.668	p-Xylene	Aromatic	C ₈ H ₁₀	106.17	1.28
17.139	m-Xylene	Aromatic	C ₈ H ₁₀	106.17	1.32
17.496	Cyclooctatetraene (104, 104, RI 0)	Alkene	C ₈ H ₈	104.15	2.05
20.048	Decane, 1-chloro-	Alkane/Chlorine	C ₁₀ H ₂₁ Cl	176.73	3.53
20.496	2-Ethyltoluene	Aromatics	C ₉ H ₁₂	120.19	0.96
20.887	2-Cyclopenten-1-one,2-methyl-	Cyclopentanone	C ₆ H ₈ O	96.13	0.79
21.715	3-Ethyltoluol	Aromatics	C ₉ H ₁₂	120.19	1.28
25.394	Undecane	Alkanes	C ₁₁ H ₂₄	156.31	2.27
25.613	Benzene, Butyl-	Aromatic	C ₁₀ H ₁₄	134.22	1.54
26.027	1-Nonyne, 7-methyl-	Alcohol	C ₁₀ H ₁₈	138.25	0.67
30.591	Carbamic acid, methyl-, phenyl ester	Ester	C ₈ H ₉ NO ₂	151.2	6.69
30.948	Benzene, (3-methylbutyl)-	Alkene	C ₁₁ H ₁₆	148.24	1.86
31.638	Ethanone, 1-(1-cyclohexen-1-yl)-	Ketones	C ₈ H ₉ F ₃ O	178.15	2.14
33.132	2-Methylphenol (108, 108, RI 1260)	Phenol	C ₇ H ₈ O	108.14	2.38
34.857	Phenol, 4-methyl-	Phenol	C ₇ H ₈ O	108.14	7.13
35.581	Tridecane	Alkanes	C ₁₃ H ₂₈	184.36	3.07
36.087	Benzene, Hexyl-	Alkene	C ₁₂ H ₁₈	162.27	1.52
36.283	Octanenitrile	Alkyl Nitriles	C ₈ H ₁₅ N	125.21	0.62
36.627	Benzene, (1,3-dimethylbutyl)-	Alkene	C ₁₉ H ₂₆ N ₂	292	0.98
37.248	2,4-Dimethylphenol	Phenol	C ₈ H ₁₀ O	122.16	1.88
39.03	Phenol, 2,3-dimethyl-	Phenol	C ₈ H ₁₀ O	122.16	0.61
39.18	4-Ethylphenol	Phenol	C ₈ H ₁₀ O	122.16	2.42
40.939	4-Ethylguaiaacol	Guaicols	C ₉ H ₁₂ O ₂	152.19	1.53
41.33	Phenol, 4-ethyl-3-methyl-	Phenol	C ₈ H ₁₅ NO ₂	157.2	0.62
44.722	Tetradecane	Alkane	C ₁₄ H ₃₀	198.39	6.76
48.999	1-Tetradecene	Alkene	C ₁₄ H ₂₈	196.37	0.6
49.332	2-Methylindole	Alcohol	C ₉ H ₉ N	131.17	0.68
52.505	7-Tetradecene	Alkene	C ₁₄ H ₂₈	196.37	0.68
61.129	Thiazolo[5-4-f]quinoline	Alcohol	C ₁₀ H ₆ N ₂ S	186	0.68
63.428	Pentadecanoic acid, 14-methyl-, methyl ester	Ester	C ₁₅ H ₃₀ O ₂	242.4	2.01
65.394	Pentadecanenitrile	Alkyl Nitriles	C ₁₅ H ₂₉ N	223	2.64
76.489	Palmitic Acid	Organic Acid	C ₁₆ H ₃₂ O ₂	256.4	2.07
81.847	Undec-10-ynoic acid	Organic Acid	C ₁₁ H ₈ O ₂	182.16	0.72

8.4.1.2 GCMS Bio-oil without catalyst at 50°C/min heating rate

The bio-oil produced at a heating rate of 50°C/min was dissolved in ethanol and was characterised for its chemical composition using liquid gas chromatography. The chromatograph for this oil is presented in Figure 78 and Table 29.

The results show that there was no significant difference from the Pyroformer oils (see Figure 67 and Table 20).

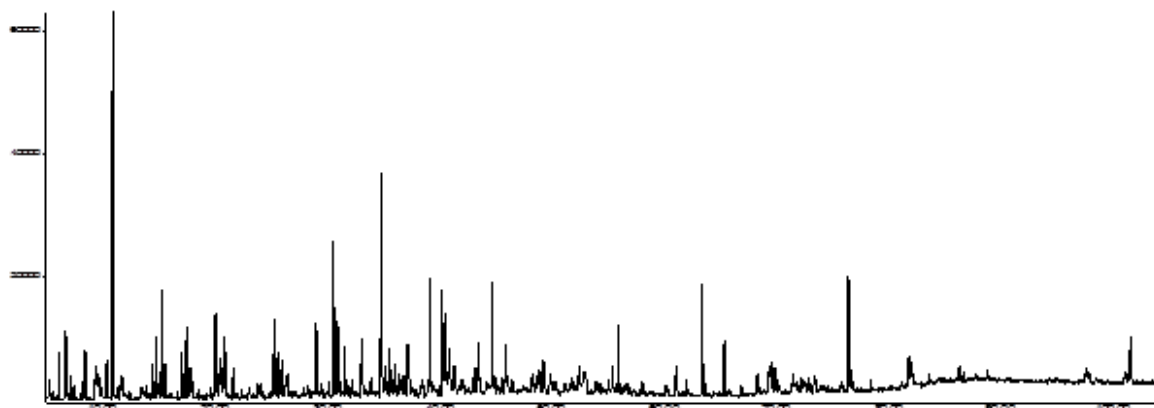


Figure 78 GC/MS analysis of BSG bench scale bio-oil at 50°C/min (chemical abundant vs. Retention time)

Again more than 100 peaks were detected corresponding to different organic compounds being identified within the spectrum. The major peaks detected and identified with the highest abundance was toluene 11.48%, phenol, 4-methyl- 7.13%, tetradecane 6.76% and carbamic acid, methyl-, phenyl ester 6.69%, these were the largest components present. The average molecular weight of the bio-oil components at the higher heating rate was determined to be 142.

Table 29 Composition of BSG bio-oil without catalysts at 50°C/min heating rate

Retention Time	Chemical Name	Chemical Group	Molecular formula	RMM	Area %
8.493	2,5-Dimethylfuran	Furan	C ₆ H ₈ O	96.13	1.51
9.654	trans,trans-1,3,5-Heptatriene	Isomer	C ₇ H ₁₀	94.15	1.88
10.413	1-Octene, 3,7-dimethyl-	Alkene	C ₁₀ H ₂₀	140.27	1.2
10.965	Toluene	Aromatic	C ₇ H ₈	92.14	11.48
11.678	Pyridine	Pyridine	C ₅ H ₅ N	79.1	0.62
14.564	Cyclopentanone	Cyclopentanone	C ₅ H ₈ O	84.12	1
15.265	Ethylbenzene	Aromatic	C ₈ H ₁₀	106.17	3.6
15.668	p-Xylene	Aromatic	C ₈ H ₁₀	106.17	1.28
17.139	m-Xylene	Aromatic	C ₈ H ₁₀	106.17	1.32
17.496	Cyclooctatetraene	Alkene	C ₈ H ₈	104.15	2.05
20.048	Decane, 1-chloro-	Alkane/Chlorine	C ₁₀ H ₂₁ Cl	176.73	3.53
21.715	3-Ethyltoluol	Aromatic	C ₉ H ₁₂	120	1.28
25.394	Undecane	Alkane	C ₁₁ H ₂₄	156.31	2.27
25.613	Benzene, Butyl-	Aromatic	C ₁₀ H ₁₄	134.22	1.54
30.591	Carbamic acid, methyl-, phenyl ester	Ester	C ₈ H ₉ NO ₂	151.2	6.69
30.948	Benzene, (3-methylbutyl)-	Aromatic	C ₁₁ H ₁₆	148.24	1.86
31.638	Ethanone,	Ketone	C ₁₄ H ₁₈ O ₇	298.29	2.14
33.132	2-Methylphenol	Phenol	C ₇ H ₈ O	108.14	2.38
34.857	Phenol, 4-methyl-	Phenol	C ₇ H ₈ O	108.14	7.13
35.581	Tridecane	Alkane	C ₁₃ H ₂₈	184.36	3.07
36.087	Benzene, Hexyl-	Aromatic	C ₁₂ H ₁₈	163	1.52
37.248	2,4-Dimethylphenol	Phenol	C ₈ H ₁₀ O	122.16	1.88
39.18	4-Ethylphenol	Phenol	C ₈ H ₁₀ O	122.16	2.42
40.939	4-Ethylguaiaicol	Guaicol	C ₉ H ₁₂ O ₂	152.19	1.53
44.722	Tetradecane	Alkane	C ₁₄ H ₃₀	198.4	6.76
65.394	Pentadecanenitrile	Alkyl Nitrile	C ₁₅ H ₂₉ N	223.4	2.64
76.489	Palmitic Acid	Organic Acid	C ₁₆ H ₃₂ O ₂	256.42	2.07

8.4.1.3 GCMS Bio-oil with the addition of secondary catalytic reactor at 850°C

The bio-oil produced at a heating rate of 50°C/min using a secondary reactor without a catalyst at 850°C was dissolved in ethanol and was characterised for its chemical composition using liquid gas chromatography. The chromatograph for this oil is presented in Figure 79 and Table 30.

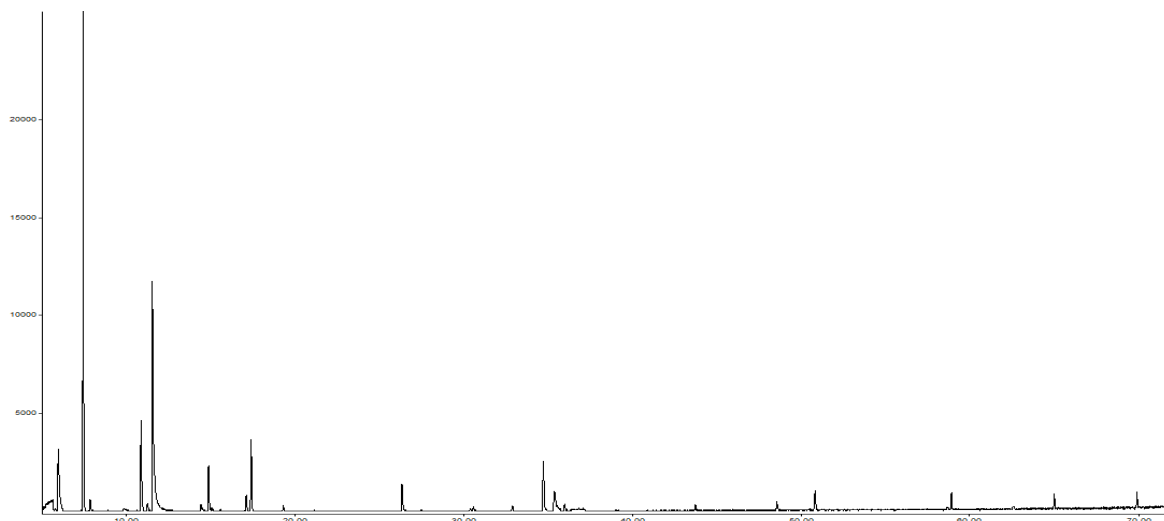


Figure 79 GC/MS analysis of BSG bench scale bio-oil at 50°C/min heating rate with secondary reactor at 850°C (no catalyst) (chemical abundant vs. Retention time)

As before, more than 100 peaks were detected corresponding to different organic compounds being identified within the spectrum. The major peaks detected and identified with the highest abundance was benzene 29.74%, pyridine (79, 79, RI0) 22.23%, toluene 7.36%, 2-propenenitrile 6.82%, cyclooctatetraene (104, 104, RI 0) 5.09%, naphthalene 4.43%, and butanedinitrile 3.01% these were the largest components present. The effects of a secondary reactor with no catalysts at 850°C had further cracked the organic components breaking down much of the phenols, furans, acids and esters. Toluene had reduced and the presence of benzene increased significantly as well as some polyacyclic aromatic hydrocarbons.

Table 30 Composition of BSG bio-oil without catalysts at 50°C/min heating rate with secondary reactor at 850°C (no catalyst)

Retention Time	Chemical Name	Chemical Group	Molecular		
			Formula	RMM	Area %
5.987	2-Propenenitrile	Alkyl Nitriles	C ₃ H ₃ N	53.1	6.82
7.458	Benzene	Aromatic	C ₆ H ₆	78.11	29.74
7.872	Thiophene	Alkene	C ₄ H ₄ S	84.14	0.73
10.884	Toluene	Aromatic	C ₇ H ₈	92.14	7.36
11.55	Pyridine (79, 79, RI 0)	Pyridines	C ₅ H ₅ N	79	22.23
14.884	Pyrrol	Alcohol	C ₄ H ₅ N	67	3.26
17.114	Phenylpropionic acid	Organic Acid	C ₉ H ₆ O ₂	146.14	1.07
17.401	Cyclooctatetraene (104, 104, RI 0)	Alkene	C ₈ H ₈	104.15	5.09
26.322	Benzene, 1-ethynyl-4-methyl-	Aromatic	C ₉ H ₈	116	2.26
32.874	Sulphur dioxide	Sulphur	H ₂ O ₃ S	82.08	0.44
34.702	Napthalene	Polyaromatic	C ₁₀ H ₈	128.17	4.43
35.357	Butanedinitrile	Alkyl Nitrile	C ₄ H ₄ N ₂	80.09	3.01
48.531	Acenaphthylene	Polyaromatic	-C ₁₂ H ₈	152-	0.99

Tables 31 and Figure 80 below illustrates the chemical groups for the chemicals detected in the bio-oils produced at 25°C/min, 50°C/min and at a catalytic temperature of 850°C but without catalysts in comparison to bio-oil produced using the pyroformer.

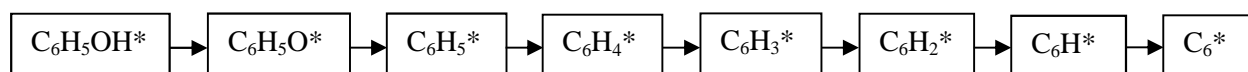
Table 31 Bio-oil chemical groups

Chemical Groups	Pyroformer	BSG 25°C/min	BSG 50°C/min	BSG 50°C/min +850°C
Alcohols	2.13	2.87	0	3.26
Alkanes	5.5	15.63	15.63	0
Alkenes	7.67	3.25	3.25	5.82
Alky Nitriles	1.57	0.62	0	9.83
Aromatic Hydrocarbons	22.68	24.54	23.88	39.36
Carboxaldehydes	0	0	0	0
Cyclopentanones	1.39	0.79	0	0
Esters	1.77	8.7	6.69	0
Furans	2.9	2.28	1.51	0
Guaicols	6.08	1.53	1.53	0
Isomers	0	1.88	1.88	0
Ketones	0.89	3.14	3.14	0
Polyaromatic Hydrocarbons	0	0	0	5.42
Phenols	15.27	15.04	13.81	0
Pyridines	0.0	0.0	0.0	0.0
Organic Acids	0	4.07	2.07	1.07
Oxygenates	0.99	0	0	0
Saccharides	0	0	0	0
Sulphurs	0	0	0	0.44
Chlorines	0	0	0	0

The bio-oils produced at two different heating rates show similarities to oils produced using the pyroformer with the large portion of chemicals detected as aromatic hydrocarbons 23-25%, phenols 13-15%, alkanes 5-15% and alkenes 6-8%. No polyaromatic hydrocarbons were produced in either of these bio-oils.

The bio-oil produced at a catalytic temperature of 850°C shows an increase of aromatic hydrocarbons of 39%, alkyl nitriles 9.8% and an increase of polyaromatic hydrocarbons of 5.4%. This is due to the thermal cracking of alkanes, esters, furans, guaicols, isomers, ketones and phenols which were not present in the bio-oil.

The decomposition of the phenolic components for instance (C₆H₅OH) is likely to occur via O-H bond cleavage rather than C-O bond cleavage. Therefore the most likely reaction pathway for phenol decomposition is as follows:



The decomposition of phenol is a continuous endothermic process leading to products of higher energies and reduced stabilities.[186]

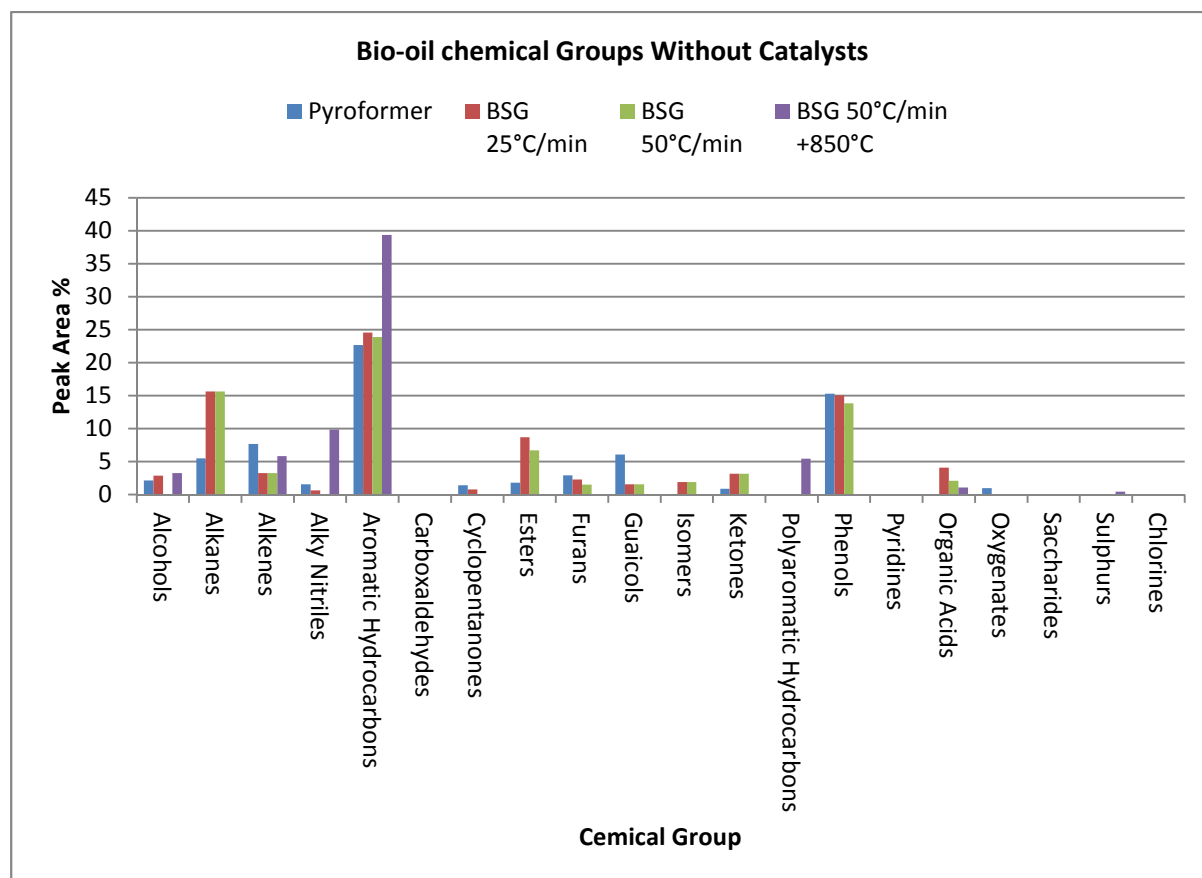


Figure 80 Chemical groups and the peak areas for non-catalytic bench scale intermediate pyrolysis bio-oil

8.4.2 Char Analysis

The char was the second largest product yield in the non-catalytic bench scale intermediate pyrolysis of BSG. The material produced was found to be very dark, brittle, coarse and very dry. It was analysed for its heating value, proximate analysis and elemental composition. Table 32 & 33 gives the proximate and elemental analysis of the char.

Table 32 Proximate analysis of char produced using bench scale reactor

Biochar	mass %			
	Moisture	Ash	Volatiles	Fixed Carbon
Pyroformer Char	3	18	21	57
25 °C/min	3	15	20	62
50 °C/min	2	14	22	62

The results show that the BSG char produced at a temperature of 450°C with heating rate 50°C/min is quite comparable to char produced from the Pyroformer. All char produced seemed to be unaffected by heating rate at the same temperature. Moisture content was very low at 3%, ash was high between 14-18%, volatiles between 20-22% and fixed carbon 57-62%. The char had a quite high energy content of 28-30 MJ/kg.

The ultimate analysis shows the char is rich in carbon at 68%, with a high level of hydrogen 3.5%, nitrogen 5.53% and sulphur 0.10% and chlorine 0.12% was detected. Oxygen 23% was determined by difference. Char obtained from barley was also analysed and was found to have a high carbon content of 66%, hydrogen 3.5%, nitrogen 1% and sulphur 0.91% and chlorine 1.34% was detected. Table 33 shows the data comparatively.

The proximate and ultimate analysis indicates that the chars produced using the bench scale intermediate pyrolysis unit is consistent with the chars obtained from the Pyroformer as described in chapter 7.

Table 33 Ultimate analysis of BSG char

Biochar	<i>Pyroformer</i>	<i>Bench Scale</i>	<i>Bench Scale</i>
	BSG Char (wt. %)	BSG char (wt.%)	Barley Char (wt.%)
C	61.8	68.24	65.93
H	4	3.47	3.51
N	5.2	5.53	1
O	27.1	22.76	28.65
S	1.9	<0.10	0.91
Cl	-	0.12	1.34
HHV (MJ/kg)	28	29	29
HHV (MJ/kg) Channiwala	28.7	30.8	29.9

The TGA and DTG combustion profile of char produced using the bench scale fixed bed pyrolysis unit is illustrated in Figure 81 below showing the weight loss. Combustion profiles were carried out in an air atmosphere. The weight loss can be seen to occur between 330°C and 900°C and peaks between 500-600°C. These peaks are largely caused by organic components that may still be present within the char solids such as cellulose and hemicelluloses fibres.

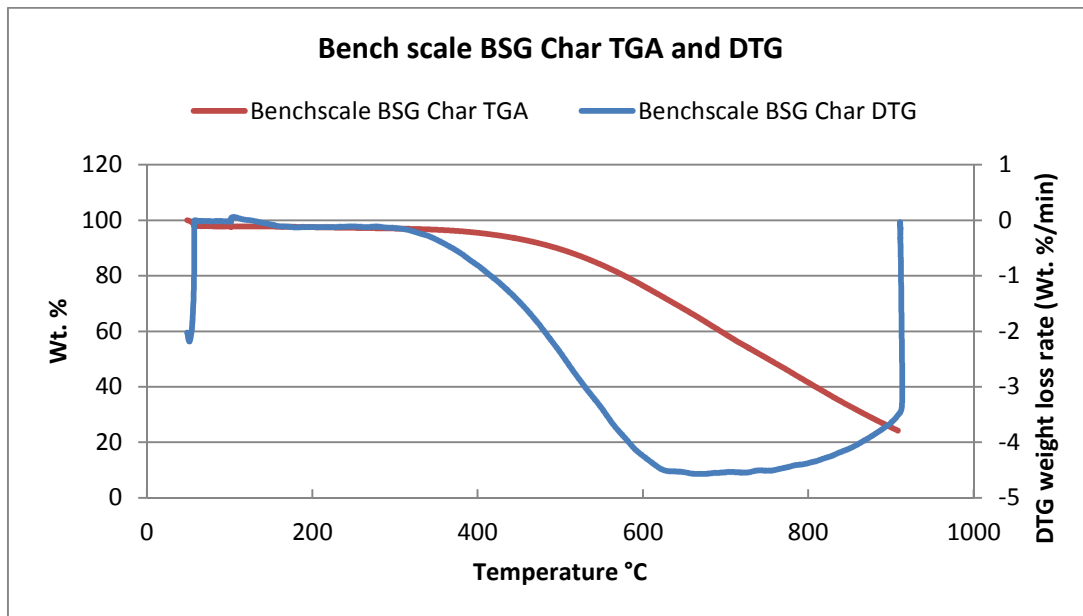


Figure 81 BSG char TGA and DTG combustion profiles

8.4.3 Permanent gases

Figure 82 shows that there was no real difference in the composition of permanent gases produced as heating rate increased. No H₂ or O₂ was produced in the bench scale experiments which is normal for pyrolysis. CO concentration was about 17 vol%, CH₄ concentration about 10vol% and CO₂ concentration about 45vol%.

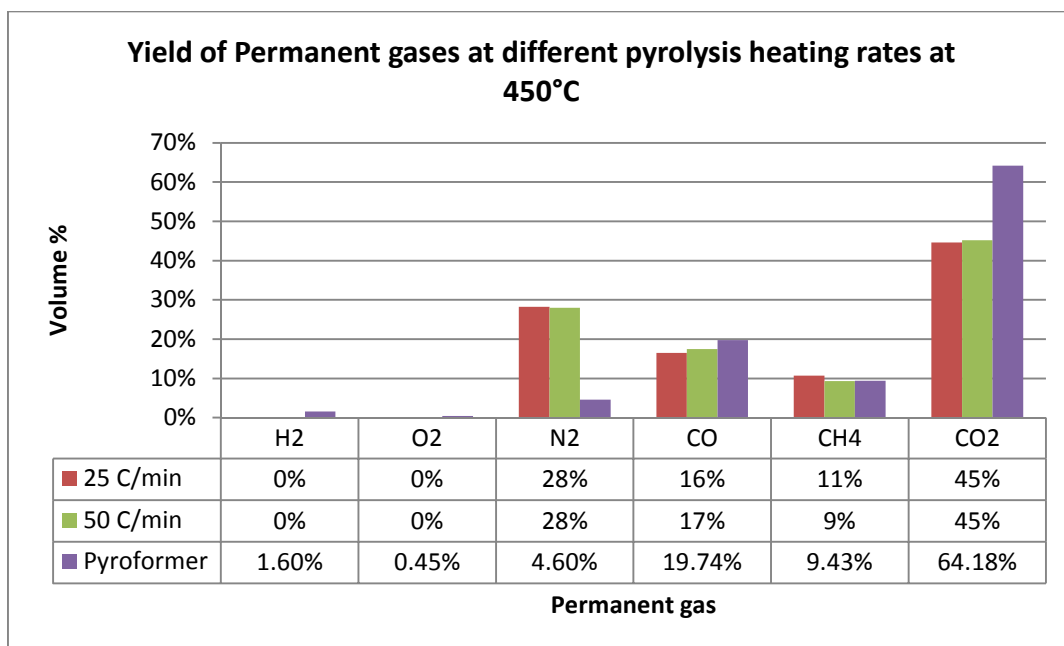


Figure 82 Comparison of the Permanent gas yields from different pyrolysis heating rates

Figure 83 illustrates the yield of permanent gases produced with the addition of a secondary catalytic reactor at different catalytic temperatures, but without catalysts. At high temperature thermal cracking had taken place as vapour was in contact with quartz wool producing more gases, in particular it was noted that H₂ was present at high temperature increasing to 10vol%, with a decrease in CO from 17vol% to 11vol%, CH₄ ranged between 9 -11vol% and an increase in CO₂ from 45vol% to 69vol%. Figure 83 shows these data comparatively.

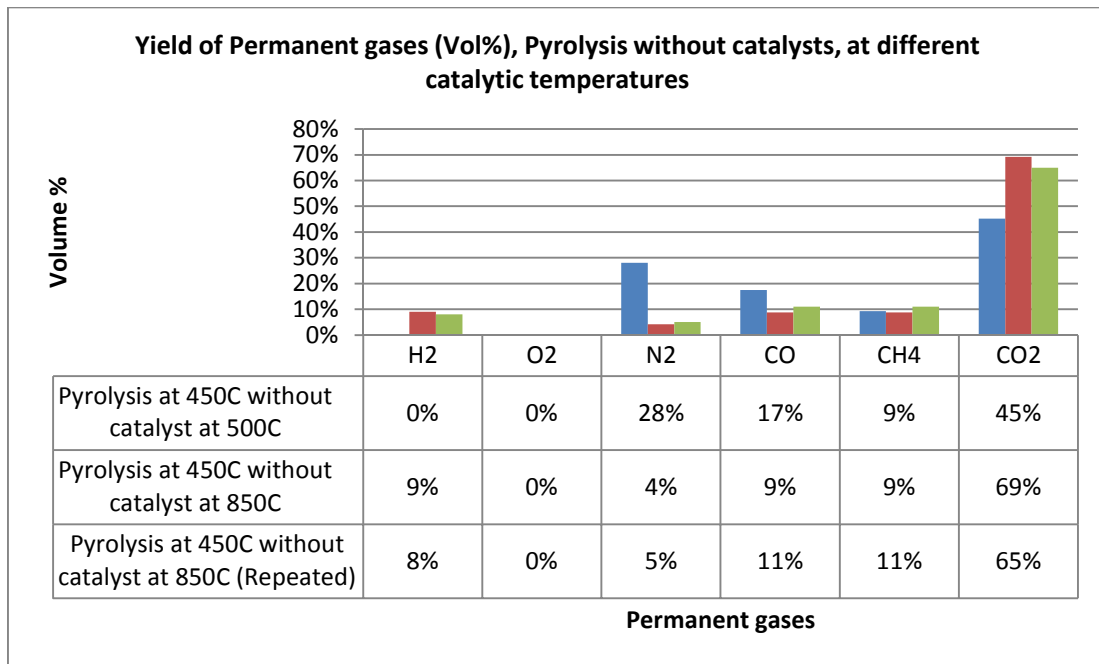


Figure 83 Comparison of the Permanent gas yields from different pyrolysis heating rates and with 2nd reactor at 500°C and 850°C (no catalyst)

8.4.3.1 Heating Value

The permanent gases were analysed post quench using an offline GC-TCD analyser and the results are given in Table 25 and Figure 84. The permanent gases detected were hydrogen, nitrogen, carbon monoxide, methane and carbon dioxide. The gases were normalised to 100%. The gases produced at the different heating rates 25°C/min and 50°C/min had a heating value of 1.12 and 1.16MJ/m³ respectively. The gas produced with a secondary catalytic reactor without any catalysts at 500°C and 850°C had a heating value of 1.31 and 1.7 MJ/m³ respectively.

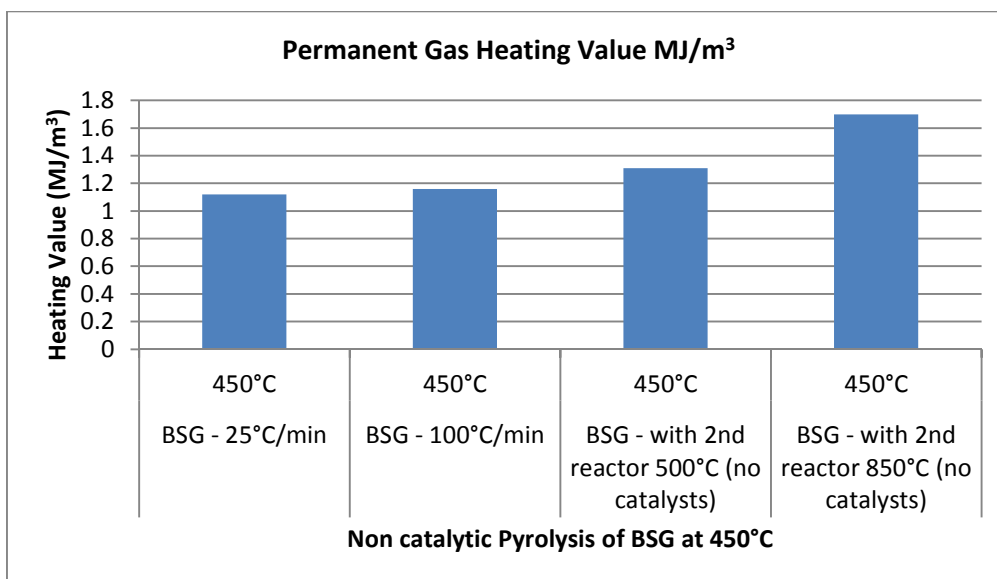


Figure 84 Permanent gas heating value of non-catalytic pyrolysis experiments

9 Catalytic Intermediate Pyrolysis Results and Discussion

9.1 Introduction

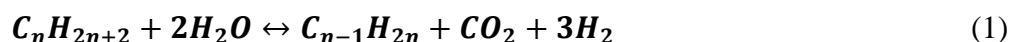
The experimental results are discussed for the intermediate pyrolysis and catalytic steam reforming of BSG feedstock. A secondary catalytic reactor was added to the bench scale pyrolysis reactor to form a close-coupled catalytic pyrolysis system to upgrade the generated hot pyrolysis vapours in situ. A high surface area commercial steam reforming nickel catalyst on an alumina support (Ni/Al₂O₃) was used as part of the catalytic experiments. Rhodium and platinum on an alumina support (Rh/Al₂O₃& Pt/Al₂O₃) were also selected and performances compared. All catalysts were prepared and supplied by Johnson Matthey Ltd[1]. Three catalytic steam reforming temperatures were selected and investigated: 500°C, 750°C and 850°C initially, without steam and then with the addition of steam. The initial catalytic experiments without steam made use of the aqueous phase or the water/steam present in the hot organic pyrolysis vapours to serve the steam reforming reactions within the secondary reactor, so as to observe quantity of syngas produced (in particular H₂ content) and the catalyst performance utilising the water already present in the system. It is anticipated that the passing of hot pyrolysis vapours over a fixed bed of catalysts will upgrade and enrich the pyrolysis gas prior to condensation in terms of heating value, due to an increased yield of methane, and hydrogen formation. Based on the experimental results obtained from the 14 runs of catalytic intermediate pyrolysis steam reforming of BSG were carried out.

9.2 Catalytic Bench Scale Intermediate Pyrolysis Reactor

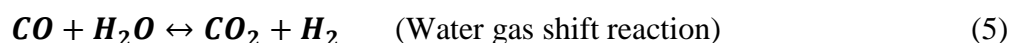
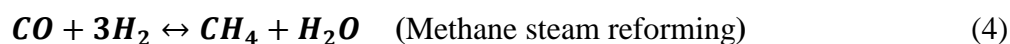
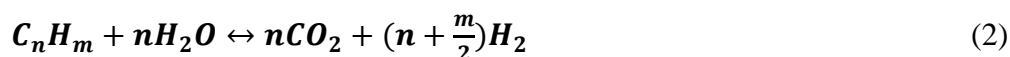
Catalyst was placed directly in the catalytic reforming reactor supported with quartz wool and the loaded reactor was then housed inside a furnace so that the catalyst bed could be heated up. The pyrolysis reactor was loaded with 100g of BSG and nitrogen purge was set at 50cm³/min and then introduced into the reactor. After reaching the desired catalytic temperature the catalysts were left for 30 minutes in a purged environment, afterwards the pyrolysis reactor heater was switched on to heat the pyrolysis reactor to the desired temperature 450°C at a heating rate of 50°C/min. The released pyrolysis vapours are then transported via nitrogen purge to the second stage catalytic reactor where steam or catalytic reforming of the pyrolysis vapours occurs.

The initial tests were to see the effect of reforming pyrolysis vapours without steam at the selected temperatures, as the presence of significant water content in the pyrolysis vapours may be sufficient for the catalytic reforming reactions to proceed. The runs without steam are then replicated using fresh catalyst samples with the addition of steam. A copper distillation kettle mounted on top of a heated plate was used to generate steam for steam reforming experiments.

The steam reforming reaction of any oxygenated organic compound can be represented as follows:



Other reactions that may take place are as follows:



These reactions are only a guide, as pyrolysis vapours contain complicated hydrocarbon chains, but also oxygenated compounds.

The mechanism of steam reforming oxygenated compounds over metal catalysts is proposed to correspond to a similar bifunctional mechanism of the reforming of hydrocarbons. The organic molecules activate or adsorb on the metal crystalline sites while water molecules are activated on the support structure. Surface hydroxyl groups are formed from water with the surface oxygen on the support. Hydrogen is produced by dehydrogenation of the organic molecule and reaction of the hydroxyl groups from the water at the metal/support interfaces.[187] A schematic of the mechanism proposed for conventional steam reforming is illustrated in Figure 85 below, however this mechanism is not very specific and do not describe the actual surface reactions which might occur.[188]

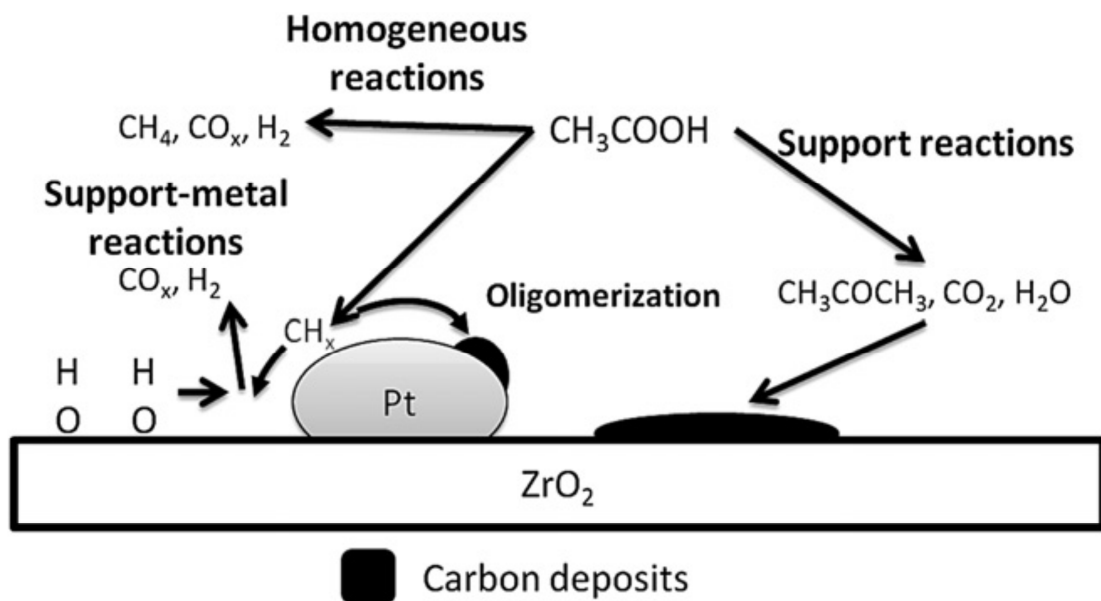


Figure 85 The bifunctional reaction mechanism, where possible side reactions are indicated as well. Figure adapted from [188]

Space velocity is defined as the inverse of residence time τ , and is usually defined as the ratio of the feed gas flow rate to the size of the reactor (units = h^{-1}). The space velocity can be defined in terms of gas hourly space velocity (GHSV) and is calculated using the following equation.

$$\text{GHSV} = \text{Feed Gas Volumetric Flow Rate} / \text{Reactor (or Catalyst) Volume} \quad (6)$$

The amount of catalysts to be used for each experiment was calculated based on achieving a space velocity of approximately $8\text{-}10,000 \text{ h}^{-1}$ as Nickel catalysts was supplied as pellets and PGM catalysts was supplied as spheres. Figure 86 & 87 below illustrates the space velocity versus the catalysts mass for both Nickel and PGM catalysts. Based on the charts 10g of Nickel was selected and 5g for each of the PGM catalysts was selected for the catalytic experiments.

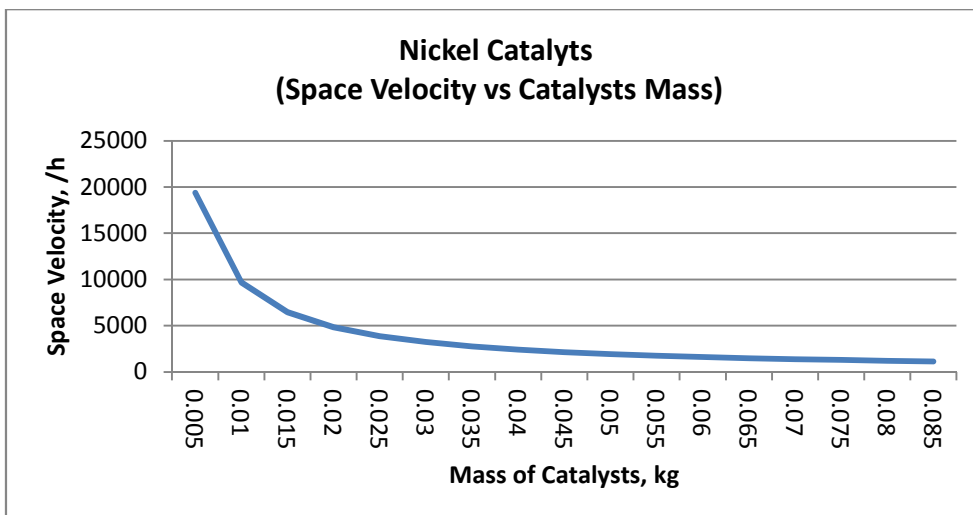


Figure 86 Space velocity vs Mass of catalysts for Nickel catalysts (supplied as pellets)

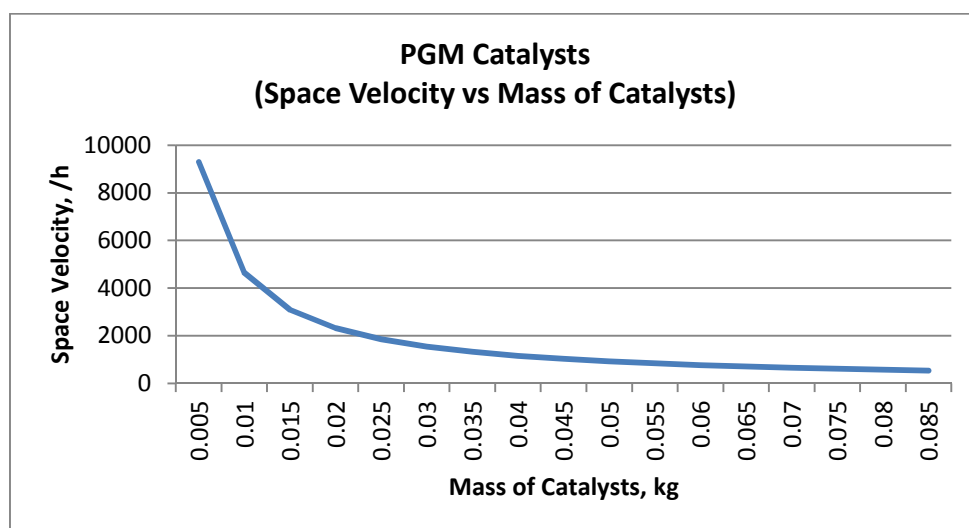


Figure 87 Space velocity vs Mass of catalysts for PGM catalysts (supplied as spheres)

9.3 Mass Balance

The mass balance sheet used for recording data can be found in APPENDIX B. During each catalytic experiment the reactor transition tubes and condensers are weighed before and after each experiment as described in the previous chapter. The quartz wool used to hold the bed was weighed before and after. The catalyst was also weighed before and after each run. For tests conducted with additional steam the amount of water added was weighed before and after each test. This allows determination of the product yields, and the overall mass balance. Much of the char was retained in the primary quartz reactor, and the transition tubes and oil-pots contained the bio-oils. Prior to weighing, all the glassware apparatus was thoroughly cleaned and dried. Photographs of Condenser 1 before and after are illustrated in Figure 88. Permanent gases composition was normalised and obtained by difference.

The analysis of the product yields properties based on methods discussed from Chapter 6, and the mass balance from the catalytic experiments are summarised in Table 34 & 35 and discussed below.

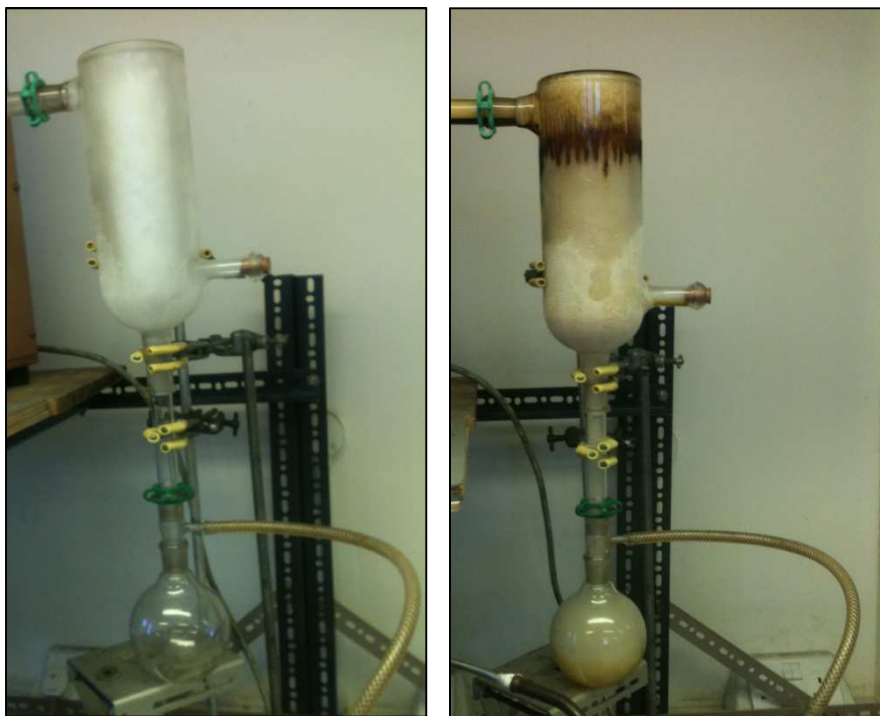


Figure 88 Condenser 1 before and after

Table 34 Summary of mass balances for catalytic experiments using commercial nickel catalysts (with and without steam)

	Unit	Catalytic reforming at 500°C	Catalytic reforming at 750°C	Catalytic reforming at 850°C	Catalytic reforming at 500°C + steam	Catalytic reforming at 750°C + steam	Catalytic reforming at 850°C + steam
Moisture content	wt.%	8%	8%	8%	8%	8%	8%
Ash content	wt.%, dry basis	4.5	4.5	4.5	4.5	4.5	4.5
Pyrolysis temperature	°C	450	450	450	450	450	450
Pyrolysis heating rate	°C/min	50	50	50	50	50	50
Catalysts		Ni/Al ₂ O ₃	Ni/Al ₂ O ₃	Ni/Al ₂ O ₃	Ni/Al ₂ O ₃	Ni/Al ₂ O ₃	Ni/Al ₂ O ₃
Catalytic reforming temperature	°C	500	750	850	500	750	850
Steam flow rate	ml/s				0.0434	0.0358	0.0408
Biomass feed	g, dry basis	100.98	100.5	100.48	100.23	100.08	100.15
<i>Pyrolysis Yields (as received):</i>							
Liquids	wt.%	40.50	26.1	21.44	24.20	8.08	11.94
Char	wt.%	32.44	32.56	31.30	31.20	32.11	31.23
Permanent gas:	wt.%	28.04	41.84	47.26	134.83	119.89	154.98
	H ₂ vol%	10%	24%	43%	32%	57%	57%
	O ₂ vol%	1%	0%	0%	0%	0%	0%
	N ₂ vol%	10%	9%	0%	12%	7%	4%
	CO vol%	17%	17%	15%	10%	25%	26%
	CH ₄ vol%	9%	14%	6%	6%	6%	13%
	CO ₂ vol%	53%	35%	36%	40%	6%	0%
HHV	MJ/kg	2.0	4.8	4.7	10.8	15.7	25.2

Table 35 Summary of mass balances for catalytic experiments using PGM catalysts (Platinum and Rhodium) with and without steam

	Unit	Catalytic reforming at 500°C with Pt	Catalytic reforming at 850°C with Pt	Catalytic reforming at 500°C with Rh	Catalytic reforming at 850°C with Rh	Catalytic reforming at 500°C with Pt+ steam	Catalytic reforming at 850°C with Pt + steam	Catalytic reforming at 500°C with Rh + steam	Catalytic reforming at 850°C with Rh + steam
Moisture content	wt.%	8%	8%	8%	8%	8%	8%	8%	8%
Ash content	wt.%, dry basis	4.5	4.5	4.5	4.5	4.5	4.5	4.5	4.5
Pyrolysis temperature	°C	450	450	450	450	450	450	450	450
Pyrolysis heating rate	°C/min	50	50	50	50	50	50	50	50
Catalysts		Pt/Al ₂ O ₃	Pt/Al ₂ O ₃	Rh/Al ₂ O ₃	Rh/Al ₂ O ₃	Pt/Al ₂ O ₃	Pt/Al ₂ O ₃	Rh/Al ₂ O ₃	Rh/Al ₂ O ₃
Catalytic reforming temperature	°C	500	850	500	850	500	850	500	850
Steam flow rate	ml/s					0.0362	0.0434	0.0338	0.0338
Biomass feed	g, dry basis	101.19	102.72	101.53	101.61	100.5	102.53	100.34	101.34
<i>Pyrolysis Yields (as received):</i>									
Liquids	wt.%	51.39	28.46	49.49	35.95	120.07	35.46	127.11	62.42
Char	wt.%	32.95	36.35	30.02	31.27	32.33	33.15	33.08	34.61
Permanent gas:	wt.%	16.85	37.91	22.02	34.39	23.1	83.92	11.72	76.31
H ₂	vol%	3%	18%	2%	12%	8%	13%	5%	14.68%
O ₂	vol%	0%	0%	0%	0%	0%	0%	0%	0.00%
N ₂	vol%	13%	1%	10%	4%	27%	1%	33%	1.89%
CO	vol%	9%	6%	6%	13%	13%	7%	12%	9.20%
CH ₄	vol%	2%	3%	3%	10%	6%	4%	3%	5.25%
CO ₂	vol%	73%	72%	79%	62%	46%	75%	47%	68.90%
HHV	MJ/kg	0.38	1.66	0.53	1.61	1.24	3.54	1.26	4.05

9.3.1 Pyrolysis and Catalytic Reforming with Commercial Nickel (Ni/Al₂O₃) Catalyst without steam

Table 34 and Figure 89, shows the yield of products from pyrolysis and catalytic steam reforming at 500°C, 750°C and 850°C without the addition of steam. The presence of catalysts led to a significant change in product distribution. The results indicate that as the reforming temperature increases permanent gases also increase, reducing the yield of condensable liquids. In comparison to the non-catalytic experiments conducted in Chapter 8 the reduction in yield for liquids is 7%, 22% and 26% at 500, 750 and 850°C respectively. Char remained the same as pyrolysis conditions remained constant.

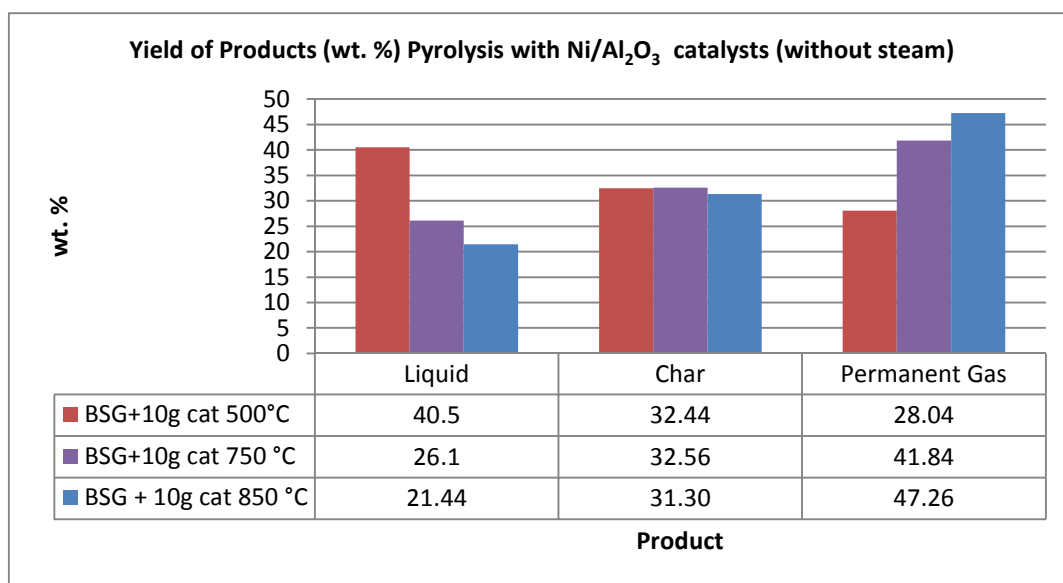


Figure 89 Comparison of the yields of products from measurements with Ni/Al₂O₃ catalysts and without steam

9.3.2 Pyrolysis and Catalytic Reforming with Commercial Nickel (Ni/Al₂O₃) with Steam

The experimental runs without steam were then replicated using fresh Nickel catalyst samples with the addition of steam. Steam was added to the second stage catalytic reactor using a copper distillation kettle mounted on a heater plate at temperatures between 350-400°C. The amount of additional steam added for each run ranged between 140-150ml.

As can be seen by Table 34 and Figure 89, the observed results shows that the presence of additional steam also has a significant effect on the product distribution at all reforming temperatures (500°C, 750°C and 850°C). The results indicate that as the reforming temperature increases with the presence of catalysts and additional steam the permanent gases also increase considerably, reducing the yield of condensable liquids further (24.20%, 8.08% and 11.94% at 500, 750 and 850°C respectively). Char remained the same as pyrolysis conditions remained constant.

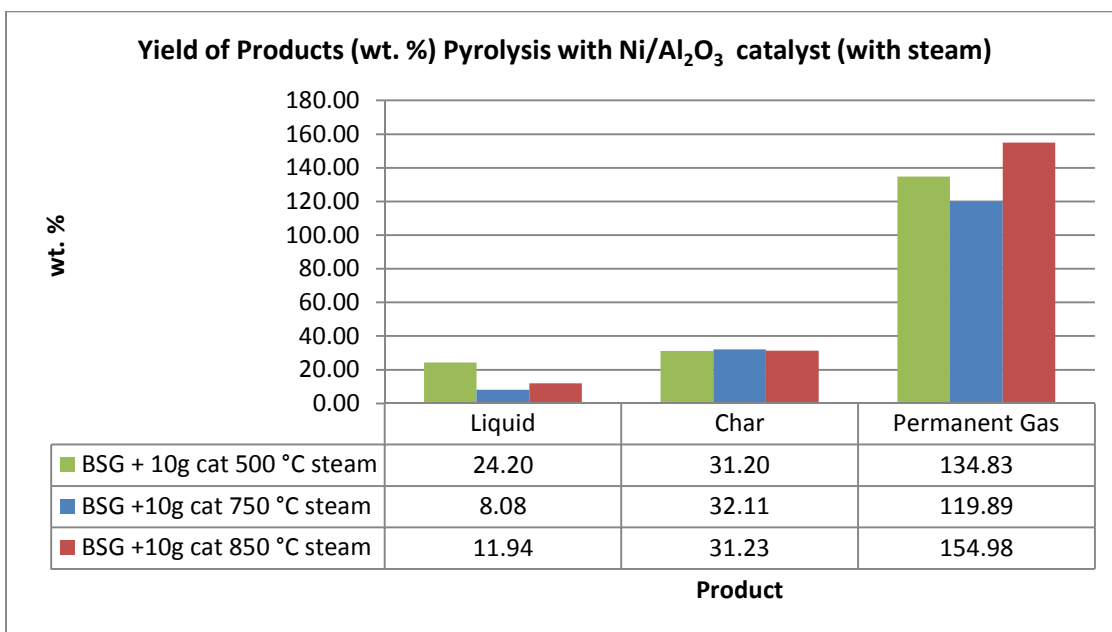


Figure 90 Comparison of the yields of products from measurements with Ni/Al₂O₃ catalysts and with steam added

9.3.3 Pyrolysis and Catalytic Reforming with PGM Catalysts (Pt/Al₂O₃) & (Rh/Al₂O₃) without Steam

Initial catalytic experiments using the PGM catalysts described earlier were repeated without the addition of steam at two different reforming temperatures were investigated at 500°C and 850°C. As observed by Table 35 and Figure 91 the results show the yield of products from pyrolysis and catalytic reforming at 500°C and 850°C without the addition of steam using both PGM catalysts.

The effect both catalysts have at the lower catalytic reforming temperature (500°C) shows very little change in the product distribution in comparison to the non-catalytic experiments. However at the higher catalytic reforming temperatures of 850°C the permanent gases increased, reducing the yield of condensable liquids. In comparison to non-catalytic experiments the reduction in yield for liquids is 19% and 12% for Pt/Al₂O₃ and Rh/Al₂O₃ catalyst which is less than the 26% reduction reported earlier using the Ni/Al₂O₃ at the same temperature.

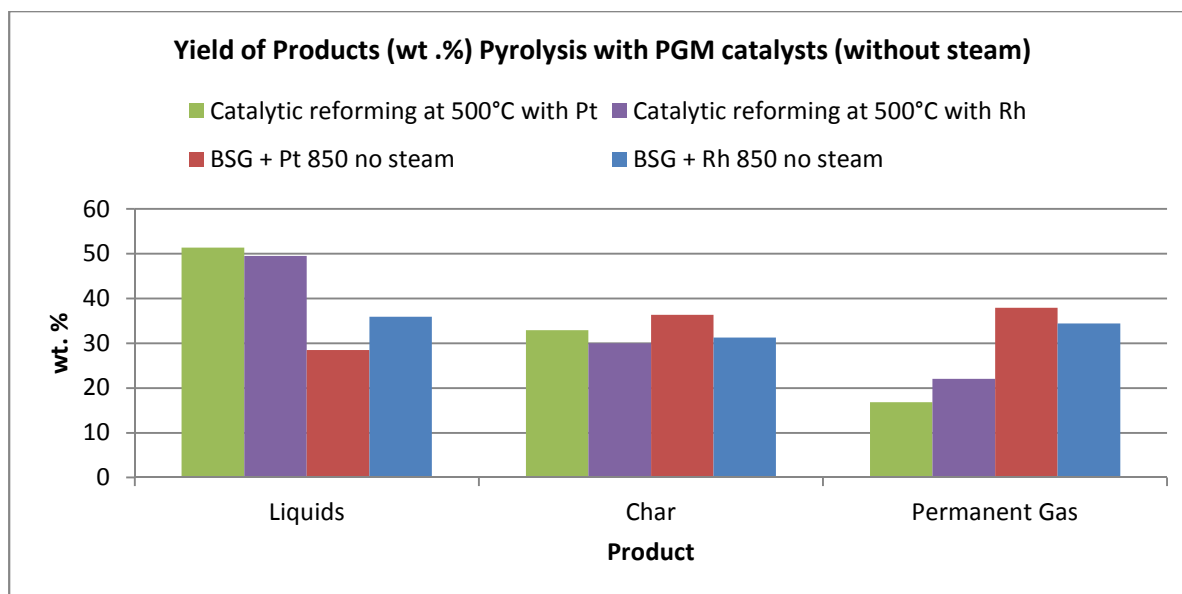


Figure 91 Comparison of the yields of products from measurements with Pt/Al₂O₃ & Rh/Al₂O₃ catalysts at low temperature and without steam

9.3.4 Pyrolysis and Catalytic Reforming with PGM Catalysts (Pt/Al₂O₃) & (Rh/Al₂O₃) with Steam

The experimental runs without steam were then replicated using fresh catalyst samples with the addition of steam. Steam was added to the second stage catalytic reactor using a copper distillation kettle mounted on a heater plate at temperatures between 350-400°C. The amount of additional steam added for each run ranged between 140-150ml.

As can be observed by Table 35, the results show that the presence of additional steam also has a significant effect on the product distribution at both reforming temperatures (500°C and 850°C).

At the lower catalytic reforming temperature of 500°C with the presence of catalyst and additional steam, the condensable liquids yield had increased 73% and 80% for both Pt/Al₂O₃ and Rh/Al₂O₃ which is a significant increase in comparison to non-catalytic experiments. The addition of steam at the lower reforming temperature had very little effect in reforming pyrolysis vapours and was found to have condensed adding to the liquids yield.

At the higher catalytic reforming temperature 850°C the liquid yield decreased 12% and permanent gases increased 62% for Pt/Al₂O₃, however for Rh/Al₂O₃ at the same conditions both liquids and permanent gas yields increased 15% and 55%. This suggests that Rh/Al₂O₃ was less effective in reducing the condensable liquids yield than Pt/Al₂O₃ and Ni/Al₂O₃.

9.4 Bio-oil Analysis

The properties of the bio-oils produced from the catalytic reforming experiments was characterized using various analytical techniques in order to determine ultimate (C, H, N, O, and S& Cl), water content, pH, acid number and heating values. Chemical composition analysis was conducted by GC/MS.

All the bio-oils produced from catalytic reforming experiments had separated into an aqueous and an organic phase except oils produced at the higher reforming temperatures with the addition of steam. The organic fraction 'bio-oil' contains the heavy condensable phase that are mainly organic components, and the aqueous fraction is the light condensable phase mainly comprising of water.

The liquids collected in the condenser system at the lower reforming temperatures (500°C) contained a mixture of water (including unreacted condensed steam) and dark brown colored oil for bio-oils. At the higher catalytic reforming temperatures the liquid content in the condenser system was a mixture of mostly water and pale yellow colored oil. The organic content was reduced in quantity, indicating an effect of the catalysts on cracking of the pyrolysis products to form gases. This can be seen in Figure 92 below comparing non-catalytic oil with catalytic oils produced using Ni/Al₂O₃ catalyst.

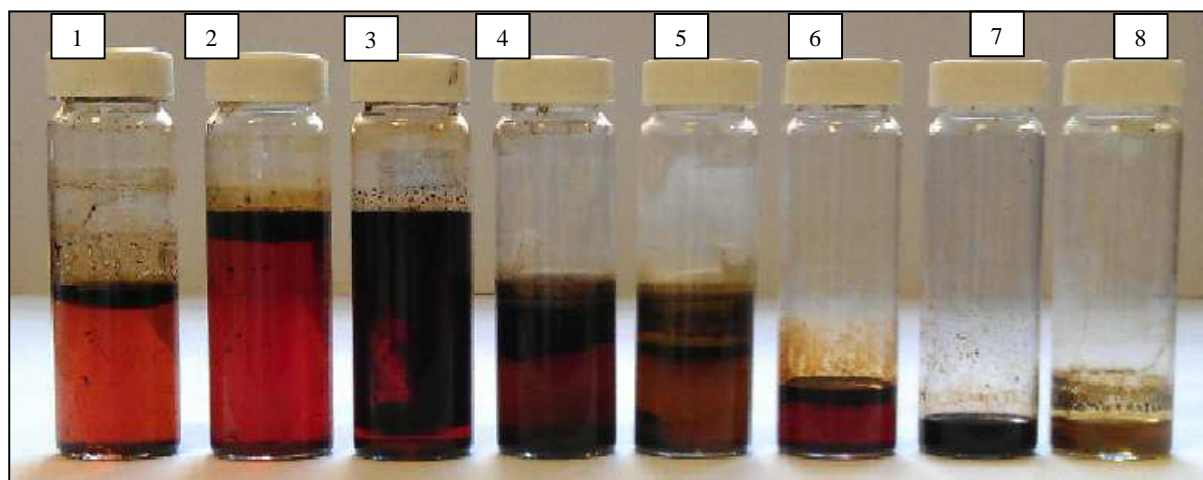


Figure 92 Comparison of Bio-oil samples

(1) at 25°C/min; (2) at 100°C/min; (3) catalytic reforming at 500°C; (4) catalytic reforming at 500°C with steam; (5) catalytic reforming at 750°C; (6) catalytic reforming at 750°C with steam; (7) catalytic reforming at 850°C; (8) catalytic reforming at 850°C with steam

Table 36 shows the compositional analysis of the bio-oils produced with nickel catalysts (Ni/Al₂O₃) at different catalytic reforming temperatures with and without the addition of steam.

Table 36 Compositional analysis of Bio-oils produced from catalytic bench scale pyrolysis/reforming experiments using Nickel catalysts (Ni/Al₂O₃)

Bio-oil	Catalytic reforming at 500°C	Catalytic reforming at 750°C	Catalytic reforming at 850°C	Catalytic reforming at 500°C + steam	Catalytic reforming at 750°C + steam	Catalytic reforming at 850°C + steam
C	58.4	47.6	70.4	70.8	68.2	48.1
H	9.3	8.6	7.5	8.9	9.7	8.1
N	3.7	4.1	3.5	5.5	4.8	3.5
S	1.7	0.8	1.3	1.3	0.1	0.1
O	26.7	38.6	17.2	13.5	17.0	40.1
Cl	0.12	0.31	0.17	0.1	0.18	0.1
Water Content:						
Organic (wt.%)	3.2	3.6	66.6	67.0	68.1	45.4
Aqueous (wt.%)	63.9	72	85.2	76.3	80	40.4
pH:						
organic	5.6	8.3	8.8	8.3	N/D	N/D
aqueous	5.3	8.28	8.9	8.3	8	8.6
Acid Number mg/g	50.34	N/D	N/D	48.81	N/D	N/D
HHV	28.7	22.7	31.7	33.9	33.4	22.2

*N/D (Could not be determined)

The C content in the oils for all experiments with Ni/Al₂O₃ with and without steam decreased as the reforming temperature increased, indicating catalytic activity and decarboxylation reactions. The high C content with catalytic reforming at 850°C may be due to experimental error.

All the oil samples contained S and Cl between 0.1-1.7% and 0.1-0.18% respectively. Visual inspection of the catalysts showed very little carbon precipitation, but the declining activity of the catalysts with time associated with S and Cl poisoning could not be assessed. However the presence of these components may lead to catalysts poisoning and eventually deactivation over long periods of time.

The pH value of all samples for both organic and aqueous phases was found to be between 5.1 and 8.9. The HHVs obtained for all oils were clearly related to the O content - the lower the O content, the higher the HHV.

The acid number of the oils without catalysts was found to be 60.2 mg/g, and at low temperature (LT) reforming with and without steam 50.34mg/g and 48.81mg/g respectively, which indicates potential corrosion problems. However at HT reforming with and without the addition of steam the acid number could not be determined. This may be due to acidic components being reformed.

Table 37 Compositional analysis of Bio-oils from catalytic bench scale pyrolysis/reforming experiments using PGM catalysts Platinum (Pt/Al₂O₃) and Rhodium (Rh/Al₂O₃)

Bio Oil Fraction	Catalytic reformin g at 500°C with Pt	Catalytic reformin g at 850°C with Pt	Catalytic reformin g at 500°C with Rh	Catalytic reformin g at 850°C with Rh	Catalytic reformin g at 500°C with Pt+ steam	Catalytic reformin g at 850°C with Pt + steam	Catalytic reformin g at 500°C with Rh + steam	Catalytic reformin g at 850°C with Rh + steam
C	74.29	23.37	74.39	33.48	72.3	29.03	71.05	36.26
H	9.58	9.7	9.32	9.08	9.21	9.37	9.82	9.15
N	3.67	2.87	3.5	3.08	2.15	2.3	2.96	2.07
S	1.5	1.02	3.16	1.31	1.1	1.07	1.7	1.25
O	10.95	62.96	9.55	52.96	15.23	58.19	14.46	51.18
Cl	0.01	0.08	0.08	0.09	0.01	0.04	0.01	0.09
HHV	36.2	13.1	36.2	17.0	34.6	15.2	35.0	18.2

Table 37 shows the compositional analysis of the bio-oils produced with PGM catalysts Platinum (Pt/Al₂O₃) and Rhodium (Rh/Al₂O₃) at two different catalytic reforming temperatures 500°C and 850°C with and without the addition of steam.

The C content in the oils for all experiments with PGM catalysts with and without the addition of steam decreased as the reforming temperature increased, indicating catalytic activity and decarboxylation reactions. However it was observed that catalytic reforming at 850°C with steam addition the bio-oil C content was higher than the oils produced at the same temperature without steam; (Pt/Al₂O₃) at 850°C 23.37 wt.% to 29.03 wt.% with steam. (Rh/Al₂O₃) at 850°C 33.48 wt.% to 36.26 wt.% with steam.

All the oil samples contained S and Cl between 1.02-3.16% and 0.01-0.09% respectively. Due to the unavailability of equipment water content, pH and acid number for oils produced using PGM catalysts could not be analysed

Gas chromatography Mass spectrometer (GCMS) analysis was conducted for all the bio-oil samples obtained with catalysis. This technique was useful to compare the oils in particular understanding chemicals that may have been formed or reformed to H₂, CO and CH₄. For most samples more than 100 peaks was detected corresponding to different organic compounds being identified within the spectrum. Each peak identified has an 'Area%' given representing each identified component as a fraction integrated over the whole mass spectrum. Each of the components identified consists of its chemical group, molecular formula and relative molecular mass (RMM).

9.4.1 GCMS Bio-oil at 500°C with Nickel (Ni/Al₂O₃) catalysts and without steam

Figure 93 shows the GC/MS mass spectrum. The major chemical components present are illustrated in Table 38. The bio-oil consists of a number of complex organic oxygenated compounds. Much of the abundant components found were aromatic hydrocarbons and alkanes, followed by phenols.

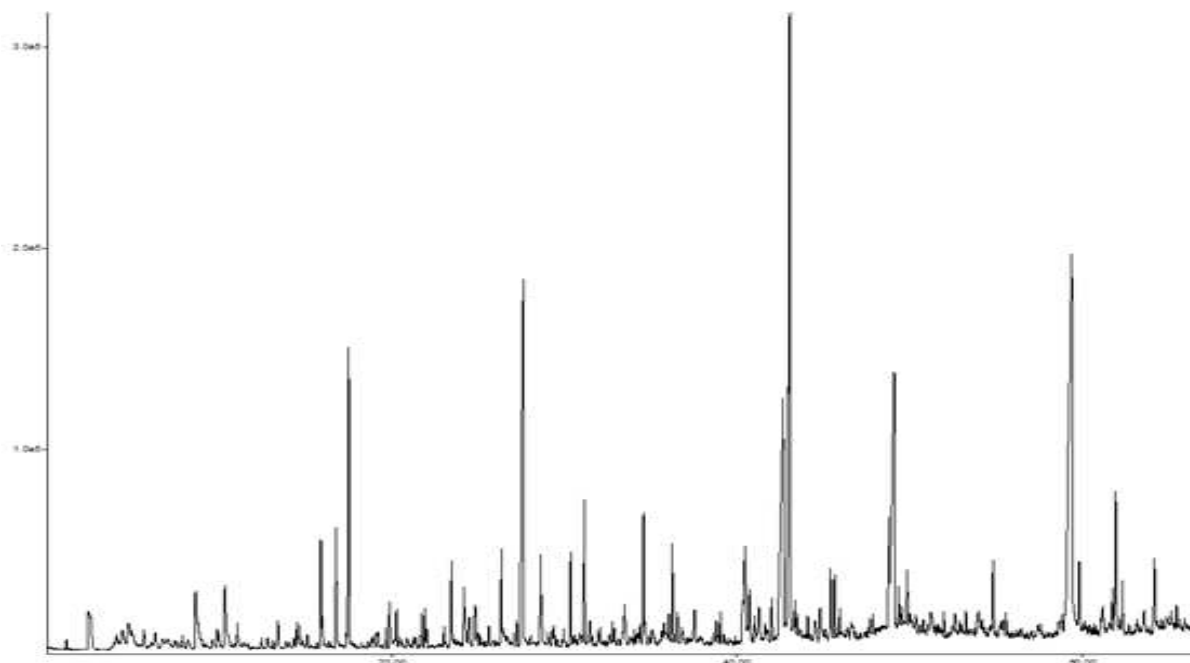


Figure 93 GC/MS analysis of BSG Intermediate pyrolysis oil after catalytic reforming at 500°C Nickel catalysts and no steam (Chemical abundant vs. Retention time)

The major peaks detected and identified with the highest abundance was acetic acid 24.26%, toluene 12.05%, pyridine 4.57%, cyclohexene, 3-(bromomethyl)-Phenol 3.08%, 1,2 cyclopentanedione, 3 methyl- 3.32%. These were the largest components present. The effect of catalysts at 500°C in comparison to non-catalytic bio-oil shows a decrease of aromatic hydrocarbons, alkanes, esters and phenols 4%, 14%, 4% and 8%. However there was an increase of alcohols, alkyl nitriles, cyclopentanones, isomers, ketones and organic acids 6%, 1.7%, 3.87%, 1%, 12.2% and 24% respectively. The average molecular weight of the bio-oil components using Nickel catalysts at 500°C was determined to be 119 which is a 17% decrease in comparison to oils produced without catalysts.

Table 38 Composition of BSG Intermediate Pyrolysis oil after catalytic reforming at 500°C Nickel catalyst and no steam

Time	Chemical Name	Chemical Group	Molecular formula	RMM	Area %
5.126	Benzene, 1,3-bis(3-phenoxyphenoxy)-	Aromatic	C ₃₀ H ₂₂ O ₄	446	3.5
5.24	Pseudoephedine, (+)-	Oxygenates	C ₁₀ H ₁₅ NO	165	2.34
6.804	2-Butanone	Ketones	C ₄ H ₈ O	72	3.18
7.23	Propanenitrile	Alkyl nitrile	C ₃ H ₅ N	55	1.7
8.368	2,5-Dimethylfuran	Furan	C ₆ H ₈ O	96	1.53
9.345	Acetic Acid	Organic Acid	C ₄ H ₇ ClO ₄ S	186	24.26
10.817	Toluene	Aromatic	C ₇ H ₈	92	12.05
11.541	Pyridine	Pyridine	C ₅ H ₅ N	79	4.57
13.507	Propanoic acid	Organic Acid	C ₃ H ₆ O ₂	74	1.93
14.416	Cyclopentanone	Cyclopentanone	C ₅ H ₈ O	84	2.29
14.691	Isooctanol	Alcohol	C ₈ H ₁₀	106	1.58
15.105	Ethylbenzene	Aromatic	C ₈ H ₁₀	106	2.65
17.324	Styrene	Aromatic	C ₈ H ₈	104	1.87
17.646	2-Cyclopenten-1-one	Cyclopentanone	C ₅ H ₆ O	82	2.68
19.865	Octane-1-chloro-	Alkane/Chlorine	C ₈ H ₁₇ CL	148	1.64
20.256	2-Propanone, 1-(acetyloxy)-	Ketone	C ₅ H ₈ O ₃	116	2.02
20.544	Butanoic acid, 3-methyl-	Organic Acid	C ₅ H ₁₀ O ₂	88	2.43
20.705	2-Cyclopenten-1-one, 3-methyl-	Cyclopentanone	C ₁₁ H ₁₆ O	96	1.84
21.498	2-Furyl Methyl Ketone	Ketone	C ₁₀ H ₁₂ O ₂		1.42
25.062	2,3-Pentanedione	Ketone	C ₅ H ₈ O ₂	100	1.66
25.223	1-Pentanol, 2-3thyl-4-methyl-	Cyclopentanone	C ₈ H ₁₈ O		1.74
25.787	3-Methyl-2-Cyclopentenone	Cyclopentanone	C ₆ H ₈ O		2.03
28.856	1,2-Cyclopentanedione, 3-methyl-	Ketone	C ₆ H ₈ O ₂	112	3.32
30.42	Phenol	Phenol	C ₆ H ₆ O	94	3.08
30.753	7-Norbornadadienyl t-butyl ether	Isomer	C ₄ H ₁₀ O		2.53
34.686	p-Cresol (107, 108, RI 1294)	Phenol	C ₇ H ₈ O	108	2.44
40.135	3,7-Dimethyl-1-octyl methylphosphonofluoridate	Alcohol	C ₁₁ H ₂₄ FO ₂ P		2.73
40.388	Cyclohexene, 3-(bromomethyl)-	Alkene	C ₇ H ₁₁ BR	82	3.53
44.504	1-Propanone, 1-(3-cyclohexen-1-yl)-2,2-dimethyl-	Ketone	C ₁₁ H ₁₈ O	166	1.46

9.4.2 GCMS Bio-oil at 750°C with Nickel (Ni/Al₂O₃) catalysts and without steam

Figure 94 shows the GC/MS mass spectrum. The major chemical components present are illustrated in Table 39.

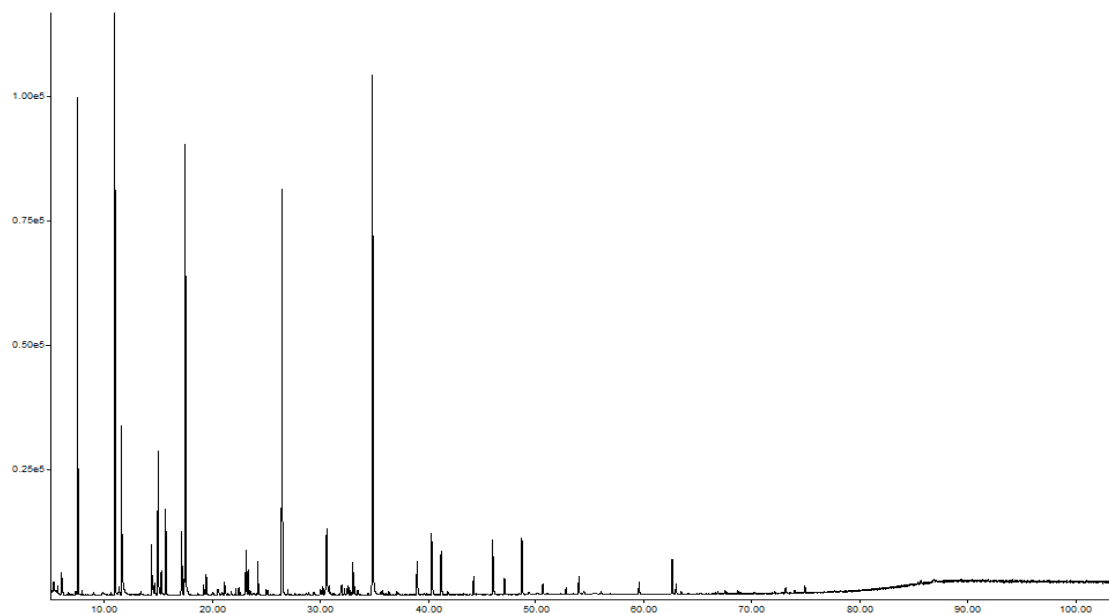


Figure 94 GC/MS analysis of BSG Intermediate pyrolysis oil after catalytic reforming at 750°C Nickel catalysts and no steam (Chemical abundant vs. Retention time)

The major peaks detected and identified with the highest abundance was naphthalene 16.27%, toluene 14%, indene 12.17%, cyclooctatetraene 11.61%, and benzene 10.01%. These were the largest components present. Much of the abundant components detected were aromatic hydrocarbons alkanes, and polyaromatic hydrocarbons followed by pyridines and alkyl nitriles. The effect of catalysts at 750°C in comparison to non-catalytic bio-oil shows a decrease of alkanes, esters, guaicol, ketones, phenols and organic acids 15.6%, 6.7%, 1.5%, 3%, 11.6% and 2.1%. However there was an increase of alcohols, alkenes, alkyl nitriles, aromatic hydrocarbons, carboxaldehydes, isomers, polyaromatic hydrocarbons and pyridines 3.7%, 8.4%, 1.4%, 17.1%, 2.7%, 25% and 1.9% respectively. The average molecular weight of the bio-oil components using Nickel catalysts at 750°C was determined to be 118 which is a 18% decrease in comparison to oils produced without catalysts.

Table 39 Composition of BSG Intermediate Pyrolysis oil after catalytic reforming at 750°C Nickel catalyst and no steam

Time	Chemical Name	Chemical Group	Molecular Formula	RMM	Area %
7.515	Benzene	Aromatic	C ₆ H ₆	78	10.01
10.964	Toluene	Aromatic	C ₇ H ₈	92	14
11.573	Pyridine	Pyridine	C ₅ H ₅ N	79	4.78
14.356	2-Methylpyridine	Pyridine	C ₆ H ₇ N	93	1.55
14.965	Pyrrol	Alcohol	C ₄ H ₅ N	67	3.69
15.264	Ethylbenzene	Aromatic	C ₈ H ₁₀	106	0.68
15.666	m-Xylene	Aromatic	C ₈ H ₁₀	106	2.3
17.127	p-Xylene	Aromatic	C ₈ H ₁₀	106	2.35
17.494	Cyclooctatetraene	Alkene	C ₈ H ₈	104	11.61
19.415	1H-Pyrrole,2-methyl-	Carboxaldehydes	C ₆ H ₉ N	95	0.56
21.128	Pyridine, 2-ethenyl-	Pyridine	C ₇ H ₇ N	105	0.4
23.105	Benzene, 1-ethenyl-2-methyl-	Aromatic	C ₉ H ₁₀	118	1.17
23.301	Benzene, 1-ethenyl-4-methyl-	Aromatic	C ₉ H ₁₀	118	0.66
24.209	Benzofuran	Furan/Aromatic	C ₈ H ₆ O	118	0.97
26.44	Indene	Aromatic	C ₉ H ₈	116	12.17
30.579	Phenol	Phenol	C ₆ H ₆ O	94	2.16
34.821	Naphthalene	Polyaromatic	C ₁₀ H ₈	128	16.27
38.937	Isoquinoline	Heterocyclic	C ₉ H ₇ N	129	1.15
40.271	Naphthahalene, 2-methyl-	Polyaromatic	C ₁₁ H ₁₀	142	2.18
41.168	Naphthahalene, 2-methyl-	Polyaromatic	C ₁₁ H ₁₀	142	1.46
44.169	Naphthahalene, 2-ethenyl-	Polyaromatic	C ₁₂ H ₁₀	142	0.59
45.939	Indole	Carboxaldehyde	C ₈ H ₇ N	117	2.12
47.032	Naphthahalene, 2-ethenyl-	Polyaromatic	C ₁₂ H ₁₀	154	0.52
48.63	Acenaphthylene	Polyaromatic	C ₁₂ H ₈	152	1.86
54.011	Fluorene	Polyaromatic	C ₁₃ H ₁₀	166	0.57
59.575	Propanenitrile, 3,3'-thiobis-	Alkyl Nitrile	C ₆ H ₈ N ₂ S	140	0.45
62.645	Phenanthrene	Polyaromatic	C ₁₄ H ₁₀	178	1.29

9.4.3 GCMS Bio-oil at 850°C with Nickel (Ni/Al₂O₃) catalysts and without steam

Figure 95 shows the GC/MS mass spectrum. The major chemical components present are illustrated in Table 40.

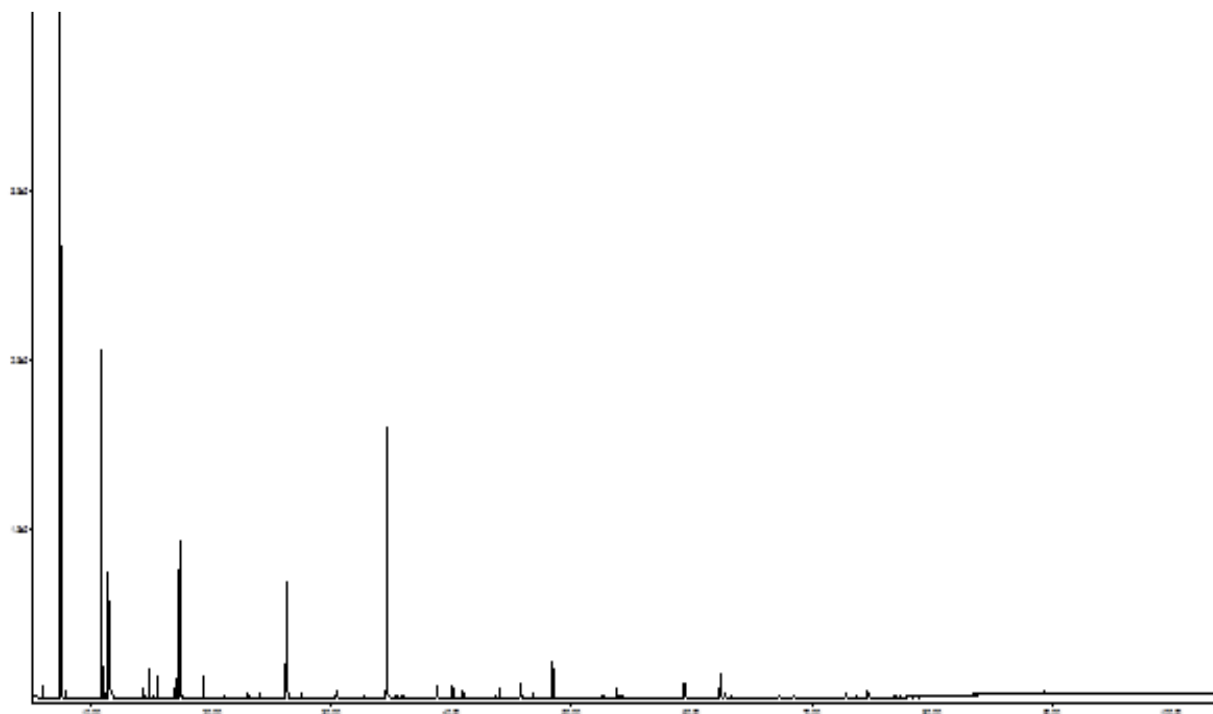


Figure 95 GC/MS analysis of BSG Intermediate pyrolysis oil after catalytic reforming at 850°C Nickel catalysts and no steam (Chemical abundant vs. Retention time)

The major peaks detected and identified with the highest abundance was benzene 25.44%, naphthalene 17.76%, toluene 15.63%, cyclotetraene 8.55%, indene 7.05%, and pyridine 6.55%. These were the largest components present. Much of the abundant components are aromatic hydrocarbons and alkanes, followed by phenols. The effect of catalysts at 850°C in comparison to non-catalytic bio-oil shows a decrease of alkanes, esters, furans, guaicol, isomers, ketones, phenols and organic acids (15.6%, 6.7%, 1.2%, 1.5%, 1.8%, 3.1%, 13.3% and 2.1%). However there was an increase of alcohols, alkenes, alkyl nitriles, aromatic hydrocarbons, and polyaromatic hydrocarbons (2.4%, 5.6%, 2.9%, 27.5%, and 24.2%) respectively. The average molecular weight of the bio-oil components using Nickel catalysts at 850°C was determined to be 121 which is a 16% decrease in comparison to oils produced without catalysts.

Table 40 Composition of BSG Intermediate Pyrolysis oil after catalytic reforming at 850°C Nickel catalyst and no steam

Time	Chemical Name	Chemical Group	Molecular formula	RMM	Area %
5.94	2-Propenenitrile	Alkyl Nitrile	C ₃ H ₃ N	53	0.68
7.412	Benzene	Aromatic	C ₆ H ₆	78	25.44
7.825	Thiophene	Alkene	C ₄ H ₄ S	84	0.32
10.815	Toluene	Aromatic	C ₇ H ₈	92	15.63
11.413	Pyridine	Pyridine	C ₅ H ₅ N	79	6.55
11.723	Pyridine	Pyridine	C ₅ H ₅ N	79	0.24
14.804	Pyrrrol	Alcohol	C ₄ H ₅ N	67	1.29
15.494	m-Xylene	Aromatic	C ₈ H ₁₀	106	1.11
17.023	Phenylethyne	Alcohol	C ₈ H ₆	102	1.15
17.311	Cyclooctatetraene	Alkene	C ₈ H ₈	104	8.55
22.933	Benzene, 1-ethenyl-3-methyl-	Aromatic	C ₉ H ₁₀	118	0.32
24.025	Benzofuran	Aromatic/Furan	C ₈ H ₆ O	118	0.33
26.244	Indene	Aromatic	C ₉ H ₈	116	7.05
30.418	Phenol	Phenol	C ₆ H ₆ O	94	0.44
34.603	Naphthalene	Polyaromatic	C ₁₀ H ₈	128	17.76
38.731	Quinoline	Heterocyclic	C ₉ H ₇ N	129	1.03
40.064	1H-Indene, 1-ethylidene-	Aromatic	C ₁₁ H ₁₀		1.28
43.951	Biphenyl-	Aromatic	C ₁₂ H ₁₀	154	0.59
45.733	Phenylacetonitrile	Alkyl Nitrile	C ₈ H ₇ N	117	0.96
46.825	Naphthalene, 2-ethenyl-	Polyaromatic	C ₁₂ H ₁₀	154	0.26
48.4	Acenaphthylene	Polyaromatic	C ₁₂ H ₈	152	2.37
52.597	Naphthalene, 1-isocyano-	Polyaromatic	C ₁₁ H ₇ N	153	0.29
53.781	Fluorene	Polyaromatic	C ₁₃ H ₁₀	166	0.59
59.357	Propanenitrile, 3,3'-thiobis-	Alkyl Nitrile	C ₈ H ₈ N ₂ S	140	1.25
62.404	Phenanthrene	Polyaromatic	C ₁₄ H ₁₀	178	1.86
62.772	Anthracene	Polyaromatic	C ₁₄ H ₁₀	178	0.43
72.89	Pyrene	Polyaromatic	C ₁₆ H ₁₀	202	0.92

9.4.4 GCMS Bio-oil at 500°C with Nickel (Ni/Al₂O₃) catalysts and steam

Oil produced at a catalytic reforming temperature of 500°C without steam was found to contain 12.05% toluene, and a high acetic acid content of 24.26%. Much of the complex mixture contained alkenes from C3-C8 groups such as benzene, ethylbenzene, and styrene. The presence of chlorine was detected with octane-1-chloro identified in the peak range, see Table 38.

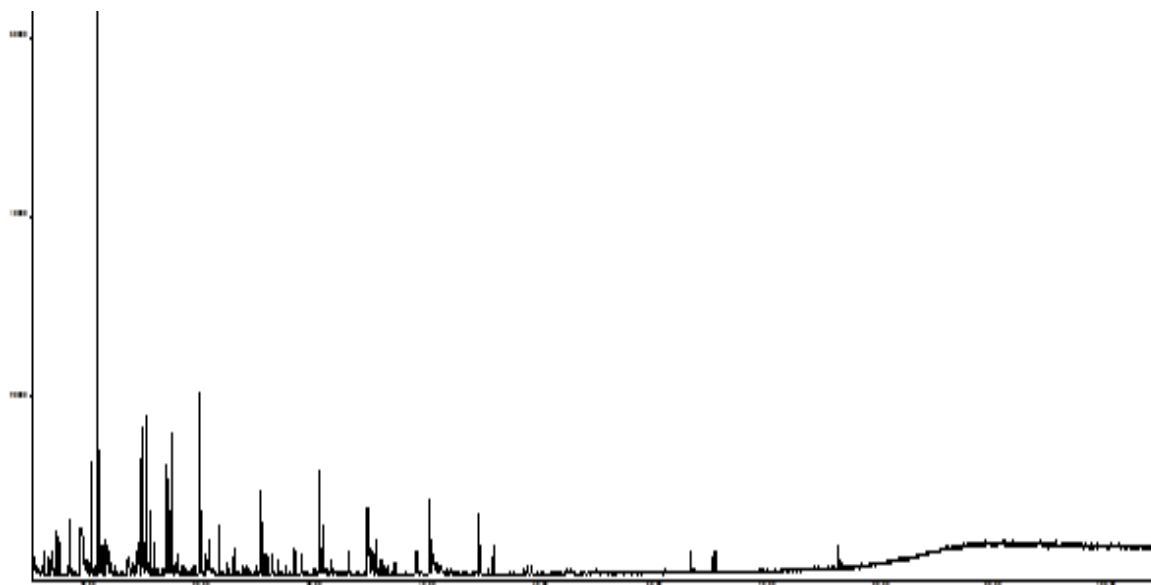


Figure 96 GC/MS analysis of BSG Intermediate pyrolysis oil after catalytic reforming at 500°C Nickel catalysts with steam (Chemical abundant vs. Retention time)

The peaks for LT reforming with and without the addition of steam (see Figure 93 & 96) are quite similar, however with the addition of steam the composition of the oils had altered. With the addition of steam at LT reforming (500°C) an increase of benzene, toluene, pyridine, cyclooctatetraene and naphthalene (25.44%, 15.63%, 6.55%, 8.55% and 17.76% respectively). This may have been due to the further cracking of phenolic components with the addition of steam. Thiophene and propanenitrile, 3,3'-thiobis- are components that contain S which can poison catalysts. Cl was not identified in the peaks, see Table 41. Formation of polycyclic aromatic hydrocarbons (PAH's) were formed such as anthracene, acenaphthylene, fluorene, naphthalene, phenanthrene and pyrene. These are cause for concern due to their carcinogenic characteristics. The average molecular weight of the bio-oil components using Nickel catalysts at 500°C with steam was determined to be 128 which is an 11% decrease in comparison to oils produced without catalysts.

Table 41 Composition of BSG Intermediate Pyrolysis oil after catalytic reforming at 500°C with steam

Time	Chemical Name	Chemical Group	Molecular formula	RMM	Area %
7.412	Benzene	Aromatic	C ₆ H ₆	78	25.44
7.825	Thiophene	Alkene	C ₄ H ₄ S	84	0.32
10.815	Toluene	Aromatic	C ₇ H ₈	92	15.63
11.413	Pyridine	Pyridine	C ₅ H ₅ N	79	6.55
14.804	Pyrrol	Alcohol	C ₄ H ₅ N	67	1.29
15.494	m-Xylene	Aromatic	C ₈ H ₁₀	106	1.11
17.023	Phenylethyne	Alcohol	C ₈ H ₆	102	1.15
17.311	Cyclooctatetraene	Alkene	C ₈ H ₈	104	8.55
26.244	Indene	Aromatic	C ₉ H ₈	116	7.05
30.418	Phenol	Phenol	C ₆ H ₆ O	94	0.44
34.603	Naphthalene	Polyaromatic	C ₁₀ H ₈	128	17.76
38.731	Quinoline	Heterocyclic	C ₉ H ₇ N	129	1.03
45.733	Phenylacetonitrile	Alkyl nitriles	C ₈ H ₇ N	117	0.96
46.825	Naphthalene, 2-ethenyl-	Polyaromatic	C ₁₂ H ₁₀	154	0.26
48.4	Acenaphthylene	Polyaromatic	C ₁₂ H ₈	152	2.37
52.597	Naphthalene, 1-isocyano-	Polyaromatic	C ₁₁ H ₇ N	153	0.29
53.781	Fluorene	Polyaromatic	C ₁₃ H ₁₀	166	0.59
59.357	Propanenitrile, 3,3'-thiobis-	Alkyl propanitrile	C ₆ H ₈ N ₂ S	140	1.25
62.404	Phenanthrene	Polyaromatic	C ₁₄ H ₁₀	178	1.86
62.772	Anthracene	:Polyaromatic	C ₁₄ H ₁₀	178	0.43
72.89	Pyrene	Polyaromatic	C ₁₆ H ₁₀	202	0.4
74.683	Pyrene	Polyaromatic	C ₁₆ H ₁₀	202	0.52

9.4.5 GCMS Bio-oil at 750°C with Nickel (Ni/Al₂O₃) catalysts and steam

Figure 97 shows the GC/MS mass spectrum. The major chemical components present are illustrated in Table 42.

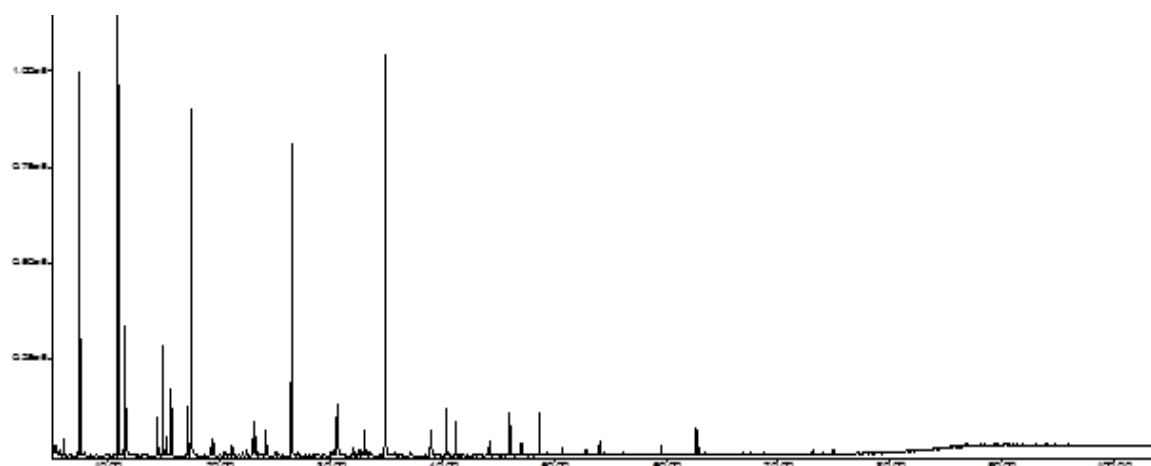


Figure 97 GC/MS analysis of BSG Intermediate pyrolysis oil after catalytic reforming at 750°C (Chemical abundant vs. Retention time)

Oil produced at HT (750°C) reforming with the addition of steam was found to have an increase in C5-C8 alkene components. The peaks when reforming at 750°C with and without the addition of the steam are similar; however with the addition of steam the peaks are smaller indicating catalytic

activity (see Figure 97). The identified components are given in Table 42. The peaks indicate cracking of phenolic components to lighter hydrocarbons, with an increase in naphthalene. The average molecular weight of the bio-oil components using Nickel catalysts at 750°C with steam was determined to be 128 which is an 11% decrease in comparison to oils produced without catalysts.

Table 42 Composition of BSG Intermediate Pyrolysis oil after catalytic reforming at 750°C with steam

Time	Chemical Name	Chemical Group	Molecular formula	RMM	Area %
5.124	Benzene, 1,3-bis(3-phenoxyphenoxy)-	Aromatic	C ₃₀ H ₂₂ O ₄	446	5.16
5.986	2-Propenitrile	Alkyl Nitrile	C ₃ H ₃ N	53	1.11
9.274	Acetic Acid	Organic Acid	C ₄ H ₇ ClO ₄ S		34.56
11.516	Pyridine	Pyridine	C ₅ H ₅ N	186	7.48
14.828	Pyrrol	Alcohol	C ₄ H ₅ N	67	2.72
17.84	Butanoic Acid	Organic Acid	C ₄ H ₈ O ₂	88	1.99
20.53	Methanimine, N-Methoxy-N-nitroso-	Oxygenates	C ₈ H ₉ N		1.71
20.783	2-Cyclopenten-1-one, 2-methyl-	Cyclopentanone	C ₆ H ₈ O	96	1.01
25.842	2-Cyclopenten-1-one, 3-methyl-	Cyclopentanone	C ₆ H ₈ O	96	1.24
26.314	Benzene, 1-ethynyl-4-methyl-	Aromatic	C ₉ H ₈	116	1.51
30.476	Phenol	Phenol	C ₆ H ₆ O	94	3.16
34.684	Naphthalene	Polyaromatic	C ₁₀ H ₈	128	3.94
35.04	Piperidine-2,5-dione	Ketone	C ₅ H ₇ NO ₂	113	4.49
40.145	2,5-Pyrrolidinedione	Ketone	C ₄ H ₅ NO ₂	99	3.69
40.364	4(1H)-Pyridinone	Ketone	C ₅ H ₅ NO	95	4.19
41.582	2-Propanol, 1-chloro-	Alcohol/Chlorine	C ₃ H ₇ ClO	95	0.47
41.95	1,4,3,6-Dianhydro-d-glucopyranose	Saccharides	C ₆ H ₈ O ₄	144	2.02
50.55	2,5-Imidazolidinedione, 1-(hydroxymethyl)	Alcohol	-		4.29
69.59	N-Morpholinomethyl-isopropyl-sulfide	Sulphur	C ₈ H ₁₇ NOS		2.08

9.4.6 GCMS Bio-oil at 850°C with Nickel (Ni/Al₂O₃) catalysts and steam

Bio-oil produced at (850°C) HT reforming with the addition of steam showed significant cracking of most PAH's and alkene groups in particular benzene and toluene, and the formation of a significant quantity of pyridine as seen in Table 43. Figure 98 illustrates the main peak of pyridine and the significant cracking and reduction of other components such as phenols, furans and some oxygenated compounds that may have been present in oils at LT reforming.



Figure 98 GC/MS analysis of BSG Intermediate pyrolysis oil after catalytic reforming at 850°C with steam
(Chemical abundant vs. Retention time)

The presence of 2-propanol, 1-chloro and propanenitrile, 3,3'-thiobis- indicate potential Cl and S poisoning of catalysts.

Table 43 Composition of BSG Intermediate Pyrolysis oil after catalytic reforming at 850°C with steam

Time	Chemical Name	Chemical Group	Molecular formula	RMM	Area %
6.01	2-Propenenitrile	Alkyl Nitriles	C ₃ H ₃ N	53	1.49
7.413	Benzene	Aromatic	C ₆ H ₆	78	1.17
10.839	Toluene	Aromatic	C ₇ H ₈	92	1.11
11.426	Pyridine	Pyridine	C ₅ H ₅ N	79	84.52
14.829	Pyrrol	Alcohol	C ₄ H ₅ N	67	2.76
50.46	2-Propanol, 1-chloro-	Alcohol/Chlorine	C ₃ H ₇ ClO	95	0.91
59.416	Propanenitrile, 3,3'-thiobis-	Alkyl nitriles	C ₆ H ₈ N ₂ S	140	6.32

In comparing the GC/MS chromatograms obtained at different reforming temperatures there was a large decrease in the number of compounds at 850°C, in comparison to those reforming temperatures 500°C and 750°C during the analysis of bio-oils. This was also observed similarly by Gilbert et al[189].

It can be seen that at the three different reforming temperatures (without steam) much of the oxygenated components in the bio-oils were not identified in the GC/MS peaks indicating these components were reformed completely. At reforming temperatures 500°C and 750°C the organic composition contain some polycyclic aromatic hydrocarbons (PAH). At LT reforming 500°C the PAH compounds identified were anthracene, fluorene, naphthalene and pyrene, while at HT reforming 750°C the quantity of PAH had decreased with some naphthalene identified. However at HT reforming 850°C PAH compounds in the bio-oil were not identified but showed some presence of benzene, toluene, pyrrol and a large fraction of pyridine. The average molecular weight of the bio-oil

components using Nickel catalysts at 850°C with steam added rate was determined to be 86 which is a 40% decrease in comparison to oils produced without catalysts.

The PAH's cause concern due to their carcinogenic and mutagenic characteristics and have been classified by the Environmental Protection Agency (EPA) as priority pollutants. By using a Ni/Al₂O₃ catalysts bed and steam reforming at high temperature close coupled to a pyrolysis unit, (PAH) 3 and 4 ring compounds such as phenanthrene, pyrene and other PAH compounds are reformed into single and two ring aromatic compounds of lower molecular weights such as benzene, toluene and styrene. This reduction could be due to higher molecular weight hydrocarbons being thermally degraded into lighter hydrocarbons[116]. This confirms the effect of the catalyst and the cracking of higher compounds and the increase of hydrogen in the syngas. Figures 99 & 100 illustrate effects of Ni/Al₂O₃ catalysts with and without steam for the chemical components detected in the bio-oils.

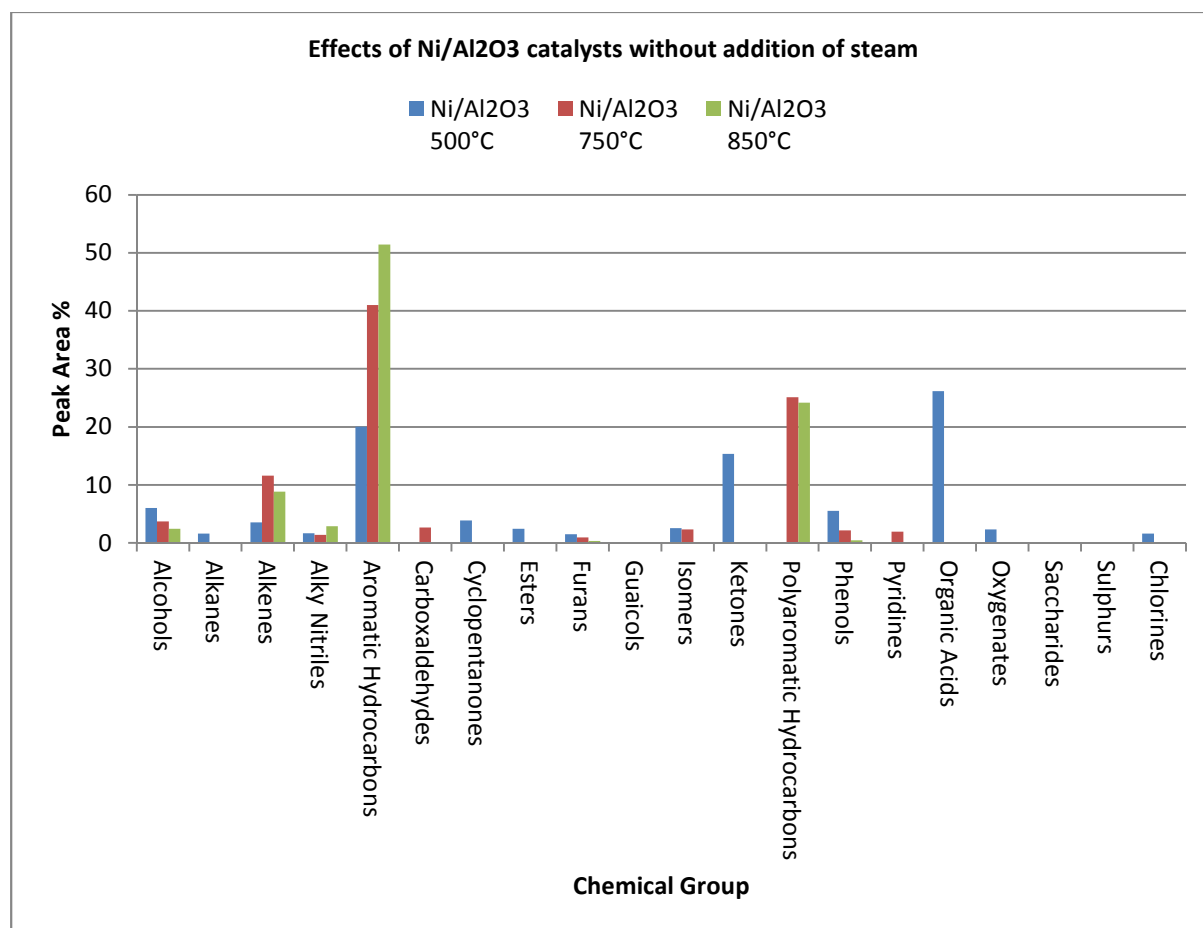


Figure 99 Effects of Nickel catalysts without steam

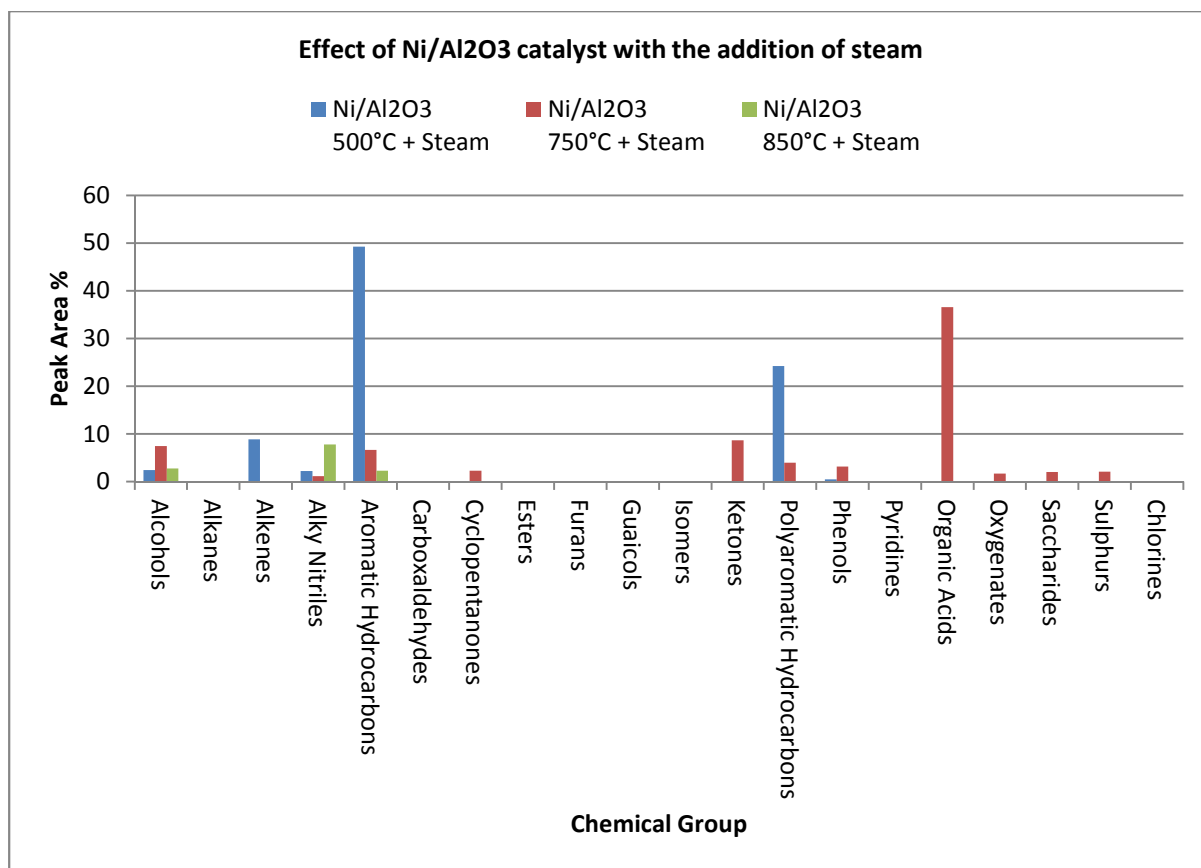


Figure 100 Effects of Nickel catalyst with the addition of steam

9.4.7 GCMS Bio-Oil at 500°C with Platinum (Pt/Al₂O₃) catalyst and without steam

Figure 101 shows the GC/MS mass spectrum. The major chemical components present are illustrated in Table 44. The bio-oil consists of a number of complex organic oxygenated compounds.

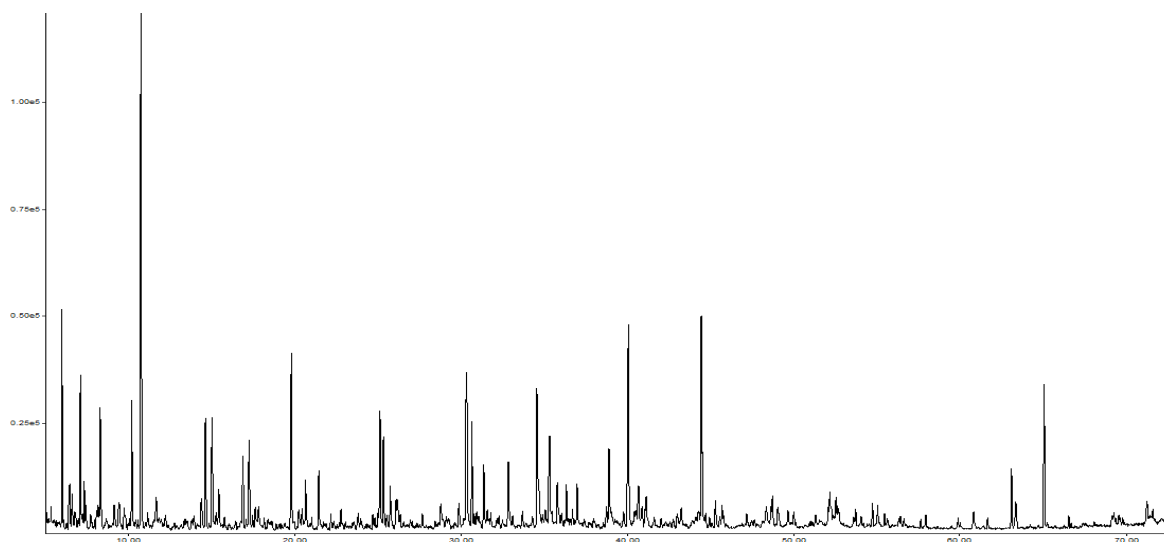


Figure 101 GC/MS analysis of BSG Intermediate pyrolysis oil after catalytic reforming 500°C with Platinum and no steam (Chemical abundant vs. Retention time)

The major peaks detected and identified with the highest abundance was toluene 10.49%, 1-tetradecene 4.55%, decane 1-chloro- 3.08% pentadecane 3.76%, carbamic acid, methyl-, phenyl ester 3.96%, hexadecanenitrile 2.77%, furan, 2-methyl- 2.53%, ethylbenzene 2.44% . These were the largest components present. The average molecular weight of the bio-oil components using Platinum catalysts at 500°C was no different in comparison to oils produced without catalysts.

Table 44 Composition of BSG Intermediate Pyrolysis oil after catalytic reforming 500°C with Platinum and no steam

Time	Chemical Name	Chemical Group	Molecular Formula	RMM	Area %
6.01	Furan, 2-methyl-	Furan	C ₅ H ₆ O	82	2.53
6.482	1,3-Cyclopentadiene, 1-methyl-	Alcohol	C ₆ H ₈	80	1.02
7.114	1-Heptene	Alkene	C ₇ H ₁₄	98	1.99
8.321	2,5-Dimethylfuran	Furan	C ₆ H ₈ O	96	2.04
10.206	Octane, 4-chloro-	Alkane/Chlorine	C ₈ H ₁₇ Cl	149	2.13
10.758	Toluene	Aromatic	C ₇ H ₈	92	10.49
15.034	Ethylbenzene	Aromatics	C ₈ H ₁₀	106	2.44
19.793	Decane, 1-chloro-	Alkane/Chlorine	C ₁₀ H ₁₅ Cl	176	3.08
21.437	Mesitylene	Alkene	C ₉ H ₁₂	120	1.08
25.322	Benzene, butyl-	Aromatic	C ₁₀ H ₁₄	134	1.48
25.518	2-Cyclopenten-1-one, 2,3-dimethyl-	Cyclopentanone	C ₇ H ₁₀ O	110	0.25
30.311	Carbamic acid, methyl-, phenyl ester	Ester	C ₈ H ₉ NO ₂	151	3.96
30.633	Benzene, pentyl-	Aromatic	C ₁₁ H ₁₆	148	1.84
31.358	Benzene, 1-methyl-4-(2-methylpropyl)-	Aromatic	C ₁₁ H ₁₆	148	1.23
32.829	Phenol, 3-methyl-	Phenol	C ₇ H ₈ O	108	1.5
33.668	Phenol, 2,5-dimethyl-	Phenol	C ₈ H ₁₀ O	122	0.36
34.542	Phenol, 3-methyl-	Phenol	C ₇ H ₈ O	108	2.92
35.772	Benzene, hexyl-	Aromatic	C ₁₂ H ₁₈	162	1
38.864	Phenol, 4-ethyl-	Phenol	C ₈ H ₁₀ O	122	1.38
40.037	1-Tetradecene	Alkene	C ₁₄ H ₂₈	196	4.55
44.416	Pentadecane	Alkene	C ₁₅ H ₃₂	212	3.76
63.108	Hexadecanoic acid, methyl ester	Ester	C ₁₇ H ₃₄ O ₂	270	1.07
63.361	2-Nonadecanone	Ketone	C ₁₉ H ₃₈ O	282	0.74
65.062	Hexadecanenitrile	Alkyl Nitrile	C ₁₆ H ₃₁ N	237	2.77

9.4.8 GCMS Bio-Oil at 850°C with Platinum (Pt/Al₂O₃) catalyst and without steam

Figure 102 shows the GC/MS mass spectrum. The major chemical components present are illustrated in Table 45.

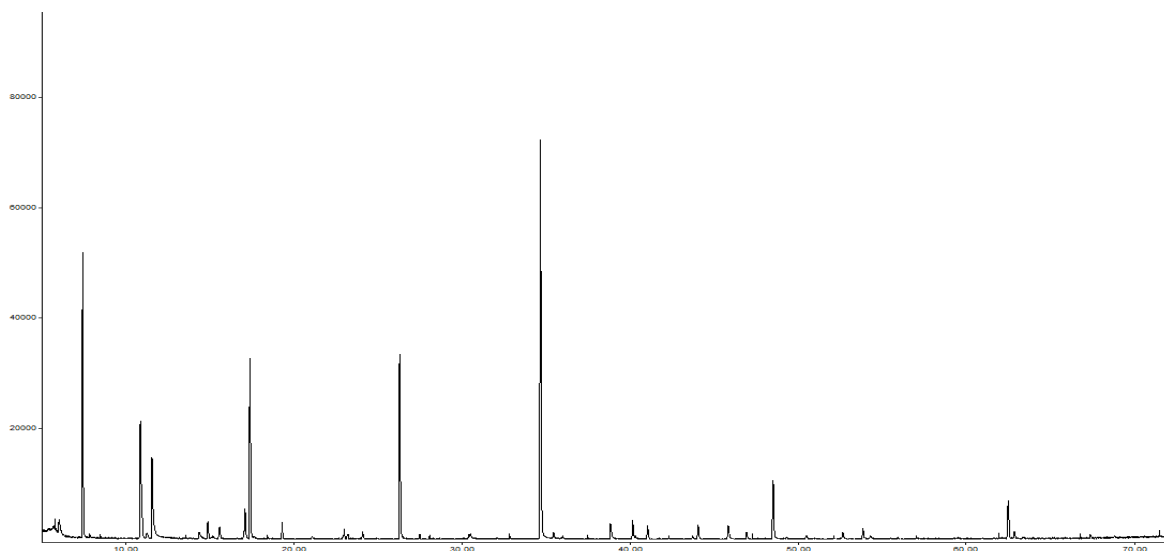


Figure 102 GC/MS analysis of BSG Intermediate pyrolysis oil after catalytic reforming 850°C with Platinum and no steam (Chemical abundant vs. Retention time)

The major peaks detected and identified with the highest abundance was naphthalene 28.97%, indene 15.33%, styrene 10.62%, toluene 9.05%, benzene 4.69%, acenaphthylene 4.35%, pyridine (79, 79, R I0) 3.55%. These were the largest components present. The average molecular weight of the bio-oil components using Platinum catalysts at 850°C was determined to be 104 which is a 27% decrease in comparison to oils produced without catalysts.

Table 45 Composition of BSG Intermediate Pyrolysis oil after catalytic reforming 850°C with Platinum and no steam

Time	Chemical Name	Chemical Group	Molecular Formula	RMM	Area %
7.366	Benzene	Aromatic	C ₆ H ₆	78	4.69
10.769	Toluene	Aromatic	C ₇ H ₈	92	9.05
11.62	Pyridine	Pyridine	C ₅ H ₅ N	79	3.55
14.769	Pyrrol	Alcohol	C ₄ H ₅ N	67	1.6
15.448	p-Xylene	Aromatic	C ₈ H ₁₀	106	1.29
16.976	Phenylethyne	Alcohol	C ₈ H ₆	102	2.69
17.252	Styrene	Aromatic	C ₈ H ₈	104	10.62
26.15	Indene	Aromatic	C ₉ H ₈	116	15.33
30.334	Phenol	Phenol	C ₆ H ₆ O	94	1.12
32.702	Bicyclo[2.2.1]hept-5-ene-2-carbonitrile	Alkyl nitrile	C ₈ H ₉ N	119	3.01
34.507	Naphthalene	Polyaromatic	C ₁₀ H ₈	128	28.97
38.749	2-Propenenitrile, 3-phenyl-, (E)-	Alkyl nitrile	C ₉ H ₇ N	-	1.61
39.979	1H-Indene, 1-ethylidene-	Aromatic	C ₁₁ H ₁₀	-	1.89
40.875	Naphthalene, 2-methyl-	Polyaromatic	C ₁₁ H ₉ BR	-	1.49
45.669	Indole	Carboxaldehyde	C ₈ H ₇ N	117	2.27
48.324	Acenaphthylene	Polyaromatic	C ₁₂ H ₈	152	4.35
62.36	9H-Fluorene, 9-methylene-	Polyaromatic	C ₁₄ H ₁₀	-	1.87

9.4.9 GCMS Bio-Oil at 500°C with Rhodium (Rh/Al₂O₃) catalyst and without steam

Figure 103 shows the GC/MS mass spectrum. The major chemical components present are illustrated in Table 46.

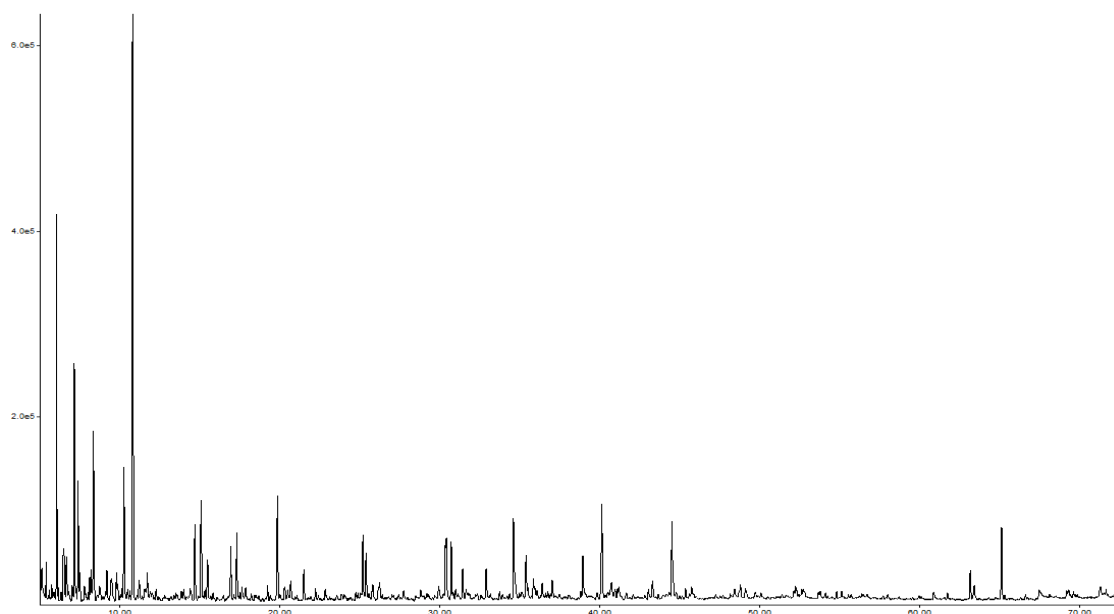


Figure 103 GC/MS analysis of BSG Intermediate pyrolysis oil after catalytic reforming 500°C with Rhodium and no steam (Chemical abundant vs. Retention time)

The major peaks detected and identified with the highest abundance was toluene 15.45%, furan, 2-methyl- 5.83%, 1-heptene 4.4%, 2,5-dimethylfuran 3.58%, 1-tetradecene 2.86%, phenol, 4-methyl- 2.82%, benzene 2.16% ethylbenzene 2.06%. These were the largest components present. The average molecular weight of the bio-oil components using Rhodium catalysts at 500°C rate was determined to be 137 which is a 5% decrease in comparison to oils produced without catalysts.

Table 46 Composition of BSG Intermediate Pyrolysis oil after catalytic reforming 500°C with Rhodium and no steam

Time	Chemical Name	Chemical Group	Molecular Formula	RMM	Area %
6.068	Furan, 2-methyl-	Furan	C ₅ H ₆ O	82	5.83
6.689	1,3-Cyclopentadiene, 1-methyl-	Alcohol	C ₆ H ₈	80	0.98
7.045	2,4-Hexadiene	Isomer	C ₆ H ₁₀	82	0.37
7.172	1-Heptene	Alkene	C ₇ H ₁₄	98	4.4
7.413	Benzene	Aromatic	C ₆ H ₆	78	2.16
8.367	2,5-Dimethylfuran	Furan	C ₆ H ₈ O	96	3.58
10.275	1-Octene	Alkene	C ₈ H ₁₆	112	2.86
10.815	Toluene	Aromatic	C ₇ H ₈	92	15.45
14.401	Cyclopentanone	Cyclopentanone	C ₅ H ₈ O	84	0.2
14.7	1-Nonene	Alcohol	C ₉ H ₁₈	126	2.06
15.102	Ethylbenzene	Aromatic	C ₈ H ₁₀	106	2.62
15.344	3-Nonene	Alcohol	C ₉ H ₁₈	126	0.21
15.493	p-Xylene	Aromatic	C ₈ H ₁₀	106	1.05
16.953	m-Xylene	Aromatic	C ₈ H ₁₀	106	1.26
17.32	Bicyclo[4.2.0] octa-1,3,5-triene	Isomer	C ₉ H ₈ O ₂	104	1.62
19.86	Hexadecane, 1-chloro-	Alkane/Chlorine	C ₁₆ H ₃₃ CL	261	2.56
25.205	1-Dodecanol, 2-methyl- (S)-	Alcohol	C ₁₃ H ₂₈ O	-	1.37
25.4	Benzene, butyl-	Aromatic	C ₁₀ H ₁₄	134	1.05
30.411	4-Trifluoroacetoxytetradecane	Alkane	C ₁₆ H ₂₉ F ₃ O ₂	310	2.03
30.722	Benzene, pentyl	Aromatic	C ₁₁ H ₁₆	148	1.36
34.606	Phenol, 4-methyl-	Phenol	C ₇ H ₈ O	108	2.82
35.399	1-Pentadecene	Alkene	C ₁₅ H ₃₀	210	1.47
38.939	Phenol, 4-ethyl-	Phenol	C ₈ H ₁₀ O	122	1.39
40.123	1-Tetradecene	Alkene	C ₁₄ H ₂₈	196	2.86
44.502	Pentadecane	Alkane	C ₁₅ H ₃₂	212	1.75
65.144	Hexadecanenitrile	Alkyl nitriles	C ₁₆ H ₃₁ N	237	1.81

9.4.10 GCMS Bio-Oil at 850°C with Rhodium (Rh/Al₂O₃) catalyst and without steam

Figure 104 shows the GC/MS mass spectrum. The major chemical components present are illustrated in Table 47.

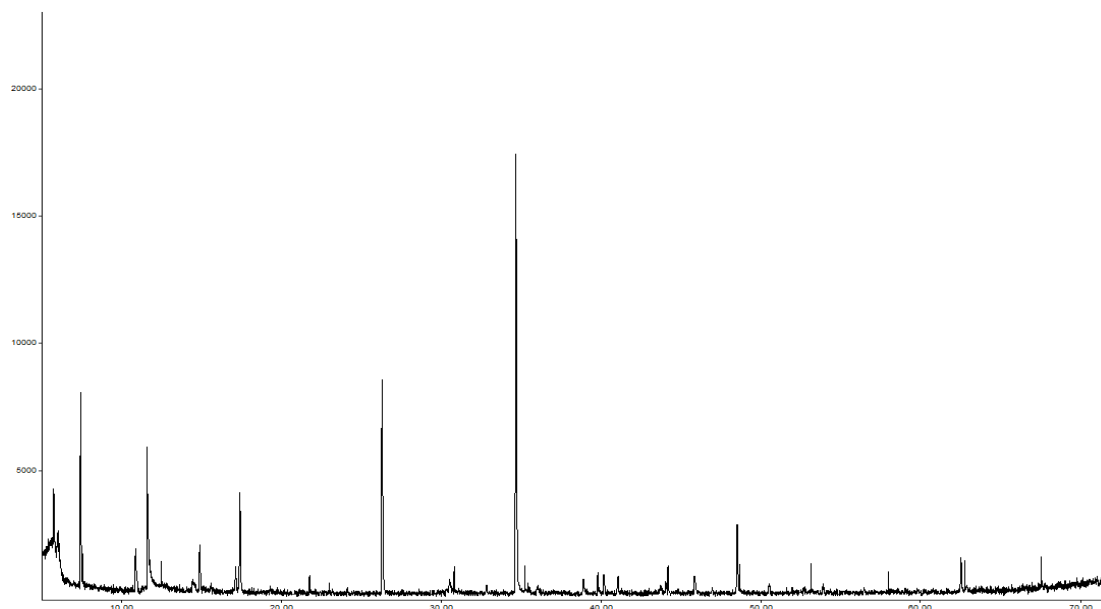


Figure 104 GC/MS analysis of BSG Intermediate pyrolysis oil after catalytic reforming 850°C with Rhodium and no steam (Chemical abundant vs. Retention time)

The major peaks detected and identified with the highest abundance was naphthalene 27.53%, benzene 13.28%, indene 11.9%, toluene 10.59%, and acenaphthylene 5.04%. These were the largest components present. The average molecular weight of the bio-oil components using Rhodium catalysts at 850°C was determined to be 123 which is a 15% decrease in comparison to oils produced without catalysts.

Table 47 Composition of BSG Intermediate Pyrolysis oil after catalytic reforming 850°C with Rhodium and no steam

Time	Chemical Name	Chemical Group	Molecular Formula	RMM	Area %
7.436	Benzene	Aromatic	C ₆ H ₆	78	13.28
10.861	Toluene	Aromatic	C ₇ H ₈	92	10.59
11.632	Pyridine	Pyridines	C ₅ H ₅ N	79	1.54
17.092	Phenylethyne	Alcohol	C ₈ H ₆	102	2.7
17.391	Cyclooctatetraene	Alkenes	C ₈ H ₈	104	10.22
26.288	Indene	Aromatic	C ₉ H ₈	116	11.9
30.45	Phenol	Phenol	C ₆ H ₆ O	94	0.77
34.657	Naphthalene	Polyaromatic	C ₁₀ H ₈	128	27.53
38.807	2-Propenenitrile, 3-phenyl-, (E)-	Alkynitrile	C ₉ H ₇ N	129-	1.46
40.129	1H-Indene, 1-ethylidene-	Aromatic	C ₁₁ H ₁₀	142-	2.57
44.014	Biphenyl	Aromatic	C ₁₂ H ₁₀	154	1.06
45.796	Indole	Carboxaldehyde	C ₈ H ₇ N	117	1.89
48.486	Acenaphthylene	Polyaromatic	C ₁₂ H ₈	152	5.04
62.51	9H-Fluorene, 9-methylene-	Polyaromatic	C ₁₄ H ₁₀	178	2.94
72.971	1,9-Dihdropyrene	Polyaromatic	C ₁₆ H ₁₂	204	1.06

9.4.11 GCMS Bio-Oil at 500°C with Platinum (Pt/Al₂O₃) catalyst and steam

Figure 105 shows the GC/MS mass spectrum. The major chemical components present are illustrated in Table 48.

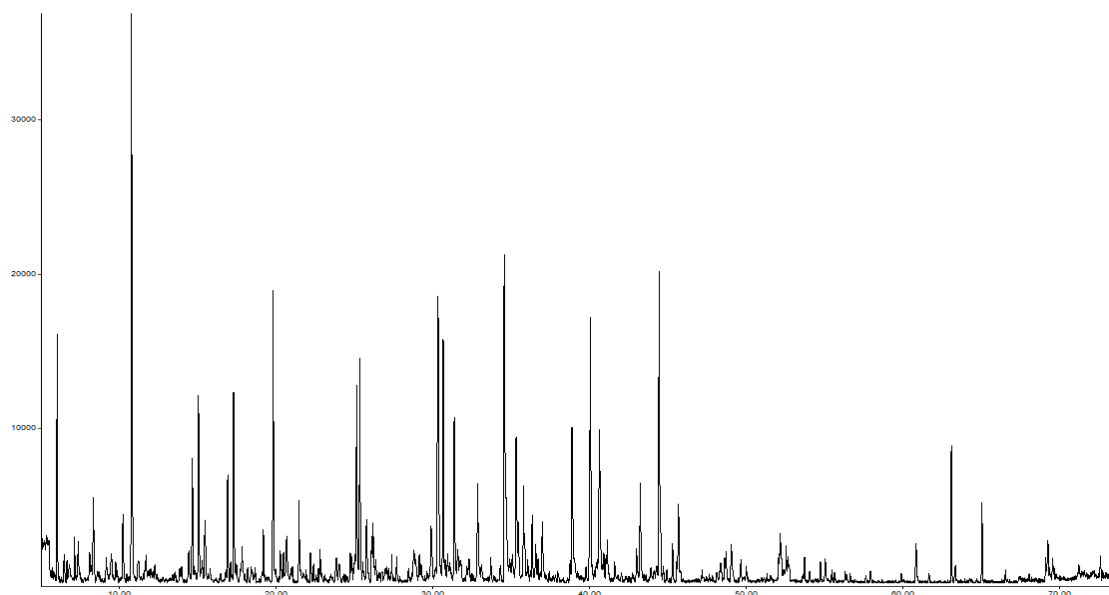


Figure 105 GC/MS analysis of BSG Intermediate pyrolysis oil after catalytic reforming 500°C with Platinum and with steam (Chemical abundant vs. Retention time)

The major peaks detected and identified with the highest abundance was toluene 9.58%, phenol, 3-methyl- 7.66%, carbamic acid, methyl-, phenyl ester 6.95%, 7-tetradecene 4.65%, decane, 1-chloro- 4.22%, benzene, pentyl- 3.5%, benzene, butyl- 3.22%, tridecane 3.14%, ethylbenzene 3.06%, benzene, 1-methyl-4-(2-methylpropyl)- 2.85%, and furan, 2-methyl- 2.56%. The average molecular weight of the bio-oil components using Platinum catalysts at 500°C with steam was determined to be 131 which is a 8.5% decrease in comparison to oils produced without catalysts.

Table 48 Composition of BSG Intermediate Pyrolysis oil after catalytic reforming 500°C with Platinum and with steam

Time	Chemical Name	Chemical Group	Molecular Formula	RMM	Area %
6.045	Furan, 2-methyl-	Furan	C ₅ H ₆ O	82	2.56
8.355	2,5-Dimethylfuran	Furan	C ₄ H ₉ NO ₂	96	1.34
10.792	Toluene	Aromatic	C ₇ H ₈	92	9.58
15.067	Ethylbenzene	Aromatic	C ₈ H ₁₀	106	3.06
15.469	p-Xylene	Aromatic	C ₈ H ₁₀	106	1.07
16.918	m-Xylene	Aromatic	C ₈ H ₁₀	106	1.6
17.297	Cyclooctatetraene	Alkene	C ₈ H ₈	104	2.85
17.849	Pentanenitrile, 4-methyl-	Alkyl nitrile	C ₆ H ₁₁ N	97	0.66
19.814	Decane, 1-chloro-	Alkane/Chlorine	C ₁₀ H ₂₁ CL	176	4.22
20.676	Cyclopentane, ethylidene-	Alkane	C ₇ H ₁₂	96	0.78
21.469	Mesitylene	Alkene	C ₉ H ₁₂	120	1.08
25.342	Benzene, butyl-	Aromatic	C ₁₀ H ₁₄	134	3.22
26.112	Benzene, (1-methylpropyl)-	Aromatic	C ₁₀ H ₁₄	134	0.71
26.193	1H-Indene, 1-chloro-2,3-dihydro-	Alkene/Chlorine	C ₉ H ₉ CL	-	0.89
30.33	Carbamic acid, methyl-, phenyl ester	Ester	C ₈ H ₉ NO ₂	151	6.95
30.652	Benzene, pentyl-	Aromatic	C ₁₁ H ₁₆	148	3.5
31.365	Benzene, 1-methyl-4-(2-methylpropyl)-	Aromatic	C ₁₁ H ₁₆	-	2.85
32.847	Phenol, 3-methyl-	Phenol	C ₇ H ₈ O	108	2.03
34.56	Phenol, 3-methyl-	Phenol	C ₇ H ₈ O	108	7.66
35.307	Tridecane	Alkane	C ₁₃ H ₂₈	184	3.14
35.456	1H-Pyrrole, 1-(2-furanylmethyl)-	Carboxaldehydes	C ₉ H ₉ NO	147	1.12
35.79	Benzene, hexyl-	Aromatic	C ₁₂ H ₁₈	162	1.29
36.341	Benzene, (1,3-dimethylbutyl)-	Aromatic	C ₁₂ H ₁₈	162	0.91
36.985	Phenol, 2,4-dimethyl-	Phenol	C ₈ H ₁₀ O	122	1
38.881	Phenol, 4-ethyl-	Phenol	C ₈ H ₁₀ O	122	2.53
40.054	7-Tetradecene	Alkene	C ₁₄ H ₂₈	196	4.65
40.617	Phenol, 4-ethyl-2-methoxy-	Phenol	C ₉ H ₁₂ O ₂	152	2.99
41.122	Benzene, (1-methylhexyl)-	Aromatic	C ₁₃ H ₂₀	-	0.8
43.226	2-Methoxy-4-vinylphenol	Phenol	C ₉ H ₁₀ O ₂	150	1.61
44.433	Tetradecane	Alkane	C ₁₄ H ₃₀	198	4.5
45.662	Indole	Alcohol	C ₈ H ₇ N	117	1.19
63.121	Pentadecanoic acid, 14-methyl-, methyl ester	Ester	C ₁₇ H ₃₄ O ₂	-	1.95
65.063	Pentadecaneitrile	Alkyl nitrile	C ₁₅ H ₂₉ N	-	1.17

9.4.12 GCMS Bio-Oil at 850°C with Platinum (Pt/Al₂O₃) catalyst and steam

Figure 106 shows the GC/MS mass spectrum. The major chemical components present are illustrated in Table 49.

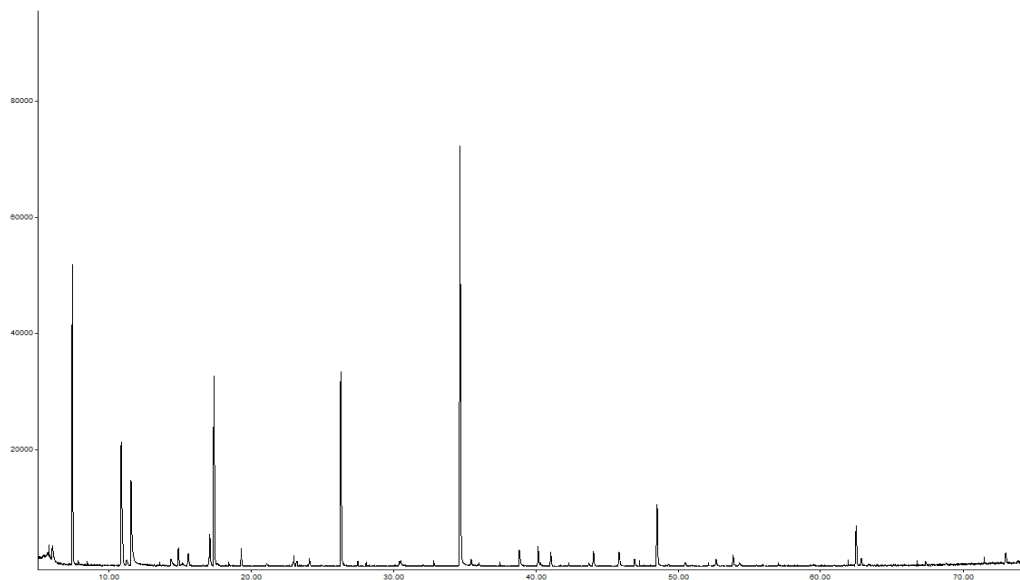


Figure 106 GC/MS analysis of BSG Intermediate pyrolysis oil after catalytic reforming 850°C with Platinum and with steam (Chemical abundant vs. Retention time)

The major peaks detected and identified with the highest abundance was naphthalene 28.75%, benzene 15.17%, indene 12.48%, cyclooctatetraene 12.01%, toluene 10.3%, pyridine (79, 79, RI0) 5.96%, acenaphthylene 4.51%. The average molecular weight of the bio-oil components using Platinum catalysts at 850°C with steam was determined to be 97 which is a 32% decrease in comparison to oils produced without catalysts.

Table 49 Composition of BSG Intermediate Pyrolysis oil after catalytic reforming 850°C with Platinum and with steam

Time	Chemical Name	Chemical Group	Molecular Formula	RMM	Area %
6.048	2-Propenenitrile	Alkyl nitrile	C ₃ H ₃ N	53	0.96
7.45	Benzene	Aromatic	C ₆ H ₆	78	15.17
10.876	Toluene	Aromatic	C ₇ H ₈	92	10.3
11.565	Pyridine	Pyridine	C ₅ H ₅ N	79	5.96
14.887	Pyrrrol	Alcohol	C ₄ H ₅ N	67	1.04
15.589	p-Xylene	Aromatic	C ₈ H ₁₀	106	0.99
17.095	Phenylethyne	Alcohol	C ₈ H ₆	-102	2.3
17.393	Cyclooctatetraene	Alkene	C ₈ H ₈	104	12.01

26.291	Indene	Aromatic	C ₉ H ₈	116	12.48
34.648	Naphthalene	Polyaromatic	C ₁₀ H ₈	128	28.75
38.809	2-Propenenitrile, 3-phenyl-,(E)-	Alkyl nitrile	C ₉ H ₇ N	129	1.22
40.131	1H-Indene, 1-ethylidene-	Aromatic	C ₁₁ H ₁₀	142	1.14
41.017	Naphthalene, 2-methyl-	Polyaromatic	C ₁₁ H ₁₀	142	0.9
44.017	Biphenyl	Aromatic	C ₁₂ H ₁₀	154	1.09
45.799	5H-1-Pyridine	Pyridine	C ₈ H ₇ N	117	1.19
48.477	Acenaphthylene	Polyaromatic	C ₁₂ H ₈	152	4.51

9.4.13 GCMS Bio-Oil at 500°C with Rhodium (Rh/Al₂O₃) catalyst and steam

Figure 107 shows the GC/MS mass spectrum. The major chemical components present are illustrated in Table 50

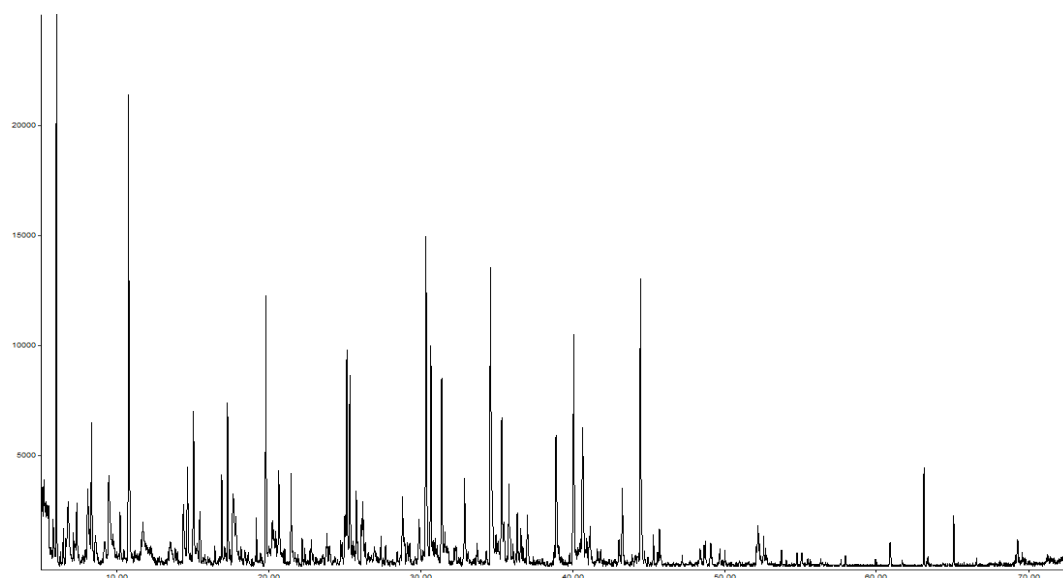


Figure 107 GC/MS analysis of BSG Intermediate pyrolysis oil after catalytic reforming 500°C with Rhodium and with steam (Chemical abundant vs. Retention time)

The major peaks detected and identified with the highest abundance was toluene 8.66%, phenol, 4-methyl- 7.44%, carbamic acid, methyl-, phenyl ester 7.21%, furan, 2-methyl- 5.85%, pentadecane 5.53%, 1-pentadecene 4.63%, decane, 1-chloro- 4.09%, ethanone, 1-(1-cyclohexen-1-yl)- 3.64%, benzene, pentyl- 3.54% o-xylene 2.88%, benzene, butyl- 2.86%, tridecane 2.79%, acetic acid (60, 60, RI 0) 2.79%, cyclooctatetraene 2.62% and phenol, 4-ethyl- 2.59%. The average molecular weight of the bio-oil components using Rhodium catalysts at 500°C with steam added was determined to be 134 which is a 6.5% decrease in comparison to oils produced without catalysts.

Table 50 Composition of BSG Intermediate Pyrolysis oil after catalytic reforming 500°C with Rhodium and with steam

Time	Chemical Name	Chemical Group	Molecular Formula	RMM	Area %
6.038	Furan, 2-methyl-	Furan	C ₅ H ₆ O	81	5.85
6.808	1-Propene, 2-methyl-3-(1-methylethoxy)-	Alkene	C ₇ H ₁₄ O	114	1.84
8.107	Butanol, 2-methyl-	Alcohol	C ₅ H ₁₂ O	88	1.62
8.348	2,5-Dimethylfuran (96, 96, RI 0)	Furan	C ₆ H ₈ O	96	1.81
9.497	Acetic Acid (60, 60, RI 0)	Organic Acid	C ₇ HNO ₃	189	2.79
10.784	Toluene	Aromatic	C ₇ H ₈	92	8.66
14.393	Cyclopentanone	Aromatic	C ₅ H ₈ O	84	1.16
14.658	4-Tridecene, (Z)-	Alkene	C ₁₃ H ₂₆	182	1.65
15.06	O-Xylene	Aromatic	C ₈ H ₁₀	106	2.88
15.474	m-Xylene	Aromatic	C ₈ H ₁₀	106	1.01
16.91	p-Xylene	Aromatic	C ₈ H ₁₀	106	1.35
17.29	Cyclooctatetraene (104, 104, RI 0)	Alkene	C ₈ H ₈	104	2.62
19.807	Decane, 1-chloro-	Alkane/Chlorine	C ₁₀ H ₂₁ CL	176	4.09
20.669	2-Cyclopenten-1-one, 2-methyl-	Cyclopentanone	C ₆ H ₈ O	96	1.52
21.462	Mesitylene	Alkene	C ₉ H ₁₂	120	1.34
25.335	Benzene, butyl-	Aromatic	C ₁₀ H ₁₄	134	2.86
26.186	Benzene, 1,2-propadienyl-	Aromatic	C ₁₁ H ₈	140 140	1.11
30.335	Carbamic acid, methyl-, phenyl ester	Ester	C ₈ H ₉ NO ₂	151	7.21
30.656	Benzene, pentyl-	Aromatic	C ₁₁ H ₁₆	148	3.54
31.369	Ethanone, 1-(1-cyclohexen-1-yl)-	Ketone	C ₈ H ₉ F ₃ O	178	3.64
32.875	Phenol, 2-methyl-	Phenol	C ₇ H ₈ O	108	1.91
34.564	Phenol, 4-methyl-	Phenol	C ₇ H ₈ O	108	7.44
35.311	Tridecane	Alkane	C ₁₃ H ₂₈	184	2.79
35.782	Benzene, hexyl-	Aromatic	C ₁₂ H ₁₈	162	1.26
37.001	Phenol, 2,4-dimethyl-	Phenol	C ₈ H ₁₀ O	122	1.11
38.897	Phenol, 4-ethyl-	Phenol	C ₈ H ₁₀ O	122	2.59
40.046	1-Pentadecene	Alkene	C ₁₅ H ₃₀	210	4.63
40.633	Phenol, 4-ethyl-2-methoxy-	Phenol	C ₉ H ₁₂ O ₂	152	3.16
43.242	2-Methoxy-4-vinylphenol	Phenol	C ₉ H ₁₀ O ₂	150	1.66
44.425	Pentadecane	Alkane	C ₁₅ H ₃₂	212	5.53
63.125	Pentadecanoic acid, 14-methyl-, methyl ester	Ester		-	1.42

9.4.14 GCMS Bio-Oil at 850°C with Rhodium (Rh/Al₂O₃) catalyst and steam

Figure 108 shows the GC/MS mass spectrum. The major chemical components present are illustrated in Table 51.

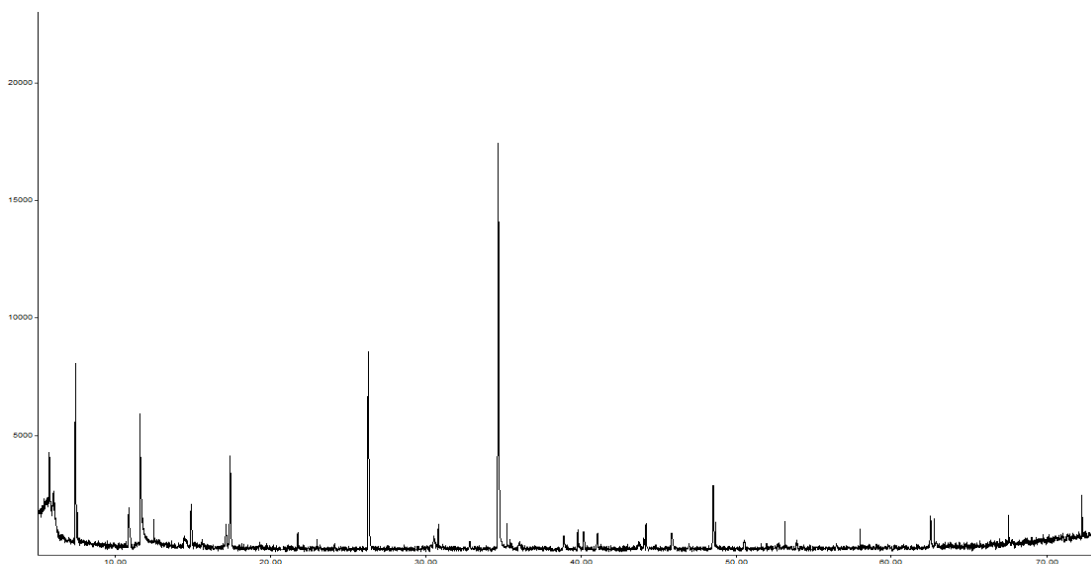


Figure 108 GC/MS analysis of BSG Intermediate pyrolysis oil after catalytic reforming 850°C with Rhodium and with steam (Chemical abundant vs. Retention time)

The major peaks detected and identified with the highest abundance was naphthalene 29.21%, cyclooctatetraene (104, 104, RI 0) 19.72%, indene 13.02%, benzene 8.32%, toluene 7.93%, pyrrol 7%, 2-propenenitrile 7.74%, acenaphthylene 2.94%, 2-methylpyridine 2.1%. The average molecular weight of the bio-oil components using Rhodium catalysts at 850°C with steam determined to be 106 which is a 26% decrease in comparison to oils produced without catalysts.

Table 51 Composition of BSG Intermediate Pyrolysis oil after catalytic reforming 850°C with Rhodium and with steam

Time	Chemical Name	Chemical Group	Molecular Formula	RMM	Area %
5.977	2-Propenenitrile	Alkyl nitrile	C ₃ H ₃ N	53	7.74
7.345	Benzene	Aromatic	C ₆ H ₆	78	8.32
10.759	Toluene	Aromatic	C ₇ H ₈	92	7.93
14.392	2-Methylpyridine	Pyridine	C ₆ H ₇ N	93	2.1
14.737	Pyrrol	Alcohol	C ₄ H ₅ N	67	7
17.231	Cyclooctatetraene (104, 104, RI 0)	Alkene	C ₈ H ₈	104	19.72
26.14	Indene	Aromatic	C ₉ H ₈	116	13.02
34.509	Naphthalene	Polyaromatic	C ₁₀ H ₈	128	29.21
48.349	Acenaphthylene	Polyaromatic	C ₁₂ H ₈	152	2.94
62.385	9H-Fluorene, 9-methylene-	Polyaromatic	C ₁₄ H ₁₀	178	2.02

Figures 109 & 110 illustrate effects of Pt/Al₂O₃ and Rh/Al₂O₃ catalysts with and without steam for the chemical components detected in the bio-oils.

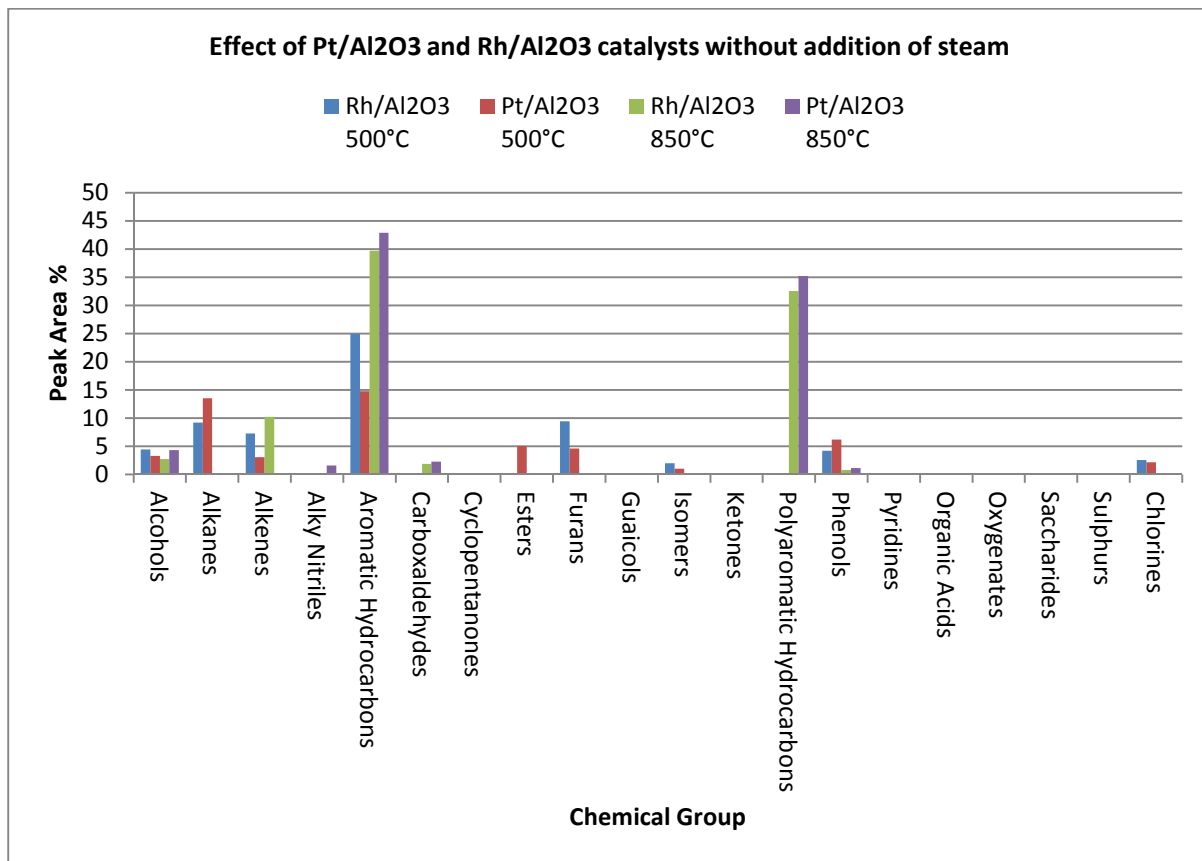


Figure 109 Effect of bio-oil chemical groups using Platinum and Rhodium Catalysts catalyst without steam

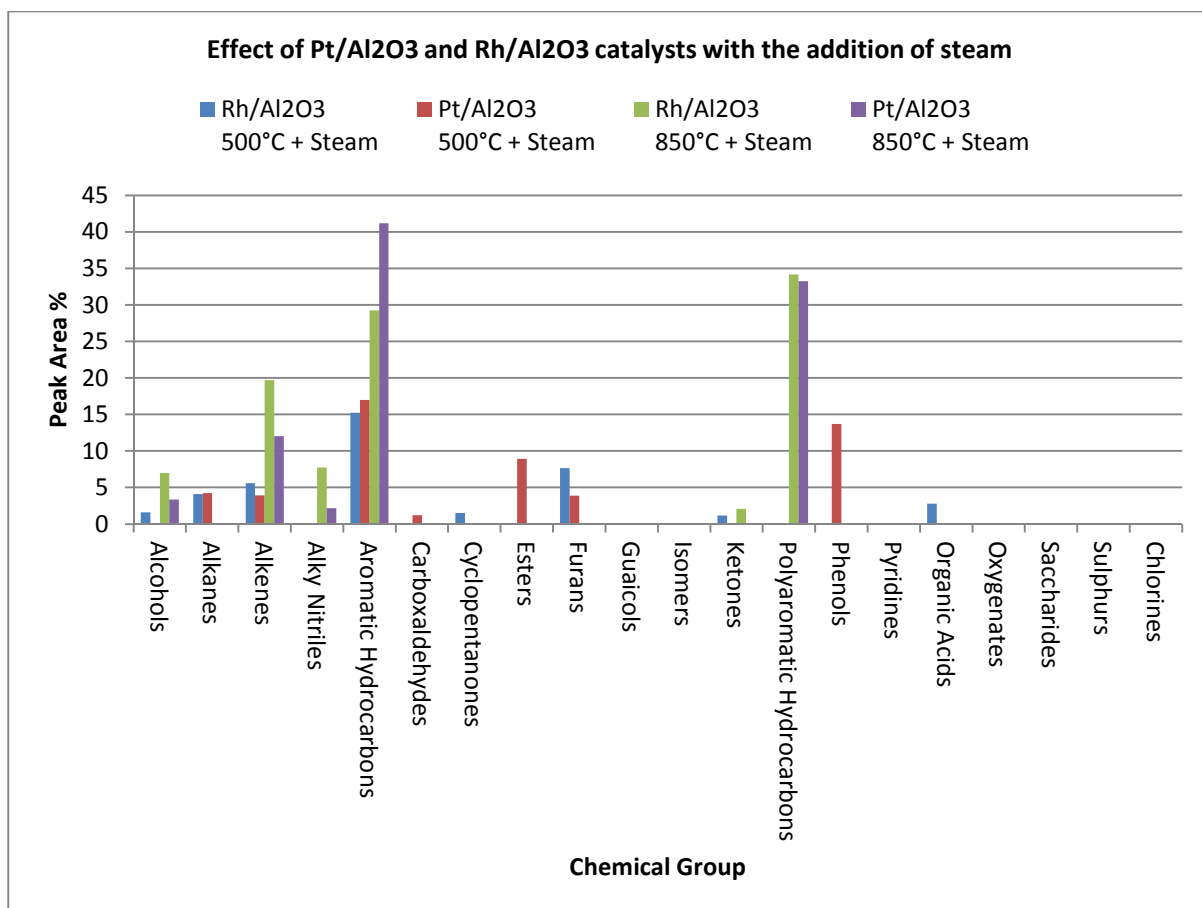


Figure 110 Effect of bio-oil chemical groups with Platinum and Rhodium catalysts with the addition of steam

9.5 Permanent gases

The effect of catalysts had a significant change in the permanent gases. Figure 111 illustrates the comparison of permanent gas yield composition produced at the three different reforming temperatures using Ni/Al₂O₃ catalysts without steam. As much as 43 vol% of hydrogen was produced at 850°C, 24 vol% at 750°C and 10% at 500°C, much higher values than without catalytic reforming. A CO₂ concentration was 35-53 vol%, CO concentrations 15-17 vol% and CH₄ 9-14 vol%.

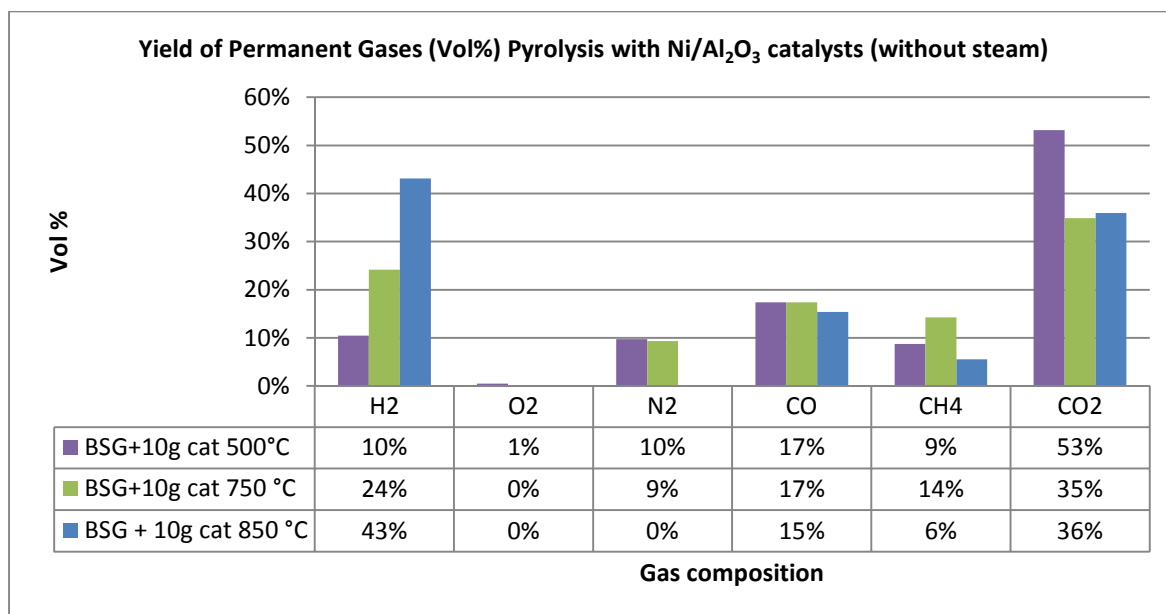


Figure 111 Comparison of the yields of Permanent gases produced from measurements with Ni/Al₂O₃ catalyst and without steam

It appears that the soluble water fraction present in the pyrolysis vapours released via dehydration reaction during pyrolysis can act as a hydrogen source during catalytic reforming.

Figure 112 illustrates the composition of permanent gases at the three different catalytic reforming temperatures with the presence of additional steam and Ni/Al₂O₃ catalysts. As much as 57vol% of hydrogen was produced at reforming temperatures of 750°C and 850°C which is an increase of about 14% in comparison to reforming at the same temperatures without steam. The increase was 22% at 500°C. CO concentration also increased by 9% at 850°C but had decreased by 7% at 500°C. This may be attributed to CH₄ concentration reduced by 6-8% at 500°C and 750°C, however increased by 7% at 850°C.

CO₂ concentration decreased by 13% at 500°C and by 31% at 750°C and was not found at 850°C. The reduction of CO₂ with catalyst shows evidence of decarboxylation reactions occurring and the promotion of both methane reforming reaction (reaction 4) and the water gas shift reaction (reaction 5). The addition of steam had increased H₂ in the product gas and this can be due to the promotion of water-gas shift reaction (reaction 5) shifted towards H₂ production in the presence of Ni/Al₂O₃ catalysts.

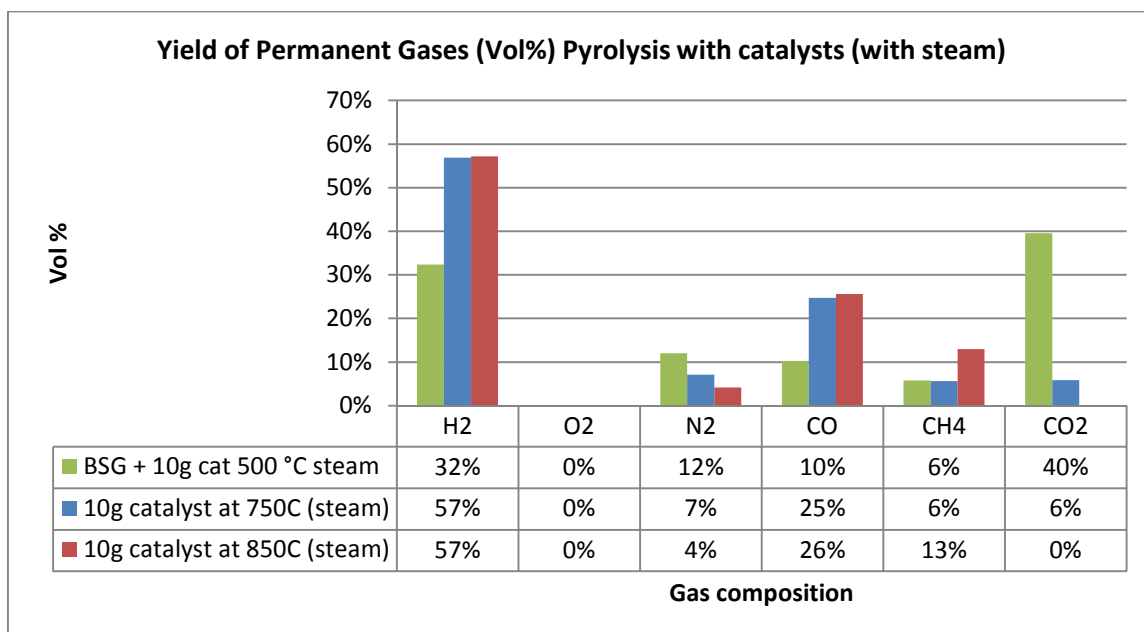


Figure 112 Comparison of the yields of Permanent gases produced from measurements with Ni/Al₂O₃ catalyst and with steam added

The effect of both PGM (Pt/Al₂O₃ and Rh/Al₂O) catalysts also had a significant change in the product gases. Figure 113 illustrates the comparison of permanent gas yield composition produced at the two different catalytic reforming temperatures without steam. At lower reforming temperature of 500°C 3vol% and 2vol% of hydrogen was produced for Pt/Al₂O₃ and Rh/Al₂O slightly higher values than without catalytic reforming but considerably less than what was reported using Ni/Al₂O₃. A CO₂ concentration was 73-79vol%, CO concentrations 6-9vol% and CH₄ 2-3vol%.

At the higher catalytic reforming temperature of 850°C 18vol% and 12vol% of hydrogen was produced for Pt/Al₂O₃ and Rh/Al₂O respectively. This confirms that at low catalytic reforming temperatures of 500°C without the presence of steam both Pt/Al₂O₃ and Rh/Al₂O catalysts are partially active in producing small quantities of hydrogen but ineffective in reducing the liquids yield.

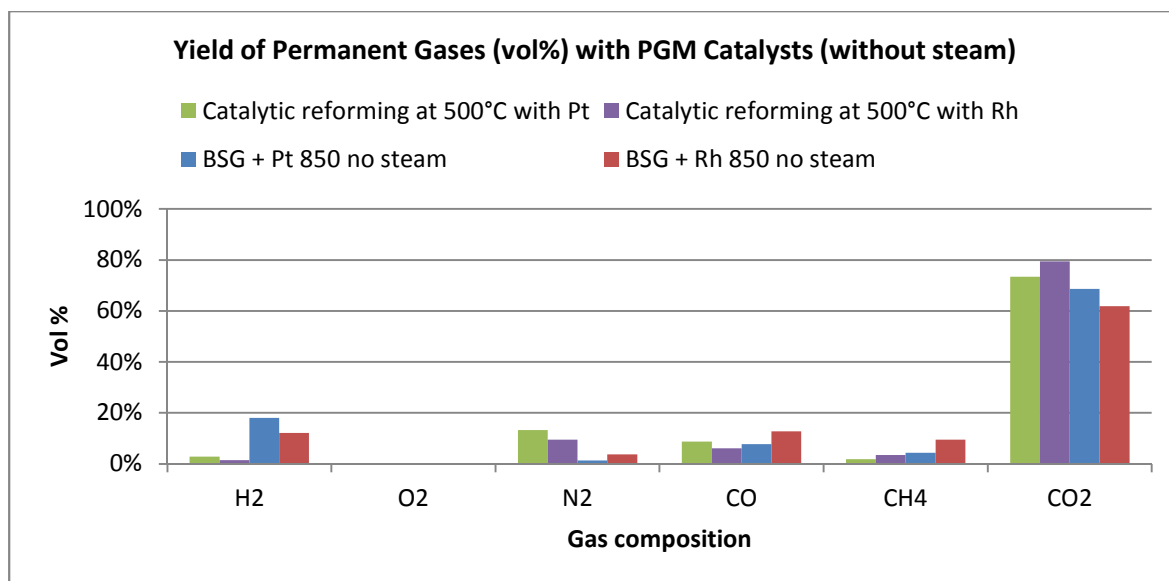


Figure 113 Comparison of the yields of permanent gases produced from measurements with Pt/Al₂O₃ & Rh/Al₂O₃ catalyst at low temperature and without steam

Figure 114 illustrates the comparison of permanent gas yield composition produced at the two different catalytic reforming temperatures with the presence of additional steam using both PGM catalysts. The presence of additional steam at the higher reforming temperatures had a significant change in the product gases.

At lower reforming temperature of 500°C 8vol% and 5vol% of hydrogen was produced for Pt/Al₂O₃ and Rh/Al₂O respectively slightly higher values than without catalytic reforming but considerably less than what was reported using Ni/Al₂O₃. A CO₂ concentration was 46-47vol%, CO concentrations 12-13vol% and CH₄ 6-3vol% for Pt/Al₂O₃ and Rh/Al₂O.

At the higher catalytic reforming temperature of 850°C and with the presence of additional steam 18vol% and 12vol% of hydrogen was produced for Pt/Al₂O₃ and Rh/Al₂O respectively. A CO₂ concentration was 75-69vol%, CO concentrations 7-9vol% and CH₄ 4-5vol% for Pt/Al₂O₃ and Rh/Al₂O.

This confirms that at low catalytic reforming temperatures of 500°C even with the presence of steam both Pt/Al₂O₃ and Rh/Al₂O₃ catalysts are partially active and ineffective in producing hydrogen and reducing condensable liquids yield in comparison to Ni/Al₂O₃ catalysts. This is likely to be that at lower reforming temperature both PGM catalysts are prone to coke formation at the catalysts surface resulting in less active site for catalysts to take effect.

There are a number of factors such that may affect the performance of catalysts they could be precious metal loading content, surface area, attrition, or deactivation by H₂S or coke/ash formation. These parameters were not able to be investigated at this time but would lead to better understanding and

evaluation of catalyst performance if a catalyst was tested over a longer period of time. This study however focused only on the effect and performance of each of the catalysts to produce a quality product gas rich in hydrogen and energy content that maybe suitable for engine applications.

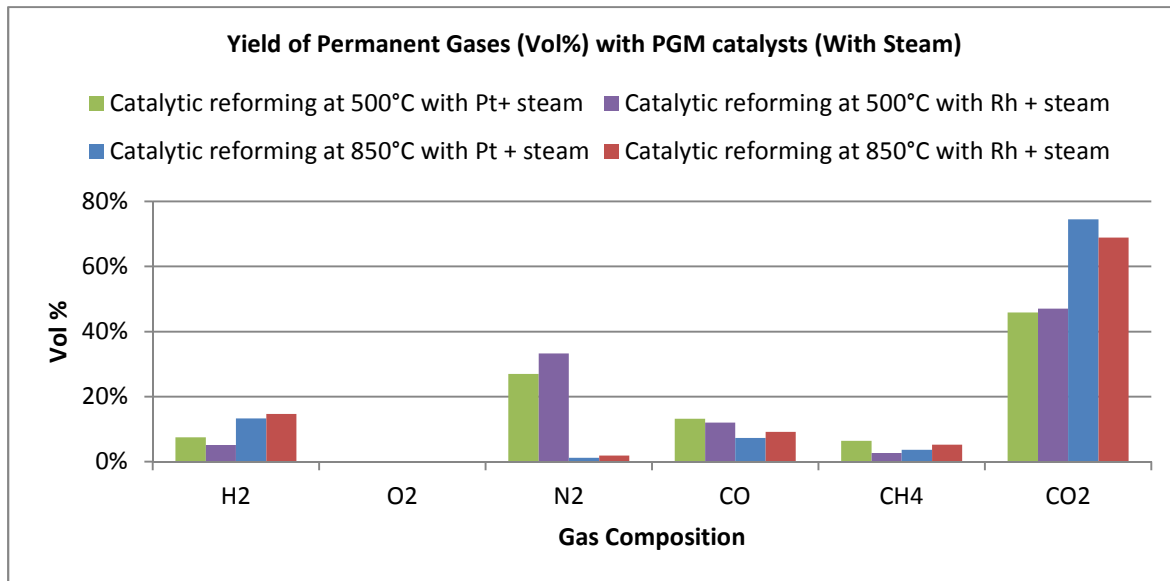


Figure 114 Comparison of the yields of Permanent gases from measurements with Al_2O_3 & $\text{Rh}/\text{Al}_2\text{O}_3$ catalysts at low temperature and with steam

All experimental results using catalysts resulted in a significant influence on the gas compositions. For maximum hydrogen production, temperatures higher than 500°C are suggested with addition of steam.

9.5.1 Heating Value

The increase of reforming temperature and the addition of steam gives an increase in the heating value of the gases see Figure 115. Pyrolysis without catalytic reforming produced a gas with a typical heating value of $1 \text{ MJ}/\text{m}^3$. Best results obtained were with $\text{Ni}/\text{Al}_2\text{O}_3$ catalysts and with steam added: at 500°C the heating value was $10.80 \text{ MJ}/\text{m}^3$, at 750°C heating value was $15.66 \text{ MJ}/\text{m}^3$ and at 850°C heating value was $25.21 \text{ MJ}/\text{m}^3$. For reforming without steam using $\text{Ni}/\text{Al}_2\text{O}_3$ catalysts at 500°C , the heating value was about $2 \text{ MJ}/\text{m}^3$, and at 750°C and 850°C the heating value was about $5 \text{ MJ}/\text{m}^3$.

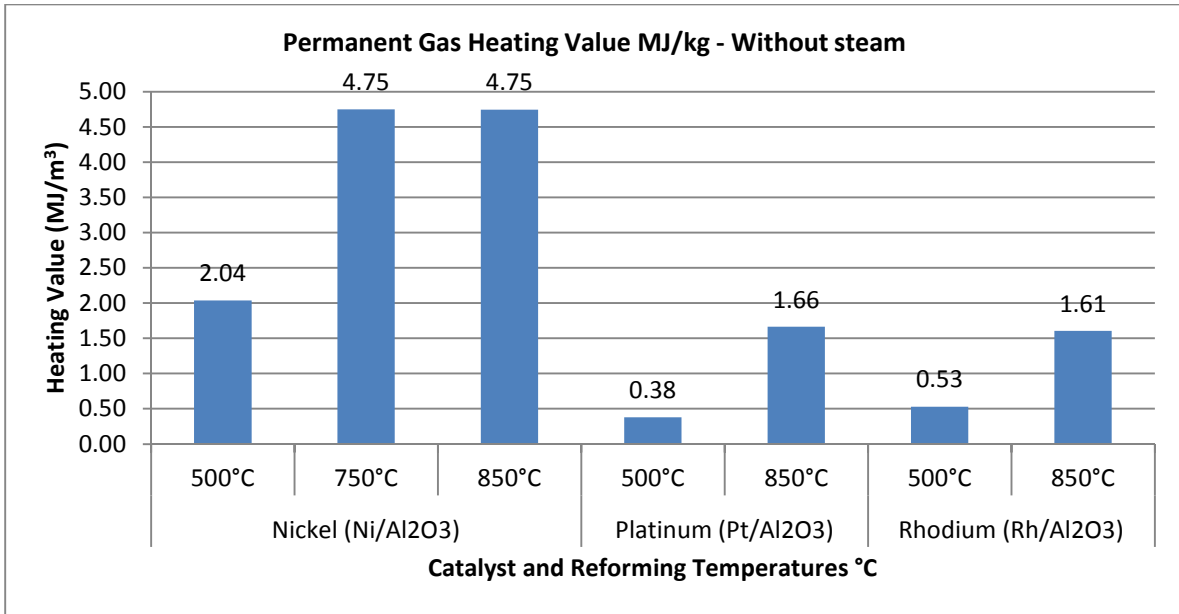


Figure 115 Comparison of permanent gas heating value of bench scale pyrolysis/reforming experiments with catalysts and without steam

Both PGM catalysts Pt/Al₂O₃ and Rh/Al₂O₃ did not perform as well as the Ni/Al₂O₃ catalyst. Again best results were with steam added at high reforming temperatures 850°C for platinum 3.54MJ/m³ and for rhodium 4.05MJ/m³ which is similar to heating value performance of a gasifier.

Without steam added at lower reforming temperatures the heating values was low for Pt/Al₂O₃ at 0.38MJ/m³ and Rh/Al₂O₃ at 0.53MJ/m³ with the addition of steam at the same temperature the values were 1.24MJ/m³and 1.26MJ/m³ respectively. This suggests that the PGM catalysts were not as active as the commercial Ni/Al₂O₃ reforming catalysts, and may be the active sites had become blocked at these temperatures when running the experiments.

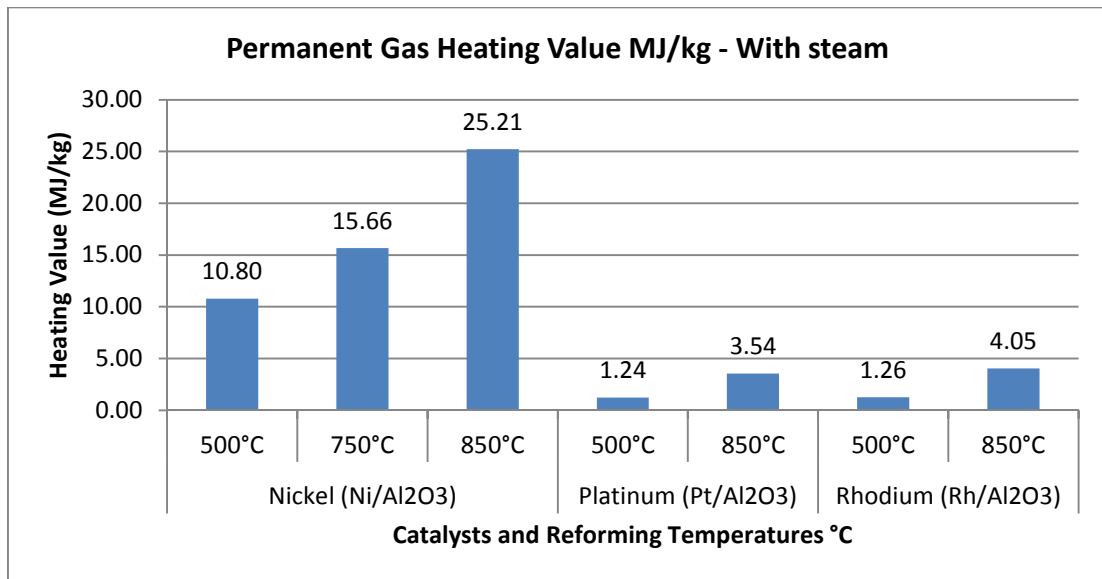


Figure 116 Comparison of permanent gas heating value of bench scale pyrolysis/reforming experiments with catalysts and with steam

10 Implications, Conclusions and Recommendations

10.1 Implications

This section aims to discuss some of the implications of the research work conducted. The original focus of this work was to investigate thermal processing of BSG using fluidised bed gasification followed by catalytic steam reforming. Unfortunately due to unforeseen circumstances a fluidised bed gasifier along with a catalytic steam reforming reactor was not available and the EBRI labs and equipment at various stages of this project was also not available.

From the review of the literature it highlighted the opportunity to explore the advanced thermochemical conversion of BSG further. There had been some studies that have explored both the pyrolysis and gasification of BSG however the quantity of searchable work was very limited. Furthermore there has been limited literature that explores intermediate pyrolysis systems.

As found by this study one of the major issues was obtaining a supply of spent grain that was dry. The BSG obtained for this study was fresh off the process and containing high moisture (67-81%) making the material difficult to handle and transport. Due to its high protein and fibre content, if left untreated at room temperature, within 3 days the material would microbiologically degrade releasing heat and strong odours that could potentially be hazardous. As a result care was given to the pre-treatment of BSG in that quantities was obtained, frozen and then later dried in preparation for experimental work. For this work a dry and densified (in the form of pellets) feedstock was required not only to prevent degradation but also to prepare the fuel so that it is suitable for thermochemical processing. Thus the moisture content was required to be reduced to approximately 8 wt.% using an oven. This required the frozen feedstock left to thaw for several hours and to then manually break up the partially frozen cake material from larger lumps into smaller ones. By doing this ensured that the broken cake material (approximately 50-100mm in size) was evenly distributed across the oven trays so that they can be dried consistently.

Initial tests had revealed that by not breaking the larger lumps before drying would prolong the drying process, and although the material would appear to be dry on the outer side however would still retain a lot of the inner bound moisture which would subsequently still lead the material to degrade overtime. Evidence of this would appear as black spots and the release of strong odours. Breaking the cake material into smaller lumps aided the drying process ensuring most of the moisture from the material could be removed.

When dry, the spent grain was then grinded to further reduce the size of the material using a cutting mill with a 1mm sieve in preparation for pelletising.

For the pelleting process some moisture was required to be added to the fuel in order to aid the binding of the pellets during pelletizing; subsequently its moisture was increased to a final moisture content of approximately 10-12 wt.%. The prepared pellets samples were then stored in closed container for allowing no exchange of moisture with atmospheric air.

The feedstock pre-treatment was a necessary but a very time consuming and labour intensive process to produce significant quantity for processing in either the Pyroformer or Gasifier both having an operating capacity of 20kg/hr.

Although there are many drying technologies available that may be suitable for drying BSG efficiently and economically both the operating and capital cost for implementing and integrating the technologies within a system would need to be carefully considered as well as the technology performance. The amount of total energy required for drying spent grain in a rotary drum dryer from an initial moisture content of 70% to a final moisture content of 10% are described in APPENDIX C. BSG pellets approximately 10-21mm in length and 5mm diameter were processed in a fixed bed downdraft gasifier, and were found to have produced a good quality syngas in terms of CO, H₂ and heating value which were comparable with those from wood chips, wood pellets and hazelnut shells.

One of the problems discovered within this study was the presence of fines due to pellets crumbling within the screw feeder which over time may restrict the gasifier throat preventing air entering and gasification reactions from occurring. It was clear after the study that the operation of this type of gasifier is very sensitive to feedstock size and quality. Upon inspection of the gasifier chamber by the removal of the gasifier top plate there was some unprocessed BSG in the middle of the gasifier bed mainly fines. Fines may have resulted in the abrasion of the surface of the pellets and overtime the fines will build up and may block the throat that can lead to obstruction of gases. Erlich & Fransson [120] reported that many gasifiers similar of this type have grid/bed shaking devices to avoid problems such as bridging and fouling. However a shaking device may form more fines due to abrasion and breakdown of BSG pellets that may block the constricted throat. Literature does not report how to overcome breakdown of pellets in this type of gasifier and dealing with fines and therefore this work could be repeated.

To overcome limitations of the fuel properties for this type of gasifier, stronger pellets would be required or better suited to reduce the formation of fines in the feed system. The pellets strength may

be increased by adding or blending it with a binding material such as wood to increase the mechanical strength of the pellet.

Another proposed solution is to produce cubes or briquettes instead of pellets with an approximate size of approximately 1 inch³ to ensure uniform size distribution, density and mechanical strength of the fuel. Cubes would allow better feeding into the gasifier and would encourage bridging of the fuel which is required within a downdraft gasifier.

The mass balance closed at 95%. The source of the error may have been due to a number of factors including the amount of BSG fines and the inability to measure the residual char in the gasifier. A more accurate method ensuring the mass balance closure was obtained would have been by placing the gasifier on a weighing scale to measure the total mass before and after each experiment however due to the size of the unit it was impractical to implement this strategy.

A slight decrease in the airflow rate to the gasifier was observed indicating some restriction within the gasifier. In order to alleviate this problem the ash grate was agitated in order to distribute the ash and allow for better distribution of the air flow to maintain gasification reactions. Therefore an ash removal system would benefit the gasification process ensuring the continual removal of ash and to keep the incoming air flow rate necessary for the gasification.

A downdraft gasifier with a capacity of 250 kW is suitable to run a combined heat and power plant, however before the gas can be used in an engine it must be cleaned. In this work tar removal was achieved using a carbon absorption filter, but tar levels downstream of the filter were not measured. The tar content in the product syngas was determined to be 1.87 g/Nm³, a figure which is similar to that of wood chips (2 g/Nm³) [173] which in comparison to other types of gasification is fairly low, but still much too high for an engine and will seriously limit the life of the engine components. Therefore the tar content would need to be reduced to acceptable levels (approximately 100g/Nm³) however this can be difficult and expensive. The water content of the product gas was 15.52 g/Nm³. High amount of water vapour in the product gas reduces its calorific value; therefore it is important to reduce the level if possible. This can be achieved by further evaporative drying of the feedstock before gasification, although it is important that the water content is not too low as some water vapour is required for the important water gas shift reactions occurring to produce hydrogen. Tar appeared to form a dark highly viscous layer on the flask surface.

In order to achieve a product gas with acceptable levels of tar to combust in an engine for CHP a gasifier will require additional process equipment downstream in terms of gas cleaning and cooling systems, comprising mainly of cyclone separators, indirect gas coolers, water separator (scrubber) and

a bag filter. The cooling of the product gas can take place in a heat exchanger which can be used to preheat the incoming air required for gasification while cooling down the product gas.

BSG pellets was initially used during the pyroformer tests, however they were also prone to break down and crumble within the screw feeder which resulted in the fuel being fed as fines into the feed inlet. This did not affect the processing of BSG under pyrolysis conditions but had an impact on reducing the fuel feed rate from 10kg/hr to 5kg/hr.

Attempts were made to feed the fines into the pyroformer at higher feed rates of up to 10kg/hr, but this resulted in the feed inlet pipe to the pyroformer to become blocked. BSG fines were fed through the feed inlet pipe and towards the exit of the pipe into the pyroformer the feed material would partially pyrolyse and stick to the surface walls resulting in a bottle neck. The partially decomposed sticky material would then cause the fresh feed material to stick to the already formed sticky material restricting the feed path into the reactor further. Therefore a slower feed rate was selected to process BSG, and a stronger pellet would be required to prevent crumbling in the feed system.

It was found that the intermediate pyrolysis of BSG using the Pyroformer reactor yielded 52% of bio-oil liquid. However the fuel characteristics of the bio-oil were too poor to be considered as a potential fuel for an engine, as there was a significant quantity of water present, bituminous solids and viscous compounds which could polymerize with age if stored at room temperature. The oily organic fraction was of more interest in this study and when visually observed appeared very viscous due to the presence of solids.

The moisture content of the organic fraction however was reported to be 6.5% ten times lower than the aqueous phase at 62%. The poor flow characteristics of the organic fraction was confirmed by the carbon residue and viscosity tests which were 1.93% and 222Cst and therefore would cause problems and result in blocking engine components such as injectors if used as a fuel in an engine for CHP.

Compositional analysis of the organic fraction was found to contain a complex mixture organic and aromatic compounds ranging from C₅-C₁₉. Alkenes in the form of benzene, toluene and xylenes were largely present and some phenolics. Alkyl Nitrile compounds were also detected which are highly toxic and therefore direct contact with skin was avoided.

Much of the energy potential however was found to be stored within the char fraction (30 wt.%) having a high carbon content and high heating value (28 MJ/kg) which can be very valuable. The char produced was very dry 3% moisture, brittle and would be useful for combustion in boilers and furnaces to provide heat for the drying of BSG or heat for the pyrolysis process. As the char has been devolatilised it may give less smoke emissions when combusted. As discussed earlier prolonged

residence time within the pyroformer promotes secondary cracking reactions and leads to coke formation, leading to a high fraction of carbon in the char product. This study was impacted due to insufficient quantity of feedstock which resulted in the inability to repeat experiments and to investigate the impact varying the solids residence time within the screws has on char yield and composition.

The pyroformer as a standalone operating unit processing BSG would be best suited to producing chars as much of the energy in the original feedstock remains in the char product. By enhancing the cracking effect of the char by varying the solids residence time within the reactor (varying inner and outer screw speeds) of the char/biomass mixing ratio, may improve this however further investigations are required.

The pyrolysis permanent gases produced have a satisfactory content of combustible fractions and energy contents and could be potential as gaseous fuel. Unlike in the case of other pyrolysis technologies such as slow pyrolysis or torrefaction, the Pyroformer was able to generate permanent gases namely H_2 , CO , CH_4 , CO_2 and N_2 . A high concentration of CH_4 9.43% and a small concentration of H_2 1.6% were detected resulting in a heating value of $6.7MJ/m^3$. The heating value was largely due to the presence of methane content making the product gas comparable to the heating value of gasification product gas from the gasification test conducted in this study earlier ($4.96 MJ/m^3$). As reported in literature earlier if air is used as the gasification medium, the combustible components in the fuel gas are diluted with nitrogen which significantly lowers the gas HHV ($4-7 MJ/Nm^3$). Oxygen blown or steam gasification produces a synthesis gas with a medium heating value ($10-18 MJ/Nm^3$)[50].

Although having a similar content of gas, the formation of the pyrolysis gas is significantly different to that of gasification product gas. The permanent gases produced under pyrolysis conditions occurs when the feedstock is decomposed in the absence of air or oxygen, therefore there is no reducing zone or oxidation taking place. The permanent gases are formed by the decomposition of cellulose, hemicellulose and secondary cracking reactions and related reforming reactions.

Generally H_2 is not expected in pyrolysis gas since there is no reduction process for hydrogen formation to occur. In the pyroformer hot char is recycled all the time, therefore contact with water vapour can lead to reaction to form CO and H_2 in a heated environment. The energy balance for the pyroformer can be found in APPENDIX D.

A catalytic steam reforming reactor was considered to be placed downstream of the Pyroformer reactor. Coupling a catalytic reactor downstream of the Pyroformer, gives the opportunity to produce a high quality hydrogen rich product gas as well as increase the permanent gas heating value. The

aqueous phase or water/steam present in the hot organic pyrolysis vapours would serve the steam reforming reactions within the catalytic reactor.

The intermediate pyrolysis step within a pyro-reforming setup would act more as a pre-conditioner step for BSG prior to downstream catalytic steam reforming. The bio-oils produced in this study were poor and found to have heavy viscous fractions of organics. This can cause potential storage and handling problems over time as well as operational problems if used directly in a catalytic reforming reactor or combusted in an engine.

Steam reforming of condensed bio-oil and its fractions into a catalytic steam reforming reactor would be problematic and a very difficult task. It cannot be totally vaporised as significant amount of residual solids can often block the feeding line and the reactor [118]. Bio-oil's tested in engines were found to achieve thermal efficiencies similar to when operating on diesel however ignition delay is longer when bio-oil is used due to poor atomisation and vaporisation of the bio-oil in the cylinder[190]. By upgrading the pyrolysis vapours in situ would alleviate the problem of reheating and vaporising the condensed bio-oil.

Due to unforeseen circumstances a catalytic steam reforming reactor was unavailable to be coupled directly to the Pyroformer. The Pyroformer would require extensive modification and the installation of additional equipment in parallel to existing equipment such as; product gas bypass, high temperature shut off valve, steam generator, catalytic steam reforming reactor, reactor heaters, heated line's, differential pressure indicators, water cooled condenser, and an electrostatic precipitator, and online gas measurement equipment. The setup would compare the pyrolysis with and without catalytic steam reforming by means of gas analysis, for determination of gas composition for instance hydrogen as well as heating value on a continuous basis.

Additional gas lines are required to the catalytic reactor to enable the pre-reduction of the metal oxide catalysts. Once the catalysts are placed inside the catalytic reactor, it is indirectly heated at temperature to approximately 600°C before a mixture of pre-reduction gas (15-40%) hydrogen/nitrogen is introduced for a couple of hours to activate the catalysts before experimentation. The oxygen is removed from the catalyst and collected as water. Nitrogen would also be required as a purge to ensure the catalysts remain in an oxygen free zone in the event of shutdown and reactor cooled down.

In order to prevent coking of the catalysts during Pyroformer start up a heated bypass stream is required with a shut off valve to divert the generated hot pyrolysis vapours initially to protect the catalysts until Pyroformer steady state has been achieved (approximately 30-45 minutes). Steady state is achieved when hot pyrolysis vapours are quenched and bio-oil is collected downstream. The shut

off valve is then opened allowing the flow of the hot pyrolysis vapours to the catalytic reactor. The timing for the introduction of steam to the catalysts should only occur during the introduction of pyrolysis vapours, otherwise the catalyst active sites may be consumed by oxygen partially deactivating the catalysts ultimately reducing their performance.

Due to this as well as time constraints of the project, a bench scale fixed bed pyrolysis reactor was constructed to simulate the Pyroformer and to carry out steam reforming experiments by adding a catalytic reactor downstream of the pyrolysis system. The Pyroformer operates continuously with char re-circulation, this was difficult to simulate in a fixed bed reactor, however the fixed bed reactor would contain a fixed portion of char which would have contact with the generated pyrolysis vapours however both the operating temperature and the heating rate were found to be more the critical parameters.

The results from initial bench scale pyrolysis studies at different heating rates showed similar yields to the Pyroformer at a heating rate of 50°C/min. The pyrolysis tests at different heating rates to see the effect on product yield and composition changes was in agreement with what was reported in literature. Tests at a high heating rate resulted in an increase in liquid yield and reduced gas yield.

The bio-oils produced when observed had phase separated and also contained very similar chemical groups and characteristics as bio-oil produced from the Pyroformer. The bio-oils produced at two different heating rates show similarities to oils produced using the Pyroformer with the large portion of chemicals detected as aromatic hydrocarbons 23-25%, phenols 13-15%, alkanes 5-15% and alkenes 6-8%. No polyaromatic hydrocarbons were produced in either of these bio-oils.

The chars were found to be brittle and dry with high carbon content and a high heating value also similar to the chars produced within the Pyroformer. The main difference observed was in the permanent gases where no hydrogen was detected in the batch fixed bed pyrolysis experiments at the low or high heating rate (25°C/min and 50°C/min); unlike the Pyroformer whereby a small quantity of hydrogen 1.6vol% was detected as was the amount of carbon monoxide. This therefore also resulted in the permanent gases having a low heating value of 1.12 and 1.16 MJ/m³ much lower than the heating value produced from the Pyroformer of 6.7 MJ/m³.

As mentioned earlier this was perhaps due to the effect hot char being continuously recycled all the time within the Pyroformer making contact with water vapour in a hot environment forming CO and H₂. Therefore the effect of recycle char was unable to be simulated in all the fixed bed reactor experiments.

By adding a catalytic reactor downstream of the batch fixed bed pyrolysis reactor made catalysts screening tests easier, in order to understand the effect of potential catalysts operating at varying operating conditions downstream of intermediate pyrolysis conditions. This offered the opportunity to carry out tests at varying catalytic reforming temperatures and provided the ability to add additional steam to the process mixing steam with pyrolysis vapours prior to entering into the catalytic reactor. The limitation of this setup was the inability to carry out continuous experiments over long durations (several of hours) to understand the long term performance of the catalysts as each experiment lasted approximately 40-50mins.

Initial studies carried out using the catalytic reactor coupled to pyrolysis reactor were as a benchmark, initially at catalysts reforming temperatures of 500°C and then at 850°C but with quartz wool in place of catalysts inside the catalytic reactor. The gas produced with a secondary catalytic reactor without any catalysts at 500°C and 850°C had a high heating value of 1.31 and 1.7 MJ/m³ respectively.

The quartz wool was found to serve two functions; firstly it will support the catalysts as a packed bed therefore preventing the catalysts from falling and secondly functions as a hot vapour filtration by capturing any char fines that can otherwise cover catalysts surface leading to catalyst deactivation. The use of quartz wool can also reduce the solids content of the bio-oil. This implies that the quartz wool would be useful for hot vapour filtration acting as a guard bed to the catalyst and reduce the amount of solids present in the bio-oils.

It appears that the presence of the secondary reactor with quartz wool at 850°C led to a reduction of liquid yields, with an increase in char and gas yields. This was due to thermal secondary reaction of pyrolysis vapours when exposed to high secondary heat.

The bio-oil produced at a catalytic temperature of 850°C shows an increase of aromatic hydrocarbons of 39%, alkyl nitriles 9.8% and an increase of polyaromatic hydrocarbons of 5.4%. This is due to the thermal cracking of alkanes, esters, furans, guaicol, isomers, ketones and phenols which were not present in the bio-oil.

Three different metal oxide catalysts Nickel, Platinum and Rhodium all supported on an alumina support were produced and supplied by Johnson Matthey Plc and were tested within this study. All catalysts were pre-reduced at Johnson Matthey and then passivated. It was unknown what proportion of metal loading was applied to the catalyst support and as a result it was unclear to understand the effect metal loading has at different steam reforming temperatures.

Initial catalytic experiments were conducted using Nickel at three different reforming temperatures of 500°C, 750°C and finally at 850°C without the addition steam, but by making use of the water

generated within the hot pyrolysis vapours as the reforming agent. The tests were then repeated by adding additional steam using fresh catalysts. Tests were conducted to see which catalysts increased the heating value of the permanent gases as well as improving the composition of the gases in terms of hydrogen production.

The results indicated that the commercial nickel catalysts performed the best out of the three catalysts producing a H₂ rich product gas at low and high reforming temperatures (500 and 850°C) with and without the present of steam producing a heating value between 11-25 MJ/m³.

Both precious group metal (PGM) catalysts Pt/Al₂O₃ and Rh/Al₂O₃ did not perform as well as the Ni/Al₂O₃ catalysts. Again best results were with steam added at high reforming temperatures 850°C for Platinum 3.54MJ/m³ and for Rhodium 4.05MJ/m³ which is similar to heating value performance of a fixed bed downdraft gasifier processing the same BSG feedstock.

At low catalytic reforming temperatures of 500°C and with the presence of steam both Pt/Al₂O₃ and Rh/Al₂O₃ catalysts were partially active and ineffective in producing hydrogen and reducing condensable liquids yield in comparison to Ni/Al₂O₃ catalysts. This is likely to be that at lower reforming temperature both PGM catalysts are prone to coke formation at the catalysts surface resulting in less active site for catalysts to take effect.

All experimental results using catalysts resulted in a significant influence on the gas compositions. For maximum hydrogen production, temperatures higher than 500°C are suggested with addition of steam. From an energetic point of view a catalytic steam reforming unit operating at 500°C with a commercial steam reforming catalyst after a pyrolysis step is better suited producing a combustible gas for a CHP in comparison to gasification which requires an operating temperature between 800°C-1000°C.

Nickel catalysts have frequently been investigated for gasification of biomass and bio-oil because of their comparatively low price and high activity. Both platinum and rhodium performed better only at high reforming temperatures producing a gas which is similar in heating value to that from a fixed bed downdraft gasifier processing the same BSG feedstock.

All the catalysts tested were capable of reforming pyrolysis vapours; however a limitation of catalytic reforming tests in this work using a batch bench scale pyrolysis unit was the ability to assess the performance of catalysts in terms of longevity as they are prone to deactivation over time. Catalysts are prone to either coking due to carbon precipitation restricting the active sites or poisoning due to H₂S being present within the gas stream leading to deactivation.

Initial catalytic tests revealed that the Nickel catalysts performed better than the three catalysts in terms of improving the heating value of the gases and composition in terms of hydrogen. However over time they are more prone to deactivation due to H₂S poisoning reducing the life span of the catalysts than the PGM catalysts. This may be the case for Nickel catalysts tested over longer periods to that of Rhodium catalysts, for instance as reported in literature earlier Rhodium catalysts in particular are recognised for its sulphur tolerance as well as resistance to carbon precipitation.

It would be of greater interest for this work to test these catalysts continuously and over several hours. Other than comparing the product gas over 40-50 min it would be interesting to compare the effects a gas containing sulphur, chlorine and carbon has on the catalysts, the product gas composition and heating value over several hours. This would give a better representation of which catalysts performs better over longer periods as well as revealing how often catalysts will require to be replaced.

Among the most important parameters found with steam reforming are catalyst bed temperature, steam/carbon ratio (S/C), gas hourly space velocity and residence time. Temperature was found to have the most profound effect on steam reforming reactions within this work with results at high temperature of 850°C showing most promise. Increasing the pyrolysis temperature from 450°C to a catalyst temperature of 850°C would require approximately 4-5% of the total gas chemical energy content, and this energy can be partly recuperated downstream. However, further testing would be required to show the effects of varying the residence time and increasing the S/C on hydrogen production.

Therefore, BSG was successfully demonstrated as a potential energy feedstock for thermochemical conversion and has the potential to produce a useable product gas with a high heating value enabling application in engines for power generation. However, much further work needs to be conducted with BSG in terms of pre-treatment and thermochemical conversion processing in order to determine the optimal process route.

10.2 Conclusion

This work has investigated the fixed bed downdraft gasification, the intermediate pyrolysis followed by the intermediate pyrolysis/reforming of Brewers Spent Grain (BSG), and the effects of tar cracking using different catalysts to attain a tar free product-fuel gas that can be suitable to run an engine, gas turbine or a combined heat and power plant. Overall the main objectives of this project have been satisfied by the following points:

- Results from pre-treatment and characterisation show that BSG can be successfully dried to a moisture content of 8% suitable for both pyrolysis and gasification.
- BSG pellets were successfully prepared by oven drying, followed by grinding and then pelletising using the roller shaft pellet mill described earlier.
- Proximate, ultimate, chemical composition, inorganic element, ash fusion and heating value analysis were conducted. BSG has a high volatile content (78% dry basis) and contains 46.6% carbon, 6.85% hydrogen, 42.26% oxygen, 3.54% nitrogen, 0.74% sulphur and 0.1% chlorine. Chemical compositional analysis has revealed that BSG is composed of 18.98% cellulose, 33.59% hemicelluloses, 12.61% lignin and 34.82% of extractives. The analysis of inorganic elements for BSG shows mainly magnesium (Mg), alumina (Al), silica (Si), phosphorous (P), potassium (K), and calcium (Ca). BSG has an ash initial deformation temperature of 1090°C, an ash softening temperature 1140°C, an ash hemispherical temperature 1180°C and an ash flow temperature of 1230°C. The heating value of BSG is approximately 18 MJ/kg on a dry basis.
- Characterisation of barley straw and wheat straw were carried as potential substitute feedstock for thermochemical processing as they were both found to be comparable to BSG. Barley straw was found to be more representative as it is also the raw material used in the brewing process.
- The fixed bed downdraft gasification of BSG pellets was successfully demonstrated in a 2 hour test at a feed rate of 4.2 kg/hr. For every kilogram of biomass fed, 2.0kg of product gas was formed.
- The product gas composition had a heating value of 4.96 MJ/m³ similar to that from other biomass feedstocks and has a composition of 11.6% H₂, 20.1% CO, 2.0% CH₄, 13.2% CO₂ and 53.2% N₂ (dry basis).

- The low concentration of H₂ content detected is low enough not to present knocking problems within an engine.[191]
- The tar content in the product syngas was 1.87 g/Nm³ which in comparison to other types of gasification processes is fairly low, but still much too high for an engine and will seriously limit the life of the engine components. The tar content would need to be reduced to acceptable levels (approximately 100g/Nm³) for use in an engine, however tar clean up can be difficult and expensive.
- Intermediate pyrolysis products bio-oil 52%, char 29% and permanent gas 21% of BSG have been produced using the Pyroformer reactor.
- The condensed bio-oil produced was found to have an organic and an aqueous phase. The two phases were separated easily using a gravimetric settler.
- The organic phase was very dark in appearance and viscous with a strong smell of carbonised organic material. The aqueous phase was red in appearance and contained some evidence of solid particles.
- The calorific value of the bio-oil (organic phase) was 20 MJ/kg, which is about half the energy content of fossil diesel. The low energy content is associated with the high oxygen content of the oil.
- Due to the high moisture, solids content and poor physical properties of the bio-oil, it is unsuitable as a fuel source in an engine without upgrading. Upon visual inspection is liquid but not homogeneous as it contained many bituminous solids and viscous compounds which overtime could polymerize with age if stored at room temperature.
- The carbon residue and ash for the bio-oil was 1.93% and 0.44% respectively which in contrast to diesel and biodiesel are relatively high and could indicate potential blockage problems in engine applications such as clogging injectors and coke formation in the combustion chamber.
- Viscosity was very high at 222 cSt; this may be due to the amount of solids present in the bio-oil and would make atomisation difficult.

- The major components detected in the bio-oils were aromatic hydrocarbons at 23% in the form of benzene, toluene and xylenes. The other major group found was phenols 15.3%, alkenes 8%, alkanes 5.5%, and Guaiacol 6.1%.
- The biochar was found to be very dry with a moisture content of 3% and containing a high ash content of 18%. The heating value for the char was found to be 26-28 MJ/kg which has higher energy content than the original feedstock.
- The biochar has high carbon content (approximately 15% higher than in the original feedstock) with oxygen determined by difference. A high level of hydrogen 4% nitrogen 5.2% and sulphur 1.9% was detected.
- The O/C ratio of the char was 0.43 and at 450°C is richer in oxygen content and may have retained the oxygen from the bio-oils, and would be expected to have mean residence time (stability) of 100-1000 years in soils.
- Hydrogen of about 1-2vol% was produced; this may be due to cracking reforming reactions taking place between hot char and pyrolysis vapours. Other species that were formed included methane and carbon monoxide.
- The heating value of the gas was 6.7MJ/m³, largely due to the high methane content. The gas can be combusted along with some char to meet heat demands of the Pyroformer or a feedstock dryer. Carbon dioxide was relatively high at 64vol% and is likely to be due to decarboxylation reactions taking place.
- Non-catalytic bench scale intermediate pyrolysis of BSG at 50°C/min heating rate yielded similar product distribution as the pyroformer.
- Non-catalytic bench scale intermediate pyrolysis of BSG showed an increase in liquid yield and a reduction in gas yield with increasing heating rates, although, char yield remained unchanged and no differences were noted in the char product composition.
- Two pyrolysis experiments were conducted as an essential reference point without catalysts prior to catalytic experiments. Quartz wool was placed inside the secondary reactor and was tested initially at 500°C and then at 850°C during the pyrolysis runs. The quartz wool was effective in capturing some char fines which otherwise may cover the catalysts surfaces

leading to catalysts deactivation. The wool contained condensed pyrolysis vapours at 500°C quartz wool contained far more char fines and condensed pyrolysis vapours than that wool which was at 850°C. This implies that the quartz wool would be useful for hot vapour filtration reducing the amount of solids present in the bio-oils.

- The presence of the secondary reactor with quartz wool at 850°C led to a reduction of liquid yields, with an increase in char and gas yields. This was due to thermal secondary reaction of pyrolysis vapours when exposed to high secondary heat.
- The major peaks detected and identified with the highest abundance was benzene 29.74%, pyridine (79, 79, RI0) 22.23%, toluene 7.36%, 2-propenenitrile 6.82%, cyclooctatetraene (104, 104, RI 0) 5.09%, naphthalene 4.43%, and butanedinitrile 3.01% these were the largest components present. The effects of a secondary reactor with no catalysts at 850°C had further cracked the organic components breaking down much of the phenols, furans, acids and esters. Toluene had reduced and the presence of benzene increased significantly as well as some polycyclic aromatic hydrocarbons.
- The amount of catalysts to be used for each experiment was calculated based on achieving a space velocity of approximately 8-10,000 h⁻¹.
- The effect of increasing the catalytic reforming temperature using a Nickel (Ni/Al₂O₃) catalyst without the addition of steam increased the yield of permanent gases 47wt.%, whilst reducing the yields of the liquids (bio-oils).
- The effect of PGM catalysts Platinum and Rhodium at the lower catalytic reforming temperature (500°C) shows very little change in the product distribution in comparison to the non-catalytic experiments without the addition of steam.
- At higher catalytic reforming temperatures of 850°C without the addition of steam the permanent gases increased, reducing the yield of condensable liquids. In comparison to non-catalytic experiments the reduction in yield for liquids is 19% and 12% for Pt/Al₂O₃ and Rh/Al₂O₃ catalyst which is less than the 26% reduction reported earlier using the Ni/Al₂O₃ catalyst at the same temperature.
- All the bio-oils produced from catalytic reforming experiments had phase separated into an aqueous and an organic phase except oils produced at the higher reforming temperatures with

the addition of steam. The organic fraction 'bio-oil' contains the heavy condensable phase that are mainly organic components, and the aqueous fraction is the light condensable phase mainly comprising of water.

- All the liquids collected in the condenser system at the lower reforming temperatures (500°C) contained a mixture of water (including unreacted condensed steam) and dark brown colored oil for bio-oils. At the higher catalytic reforming temperatures the liquid content in the condenser system was a mixture of mostly water and pale yellow colored oil. The organic content was reduced in quantity, indicating an effect of the catalysts on cracking of the pyrolysis products to form gases.
- Liquid yields decreased significantly as reforming temperature increased using Nickel (Ni/Al₂O₃) catalyst in comparison to non-catalytic experiments the reduction in yield for liquids was 7%, 22% and 26% at 500, 750 and 850°C respectively, and decreased further with the addition of steam using Nickel (Ni/Al₂O₃) catalyst (24.20%, 8.08% and 11.94% at 500, 750 and 850°C respectively).
- With the addition of steam and at the lower catalytic reforming temperature of 500°C the condensable liquids yield had increased 73% and 80% for both Pt/Al₂O₃ and Rh/Al₂O₃ which is a significant increase in comparison to non-catalytic experiments. Steam addition had very little effect and was found to have condensed adding to the liquid yields.
- The addition of steam at the lower reforming temperature using PGM catalysts had very little effect in reforming pyrolysis vapours in comparison to what was reported with Nickel catalysts under similar process conditions.
- At the higher catalytic reforming temperature 850°C the liquid yield decreased 12% and permanent gases increased 62% for Pt/Al₂O₃, however for Rh/Al₂O₃ at the same conditions both liquids and permanent gas yields increased 15% and 55%. This suggests that Rh/Al₂O₃ was less effective in reducing the condensable liquids yield than Pt/Al₂O₃ and Ni/Al₂O₃.
- At the three different reforming temperatures (without steam) using the Nickel catalysts much of the oxygenated components in the bio-oils were not identified in the GC/MS peaks indicating these components were reformed completely.

- At reforming temperatures 500°C and 750°C the organic composition contain some polycyclic aromatic hydrocarbons (PAH). The PAH's cause concern due to their carcinogenic and mutagenic characteristics and have been classified by the Environmental Protection Agency (EPA) as priority pollutants. PAH collected in liquids can be problematic when handling and any contact with human skin and inhalation of the fumes should be avoided.
- At the lower reforming temperature of 500°C the PAH compounds identified were anthracene, fluorene, naphthalene and pyrene, while at HT reforming 750°C the quantity of PAH had decreased with some naphthalene identified.
- However at HT reforming 850°C PAH compounds in the bio-oil were not identified but showed some presence of benzene, toluene, pyrrol and a large fraction of pyridine.
- Using a Ni/Al₂O₃ catalysts bed and steam reforming at high temperature 850°C close coupled to a pyrolysis unit, (PAH) 3 and 4 ring compounds such as phenanthrene, pyrene and other PAH compounds are reformed into single and two ring aromatic compounds of lower molecular weights such as benzene, toluene and styrene.
- Both PGM catalysts Platinum and Rhodium at high reforming temperatures of 850°C with and without the addition of steam was found to have increased the aromatic hydrocarbon and polycyclic aromatic hydrocarbons within the liquids yields.
- The C content in the oils for all experiments with Ni/Al₂O₃, Pt/Al₂O₃ and Rh/Al₂O₃ catalysts with and without steam decreased as the reforming temperature increased, indicating catalytic activity and decarboxylation reactions occurring.
- The higher heating value values (HHVs) obtained for all oils produced using Ni/Al₂O₃, Pt/Al₂O₃ and Rh/Al₂O₃ with and without steam ranged between 18 - 36MJ/kg and were clearly related to the O content - the lower the O content, the higher the HHV.
- All the oil samples contained S and Cl between 0.1-1.7% and 0.1-0.18% respectively. The presence of S and Cl could lead to catalyst poisoning and therefore lifetime limitation of the catalysts although this could not be assessed. Further test would be required over longer periods to assess this.

- The effect of catalyst, steam and increasing reforming temperature shows a reduction in the molecular weight of the bio-oil. Non catalytic tests at differing heating rate indicates a MW of 145, at low temperature reforming (500°C) with steam using a Ni/Al₂O₃ catalyst the molecular weight decreased 128 and at high reforming temperature (850°C) the molecular weight decreased to 86.
- The comparison of permanent gas yield composition produced at the three different reforming temperatures using Ni/Al₂O₃ catalysts without steam as much as 43 vol% of hydrogen was produced at 850°C, 24 vol% at 750°C and 10% at 500°C, much higher values than without catalytic reforming. A CO₂ concentration was 35-53 vol%, CO concentrations 15-17 vol% and CH₄ 9-14vol%.
- Catalytic reforming of the pyrolysis vapours using Nickel (Ni/Al₂O₃) catalyst with the addition of steam produced a significant increase in permanent gases mainly (H₂ and CO) with H₂ content exceeding 50 vol % at higher reforming temperatures.
- At lower reforming temperature of 500°C 3vol% and 2vol% of hydrogen was produced for Pt/Al₂O₃ and Rh/Al₂O slightly higher values than without catalytic reforming but considerably less than what was reported using Ni/Al₂O₃. A CO₂ concentration was 73-79vol%, CO concentrations 6-9vol% and CH₄ 2-3vol%.
- The permanent gas yield composition produced at low catalytic reforming temperatures 500°C without steam for PGM catalysts show that 3vol% and 2vol% of hydrogen was produced for Pt/Al₂O₃ and Rh/Al₂O slightly higher values than without catalytic reforming but considerably less than what was reported using Ni/Al₂O₃. A CO₂ concentration was 73-79vol%, CO concentrations 6-9vol% and CH₄ 2-3vol%.
- At the higher catalytic reforming temperature of 850°C and with the presence of additional steam 18vol% and 12vol% of hydrogen was produced for Pt/Al₂O₃ and Rh/Al₂O respectively. A CO₂ concentration was 75-69vol%, CO concentrations 7-9vol% and CH₄ 4-5vol% for Pt/Al₂O₃ and Rh/Al₂O.
- This confirms that at low catalytic reforming temperatures of 500°C even with the presence of steam both Pt/Al₂O₃ and Rh/Al₂O₃ catalysts are partially active and ineffective in producing hydrogen and reducing condensable liquids yield in comparison to Ni/Al₂O₃ catalysts. This is

likely to be that at lower reforming temperature both PGM catalysts are prone to coke formation at the catalysts surface resulting in less active site for catalysts to take effect.

- Both PGM catalysts Pt/Al₂O₃ and Rh/Al₂O₃ did not perform as well as the Ni/Al₂O₃ catalysts in terms of reducing liquid yields, increasing permanent gases and the heating value.
- Pyrolysis without catalytic reforming produced a gas with a typical heating value of 1 MJ/m³. Best results obtained were with Ni/Al₂O₃ catalysts and with steam added: at 500°C the heating value was 10.80 MJ/m³, at 750°C heating value was 15.66 MJ/m³ and at 850°C heating value was 25.21 MJ/m³. For reforming without steam using Ni/Al₂O₃ catalysts at 500°C, the heating value was about 2MJ/m³, and at 750°C and 850°C the heating value was about 5 MJ/m³.
- Without steam added at lower reforming temperatures the heating values was low for Pt/Al₂O₃ at 0.38MJ/m³ and Rh/Al₂O₃ at 0.53MJ/m³ with the addition of steam at the same temperature the values were 1.24MJ/m³ and 1.26MJ/m³ respectively. This suggests that the PGM catalysts were not as active as the commercial Ni/Al₂O₃ reforming catalysts, and may be the active sites had become blocked at these temperatures when running the experiments.
- Best results were with steam added at high reforming temperatures 850°C for Platinum 3.54MJ/m³ and for Rhodium 4.05 MJ/m³ which is similar to heating value performance of a fixed bed downdraft gasifier.
- All experimental results using catalysts resulted in a significant influence on the gas compositions. For maximum hydrogen production, temperatures higher than 500°C are suggested with addition of steam.

10.3 Recommendation

The following work is recommended to take this project further:

- Obtaining and conducting the pre-treatment of BSG feedstock for this study was extremely difficult and labour intensive. High moisture and microbial degradation made the feedstock extremely difficult to transport and store. As a result this limited the amount of BSG available to conduct further pilot scale experiments. Drying a large bulk of BSG in a rotary drum dryer would be recommended focusing on removing the large quantity of moisture and the breakdown of the material within the rotary drum into fines.
- BSG pellets were likely to breakdown within feeding system and therefore a stronger pellet would be recommended to improve its mechanical strength by either blending BSG with either wood, adding a binding agent during palletisation or to produce cubes. This would focus on extending trials to improve the feeding characteristics of BSG or to optimise a feed system.
- Downdraft gasification tests should be repeated with an increased duration of experiment. However stronger BSG pellets are required that could perhaps be bounded together with starch as a binding agent, so that the pellets hold their form during the feeding process and do not crumble. BSG cubes could also be investigated as Cubes would allow better feeding into the gasifier and would encourage bridging of the fuel which is required within a downdraft gasifier.
- Gasification of BSG should be attempted using fluidised bed systems, both bubbling or circulating configurations and further coupling of these reactors to steam reforming reactors to crack tars and reform methane into CO and H₂ producing a gas that could be combusted in an engine for heat and power.
- Further Intermediate pyrolysis experiments should be carried out using the Pyroformer under a range of operating conditions focusing on both the yields of the pyrolysis products, and the quality of the bio-oil portion of the liquid product. The area of interest would be to vary the speeds of both the inner twin coaxial screws to see the effects of char recycle in the reactor. Bio-oils should be investigated further looking to further improve its characteristics as a fuel for engines focusing on reducing its viscosity by filtering out the solids and blending it with either bio-diesel or adding surfactants

- A catalytic steam reforming reactor should be incorporated downstream of the Pyroformer to conduct continuous catalytic pyrolysis experiments with on-line gas measurement. Further experiments at longer residence time's maybe (10's of hours) timescale should be performed to test for catalysts durability and longevity as well as to replicate studies with the use of Nickel, Rhodium and Platinum catalysts.
- The lifetime and longevity of the catalysts and the causes for deactivation should be investigated, considering effects such as tar cracking, coking (carbon precipitation), poisoning by sulphur and chlorine and the impact on the gas composition and heating value.
- To expand research on investigating pyro-steam reforming and coupling the reactor to a CHP engine to understand the use of product gas as a fuel, the engine performance as well as the emissions. The research should also aim to recirculate the waste heat from the exhaust gases for reuse in the process as drying medium or as a heating medium for the reactors. Char should be investigated as a potential fuel to be combusted to raise heat for the drying process or to raise process steam.
- To expand research on investigating different gasification regimes coupled with gas clean up technologies such as scrubbers, bag filters, or catalytic reforming reactors to reduce tar formation. The work should then follow testing the gas in a CHP engine to understand the performance of the gas, the engine performance and engine emissions. The research should also aim to recirculate the waste heat from the exhaust gases for reuse in the process as drying medium or as a heating medium for the reactors.
- An economic and environmental evaluation for each of the processes should be carried out to determine the feasibility of implementing either pyrolysis or gasification technologies. This would be to estimate the total plant capital costs, operating costs and payback time of either of the technologies.

References

1. Johnson Matthey Technology Centre, B.C.R., Sonning Common, Reading, West Berkshire RG4 9NH.
2. McKendry, P., *Energy production from biomass (part 1): overview of biomass*. Bioresource Technology, 2002. **83**(1): p. 37-46.
3. Mussatto, S.I., G. Dragone, and I.C. Roberto, *Brewers' spent grain: generation, characteristics and potential applications*. Journal of Cereal Science, 2006. **43**(1): p. 1-14.
4. Ben-Hamed, U., Seddighi, H., and Thomas, K, *Economic Returns of Using Brewery's Spent Grain in animal feed*. World Academy of Science, Engineering and Technology 50 2011, 2011: p. 695-698.
5. Sire, T.S., *Spent brewery grains as substrate for the production of cellulases by Trichoderma reesei QM9414*. Industrial microbiology, 1990. **5**(1): p. 153-158.
6. Tavasoli, A., Ahangari, M. G., Soni, C., & Dalai, A. K, *Production of hydrogen and syngas via gasification of the corn and wheat dry distillers grains (DDGS) in a fixed bed micro reactor*. Fuel Processing Technology, 2009: p. 472-482.
7. Jay, A.J., et al., *A systematic micro-dissection of brewers' spent grain*. Journal of Cereal Science, 2008. **47**(2): p. 357-364.
8. Franciso prieto Garcia, J.P.M., Maria A. Mendez Marzo, Luis A. Bello Perez, Alma D.Roman Gutierrez, *Modification and Chemical Characterisation of Barley Starch*. International Journal of Applied Science and Technology, 2012. **2**.
9. Nuno G.T. Meneses, S.M., José A. Teixeira, Solange I. Mussatto, *Influence of extraction solvents on the recovery of antioxidant phenolic compounds from brewer's spent grains*. Separation and Purification Technology, 2013. **108**: p. 152-158.
10. B. Bartolome, M.S., J.J. Jimenez, M. J. del Nozal & C. Gomez-Cordoves, *Pentoses and Hydroxycinnamic Acids in Brewers Spent Grain*. Journal of Cereal Science, 2002. **36**: p. 51-58.
11. Santos, M., et al., *Variability of brewer's spent grain within a brewery*. Food Chemistry, 2003. **80**(1): p. 17-21.
12. C. Di Blasi, C.B., and A. Galgano, *Biomass Screening for the Production of Furfural via Thermal Decomposition*. Ind. Eng. Chem Res, 2010: p. 2658-2671.
13. Stroem, L.K., D.K. Desai, and A.F.A. Hoadley, *Superheated steam drying of Brewer's spent grain in a rotary drum*. Advanced Powder Technology, 2009. **20**(3): p. 240-244.
14. Øyvind Vessia, P.F., Øyvind Skreiberg, *Biofuels from lignocellulosic materials: In the Norwegian context 2010* 2005, Norwegian University of Science and Technology. p. 101.
15. <http://www.biomassenergycentre.org.uk>. *Biomass Energy Potential*. 24/07/2010.
16. Overend, D.O.H.a.R.P., *Biomass, Renewable Energy*. 1987: British Library Cataloguing in Publication Data.
17. [http://www.steve.gb.com/images/molecules/sugars/cellulose_\(hydrogen_bonding\).png](http://www.steve.gb.com/images/molecules/sugars/cellulose_(hydrogen_bonding).png). *Image structure of Cellulose*. 24/07/2010 [cited 2010 24/07/2010].
18. <http://www.electregy.com>. *Image, structure of Hemicellulose*. 2010 [cited 2010 24/07/2010].
19. <http://www.scq.ubc.ca/wp-content/uploads/2007/01/lignin.gif>. *Image structure of Lignin*. [cited 2010 24/07/2010].
20. Dinesh Mohan , C.U.P., Jr.,† and Philip H. Steele §, *Pyrolysis of Wood/Biomass for Bio-oil: A Critical Review*. Energy and Fuels, 2006. **20**(9): p. 848-889.
21. K. Raveendrana, A.G., Kartic C. Khilarb, *Influence of mineral matter on biomass pyrolysis characteristics*. Fuel, 1995. **74**(12): p. 1812-1822.
22. Bridgwater, A.V., *Review Paper; Biomass Fast Pyrolysis*. Bioresource technology, 2004. **85**(2): p. 21-49.
23. <http://www.bgg.mek.dtu.dk/upload/subsites/mek-bgg/about/pyrolysis.jpg>. *Image for Pyrolysis of wood*. 2010 [cited 2010 15/08/2010].
24. A. Zabaniotou, O.I., E. Antonakou, A. Lappas, *Experimental study of pyrolysis for potential energy, hydrogen and carbon material production from lignocellulosic biomass*. International Journal of Hydrogen Energy 33, 2008: p. 2433-2444.

25. A. Hornung, A.A.a.S.S., *Intermediate Pyrolysis: A sustainable biomass-to-energy-concept-Biothermal Valorisation of Biomass (BtVB) process*. Journal of Scientific and Industrial Research Vol.70, 2011: p. 664-667.
26. Bridgwater, A.V., *The production of biofuels and renewable chemicals by fast pyrolysis of biomass*. International Journal of Global Energy Issues, 2007(27 (2)).
27. Kockar, C.A.a.O.M., *Characterization of slow pyrolysis oil obtained from linseed (Linum usitatissimum L.)*. Journal of Analytical and Applied Pyrolysis, 2008. **85**(1-2): p. 151-154.
28. Marion Carrier, T.H., Johann Gorgens, Hansie Knoetze, *Comparison of slow and vacuum pyrolysis of sugar cane bagasse*. Journal of Analytical and Applied Pyrolysis, 2011. **90**(1): p. 18-26.
29. Anh N. Phan, C.R.a.c.i., E-mail the corresponding author, Vida N. Sharifi, Jim Swithenbank, *Characterisation of slow pyrolysis products from segregated wastes for energy production*. Journal of Analytical and Applied Pyrolysis, 2008. **81**(1): p. 65-71.
30. Bridgwater, A.V., *Principles and practice of biomass fast pyrolysis processes for liquids*. Journal of Analytical and Applied Pyrolysis, 1999. **51**(1-2): p. 3-22.
31. Bridgwater, A.V., *Upgrading biomass fast pyrolysis liquids*. Environmental Progress & Sustainable Energy, 2012. **32**(2): p. 261-268.
32. Meier, D., et al., *State-of-the-art of fast pyrolysis in IEA bioenergy member countries*. Renewable and Sustainable Energy Reviews, 2013. **20**(0): p. 619-641.
33. M. Mann, E.C., S. Czernik and D. Wang *Biomass to Hydrogen via pyrolysis and reforming*.
34. Ursel Hornung, D.S., Andreas Hornung, Vander Tumiatti, Helmet Seifurt, *Sequential pyrolysis and catalytic low temperature reforming of wheat straw*. Journal of Analytical and Applied Pyrolysis, 2009(85): p. 145-150.
35. Wu C. , H.Q., Sui M., Yan Y. and Wang F. , *Hydrogen production via catalytic steam reforming of fast pyrolysis bio-oil in a two-stage fixed bed reactor system*. Fuel processing technology, 2008. **89**(12): p. 1306-1316.
36. Apfelbacher, A.H.A., *Combined pyrolysis reformer*, in *Thermal Treatment of biomass*, A.U. European Bioenergy Research Institute (EBRI), Birmingham, UK, Editor. 2008.
37. C. M. Roggero, V.T., A. Scova, C. De Leo, A. Binello & G. Cravotto, *Characterization of Oils from Haloclean Pyrolysis of Biomasses*. Energy Sources, Part A, 2011. **33**: p. 467-476.
38. Yang, H., et al., *Characteristics of hemicellulose, cellulose and lignin pyrolysis*. Fuel, 2007. **86**(12-13): p. 1781-1788.
39. Zhang Qi, C.J., Wang Tiejun, Xu Ying., *Review of biomass pyrolysis oil properties and upgrading research.*. Energy Conversion and Management 48, 2007. **48**: p. 87-92.
40. Oasmaa, A.a.S.C., *Fuel Oil Quality of Biomass Pyrolysis Oils State of the Art for the End Users*. Energy & Fuels, 1999. **13**(4): p. 914-921.
41. Abdullah N, G.H., *Bio-oil derived from empty fruit bunches*. Fuel, 2008. **87**: p. 2606-2613.
42. Abdullah N, G.H., Sulaiman F, *Fast pyrolysis of empty fruit bunches*. Fuel, 2010. **89**: p. 2166-2169.
43. Chiamonti D, O.A., Solantausta Y., *Power generation using fast pyrolysis liquids from biomass*. Renewable and Sustainable Energy Reviews, 2007. **11**: p. 1056-1086.
44. Oasmaa A, S.Y., Arpiainen V, Kuoppala E, Sipilä K, *Fast pyrolysis bio-oils from wood and agricultural residues*. Energy and Fuels, 2009. **24**: p. 1380-1388.
45. Patwardhan PR, S.J., Brown RC, Shanks BH, *Influence of inorganic salts on the primary pyrolysis products of cellulose*. Bioresource Technology, 2010. **101**: p. 4646-4655.
46. Butler, E., et al., *A review of recent laboratory research and commercial developments in fast pyrolysis and upgrading*. Renewable and Sustainable Energy Reviews, 2011. **15**(8): p. 4171-4186.
47. Williams, P.A.H.a.P.T., *Influence of temperature on the products from the flash pyrolysis of biomass*. Fuel, 1996. **75**(9): p. 1051-1059.
48. Williams, P.T. and S. Besler, *The influence of temperature and heating rate on the slow pyrolysis of biomass*. Renewable Energy, 1996. **7**(3): p. 233-250.
49. Rauch, H.B.R., *Review of application of gases from biomass gasification in Handbook Biomass Gasification*, H.A.M. Knoef, Editor. 2006: Biomass Technology Group (BTG), Netherlands. p. 33.

50. Rajvanshi, A.K., *Biomass Gasification, in Alternative Energy in Agriculture*. 1986.
51. http://biocharfarms.org/biochar_production_energy/. *Downdraft Gasification*. Available from: http://biocharfarms.org/biochar_production_energy/, .
52. Kantarelis, E., W. Yang, and W. Blasiak, *Effect of zeolite to binder ratio on product yields and composition during catalytic steam pyrolysis of biomass over transition metal modified HZSM5*. *Fuel*, 2014. **122**(0): p. 119-125.
53. R, H.H.R., *Gas cleaning for synthesis application*. *Thermal Biomass Conversion*, ed. A.V. Bridgwater. 2009: London: Chris Fowler International.
54. Sangeeta Chopra, A.K.J., *A Review of Fixed Bed Gasification Systems for Biomass*. *Agricultural Engineering International: CIGR E-journal*, 2007. **IX**: p. 1-26.
55. F. G. van den Aarsen, W.P.M.v.S., Europäische Kommission Generaldirektion Wissenschaft, Forschung und Entwicklung, *A Review of Biomass Gasification: A Report to the European Community DG-XII JOULE Programme*. 1994: p. 176.
56. Sadaka, D.S. *Gasification*. [cited 23/05/2013; Available from: <http://bioweb.sungrant.org/NR/rdonlyres/F4AE220B-0D98-442C-899F-177CFD725ADD/0/Gasification.pdf>.
57. Safitri, A., *Biomass gasification using bubbling fluidized-bed gasifier: investigation of the effect of different catalysts on tar reduction*, in *Chemical Engineering and Chemistry*. 2005, Technische Universiteit Eindhoven. p. 126.
58. Basu, P., *Chapter 6 Design of Biomass Gasifier*, in *Biomass Gasification and Pyrolysis*. 2010. p. 167-228.
59. Couto, N., et al., *Influence of the Biomass Gasification Processes on the Final Composition of Syngas*. *Energy Procedia*, 2013. **36**(0): p. 596-606.
60. Thornhill, D. *Fluid Mechanics for fluidized beds*. 2013; Available from: http://faculty.washington.edu/finlayso/Fluidized_Bed/FBR_Fluid_Mech/fluid_bed_fbr.htm
61. S.V.B. van Paasen, J.H.A.K., H.J. Veringa, *Tar formation in a fluidised-bed gasifier; impact of fuel properties and operating conditions* ECN-C-04-013, 2004: p. 11.
62. D. Kunni, O.L., *Fluidization Engineering*. 1991, London: Butterworth-Heinemann.
63. Warnecke, R., *Gasification of biomass: comparison of fixed bed and fluidized bed gasifier*. *Biomass and Bioenergy*, 2000. **18**(6): p. 489-497.
64. X.T. Li, C.J.L., A.P. Watkinson, H.P. Chen, J.R. Kim, *Biomass gasification in a circulating fluidised bed* *biomass and Bioenergy*, 2003. **26**: p. 171-193.
65. Bridgwater, A.V., *The technical and economic feasibility of biomass gasification for power generation*. *Fuel*, 1995. **74**(5): p. 631-653.
66. Larson, E.D., *Small-Scale Gasification-Based Biomass Power Generation*. *Biomass Workshop*, 1998.
67. Sang jun Yoon, Y.-C.C., Jae-Goo Lee, *Hydrogen Production from biomass tar by catalytic steam reforming*. *Energy Conversion and Management* 2010. **51**(1): p. 42-47.
68. Evans, T.A.M.a.R.J., *Biomass Gasifier "Tars": Their Nature, Formation, and Conversion*. NREL/TP-570-25357, 1998.
69. Laurent, E., A. Centeno, and B. Delmon, *Coke Formation during the Hydrotreating of Biomass Pyrolysis Oils: Influence of Guaiacol Type Compounds*, in *Studies in Surface Science and Catalysis*, B. Delmon and G.F. Froment, Editors. 1994, Elsevier. p. 573-578.
70. Maggi, R. and B. Delmon, *A review of catalytic hydrotreating processes for the upgrading of liquids produced by flash pyrolysis*, in *Studies in Surface Science and Catalysis*, B.D. G.F. Froment and P. Grange, Editors. 1997, Elsevier. p. 99-113.
71. Mullen, C.A., A.A. Boateng, and S.E. Reichenbach, *Hydrotreating of fast pyrolysis oils from protein-rich pennycress seed presscake*. *Fuel*, 2013. **111**(0): p. 797-804.
72. Pinto, F., et al., *Production of bio-hydrocarbons by hydrotreating of pomace oil*. *Fuel*, 2014. **116**(0): p. 84-93.
73. Pstrowska, K., et al., *Hydroprocessing of rapeseed pyrolysis bio-oil over NiMo/Al₂O₃ catalyst*. *Catalysis Today*, 2014. **223**(0): p. 54-65.
74. Paul T. Williams, N.N., *Comparison of products from the pyrolysis and catalytic pyrolysis of rice husks*. *Energy*, 1999. **25**: p. 493-513.

75. Aho, A., et al., *Catalytic Pyrolysis of Biomass in a Fluidized Bed Reactor: Influence of the Acidity of H-Beta Zeolite*. Process Safety and Environmental Protection, 2007. **85**(5): p. 473-480.
76. Aho, A., et al., *Catalytic pyrolysis of woody biomass in a fluidized bed reactor: Influence of the zeolite structure*. Fuel, 2008. **87**(12): p. 2493-2501.
77. Horne, P.A. and P.T. Williams, *Premium quality fuels and chemicals from the fluidised bed pyrolysis of biomass with zeolite catalyst upgrading*. Renewable Energy, 1994. **5**(5-8): p. 810-812.
78. Horne, P.A. and P.T. Williams, *The effect of zeolite ZSM-5 catalyst deactivation during the upgrading of biomass-derived pyrolysis vapours*. Journal of Analytical and Applied Pyrolysis, 1995. **34**(1): p. 65-85.
79. Iliopoulou, E.F., et al., *Catalytic upgrading of biomass pyrolysis vapors using transition metal-modified ZSM-5 zeolite*. Applied Catalysis B: Environmental, 2012. **127**(0): p. 281-290.
80. Li, J., et al., *Catalytic fast pyrolysis of biomass with mesoporous ZSM-5 zeolites prepared by desilication with NaOH solutions*. Applied Catalysis A: General, 2014. **470**(0): p. 115-122.
81. Mante, O.D., F.A. Agblevor, and R. McClung, *A study on catalytic pyrolysis of biomass with Y-zeolite based FCC catalyst using response surface methodology*. Fuel, 2013. **108**(0): p. 451-464.
82. Mante, O.D., et al., *Catalytic pyrolysis with ZSM-5 based additive as co-catalyst to Y-zeolite in two reactor configurations*. Fuel, 2014. **117, Part A**(0): p. 649-659.
83. Mihalcik, D.J., C.A. Mullen, and A.A. Boateng, *Screening acidic zeolites for catalytic fast pyrolysis of biomass and its components*. Journal of Analytical and Applied Pyrolysis, 2011. **92**(1): p. 224-232.
84. Nguyen, T.S., et al., *Catalytic upgrading of biomass pyrolysis vapours using faujasite zeolite catalysts*. Biomass and Bioenergy, 2013. **48**(0): p. 100-110.
85. Williams, P.T. and P.A. Horne, *Characterisation of oils from the fluidised bed pyrolysis of biomass with zeolite catalyst upgrading*. Biomass and Bioenergy, 1994. **7**(1-6): p. 223-236.
86. Ligang Wei, S.X., Li Zhang, Changou Liu, Hui Zhu, Shuqin Liu, *Steam gasification of biomass for hydrogen-rich gas in a free fall reactor*. Hydrogen Energy, 2006.
87. David Sutton, B.K., Julian R.H. Ross, *Review of literature on catalysts for biomass gasification*. Fuel processing technology, 2001. **73**: p. 155-173.
88. Sundac, N., *Catalytic cracking of tar from biomass gasification*. 2007.
89. Pangmei L.v, J.C., Teijun Wang, Yan Fu and Yong Chen, *Hydrogen-Rich Gas Production from Biomass Catalytic Gasification*. Energy & Fuels, 2004. **18**: p. 228-233.
90. Corella, J.A., M. P.; Gil, J.; Caballero, M. A., *Biomass Gasification in Fluidized Bed: Where to Locate the Dolomite?* Fuel, 1999. **13**(6): p. 1122-1127.
91. Delgado, J.A., M. P.; Corella, J., *Calcined Dolomite, Magnesite, and Calcite for Cleaning Hot Gas from a Fluidized Bed Biomass Gasifier with Ateam: Life and Usefulness*. Ind. Eng. Chem. Res., 1996. **37**: p. 3637-3643.
92. Simell, P.A.L.I., J. K.; Bredenberg, J. B., *Catalytic Purification of Tarry Fuel Gas with Carbonate Rocks and Ferrous Materials*. fuel, 1992. **71**: p. 211-218.
93. Simell, P.A.L.I., J. K.; Kurkela, E. A., *Tar-Decomposing Activity of Carbonate Rocks under High CO₂ Pressure*. Fuel, 1995. **74**(6): p. 938-945.
94. Walawender, W.P.G., S.; Fan, L., *Steam Gasification of Manure in Fluidized Bed. Influence of Limestone as Bed Additive*. Energy from Biomass, (1981): p. 517-527.
95. Abu El-Rub, Z.B., E. A.; Brem, G., *Removal of Naphthalene as the Model Tar Compound on Calcined Dolomites, Olivine and Commercial Nickel Catalyst in a Fixed Bed Tubular Reactor*. In 12th European Conference for Energy, Industry and Climate Protection, 17-21 June 2002, Amsterdam, The Netherlands; ETA: Florence and WIP: Munich,; p. 607-610.
96. Courson, C.M., E.; Petit, C.; Kiennemann, A., *Development of Ni Catalysts for Gas Production from Biomass Gasification. Reactivity in Steam- and Dry-Reforming*. Catal. Today, 2000. **63**: p. 427-437.
97. Rapagna, S.J., N.; Kiennemann, A.; Foscolo, P. U., *Steam Gasification of Biomass in a Fluidized-Bed of Olivine Particles*. Biomass Bioenergy, 2000. **19**: p. 187-197.

98. S. Rapagna, H.P., C. Petit, A. Kiennemann, P.U. Foscolo, *Development of catalysts suitable for hydrogen or syn-gas production from biomass gasification*. Biomass and Bioenergy, 2002. **22**: p. 377-388.
99. Garcia, L.S., J. L.; Salvador, M. L.; Bilbao, R; Arauzo, J., *Assessment of Coprecipitated Nickel-Alumina Catalysts, for Pyrolysis of Biomass.*, in *In Developments in Thermochemical Biomass Conversion*, A.V. Bridgwater, Boocok, D. G. B., Editor. 1997: Eds.;Blackie Academic and Professional: London,. p. 1158-1169.
100. Christoph Pfeifer, H.H., *Development of catalytic tar decomposition downstream from a dual fluidized bed biomass steam gasifier*. Powder Technology, 2008. **180**: p. 9-16.
101. Jose Corella, A.O.a.P.A., *Biomass Gasification with Air in Fluidized Bed: Reforming of the Gas Composition with Commercial Steam Reforming Catalysts*. Ind. Eng. Chem Res, 1998. **37**: p. 4617-4624.
102. Aznar, M.P.C., M. A.; Gil, J.; Martin, J. A., *Commercial Steam Reforming Catalysts to Improve Gasification with Steam-Oxygen Mixtures. 2. Catalytic Tar Removal*. Ind. Eng. Chem. Res., 1998. **37**: p. 2668-2680.
103. Caballero, M.A.A., M. P.; Gil, J.; Martin; J. A.; Frances, E.; Corella, J., *Commercial Steam Reforming Catalysts To Improve Biomass Gasification with Steam-Oxygen Mixtures. 1. Hot Gas Upgrading by the Catalytic Reactor*. Ind. Eng. Chem. Res., 1997 **36**(12): p. 5227-5239.
104. Engelen, K.Z., Y.; Draelants, D.; Baron, G, *A novel Catalytic Filter for Tar Removal from Biomass Gasification gas: Improvement of the Catalytic Activity in the Presence of H₂S*. Chem. Eng. Sci, 2003: p. 665-670.
105. Forzatti, P.L., L, *Catalyst Deactivation*. Catal. Today, 1999. **52**: p. 165-181.
106. Hepola, J.S., P. , *Sulphur Poisoning of Nickel-Based Hot Gas Cleaning Catalysts in Synthetic Gasification Gas. II. Chemisorption of Hydrogen Sulphide*. Applied Catalysis, 1997: p. 305-321.
107. Z. Abu El-Rub, E.A.B.a.G.B., *Review of catalysts for Tar elimination in biomass gasification processes*. 2004 American Chemical Society Published on Web, 2004(43): p. 6911-6919.
108. Yang, Y., et al., *Characterisation of waste derived intermediate pyrolysis oils for use as diesel engine fuels*. Fuel, 2013. **103**(0): p. 247-257.
109. Hossain AK, O.M., Siddiqui SU, Yang Y, Brammer J, Hornung A, et al, *Hossain AK, Ouedi M, Siddiqui SU, Yang Y, Brammer J, Hornung A, et al*. Fuel, 2013. **105**(0): p. 135-142.
110. Janat Samanyaa, Andreas Hornunga, Andreas Apfelbachera, Peter Valeb, *Characteristics of the upper phase of bio-oil obtained from co-pyrolysis of sewage sludge with wood, rapeseed and straw*. Journal of Analytical Applied Pyrolysis, 2011. **94**: p. 120-125.
111. Michael Becidan, O.S., Johan E. Hustad, *Experimental study on pyrolysis of thermally thick biomass residues samples: Intra-sample temperature distribution and effect of sample weight ("scaling effect")*. Fuel, 2007. **86**: p. 2754-2760.
112. Charles A. Mullen , A.A.B., Neil M. Goldberg, Isabel M. Limab, David A. Laird, Kevin B. Hicks, *Bio-oil and bio-char production from corn cobs and stover by fast pyrolysis*. Biomass and Bioenergy, 2010: p. 67-74.
113. Asadullah, M., et al., *Production of bio-oil from fixed bed pyrolysis of bagasse*. Fuel, 2007. **86**(16): p. 2514-2520.
114. Chidi E. Efika, C.W., Paul T. Williams, *Syngas production from pyrolysis-catalytic steam reforming of waste biomass in a continuous screw kiln reactor*. Journal of Analytical and Applied Pyrolysis, 2012. **95**: p. 87-94.
115. Aimaro Sanna, S.L., Rob Linforth, Katherine A. Smart, John M. Andresen, *Bio-oil and bio-char from low temperature pyrolysis of spent grains using activated alumina*. Bioresource Technology, 2011. **102**(22): p. 10695-10703.
116. Paula H. Blanco, C.W., Jude A. Onwudili, Valerie Dupont, Paul T. Williams, *Catalytic Pyrolysis/Gasification of Refuse Derived Fuel for Hydrogen Production and Tar Reduction: Influence of Nickel to Citric Acid Ratio Using Ni/SiO₂ Catalysts*. Waste and Biomass Valorisation, 2013.
117. Paula H. Blanco, C.W., Jude A. Onwudili, and Paul T. Williams, *Characterization of Tar from the Pyrolysis/Gasification of Refuse Derived Fuel: Influence of Process Parameters and Catalysis*. Energy and Fuels, 2012. **26**: p. 2107-2115.

118. Robert J. Evans, E.C.C., Calvin Feik, Richard French, Steven Phillips, Jalal Abedi, Yaw D. Yeboah, Danny Day, Jan Howard, Dennis Mcgee and Matthew J. Realff, *Renewable hydrogen production by catalytic steam reforming of peanut shells pyrolysis products*. Fuel, 2002. **47**: p. 757-758.
119. Hao Qinglan, W.C., Lu Dingqiang, Wang Yao, Li Dan, Li Guiju, *Production of hydrogen-rich gas from plant biomass by catalytic pyrolysis at low temperature*. International Journal of Hydrogen Energy, 2010. **35**: p. 8884-8890.
120. Catharina Erlich [†], T.H.F., *Downdraft gasification of pellets made of wood, palm-oil residues respective bagasse: Experimental study*. Applied Energy, 2011: p. 899-908.
121. Hayati Olgun a, Sibel Ozdogan b, Guzide Yinesor b, *Results with a bench scale downdraft biomass gasifier for agricultural and forestry residues*. Biomass and Bioenergy, 2011. **35**: p. 572-580.
122. Pratik N. Sheth , B.V.B., *Experimental studies on producer gas generation from wood waste in a downdraft biomass gasifier*. Bioresource Technology, 2009. **100**: p. 3127-3133.
123. P. Plis*, R.K.W., *Theoretical and experimental investigation of biomass gasification process in a fixed bed gasifier*. Energy, 2010: p. 1-8.
124. Hiroyuki Okamoto, Y.K., T. Minowa and T. Ogi, *Catalytic Conversion of High Moisture Spent Grains to a Gaseous Fuel*. MBBA, 1999.
125. Poulston, A.M.S.S., *Catalytic tar destruction from model biomass gasification streams, in Bioten Conference*. Johnson Matthey Technology Centre, 2010.
126. Cho, M.-H., et al., *Two-stage air gasification of mixed plastic waste: Olivine as the bed material and effects of various additives and a nickel-plated distributor on the tar removal*. Energy, (0).
127. Devi, L., et al., *Catalytic decomposition of biomass tars: use of dolomite and untreated olivine*. Renewable Energy, 2005. **30**(4): p. 565-587.
128. Hu, G., et al., *Steam gasification of apricot stones with olivine and dolomite as downstream catalysts*. Fuel Processing Technology, 2006. **87**(5): p. 375-382.
129. Wang, T.J., et al., *The steam reforming of naphthalene over a nickel–dolomite cracking catalyst*. Biomass and Bioenergy, 2005. **28**(5): p. 508-514.
130. Zhang, R., H. Wang, and X. Hou, *Catalytic reforming of toluene as tar model compound: Effect of Ce and Ce–Mg promoter using Ni/olivine catalyst*. Chemosphere, 2014. **97**(0): p. 40-46.
131. Tiejun Wang, J.C., Xiaoqin Cui, Qi Zhang, Yan Fu, *Reforming of raw fuel gas from biomass gasification to syngas over highly stable nickel–magnesium solid solution catalysts*. Fuel processing technology, 2006. **87**(5): p. 421-428.
132. M. Asadullah, M.A.R., M.M. Ali, M.S. Rahman, M.A. Motin, M.B. Sultan, M.R. Alam, *Production of bio-oil from fixed bed pyrolysis of bagasse*. Fuel, 2007. **86**: p. 2514-2520.
133. Yang Y, B.J., Ouadi M, Samanya J, Hornung A, Xu HM, et al, *Characterisation of waste derived intermediate pyrolysis oils for use as diesel engine fuels*. Fuel, 2013. **103**: p. 247-257.
134. Ouadi, M., et al., *The intermediate pyrolysis of de-inking sludge to produce a sustainable liquid fuel*. Journal of Analytical and Applied Pyrolysis, 2013. **102**(0): p. 24-32.
135. Sanna, A.L., Sujing; Linforth, Rob; Smart, Katherine A.; Andrésen, John M., *Bio-oil and bio-char from low temperature pyrolysis of spent grains using activated alumina*. Bioresource Technology, 2011. **102**(22): p. 10695-10703.
136. 9PK, *System Granular/Pelletizer operation book*, SCA Machinery.
137. 14774-3, *British Standard Solid biofuels. Determination of Moisture Content, Oven dry method. Moisture in general analysis sample*. 2009.
138. 14775, *Solid biofuels. Determination of ash content*. 2009.
139. 15148, *Solid biofuels. Determination of the content of volatile matter*. 2009.
140. Medac Ltd, A., Chobham Business Centre, Chertsey Road, Chobham, Surrey, GU24 8JB.
141. Foss Analytical AB, AB, *Determination of Acid Detergent Fibre (ADF) and Acid Detergent Lignin (ADL) using Fibercap TM 2021/2023*, 2003.
142. Foss Analytical AB, *Determination of Amylase Treated Neutral Detergent Fibre using the Fibertec System according to AOAC 2002:04/ISO 16472:2005*, 2003.

143. Du Li, Y.P., Rossnagel BG, Christensen DA, McKinnon JJ., *Physicochemical characteristics, hydroxycinnamic acids (ferulic acid, P-coumaric acid) and their ratio, and in situ biodegradability: comparison of genotypic differences among six barley varieties*. Journal Agriculture Food Chemistry, 2009. **57**(11): p. 4777-83.
144. Marchwood Scientific Services, M.I.P., Marchwood, Southampton, SO40 4PB.
145. 15404, B.S.E., *Ash Fusion Temperature*.
146. D5865, A., *Heating Value*.
147. Jigisha Parikh, S.A. Channiwala, G.K. Ghosal, *A correlation for calculating HHV from proximate analysis of solid fuels*. Fuel, 2005. **84**: p. 487-494.
148. CHANNIWALA, S.P., PP, *A unified correlation for estimating HHV of solid, liquid and gaseous fuels*. Fuel, 2002. **81**(8): p. 1051-1063.
149. E203, A.S., *Titration*.
150. D445, A.S., *Viscosity*.
151. D7236, A.S., *Flash Point*.
152. D482, A.S., *Ash Content*
153. D189, A.S., *Conradson Carbon Residue*.
154. D130, A.S., *Corrosivity*.
155. McKendry, P., *Energy production from biomass (part 3): gasification technologies*. Bioresource Technology, 2002. **83**(1): p. 55-63.
156. Ghetti, P., L. Ricca, and L. Angelini, *Thermal analysis of biomass and corresponding pyrolysis products*. Fuel, 1996. **75**(5): p. 565-573.
157. Sanchez-Silva, L., et al., *Thermogravimetric–mass spectrometric analysis of lignocellulosic and marine biomass pyrolysis*. Bioresource Technology, 2012. **109**(0): p. 163-172.
158. waste, E.P.C.D.f.b.a.; Available from: <https://www.ecn.nl/phyllis2/>.
159. Eoin Butler, G.D., Dietrich Meier, Kevin McDonnell, *A review of recent laboratory research and commercial developments in fast pyrolysis and upgrading*. Renewable and Sustainable Energy Reviews, 2011. **15**: p. 4171-4186.
160. Lijun Wang, C.L.W., David D. Jones, Milford A. Hanna, *Contemporary issues in thermal gasification of biomass and its application to electricity and fuel production*. Biomass and Bioenergy, 2008. **32**(7): p. 573-581.
161. P. Thy, B.M.J.a.C.E.L., *High Temperature Melting Behaviour of Urban Wood Fuel Ash*. Energy & Fuels, 1999. **13**: p. 859-850.
162. Sandberg, J., *Fouling in biomass fired boiler*, in *School of Sustainable Development of Society and Technology*. 2011, Malardalen University Sweden
163. Thomas R. Miles, L.L.B., Richard W. Bryers, Bryan M.Jenkins, Laurence L.Oden, *Alkali depositis found in biomass power plants: A preliminary investigation of their extent and nature*. 1996. **2**(NREL/TP-433-8142).
164. Nowakowski, D.J., et al., *Potassium catalysis in the pyrolysis behaviour of short rotation willow coppice*. Fuel, 2007. **86**(15): p. 2389-2402.
165. All Power Labs, M.S.B., CA 94710. *GEK Gasifier*. Available from: <http://www.gekgasifier.com/>.
166. Ouadi, M., et al., *Fixed bed downdraft gasification of paper industry wastes*. Applied Energy, 2013. **103**(0): p. 692-699.
167. W. van de Kamp, P.d.W., U. Zeilke, M. Soumalainen, H. Knoef, J. Good, T. Liliedahl, C. Unger, M. Whitehouse, J. Neeft, H. van de Hoek, J. Kiel, *Tar measurement standard for sampling and analysis of tars and particles in biomass gasification product gas*. ECN-RX--05-185, 2005.
168. Sastry, A.B.a.R.C., *Biomass Gasification Processes in Downdraft Fixed Bed Reactors: A Review*. International Journal of Chemical Engineering and Applications, 2011. **2**(6): p. 425-433.
169. Chao Gai , Y.D., *Experimental study on non-woody biomass gasification in a downdraft gasifier*. International Journal of Hydrogen Energy, 2012(37): p. 4935-4944.
170. Nakorn Tippayawong, C.C., Anucha Promwungkwa and Presert Rerkkiranrai, *Clean Energy from Gasification of Biomass for Sterilization of Mushroom Growing Substrates*. International Journal of Energy, 2011. **5**(4): p. 96-103.

171. P.R. Bhoi, R.N.S., A. M. Sharma and S. R. Patel, *Performance evaluation of open core gasifier on multi-fuels*. Biomass and Bioenergy, 2006. **30**: p. 575-579.
172. B. S. Pathak, S.R.P., A.G. Bhave, P. R. Bhoi, A.M.Sharma and N.P. Shah, *Performance evaluation of an agricultural residue-based modular throat-type downdraft gasifier for thermal application*. Biomass and Bioenergy, 2008. **32**: p. 72-77.
173. S.C. Bhattacharya*, A.H.M.M.R.S., Hoang-Luong Pham, *A study on wood gasification for low tar gas production*. Energy 24, 1998: p. 285-296.
174. US Department of Energy, H.o.B.D.G.E.S., US Government, Washington DC, USA, 1988.
175. Hornung A, A.A.T.t.o.b., *UK patent application GB2460156A*. 2009.
176. M. Ouadi, J.G.B., Y. Yang, A. Hornung, M. Kay, *The intermediate pyrolysis of de-inking sludge to produce a sustainable liquid fuel*. Journal of Analytical Applied Pyrolysis, 2013. **102**: p. 24-32.
177. Melisa Bertero, G.d.I.P., Ulises Sedran, *Fuels from bio-oils: Bio-oil production from different residual sources, characterisation and thermal conditioning*. Fuel, 2012. **95**: p. 263-271.
178. P. Weerachanchai, C.T., and M. Tangsathitkulchai., *Phase behaviours and fuel properties of bio-oil-diesel-alcohol blends*. Engineering and Technology, World academy of science, 2009: p. 387-393.
179. Yu F, D.S., Chen P, Liu Y, Olson A, Kittleson D & Ruan R, *Physical and chemical properties of bio-oils from microwave pyrolysis of corn stover*. Applied bichemistry and biotechnology, 2007. **136-140**: p. 957-970.
180. Waheed, Q.M.K. and P.T. Williams, *Hydrogen Production from High Temperature Pyrolysis/Steam Reforming of Waste Biomass: Rice Husk, Sugar Cane Bagasse, and Wheat Straw*. Energy & Fuels, 2013. **27**(11): p. 6695-6704.
181. Kyle Crombie, O.M., Saran P. Sohi, Peter Brownsort and Andrew Cross, *The effect of pyrolysis conditions on biochar stability as determined by three methods*. bioenergy, 2013. **5**: p. 122-131.
182. Phan, A.N., V. Sharafi, and J. Swithenbank, *Effect of bed depth on characterisation of slow pyrolysis products*. Fuel, 2009. **88**(8): p. 1383-1387.
183. Muhammad S. Abu Bakar, J.O.T., *CATALYTIC PYROLYSIS OF RICE HUSK FOR BIO-OIL PRODUCTION*. Journal of Analytical and Applied Pyrolysis, 2012: p. 1-17.
184. H. Haykiri-Acma, A.B., S. Yaman, *Effects of fragmentation and particle size on the fuel properties of hazelnut shells*. Fuel, 2013. **112**: p. 326-330.
185. Onay, O., *Influence of pyrolysis temperature and heating rate on the production of bio-oil and char from safflower seed by pyrolysis, using a well-swept fixed-bed reactor*. Fuel processing technology, 2007. **88**(5): p. 523-531.
186. Shurong Wang, X.L., Fan Zhang, Qinjie Cai, Yurong Wang, Zhongyang Lao, *Bio-oil catalytic reforming without steam addition: Application to hydrogen production and studies on its mechanism*. International Journal of Hydrogen Energy, 2013. **38**: p. 16038-16047.
187. Pedro J, O.-t., *Stewam reforming of bio-oil: Effect of bio-oil composition and stability*, in *Iowa State University*. 2008, Iowa State University: Digital Repositry @ Iowa State University.
188. R. Trane, S.D., M.S Skjpth-Rasmussen, A.D. Jensen, *Catalytic Steam reforming of bio-oil*. International Journal of Hydrogen Energy, 2012. **37**: p. 6447-6472.
189. P. Gilbert, C.R., V. Sharifi, J. Swithenbank, *Tar reduction in pyrolysis vapours from biomass over a hot char bed*. Bioresource Technology, 2009. **100**(23): p. 6045-6051.
190. Lei Zhang, S.-C.K., *Multicomponent vaporization modeling of bio-oil and its mixtures with other fuels*. Fuel, 2012. **95**: p. 471-480.
191. Hailin Li, G.A.K., *Knock in spark ignition hydrogen engines*. International Journal of Hydrogen Energy 2003. **29**: p. 859-865.
192. Capucine Dupont , R.C., Guillaume Gauthier, François Toche, *Heat capacity measurements of various biomass types and pyrolysis residues*. Fuel, 2014. **115**: p. 644-651.

Appendix A: Published Work

Publication made during the course of this study is listed below:

1. A.S.N. Mahmood, J.G. Brammer, A. Hornung, A. Steele, S. Poulston. The intermediate pyrolysis and catalytic steam reforming of Brewers spent Grain. *Journal of Analytical and Applied Pyrolysis* , Volume 103, September 2013, Pages 328-342 (Article accepted)
<http://dx.doi.org/10.1016/j.jaap.2012.09.009>
2. Y. Yang, J.G. Brammer, A.S.N. Mahmood, A. Hornung. Intermediate pyrolysis of biomass energy pellets for producing sustainable liquid, gaseous and solid fuels. *Bio resource Technology* – (Accepted 9 July 2014)
<http://dx.doi.org/10.1016/j.biortech.2014.07.044>

Appendix B: Mass Balance Sheets

Run:

Date:

Sample:

	1	2	3
Moisture Content			
Ash Content			

Pyrolysis rig				
Component	Weight before (g)	Weight after (g)	Difference	Nature
Feed				
Quartz reactor tube 1				
Quartz reactor tube 2				
Quartz wool 1				
Quartz wool 2				
Receiver bend 1				
Glass tube				
Dry ice condenser 1				
Oil pot connector 1				
Oil pot 1				
Tube to 2nd condenser				
Dry ice condenser 2				
Oil pot connector 2				
Oil pot 2				
Tube to cotton wool filter				
Cotton wool filter				
Tube to Quencher				
Quencher				
Liquids collected				
Char collected				
Small quartz tube				
Catalyst				

Notes:

Yields (as received)	Weight (g)	Weight (%)
Total Liquid		
Char		
Gas (by difference)		

--

Liquids (phase separation)	Weight (g)	Weight (%)
Aqueous phase		
Oil phase		

Liquids	Aqueous yield	Organic Liquid
Water (KF titration)		

Yields (dry basis)	Weight (g)	Weight (%)
Total Liquid		
Char		
Gas (by difference)		

Feed (dry)

Secondary Catalytic Reactor

TIME (min)	CARBOLITE REACTOR TEMPERATURE (°C)	CATALYST BED TEMPERATURE (°C)	N2 FLOWRATE (cm ³ /min)

Appendix C: Energy Required for Drying Spent Grains

ASSUMPTIONS:

1 Year is equal to 8000 Hours

Spent grain available on Brewery site 100,000 t/y having a moisture content of 70% at a temperature of 20°C

Final moisture content required is 10% using a Rotary Drum Dryer operating at 100°C

To dry the total available spent grain of 100,000 per year which contains 70% moisture content to a 10% moisture content required for thermochemical conversion (either pyrolysis or gasification) will be carried out using a rotary drum dryer.

100,000t/y at 70% is equal to 12.5t/hr of spent grain material of which 8.75t/hr is water and the remaining 3.75t/hr is the amount of solids.

When the spent grain is dried to 10% moisture content, there are 3.75t/hr of dry solids and 0.375t/hr of water.

The amount of water to be evaporated is therefore $(8.75 - 0.375) = 8.375$ t/hr = 2.326 kg/s

Therefore the remaining water is 0.104kg/s and 1.042kg/s of dry solids.

The temperature at the exit of the dryer is 100°C. The energy required in the dryer is to evaporate the water (2.592) plus that to raise the remaining water to 100°C (0.335MJ/kg) plus to heat the solids to 100°C (assuming a C_p value of 1.3KJ/kgC)[192].

Therefore the Total Energy = $(2.326 * 2.592) + (0.104 * 0.335) + (1.042 * 0.0013 * 80) = \mathbf{6.03 MW}$

Appendix D: Proformer Mass & Energy Balance

Basis: Assumed 100,000 t/yr of spent grain with 70% moisture dried to 10%.

A mass and energy balance was performed around the new intermediate pyrolysis 'Pyroformer' reactor based on the processing of BSG as a feedstock. In order to obtain the energy balance the following equation is used:

$$Q = \dot{m}C_p\Delta T \quad (18)$$

Where:

Q = Energy (MJ)

\dot{m} = mass feedrate (kg/hr.)

C_p = specific heat capacity (MJ/kg)

ΔT = temperature difference (°C)

BSG INPUT:

BSG is dried to a moisture content of 10%; the fuel enters the reactor at an operating temperature of 450°C.

Heating value of BSG as measured at Aston University is 18MJ/kg at an ambient temperature of 20°C

BSG chemical energy in to reactor = (1.042 + 0.1406) = 1.146kg/s * 18MJ/kg = **20.628 MW**

PRODUCT OUTPUTS:

Condensable Organic Vapours (Volatiles)

1.146kg/s of BSG yields 50 wt.% of condensed organic vapours or 0.573kg/s of which comprises of 20.85 wt.% (0.119kg/s) organic vapours and 79.15 wt.% (0.45kg/s) aqueous phase. The energy found in the organic phase was = **20.39 MJ/kg (see section 7.3.1)**

Chemical energy in organic vapours/volatiles = 0.573 * 20.39 = **11.68MW**

Sensible heat of major volatiles at 508K: $Q = \sum mC_p \Delta T$

Toluene = 1.887 KJ/kg K

Ethylbenzene = 1.976 KJ/kg K

Phenol = 1.742 KJ/kg K

Average = 1.87KJ/Kg K = 0.00187 MJ/kg K

Sensible heat of volatiles = 0.537 * 0.00187 * (450-20) = **0.43MW**

Total energy of condensable volatiles = 0.43 + 11.68 = **12.11 MW**

Total water vapour produced = $0.79 * 1.146 = 0.905\text{kg/s}$

Sensible heat of water vapour at $C_p = 1.98 \text{ KJ/kgK} = 0.905 * 0.00198 * 430 = \mathbf{0.77\text{MW}}$

Char (Solid Residue)

30 wt.% of the BSG feed entering the reactor is left as char (solid residues)

Amount of char leaving the reactor is $(1.146 * 0.3) = 0.344\text{kg/s}$

HHV of char measured at Aston University = 28 MJ/kg

Chemical energy in Char = $0.334 * 28 = \mathbf{9.35\text{MW}}$

Permanent Gases

The amount of permanent gases produced was obtained by difference at 20 wt. %

Amount of gas leaving the reactor = $1.146 * 0.2 = 0.2292 \text{ kg/s}$

Composition of gas obtained discounting N_2 :

$\text{H}_2 = 1.6 \text{ vol\%}$ (HHV = 13.2 MJ/Nm^3)

$\text{CO} = 19.74 \text{ vol\%}$ (HHV = 13.1 MJ/Nm^3)

$\text{CH}_4 = 9.43 \text{ vol\%}$ (HHV = 41.2 MJ/Nm^3)

Total HHV of Gas = $(0.016 * 13.2) + (0.1974 * 13.2) + (0.0943 * 41.2) = 6.7 \text{ MJ/Nm}^3$

Average density of gas at STP = 1.61 kg/Nm^3

Total Volume of Gas produced = $0.2292 / 1.61 = 0.1423 \text{ Nm}^3/\text{s}$

Chemical energy in gas = $0.1423 * 6.7 = \mathbf{0.95\text{MW}}$

Sensible heat of permanent gases:

Gas densities at 450°C

$\text{CO} = 0.47\text{kg/m}^3$, mass in $1\text{m}^3 = 0.1974 * 0.47 = 0.093 \text{ kg}$

$\text{CH}_4 = 0.27\text{kg./m}^3$, mass in $1\text{m}^3 = 0.094 * 0.27 = 0.025 \text{ kg}$

$\text{CO}_2 = 0.47 \text{ kg/m}^3$, mass in $1\text{m}^3 = 0.642 * 0.47 = 0.302 \text{ kg}$

Total mass in $1\text{m}^3 = 0.419 \text{ kg/m}^3$

Mass fractions: $\text{CO} = 19.7\%$, $\text{CH}_4 = 9.4\%$, $\text{CO}_2 = 64.2\%$ and $\text{H}_2 = 1.6\%$

Average C_p Values

$\text{CO} = 1.064 \text{ KJ/kg K}$, $\text{CH}_4 = 0.74\text{KJ/kg K}$, $\text{CO}_2 = 1.014\text{KJ/kg K}$

Average $C_p = (1.064 * 0.197) + (0.74 * 0.094) + (1.014 * 0.642) = 0.93 \text{ KJ/kg K}$

Sensible energy of gas = $0.2292 * 0.00093 * (450-20) = \mathbf{0.092MW}$

Total Energy of Gas = $0.95 + 0.0092 = \mathbf{0.952MW}$

The energy required for heating the pyrolysis unit (as determined by Aston University) is approximately 10% of chemical energy of the feed = $0.10 * 11.68 = \mathbf{1.168MW}$

Pyro – Steam Reformer – Pilot Scale Test

Mass and Energy Balance (Pyroformer reactor):

Basis 1 hour:

Fuel input at 5kg/hr with a 10 wt.% moisture content was added to the pyroformer (operating at 450°C and at atmospheric conditions) had a heating value of 18MJ/kg.

Therefore $(5*18) = \mathbf{90MJ/kg}$

Three product streams were available in the form of a solid, liquid and gas in fractions 30 wt.%, 50 wt.% and 20 wt.%.

Liquids:

The bio-oil fraction was approximately 50 wt.% (of which 20% organic fraction, 80% aqueous – mainly water) of the overall products yielded and had a heating value of 20MJ/kg. The assumed Cp value of the organics in the liquid phase is 1.8KJ/KgK.

Therefore $(5*0.5*20) = \mathbf{50MJ/kg}$

Solids/Char:

The char fraction was approximately 30 wt.% of the overall products yielded and had a heating value of 28MJ/kg. The assumed Cp value of the char is 1.4KJ/kgK[192]

Therefore $(5*0.3*28) = \mathbf{42MJ/kg}$

Permanent Gases:

The permanent gas yields was measured to have a heating value of $\mathbf{6.7 MJ/Nm^3}$

Therefore $(5*0.2*6.7) = \mathbf{6.7MJ/kg}$

Energy available in three product streams in one hour:

Char: $5 * 0.3 * 0.0014 * (450-20) = 0.9 \text{ MJ}$

Bio-oil: $5 * 0.5 * 0.0018 * (450-20) = 1.9 \text{ MJ}$

Permanent Gas: $5 * 0.2 * 0.0012 * (450-20) = 0.2 \text{ MJ}$

Case 1 – Pyro-steam reforming at 500°C

The potential energy sent to the catalytic reactor operating at 500°C

$$\text{Oil/Pyrolysis vapour:} \quad (5 * 0.5 * 0.0018) * (500 - 450) = 0.225\text{MJ}$$

$$\text{Permanent gases:} \quad (5 * 0.2 * 0.0012) * (500-450) = 0.06 \text{ MJ}$$

$$\text{Total Energy} = \mathbf{0.285 \text{ MJ}}$$

Total Energy required to heat up the catalytic reactor from gases generated 450°C to 500°C is therefore =

$$[0.285 / (6.7 + 50) * 100] = \mathbf{0.5\%}$$

Case 2 – Pyro-Steam Reforming at 750°C

The potential energy sent to the catalytic reactor operating at 750°C:

$$\text{Oil/Pyrolysis vapour:} \quad (5 * 0.5 * 0.0018) * (750 - 450) = 1.35\text{MJ}$$

$$\text{Permanent gases:} \quad (5 * 0.2 * 0.0012) * (750-450) = 0.36 \text{ MJ}$$

$$\text{Total Energy} = \mathbf{1.71 \text{ MJ}}$$

Total Energy required to heat up the catalytic reactor from gases generated 450°C to 750°C is therefore =

$$[1.71 / (6.7 + 50) * 100] = \mathbf{3.01\%}$$

Case 3 – Pyro-Steam Reforming at 850°C

The potential energy sent to the catalytic reactor operating at 850°C:

$$\text{Oil/Pyrolysis vapour:} \quad (5 * 0.5 * 0.0018) * (850 - 450) = 1.8\text{MJ}$$

$$\text{Permanent gases:} \quad (5 * 0.2 * 0.0012) * (850-450) = 0.48 \text{ MJ}$$

$$\text{Total Energy} = \mathbf{2.28 \text{ MJ}}$$

Total Energy required to heat up the catalytic reactor from gases generated 450°C to 850°C is therefore =

$$[2.28 / (6.7 + 50) * 100] = \mathbf{4.01\%}$$

A recuperated heat exchanger can be added to the catalytic reactor to partly recover the heat downstream.

Appendix E: GEK Downdraft Gasifier Energy Balance

Based on the assumption:

All reactions reach equilibrium, therefore there is no residual solid carbon.

Gasifier walls are heavily lagged using rock wool therefore wall heat losses to the surroundings by conduction are considered negligible.

All streams entering at ambient conditions are calculated at a reference temperature of 20°C.

All operating conditions as per laboratory scale unless stated.

Sensible heat from the system is not recovered.

GEK Gasification test:

Basis 2 hour trial run

Fuel Input into the gasifier = 9kg/hr, 0.0025 kg/s

Average HHV of feedstock = 18MJ/kg

Chemical energy into the gasifier = 0.045 MJ

From lab scale energy balance calculations 1kg of feed yields approximately 2.76Nm³ of product gas with an average calorific value of 4.96 MJ/Nm³

Volumetric flow rate of product gas out of gasifier = 0.365* 2.76 = 1.01 Nm³/s

Chemical energy of product gas out of gasifier = 1.01 * 4.96 = 5.01 MJ

Commercial Case – Downdraft Gasification

Assumption based on 100,000 t/y of spent grain available at 70% moisture content dried to 10%.

Drying of BSG energy requirements to 10% moisture content is 6MW.

Once feed has been dried to 10 wt.% moisture the solid is pelletised and enters the gasifier at a flow rate of 1.146kg/s.

Average HHV of feedstock = 18 MJ/kg

The chemical energy of feedstock into the gasifier = (1.042 + 0.104) = 1.146kg/s, (1.146 * 18) = **20.628 MW**

From lab scale energy balance calculations 1kg of feed yields approximately 2.76Nm³ of product gas with an average calorific value of 4.96 MJ/Nm³

Volumetric flow rate of product gas out of gasifier = $0.365 * 2.76 = 1.01 \text{ Nm}^3/\text{s}$

Chemical energy of product gas from gasifier = $1.01 * 4.96 = \mathbf{5.01MW}$

No further heat recovery from sensible heat, water condensate or the ash will be recovered by the system and therefore are not considered in this energy balance. The net available energy from the product gas would therefore be **5.01MWth**.